University of Naples Federico II

Polytechnic School and of Basic Sciences

Doctoral Program in Earth, Environmental, and Resource Sciences

XXXVII Cycle



Ph.D. Thesis in Applied Hydrogeology

Climate change effects on the groundwater recharge and groundwater availability of a karst aquifer in southern Italy. The case study of Avella Mts. strategic karst aquifer (Campania)

Supervisor
Prof. Vincenzo Allocca

Ph.D. Student
Paola Petrone

Co-supervisor
Prof. Pantaleone De Vita

Ph.D. Program Coordinator
Prof. Luigi Ferranti

La borsa di dottorato è stata cofinanziata con risorse del
Programma Operativo Nazionale Ricerca e Innovazione 2014-2020, risorse FSE REACT-EU
Azione IV.4 “Dottorati e contratti di ricerca su tematiche dell’innovazione”
e Azione IV.5 “Dottorati su tematiche Green”

Ph.D. on Green Topics with Industrial Characterization

P.O.N. Research and Innovation 2014-2020

Climate change effects on the groundwater recharge and groundwater availability of a karst aquifer in southern Italy. The case study of Avella Mts. strategic karst aquifer (Campania)

Ph.D. Student
Paola Petrone

Industrial partner
GORI SpA

Abstract

Karst aquifers are among the most important groundwater reservoirs in many regions of the world, as they provide drinking water and support industrial and agricultural activities. These aquifers are essential for socio-economic development, groundwater-dependent ecosystems and environmental sustainability. Unfortunately, these aquifers are increasingly vulnerable to threats from unsustainable exploitation, pollution and the effects of climate change with negative impacts on both the quantity and quality of groundwater resources.

This Ph.D. thesis focused on the complex challenge of estimating the recharge and availability of groundwater resources of Avella Mts. karst aquifer, with particular attention to the impacts of climatic change. The Avella Mts. system was selected as a sample aquifer for its strategic hydrogeological importance at the regional scale. For the study area, characterised by significant climatic variability, geomorphological and stratigraphic complexity, due to the presence of discontinuous ash-fall pyroclastic soil cover and a lack of systematic data at high altitudes, this research highlighted the importance of estimating groundwater recharge and identifying the factors that affect this process, considering the strategic relevance of this aquifer for current and future water supply. For this research, an integrated multi-method, multi-temporal and multi-scale approach was applied, which represents a valuable tool for developing strategies to ensure sustainable use of groundwater resources in both the short and long term.

An important first step in this study was the revision of the hydrogeological conceptual model of the Avella Mts. This updated model defines the lithology of the aquifer, its deep geometry and, for the first time, the groundwater flow scheme, identifying a compartmentalised aquifer system consisting of five distinct basins.

At the aquifer scale, recharge was estimated using the Turc formula and MODIS satellite data ranged from 7.30 to 6.90 m^3/s, with strong agreement between methods, confirming their validity. A comprehensive multi-scale water balance was performed using the Soil Water Balance (SWB) model. The results show a high spatio-temporal variability of recharge and a budget imbalance within the aquifer and its groundwater basins, which is particularly pronounced during drought years, as evidenced by the drying up of springs and streams.

This research used Regional Climate Models (RCMs) projections to assess the impact of climate change on groundwater recharge under the IPCC Representative Concentration Pathways (RCP4.5 and RCP8.5). The projections indicated reductions in recharge in the

short, medium and long term compared to the historical reference period of up to 50% by 2100 for the most catastrophic scenario RCP8.5.

The study was also extended to the piedmont sector of the Avella Mts., corresponding to the Baiano district. This area is of great hydrogeological interest because it hosts a piedmont karst aquifer that has been used for a long time to supply groundwater to local communities. At the sectoral scale were estimated: i) groundwater recharge through the hydrological balance; ii) aquifer productivity through pumping tests; iii) groundwater hydrochemical quality. The results show significant groundwater resources, high groundwater quality and yield for this sector of the aquifer.

At the site-specif scale, field surveys and laboratory analyses improved our knowledge of the hydrogeological role of the ash-fall pyroclastic soil cover on the recharge processes of the karst aquifer. This knowledge is constantly increasing through the design and implementation of an experimental observatory equipped in the Foce hydrogeological basin, where all the parameters of the hydrogeological balance are measured continuously and in real-time by an integrated monitoring system. The installed instruments allow the continuous monitoring of the following hydrological variables: i) precipitation and air temperature, by means of weather stations located inside and outside the forest; ii) soil water content to a depth of 1.20 m, by means of multilevel probes; iii) matric potential by means of water potential sensors; iv) water infiltration by means of a natural multilevel lysimeter with data logger; v) total runoff, by means of a Venturi channel and a radar sensor with data logger; vi) piezometric levels and spring discharges, by means of level and velocity sensors with data logger. Data from this monitoring, combined with detailed stratigraphic characterisation and hydraulic parameter determination, were used to implement and calibrate the HYDRUS-1D numerical model for a 3-year simulation period of hydrogeological variables (e.g. infiltration and evapotranspiration). The simulation results emphasized seasonal dynamics of the hydrogeological variables in the unsaturated zone and the role of canopy interception in modifying effective precipitation.

The results obtained are considered particularly significant as they represent an improvement of the hydrogeological knowledge that, for most aquifers of the southern Apennines, seems to be only general and not suitable for the application of advanced models aimed at estimating the effects of climate change scenarios. Finally, the proposed approach is

designed to be exportable to other karst aquifers of southern Italy and the world, with similar characteristics.

Keywords: karst aquifer, groundwater recharge, climate change, numerical modelling, southern Appennines.

List of publications

Published

- Petrone, P., De Vita, P., Marsiglia, P., Allocca, P., Coda, S., Cusano, D., Lepore, D., Allocca, V., 2024. Hydrogeological conceptual model and groundwater recharge of Avella Mts. karst aquifer (southern Italy): A literature review and update. J. Hydrol. Reg. Stud. 54, 101871. https://doi.org/10.1016/j.ejrh.2024.101871.
- Aquino A., Petrone P., Ginolfi M., Mazzarotti C., Rosamilia S., Aquino S., Allocca V., 2024. Prospettive di utilizzo di acquiferi carsici pedemontani: il caso studio del Mandamento di Baiano (Appennino meridionale, Italia). *Prospective for using of piedmont karst aquifers: the case study of the Baiano District (southern Apennines, Italy)*. Geologia Tecnica & Ambientale, 15-24.

Submitted

- Petrone, P., De Vita, P., Allocca, P., Coda, C., Cusano D., Kodešová, R., Lepore, D., Allocca V., 2025. Multiscale soil water balance for sustainable groundwater management of a local transboundary karst aquifer. Groundwater for Sustainable Development.

In progress

- Impacts of climate change on the groundwater recharge of the Avella Mts. karst aquifer by Regional Climate Models.
- Groundwater recharge estimation using HYDRUS-1D model in Foce hydrogeological karst observatory.

List of figures

Figure 1 – a) Karst aquifers of southern Apennines; b) Excerpt from geological map (Vitale and Ciarcia, 2018, modified).

Figure 2 - Groundwater circulation scheme of the Avella karst aquifer (De Vita et al., 2018, modified).

Figure 3 – Hydrogeochemical characterisation of groundwater.

Figure 4 – a) Regional distribution model of ash-fall pyroclastic deposits in the area surrounding the Somma-Vesuvius volcano (De Vita and Nappi, 2013, modified); b) land use map (Corine Land Cover, 2018).

Figure 5 – Monthly rainfall and air temperature regime.

Figure 6 - a) Groundwater-dependent ecosystems of Avella Mts.; b) Recharge and outflow areas for the provinces of Campania region.

Figure 7 - a) Study area location.; b) Excerpt from the geological map of Italy at 1:50.000 scale (from ISPRA, modified), Ercolano (N. 448) and Avellino (N. 449) sheets.

Figure 8 – Example of stratigraphic log representative of the depositional sequence exposed in the highest portion of the alluvial fans (De Vito et al., 1998, modified).

Figure 9 – a) Sarno Mts. location; b) Excerpt from geological map (Vitale and Ciarcia, 2018, modified); c) Excerpt of Foce experimental hydrogeological basin from hydrogeological map of Avella Mts.

Figure 10 - Distribution model of ash-fall soil pyroclastic deposits in Sarno Mts. (Fusco et al., 2017, modified).

Figure 11 - Representative stratigraphic setting of soil covers mantling (Fusco et al., 2022, modified).

Figure 12 - Estimated time series of SWD in comparison with the annual rainfall cumulative curves with yearly maximum (red dots) and minimum values (blue dots). Dashed horizontal lines represent SAT (blue), FC (green) and PWP (red) (Fusco et al., 2017).

Figure 13 – Location of the study area. a) Avella Mts., Partenio and Sarno River Regional Parks, and groundwater-dependent ecosystems (https://www.sciencedirect.com/topics/earth-and-planetary-sciences/groundwater-dependent-ecosystem) of Sarno, Sabato and Regi Lagni rivers; b**)** Geological map (from Vitale and Ciarcia, 2018, modified); c) Corine Land Cover (2018) simplified; d) Well-fields, wells, boreholes, and basal springs used for drinking water supply by public bodies, companies and private users; **e)** Tapped basal springs and aqueduct systems.

Figure 14 – Location sketch, date of construction, and characteristics of basal spring tapping works. a) S. Maria La Foce spring; b) S. Marina di Lavorate spring; c) Mefito and Calabricito springs; d) Cerola spring; e) Laura e Labso springs; f) Mercato and Palazzo springs; g) S. Mauro spring.

Figure 15 - Previous hydrogeological schemes of Avella Mts.: a) from Civita et al. (1973) modified; b) from Celico (1978) modified; c) from Celico (1983) modified; d) from Budetta et al. (1994) modified; e) from Allocca et al. (2008) modified; f) from De Vita et al (2018) modified.

Figure 16 – Flow chart showing the workflow developed for the definition of the hydrogeological conceptual model and water balance of Avella Mts.

Figure 17 – Novel hydrogeological conceptual model of Avella Mts.

Figure 18 – a) Planimetric distribution of the meteorological stations network; b) Hypsometric curve and distribution of gauges with altitude; c) Linear regression model of mean annual precipitation (2000-2019 period); d) Linear regression model of mean annual air temperature (2000-2019 period).

Figure 19 – Distributed models of: a) mean annual precipitation; b) mean annual air temperature; c) mean annual AET (Turc, 1954); d) mean annual AET (MODIS); e) mean annual GR (calculated by AET Turc); f) mean annual GR (calculated by AET MODIS).

Figure 20 – Comparison between previous schemes a) Civita et al. (1973); b) Celico (1978; 1983); Budetta et al. (1994); De Vita et al. (2018); and c) proposed hydrogeological model; d) Comparison between previous and proposed water balances.

Figure 21 – a) Map of TBAs in the world (IGRAC, 2021, modified); b) Map of TBAs in Europe (IGRAC, 2021, modified); c) Map of potential Italian Alpine and Apennines TBAs; d) Map of karst RTBAs and LTBAs in Campania region.

Figure 22 – a) Hydrogeological map of Avella Mts (Petrone et al., 2024, modified). Hydrogeological complexes: 1. Pyroclastic-alluvial; 2. Pyroclastic deposits; 3. Sandstone; 4. Argille Varicolori; 5. Marly limestone; 6. Limestone; 7. Groundwater contour (m a.s.l.); 8. Groundwater flow direction; 9. Groundwater flow divide; 10. Freshwater basal spring; 11. Mineralized basal spring; 12. Dried basal spring; 13. Groundwater basin; 14. River; 15. Study area; 16. Provincial boundary; 17. Endoreic area; 18. Swallow hole; 19. Cave; 20. Sinkhole; b) Total thickness (isopach) map of ash-fall deposits in the area surroundings the Somma-Vesuvius volcano (De Vita et al., 2006; De Vita and Nappi, 2013, modified); c) Seasonal rainfall and air temperature regime.

Figure 23 – a) Comparison between demographic growth, withdrawals, and no. of capture structures. b) Waterwork for drinking use. 1. Spring captured by Acquedotto Campano; 2. Spring captured by GORI SpA; 3. Spring captured by Alto Calore Servizi SpA; 4. Spring captured by municipal waterwork; 5. Well used for drinking water supply by GORI; 6. GORI SpA well; Alto Calore Servizi SpA well; 7. municipal waterwork well; 8. ABC Napoli wells field; 9. Acquedotto Campano wells Field; 10. GORI SpA wells field; 11. Alto Calore Servizi SpA wells field; 12. Study area; 13. Provincial boundary.

Figure 24 – Procedure used to implementation of the SWB code. a) Elevation map with the location of the meteorological stations; b) Flow direction map; c) Available water content map; d) Land use map; e) Hydrological soil group map.

Figure 25 – Spatial (a) and temporal distribution of annual GR (b and c), annual GRC (d) and annual GRY (e).

Figure 26 – Spatial (a) and temporal distribution of monthly GR (b and c), monthly GRC (d) and monthly GRY (e).

Figure 27 – Temporal variations of the daily GR (a and b), daily GRC (c) and daily GRY (d). The colors indicate the days of the month; each month is divided into four boxes (a, b, c, and d).

Figure 28 – a) Springs inventory map and registry of authorized wells. 1. Basal spring captured by drinking use; 2. Basal spring captured by agriculture use; 3. Basal spring captured by hydroelectric use; 4. Dried basal spring captured by drinking use; 5. High-altitude spring captured by drinking use; 6. Uncaptured high-altitude spring. 7. Well for drinking use; 8. Wells field for drinking use; 9. Well for domestic use; 10. Well for agriculture use; 11. Well for industrial use; b) Number and percentage of basal and high-altitude springs for different use; c) Spring water discharge in m^3/s and percentage of total springs, including basal and high-altitude springs for different use; d) Number and percentage of wells for different use; e) Well withdrawals in m^3/s and percentage for different use.

Figure 29 – Comparison between groundwater recharge and withdrawal at the aquifer (a and b) and basin scale (c and d).

Figure 30 – Multiple comparison between spring discharges, withdrawals (a, d, g, j, m, p and, s), simplified hydrogeological conceptual models (b, e, h, k, n, q, t, l, o, r and, u) and changes before and after development (c, f, i, l, o, r and, u). 1. Active spring; 2. Dried spring; 3. Dried spring partially reactived; 4. Spring box; 5. Drainage tunnel; 6. Wells; 7. Drainage tunnel with wells; 8. Karstic conduit; 9. Normal fault; 10. Groundwater flow direction; 11. Piezometric level; 12. Buried stream; 13. Dried stream; 14. River.

Figure 31 – a) Hydrogeological map of Avella Mts. (Petrone et al., 2024, modified); b) Seasonal rainfall and air temperature regime.

Figure 32 – a) Map of mean annual observed precipitation; b) map of mean annual RCMs precipitation; c) map of mean annual observed temperature; d) map of mean annual RCMs temperature; mean time series graphs extracted from each pixel of e) OBS_P; f) $E15_{Avella\text{-}P}$; g) OBS_T; h) $E15_{Avella\text{-}T}$. Symbology: 1) OBS_P from 1950 to 2005; 2) OBS_P from 1950 to 1996; 3) OBS_P from 1997 to 2005; 4) OBS_T from 1950 to 2005; 5) OBS_T from1950 to 1996; 6) OBS_T from1997 to 2005; 7) $E15_{Avella\text{-}P}$ from 1950 to 2005; 8) $E15_{Avella\text{-}T}$ from 1950 to 2005; 9) study area; 10) RCMs cell; 11) number of RCMs cell.

Figure 33 – a) Box plot of OBS_P, $E15_{Avella\text{-}P}$ and $E15_{Avella\text{-}P}$ corrected; b) Box plot of OBS_T, $E15_{Avella\text{-}T}$ and $E15_{Avella\text{-}T}$ corrected.

Figure 34 - Time series of the “historical” period (1950–2005) and scenarios (2006–2100) under RCP8.5 and RCP4.5 pathways: a) mean annual precipitation; b) mean annual air temperature; c) mean annual ETR; d) mean annual P-ETR.

Figure 35 – a) Map of RCM historical mean annual groundwater recharge; maps of RCM recharge variation for the RCP4.5 scenario in the: b) short term, c) medium term; d) long term and for the RCP8.5 scenario in the: e) short term, f) medium term; g) long term; h) MAGRI time series for the historical period (1950-2005) and projected scenarios (2006 to 2100) for both RCP4.5 and RCP8.5 pathways.

Figure 36 – Comparison of recharge values estimated using Turc formula, MODIS data and SWB methods with those from RCMs under RCP8.5 and RCP4.5 pathways.

Figure 37 - a) Basin-scale groundwater flow scheme of the Avella Mts karst aquifer, with ubication of basal and perched springs, wells, and meteoclimatic stations (P and T). b) Hydrogeological map of the Baiano district piedmont karst aquifer (De Vita et al., 2018 modified).

Figure 38 - Flow chart of the SWB model implemented to estimate the water budget.

Figure 39-Well stratigraphies and pumping tests with increasing discharge steps. 1) Pyroclastic deposits; 2) Clay deposits; 3) Calcareous debris; 4) Campanian Gray Tuff; 5) Gravel and silty deposits; 6) Limestone; 7) Dolomite; 8) Piezometric level.

Figure 40 - (a) Map of mean-annual recharge (2008÷2022) of the Baiano district piedmont karst aquifer of ; (b) and (c) inter-annual variability of recharge (mm/a and m^3/s).

Figure 41 - Characteristic curve of the tested wells showing critical discharge and critical drawdown (red dot).

Figure 42 - Comparison of Q_s-T values of pumping tests performed in Italian carbonate aquifers (Fabbri, 1997; Valigi et al., 2021) and in wells in the study area.

Figure 43 - (a) Piper diagram of the analyzed samples; b) Shöeller-Berkaloff diagram of the analyzed water samples from the perched springs and Well 1; c) Shöeller-Berkaloff diagram of the analyzed water samples from the basal springs (Celico et al., 1980).

Figure 44 – a) Hydrogeological map of Avella Mts. (Petrone et al., 2024, modified); b) Excerpt from the hydrogeological map; c) Excerpt from the map of the pyroclastic deposits

thickness (De Vita and Nappi, 2013, modified); d) Excerpt from land use map (Corine Land Cover, 2018, simplified).

Figure 45 – Foce hydrogeological observatory: a) ubication of monitoring stations; b) weather station; c) multilevel probes for the soil water content measurements; d) groundwater level sensor; e) multi-level lysimeter station; f) Venturi channel.

Figure 46 – a) 1D Geological model of the monitoring station site; b) SWRCs for B and C horizon.

Figure 47 – Results of hydrogeological monitoringa) Comparison between precipitation measured inside and outside the forest; b) spring hydrogram of S. Maria La Foce spring; c) infiltration measured by multilevel lysimeter; d) superficial runoff; e) soil water content at different depths; 7) average monthly water content for 2022, 2023 and 2024.

Figure 48– a) The hydrogeological variables simulated by HYDRUS-1D; b) simulation during wet and cold months c) simulation during dry and warm months; d) 1D geological model implemented in HYDRUS-1D.

List of tables

Table 1 - Summary table of previous water balances of Avella Mts. P, mean annual precipitation; T, mean annual air temperature; AET, mean annual actual evapotranspiration; GR, mean annual groundwater recharge; GRC, Groundwater Recharge Coefficient; SGR, mean annual Specific Groundwater Recharge (mean annual groundwater recharge for unit area); * No. of stations used to reconstruct distributed models of P and T at the regional scale; (C) Coutagne; (T) Turc; (TM) Thornthwaite-Mather; (M) MODIS; (**) average value.

Table 2 – Hydrogeological domains, characteristics, and hydraulic properties of hydrogeological complexes of Avella Mts.. (P) Porosity; (F) Fracturing; (K) Karst; (FW) Freshwater; (MW) Mineralized water.

Table 3 – Updated water balances of Avella Mts.. P, mean annual precipitation; T, mean annual air temperature; AET, mean annual actual evapotranspiration; GRC, groundwater recharge coefficient; GR, groundwater recharge; SGR, mean annual Specific Groundwater Recharge; (*) average value.

Table 4 - Summary of water point types, total count, depth range (min–max) for wells, use, and data sources.

Table 5 – Mean annual precipitation and temperature over the period 1954-1984, observed values (OBS_P and OBS_T), Bias $E15_{Avella}$ (Bias $E15_{Avella\ -P}$ and Bias $E15_{Avella\ -T}$), $E15_{Avella}$ corrected ($E15_{Avella-P}$ corr and $E15_{Avella-T}$ corr).

Table 6 - Mean annual groundwater recharge and variation (%) against the historical period estimated for three consecutive decades: 2011–2040 (short term), 2041–2070 (medium term), and 2071–2100 (long term).

Table 7 - Chemical-physical and microbiological parameters (minimum and maximum values) of the water from the perched springs and Well 1, for the period 2018-2023, and hydrochemical data (Celico et al., 1980) of the basal springs (Calabricito, Mefito, Santa Maria la Foce, Mercato-Palazzo, Cerola, Santa Marina di Lavorate).

Table 8 - Hydraulic parameters of the aquifer-well system estimated through pumping tests.

Table 9 - Physical-volumetric and index parameters and AGI classification of soil samples from laboratory tests.

Table 10 - Parameters of hydraulic characterization.

List of acronyms and abbreviations

ABC	Acqua Bene Comune
APC	Ancient Pyroclastic Complex
ATO	Ambito Territoriale Ottimale
AWC	Available Water Capacity
CARG	Cartografia Geologica
CIP	Coefficiente di Infiltrazione Potenziale
Csb	Warm temperate climate with dry and warm summer
DEM	Digital Elevation Model
FC	Field Capacity
FW	Freshwater
GB	Groundwater Basin
GCMs	General Circulation Models
GIS	Geographic Information System
GORI	Gestione Ottimale Risorse Idriche
GR	Groundwater Recharge
GRC	Groundwater Recharge Coefficient
GRY	Groundwater Recharge Yield
HSG	Hydrological Soil Group
IPCC	Intergovernmental Panel on Climate Change
ISPRA	Istituto Superiore per la Protezione e la Ricerca Ambientale
K	Karst
LTBAs	Local Transboundary Aquifers

LTBAs	Local Transboundary Aquifers
MAGRI	Mean Annual Groundwater Recharge Index
MODIS	Moderate Resolution Imaging Spectroradiometer
MW	Mineralized water
NAO	North Atlantic Oscillation
OBS	Observation
PWP	Permanent Wilting Point
RCMs	Regional Climate Models
RCP	Representative Concentration Pathways
RPC	Recent Pyroclastic Complex
RTBAs	Regional Transboundary Aquifers
SAT	Saturation
SCI	Site of Community Importance
SGR	Specific Groundwater Recharge
SIMN	Servizio Idrografico e Mareografico Nazionale
SWAT	Soil and Water Assessment Tool
SWB	Soil Water Balance
SWD	Soil Water Depth
SWRCs	Soil Water Retention Curves
TBAs	Transboundary Aquifers
USCS	Unified Soil Classification System
USDA	United States Department of Agriculture
USGS	United States Geological Survey

List of symbols

AET	Actual Evapotranspiration
CI	Consistency Index
CIP	Coefficient of Potential Infiltration
CO_2	Carbon dioxide
Dr	Relative density
e	Void index
Ep_i	Potential Evapotranspiration
ETR	Evapotranspiration
F	Inflow
h	Soil matric pressure head
I	Annual heat index
Ie	Effective Infiltration
In	Interception
k	Correction coefficient in Thornthwaite-Mather formula
K (h)	Unsaturated hydraulic conductivity function
K_{sat}	Saturated hydraulic conductivity
LI	Liquid Index
m	Empirical parameter of van Genuchten equation
n	Pore size distribution parameter
n	Porosity
O	Outflow – Surface runoff
OMC	Organic Matter Content

P	Precipitation
PI	Plasticity Index
P_{in}	Precipitation measured inside the forest
P_{out}	Precipitation measured outside the forest
Q_c	Critical discharge
Q_s	Specific capacity
R	Runoff
S	Sink term
SI	Shrinkage Index
Sn	Snow
T	Temperature
T	Trasmissivity
t	Time
w_L	Liquid limit
w_P	Plastic limit
w_S	Shrinkage limit
z	Vertical coordinate
α	Inverse of the air entry head in van Genuchten equation
α	Empirical exponent in Thornthwaite-Mather formula
Δh_c	Critical drawdown
$\Delta\theta$	Variation in soil moisture
θ	Volumetric water content
θ_{FC}	Water content corresponding to the Field Capacity
θ_{PWP}	Water content corresponding to Permanent Wilting Point

θ_r	Residual volumetric water content
θ_s	Saturated volumetric water content
Υ_{dry}	Dry unit weight
Υ_{nat}	Natural unit weight
Υ_s	Specific gravity
Υ_{sat}	Saturated unit weight

INDEX

1. Introduction 19
1.1 State of the art on karst aquifers in southern Italy 19
1.2 Ph.D. work steps 22

2. Study areas 24
2.1 Avella Mts. karst aquifer 24
2.2 Baiano District piedmont karst aquifer 32
2.3 Foce hydrogeological karst observatory 35

3. Data and methodologies 42
3.1 Cartographic and hydrogeological database 42
3.2 Water balance by empirical approach and numerical code 42
3.3 Spring inventory map and wells registry 42
3.4 Regional Climate Models (RCMs) 43
3.5 Pumping tests and groundwater quality 43
3.6 Characterization of Foce hydrogeological karst observatory 43
3.7 Hydrological monitoring system 43
3.8 Numerical modelling of water balance 44

4. Results 45
4.1 Hydrogeological conceptual model and groundwater recharge of Avella Mts. karst aquifer (southern Italy): A literature review and update 45
4.2 A multiscale soil water balance for sustainable groundwater management of a local transboundary karst aquifer 83
4.3 Impacts of climate change on groundwater recharge of Avella Mts. karst aquifer by Regional Climate Models 112
4.4 Prospective for using of piedmont karst aquifers: the case study of the Baiano District (southern Apennines, Italy) 133
4.5 Groundwater recharge estimation using HYDRUS-1D model in Foce hydrogeological karst observatory 153

5. Conclusions 178

Acknowledgments 179

References 180

1. Introduction

1.1 State of the art on karst aquifers in southern Italy

Karst aquifers are among the most valuable hydrogeological systems worldwide as they host significant groundwater resources supplied for human activities. The karst landscapes, which develop in various geological and climatic contexts, are formed through the dissolution of carbonate rocks and are characterised by typical karst features such as endorheic plateaus, poljes, sinkholes, caves, and swallow holes, which strongly influence groundwater circulation. Karst aquifers cover approximately 20% of the Earth's surface providing groundwater to about 25% of the global population (Ford and Williams, 2007). Furthermore, these aquifers support many natural landscapes and ecosystems of great biodiversity and geodiversity, which are dependent on the availability and quality of groundwater resources (Goldscheider, 2012; Kresic and Stevanović, 2010).

In Europe and the Mediterranean region, many large urban areas are fed, entirely or partially, by water from karst aquifers (Ford and Williams, 2007).

In Italy, about 18% of the surface is composed of carbonate rocks. In some southern Italian regions, such as Abruzzo, Lazio, Molise, Campania and Basilicata, the percentage of carbonate reliefs is much higher, reaching about 45%. These carbonate massifs host huge karst aquifers that feed basal springs with discharge of up to 6.0 m^3/s and are characterised by a mean groundwater yield of $4{,}100 \times 10^{-6}$ m^3 $year^{-1}$ and a mean specific groundwater yield varying between 0.025 and 0.045 m^3 s^{-1} km^{-2} (Celico, 1983; Allocca et al., 2007; De Vita et al., 2018). The high yield is linked to specific geomorphological, hydrogeological, land use and soil characteristics of the carbonate mountains. The high permeability of the rocks, high rainfall rates, large endorheic areas and Vesuvian and Phlegraean ash-fall pyroclastic soils allowed the development of dense woody vegetation that slows down rainfall and supports high infiltration and recharge rates. Moreover, due to the excellent hydrochemical quality of their groundwater, the karst aquifers of southern Italy are used for drinking, agriculture, industry, energy, thermal and mineral purposes (Celico, 1983; Allocca et al., 2007) and play a vital role in the ecological flow of rivers, mountain lakes and wetlands, both coastal and inland (Allocca et al., 2014).

However, these aquifers are subject to strong climatic variability related to the North Atlantic Oscillation (De Vita et al., 2012), resulting in significant inter-annual variability in groundwater recharge and availability, spring discharges and piezometric levels. As various studies outlined, the effects of climate change will significantly impact the hydrological cycle, increasing air temperature and the intensity and frequency of extreme hydroclimatic events in many regions of the world (Compagnucci et al., 2001; IPCC, 2014). The Mediterranean region, of which Italy is the central part, is recognised as a major hotspot of climate change, where drought is becoming a more frequent challenge (Vicente-Serrano et al., 2014) due to future projections of increasing air temperature and decreasing annual precipitation (Giorgi, 2006).

Given the significant climatic variability and its impact on groundwater recharge and availability, understanding the recharge processes and accurate quantitative estimates of groundwater volumes in karst systems in southern Italy, based on multi-method, multi-temporal and multi-scale approaches, are essential for ensuring the sustainable use and management of these resources in both the short and long term. The importance of these requirements is amplified by the intensive exploitation of groundwater from karst aquifers by regional and inter-regional aqueduct systems in southern Italy (Allocca et al., 2007).

However, recharge is difficult to estimate, both because it exhibits spatial and temporal variability and because its direct quantitative assessment is complex. This difficulty is particularly evident in the southern Apennines, where direct assessment of the hydrological variables required to estimate the recharge of the karst aquifers is very challenging. This is mainly due to the lack of high-altitude rain gauges and hydrometric stations, which limits the direct measurement of key water balance parameters such as precipitation, temperature, evapotranspiration and surface water runoff (Allocca et al., 2014). To overcome these limitations, the integration of ground-based hydrological and remote sensing data is a useful approach to reduce uncertainties and improve high-altitude recharge estimates without field measurements and time series. Ruggieri et al. (2021) used remote sensing data collected by the Moderate Resolution Imaging Spectrometer (MODIS) satellite to estimate actual evapotranspiration and groundwater recharge at regional and mean annual scale for 40 carbonate aquifers located in a large area of the southern Apennines. This approach highlights the potential of MODIS data to address the challenges posed by the scarcity of

high-altitude measurements, improving the accuracy of recharge estimations in complex mountainous environments.

Although field hydrogeological research and groundwater studies of karst aquifers in southern Italy have a long tradition starting from the 1960s, there is a lack of examples of equipped karst basins as natural hydrogeological observatories for continuous multiparametric field measurements in space and time of all hydrological variables of the water balance.

In the last half-century, the hydrogeological knowledge of the karst aquifers of southern Italy has advanced considerably thanks to the experimental studies carried out in the framework of Special Project 29 of the Cassa per il Mezzogiorno (Celico, 1983) and to numerous field studies conducted by universities, research institutes and private and public entities. These advances include:

- development of hydrogeological conceptual models at regional and basin scale (Allocca et al., 2007; De Vita et al., 2018);
- analysis of the impact of climate change on recharge processes and spring discharges (De Vita et al., 2012; Lepore et al., 2024);
- estimation of recharge coefficients at different spatial (regional and local) and temporal (mean annual, monthly and single rainfall event) scales (Allocca et al., 2014; 2015);
- study of the influence of faults on groundwater circulation and the hydraulic behaviour of epikarst (Petrella et al., 2007; Petrella et al., 2008; Celico et al., 2010);
- long-term spring discharge analyses (Fiorillo, 2009; Fiorillo and Guadagno, 2012; Fiorillo, 2013);
- studies on microbial contamination in karst waters (Celico et al., 2004; Naclerio et al., 2008);
- use of MODIS satellite data for groundwater recharge estimation (Ruggieri et al., 2021);
- assessment of aquifer vulnerability to pollution (Cusano et al., 2019, 2023; Tufano et al., 2020);
- evaluation of the effect of the ash-fall pyroclastic soil on groundwater recharge in peri-volcanic karst aquifer (Cusano et al., 2024a, 2024b).

1.2 Ph.D. work steps

This Ph.D. thesis aimed to analyse the effects of climate change on groundwater recharge and availability in a representative karst aquifer of the southern Apennines. The study focused on Avella Mts. karst aquifer, which was selected as the sample area due to its strategic hydrogeological importance at the regional scale. The research aimed to estimate the multi-temporal recharge using a multi-method approach, integrating physically based, empirical and numerical models, experimental monitoring, field hydrological data, laboratory studies and remote sensing observations. This multi-scale approach allows a comprehensive assessment of groundwater recharge, capturing both long-term and short-term variations from aquifer to basin to site-specific scales, at annual, monthly, daily and hourly timescales.

The research was conducted in three main phases whose contents are described below:

1) Hydrogeological database implementation.
   - Study of the scientific literature on the selected aquifer.
   - Collection of cartographic and numerical data of time series of hydrogeological quantities (rainfall, air temperature, spring flow, groundwater levels) measured on the ground and remotely (e.g. MODIS real evapotranspiration satellite data).
   - Collection of the pumping tests and groundwater quality data;
   - Acquisition of precipitation and air temperature projection data from Regional Climate Models (RCMs);
2) Field and laboratory activities.
   - Design and implementation of an experimental hydrological observatory consisting of a monitoring system for the real-time estimation and modelling of the hydrological balance and groundwater recharge processes.
   - Field and laboratory tests for stratigraphic and hydraulic characterisation and determination of physical-volumetric and index properties of sample pyroclastic soils.
3) Data processing and modelling.
   - Update of the hydrogeological conceptual model at the aquifer scale.
   - Estimation of water balance by empirical approach and numerical code across multi-spatial and multi-temporal scales.

- Analysis of temporal and spatial variation of the historical time series of hydrogeological parameters and data collected from monitoring activities.
- Modelling, calibration and validation of recharge scenarios based on RCMs projections.
- Hydrogeological and hydrogeochemical characterisation at sectorial scale of the piedmont karst aquifer.
- Implementation of a numerical model calibrated based on hydrological and monitoring data, for the simulation of evapotranspiration and infiltration processes in the ash-fall pyroclastic soil cover using HYDRUS-1D.

This thesis is a paper-based thesis. It is divided into five chapters and includes the compilation of five scientific manuscripts, two of which were published, one submitted and two are in preparation.

Chapter 1 is the general introduction, which describes the hydrogeological framework in which this research takes place and presents its objectives and phases. Chapter 2 briefly describes the main characteristics of the study area at different scales of analysis: the Avella Mts. karst aquifer, the Baiano piedmont karst aquifer and Foce karst hydrogeological observatory. Chapter 3 provides a summary of the data and methods used. Chapter 4 presents the results of this research, divided into five scientific manuscripts. Chapters 5 correspond to the conclusions.

The Ph.D. project is part of the "Programma Operativo Nazionale (PON) - Ricerca e Innovazione 2014-2020", which aims to promote innovation, sustainable development and scientific progress in the environmental and socio-economic fields. The research was also developed in collaboration with the industrial partner GORI SpA (Gestione Ottimale Risorse Idriche), the managing company of the integrated water service for ATO3 (Ambito Territoriale Ottimale) of the Sarnese-Vesuviano district in Campania region. This collaboration allowed the establishment of the experimental hydrological observatory. Finally, a visiting period from April 2nd to July 28th 2024, at the Czech University of Life Sciences in Prague supported the numerical modelling phase.

2. Study areas

In this chapter, the three study areas are briefly described.

2.1 Avella Mts. karst aquifer

Geological and geomorphological setting

The focus area of the Ph.D. study is the Avella Mts. karst aquifer which is part of a large carbonate system of the southern Apennines (southern Italy) including 40 karst aquifers and extending 8,560 km^2 (Fig. 1a). The mountain system hosts a well-defined karst aquifer (Celico,1983), recognized as one of the most important environmental resources in Campania region (southern Italy – Allocca et al., 2014). Its average annual specific groundwater yield reaches a value of up to 0.037 $m^3/s/km^2$, one of the highest for the karst aquifers of the Mediterranean area.

The Avella Mts. extending approximately 370 km^2 are delimited to the west by the Campanian plain and to the north and south by the alluvial plains of Isclero and Solofrana rivers, respectively (Fig. 1b). The carbonate system consists of three mountain ridges, separated from each other by wide valleys with marine, alluvial, and pyroclastic sediments of Late Pleistocene to Holocene age (Del Prete, 2005). The northern ridge, known as the Avella-Partenio group, reaches the highest altitudes, with Monte Vergine (1,439 m) and Ciesco Bianco (1,579 m). This ridge is separated from Pizzone one by Baiano valley, while Lauro valley is situated between Pizzone and Sarno ridges.

From a geological point of view, the Avella Mts. are mainly composed of fractured and karstified Mesozoic-Cenozoic carbonate rocks of the Apennine platform domain belonging to the “Monti Picentini and Lattari” and “Monti di Avella” tectonic units (D’Argenio et al., 1973; Bonardi et al., 1988b; ISPRA, 2017), about 2,800 meters thick. This carbonate series from the base upwards consists of Norian-Hettangian dolomites, Jurassic-Lower Cretaceous dolomitic limestones and Cretaceous limestones, characterized by a complex network of NW-SE and SW-NE oriented faults and fractures (Vitale and Ciarcia, 2018). The average

slope of the Avella Mts. is 30-35° and is the result of the morphological evolution of the original fault scarps (Brancaccio et al., 1978). Wide summit plateaus with slopes less than 5% are typical in the study area, as well as epigean karst landforms such as endorheic areas, swallow holes and sinkholes (Bull, 2007; Allocca et al., 2014) and hypogean ones, including karst conduits. Both significantly influence recharge processes and contribute to ground instabilities (Valente et al., 2021; Santo et al., 2019).

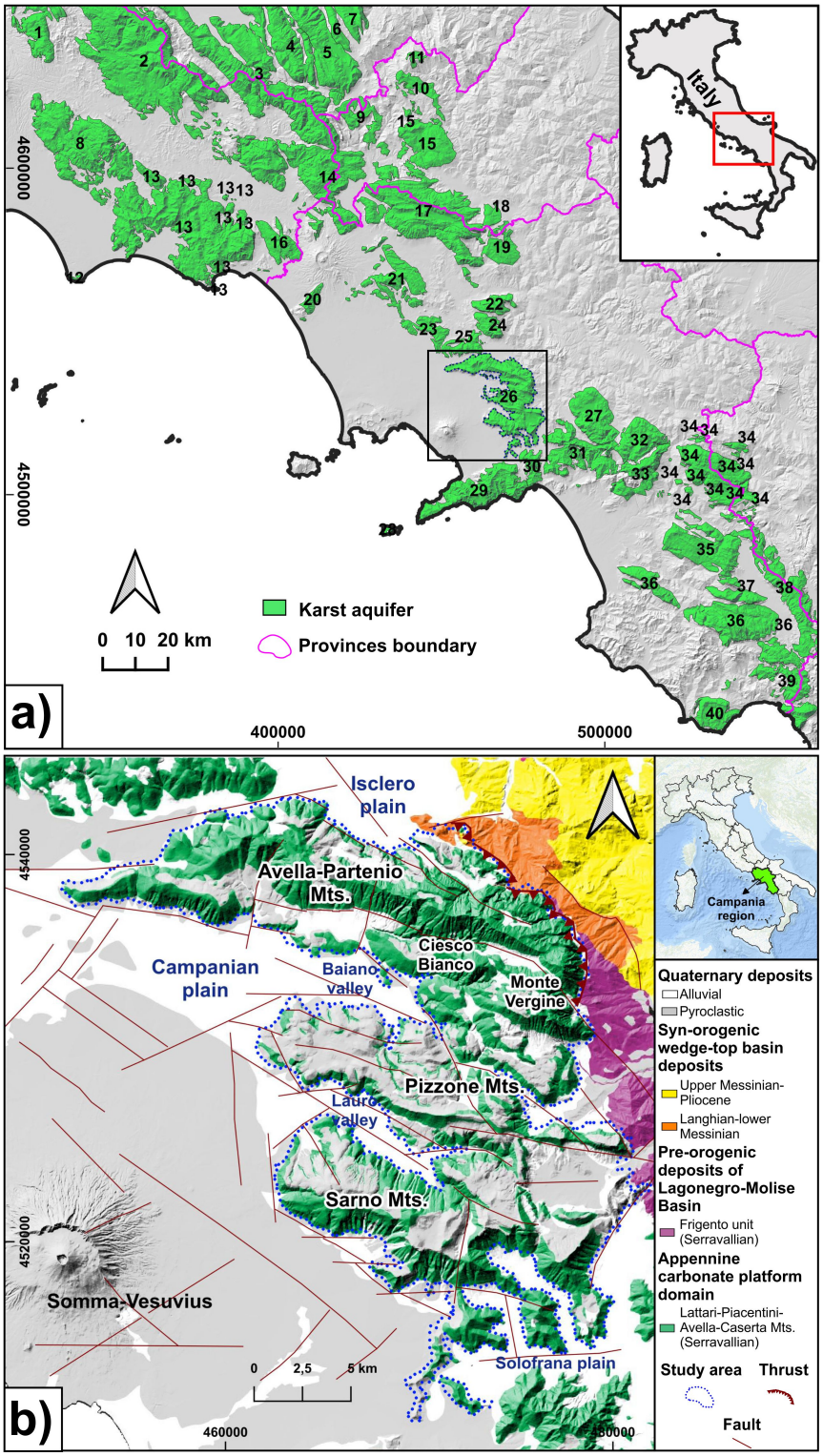


Figure 1 – a) Karst aquifers of southern Apennines; b) Excerpt from geological map (Vitale and Ciarcia, 2018, modified).

Hydrogeology and hydrochemistry

The hydrostratigraphic boundaries of karst aquifer result from a combination of sedimentary processes, tectonic deformation and hydraulic properties of the surrounding deposits. The carbonate hydrostructure is bounded:

- to the northeast by low permeable terrigenous deposits, including pre- and syn-orogenic sandstones and clays, which act as an aquiclude and are juxtaposed laterally by thrust;
- from the northwest to the south by low to moderate permeable alluvial deposits and Vesuvian and Phlegraean ash-fall and ash-flow pyroclastic deposits, which act as an aquitard and are in tectonic contact by normal fault;
- to the southeast by low to moderate permeable alluvial, detrital, and pyroclastic deposits of Solofrana Valley (Civita et al., 1970; Celico and de Riso, 1978), which act as an aquitard.

In this hydrogeological framework, a complex direct and inverse faults system is responsible for the horizontal compartmentalization of basal groundwater circulation in a typical basin-in-series system (Civita et al., 1970; Celico and de Riso, 1978). As part of the groundwater circulation scheme of the aquifer (Civita et al., 1970; Celico and de Riso,1978; Celico, 1978; 1983) the basal groundwater flow feeds three main spring groups at the base of the slope (Fig. 2), where the aquifer is in contact with the impermeable belt (Nicotera and Civita, 1969a; 1969b):

1. Cancello spring group, in the north-western sector, was characterized by Calabricito and Mefito springs (30 and 28 m a.s.l.);
2. Sarno spring group, in the southern sector, was represented originally by S. Maria La Foce (32 m a.s.l.), Mercato and Palazzo (26 and 24 m a.s.l.), Cerola (28 m a.s.l.), S. Marina di Lavorate (28 m a.s.l.) and S. Mauro springs (27 m a.s.l.);
3. Laura and Labso springs (185 and 199 m a.s.l.), in the south-eastern sector.

Before the construction of the water capture works (Celico, 1983; Allocca et al., 2007), between the 1920s and 1950s, the discharge rates of the main springs were collected by systematic measurements carried out by the National Hydrological Service of Naples and the Cassa per il Mezzogiorno. These studies reported average flows of 1.20 m^3/s for the Cancello spring group, 8.4 m^3/s for the Sarno spring group, and 0.15–0.25 m^3/s for the Laura and Labso springs, further fed by a complex system of karstic channels directly connected to the sinkhole of the Forino basin (Celico, 1983; Santo et al., 1998).

In the carbonate succession, hydrostratigraphic contacts cause local and vertical compartmentalization of shallow groundwater circulation in perched aquifers. These latter supply high-altitude springs characterised by non-permanent hydrological regimes depending on seasonality.

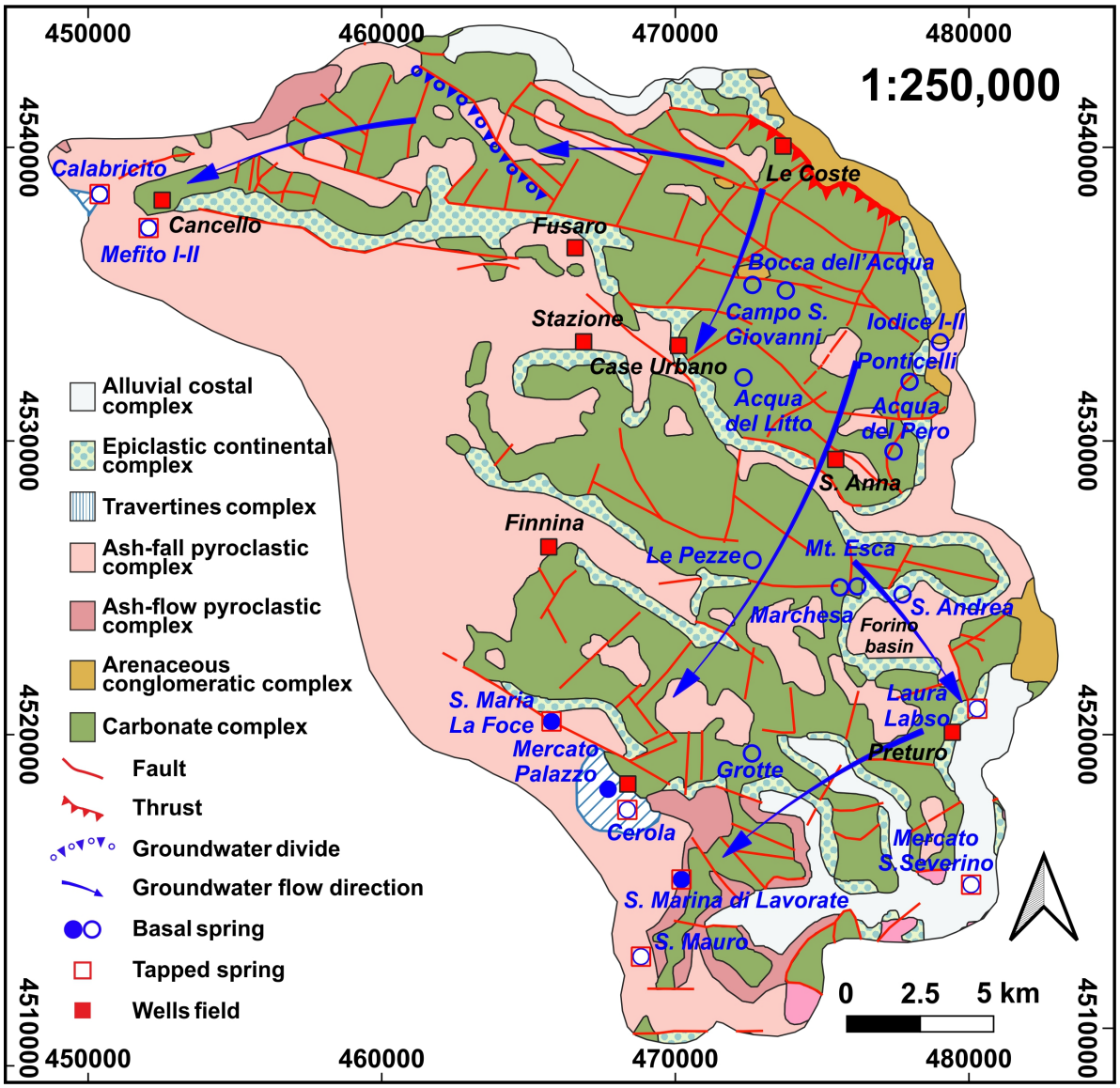


Figure 2 - Groundwater circulation scheme of the Avella karst aquifer (De Vita et al., 2018, modified).

Beyond the basal and high-altitude springs, an additional natural outflow of the hydrogeological system is represented by the deep diffuse groundwater flow towards the pyroclastic-alluvial deposits of the Campanian plain and the Baiano valley, relatively more permeable.

According to Celico et al. (1980), the groundwater of Avella karst aquifer has calcium-bicarbonate facies (Fig. 3).

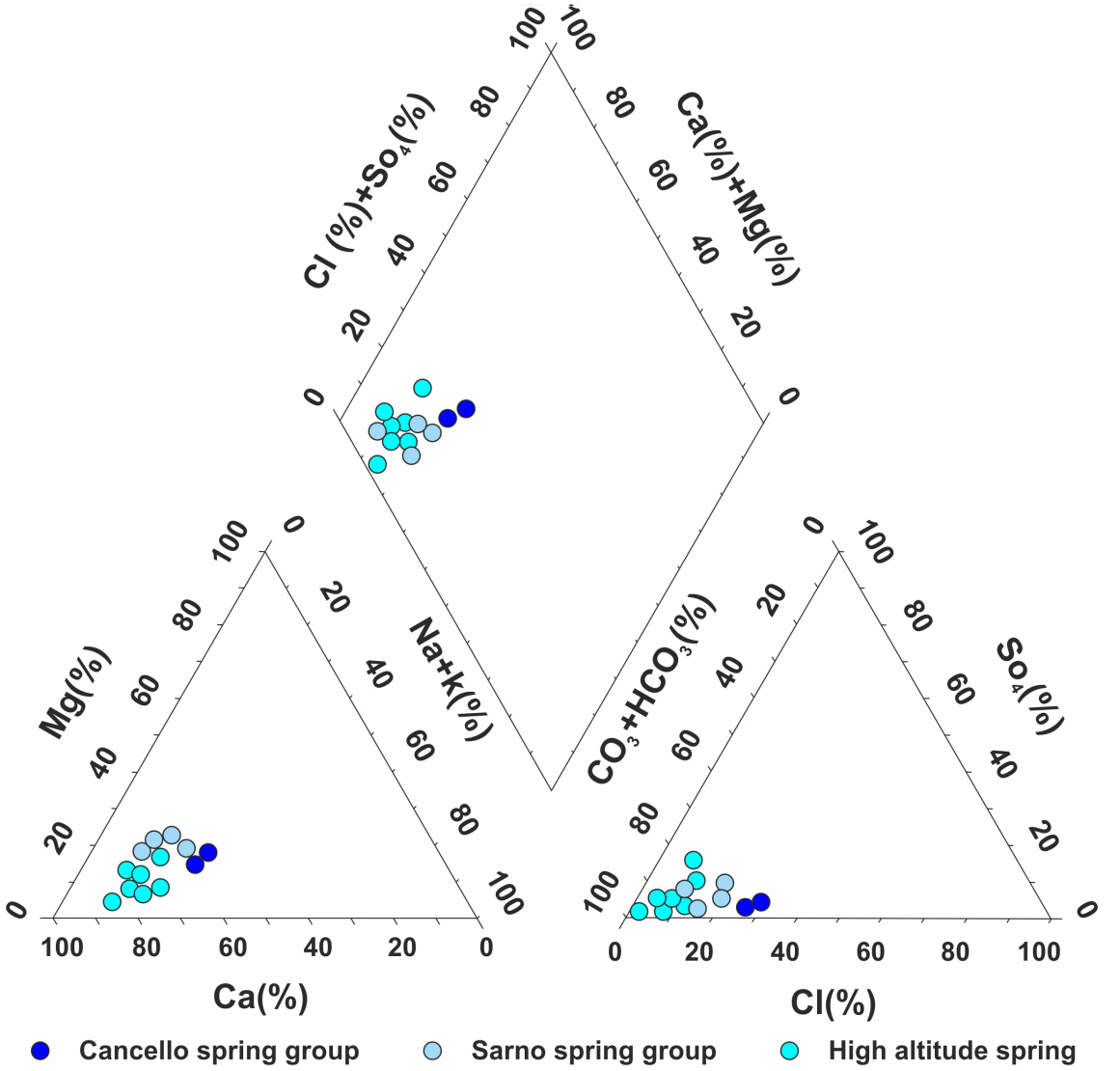


Figure 3 – Hydrogeochemical characterisation of the groundwater.

However, hydrochemical analyses show differences in the degree of mineralisation observed in the Cerola and Calabricito springs characterised by higher CO_2 contents (between 250 and 350 mg/l). These differences depend on the specific hydro-structural configuration of the aquifer discharge area, where the deepening of the groundwater flow paths occurs.

These authors also determined the isotopic age of the groundwater through an isotopic characterisation study. Mineralised water is between 20 and 25 years old because it is more deeply stored where it remains longer. As a result, it warms up and becomes enriched in

minerals due to prolonged contact with rocks and acquires a higher concentration of dissolved gases. In contrast, fresh water for drinking water use has a much lower isotopic age and degree of mineralisation. Its residence time within the rock is shorter, with an estimated average age of 2.5-3 years.

Moreover, phenomena of interaction between the carbonate hydrostructure and the pyroclastic-alluvial aquifer of Solofrana valley are hypothesized (Celico, 1983), confirmed by the occurrence of sodium and potassium in the water of S. Marina di Lavorate and S. Mauro springs.

Soil covers mantling features

The carbonate bedrock of the study area is covered by singular alkali-potassic ash-fall pyroclastic deposits (De Vita et al., 2006b; Santo et al., 2008) derived from past explosive eruptions of the Somma-Vesuvius volcano. Its thickness ranges based on the dispersion axes, distance from volcanic structure and topography (Fig. 4a) and reaches approximately a maximum of 8 metres on steep slopes (up to 40°), next to the volcano, and up to 50 meters in endorheic areas (Fusco et al., 2017).

These deposits are characterised by sandy-loam grain size (Allocca et al., 2014) and strongly affect recharge processes (Allocca et al., 2015; Fusco et al., 2017), epikarst development (Petrella et al., 2007; Celico et al., 2010), groundwater chemistry and the transport of some microbial contaminants (Celico et al., 2006; Allocca et al., 2008; Naclerio et al., 2008).

Soils formed by pedogenic processes involving pyroclastic deposits contributed to the development of different vegetation cover and land uses that affect seepage dynamics (Celico et al., 2010; De Vita and Nappi, 2013; Manna et al., 2013b). In this context, the cover soils act as a natural water storage system, retaining water moisture during the rainy autumn and winter months, which is released gradually during the hot season to support evapotranspiration processes. For the land use type, 10 classes were recognised (Fig. 4b). Along the steep slopes dense deciduous forests (typically beech groves) dominate, up to the highest altitudes. In the endorheic karst areas and piedmont regions, agricultural lands (such as chestnut and hazelnut groves up to about 1000 meters) and natural grasslands with limited urban areas are prevalent.

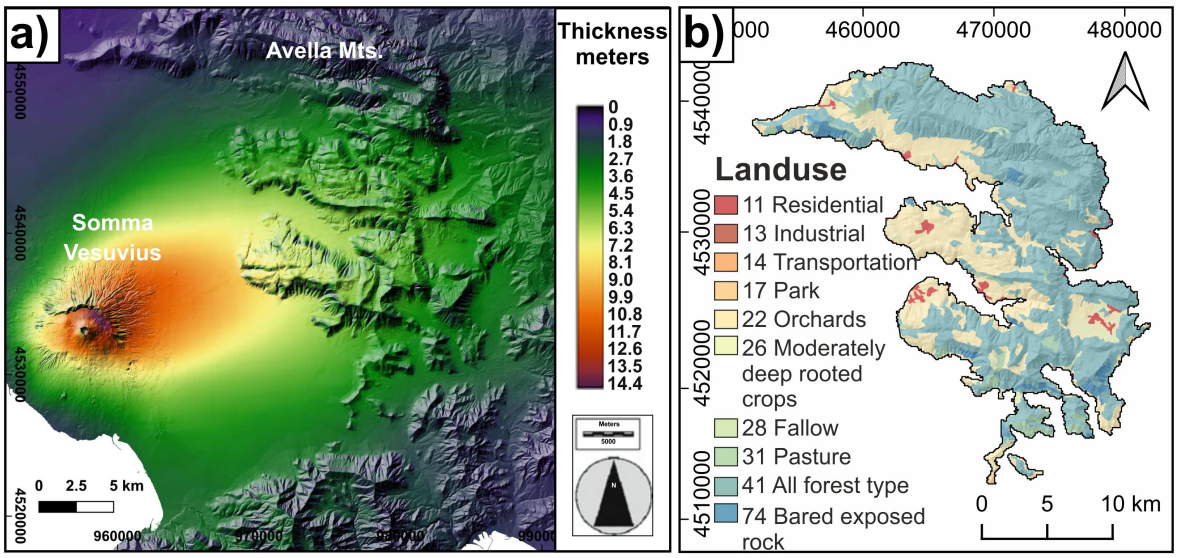


Figure 4 – a) Regional distribution model of ash-fall pyroclastic deposits in the area surrounding the Somma-Vesuvius volcano (De Vita and Nappi, 2013, modified); b) land use map (Corine Land Cover, 2018).

Climatic characteristics

The groundwater recharge processes of Avella karst aquifer are strongly affected by the local climate and its temporal variations. The climate of the study area is Mediterranean-mild type (CSb) (Beck et al., 2018) and falls into the temperate zone according to Köppen's climate classification (Köppen, 1936; Geiger, 1954). The summers are dry and very hot and the rainfall regime varies from the Mediterranean to the sublittoral Apennines type (Bandini, 1931), with maximum values occurring mainly in autumn and winter. The mean monthly air temperature is highest in August reaching 25 °C and lowest in January decreasing to 7 °C. Meanwhile, average monthly rainfall ranges from 190 mm in November to 30 mm in August (Fig. 5). As reported by Allocca et al. (2014) and Ruggieri et al. (2021), the mean annual cumulative rainfall is 1320 mm, while the mean annual air temperature is 14.4 °C. Time series of precipitation and air temperature were collected from 23 rain gauges and 11 air temperature stations belonging to the regional hydro-meteorological monitoring network of the Civil Protection of Campania Region. The elevation of these stations ranges from 14 to 840 m a.s.l. The medium- to long period climate variability for this sector of the Mediterranean basin is strongly affected by the North Atlantic Oscillation (NAO – De Vita et al., 2012; Manna et al., 2013a), which directly impacts the aquifer recharge processes. Positive NAO phases are characterized by dry winters with low rainfall, causing a reduction

of piezometric levels and spring discharges. On the other hand, negative NAO phases are characterized by wet winters with above-average rainfall which helps to restore water levels and ensure a steady flow of springs.

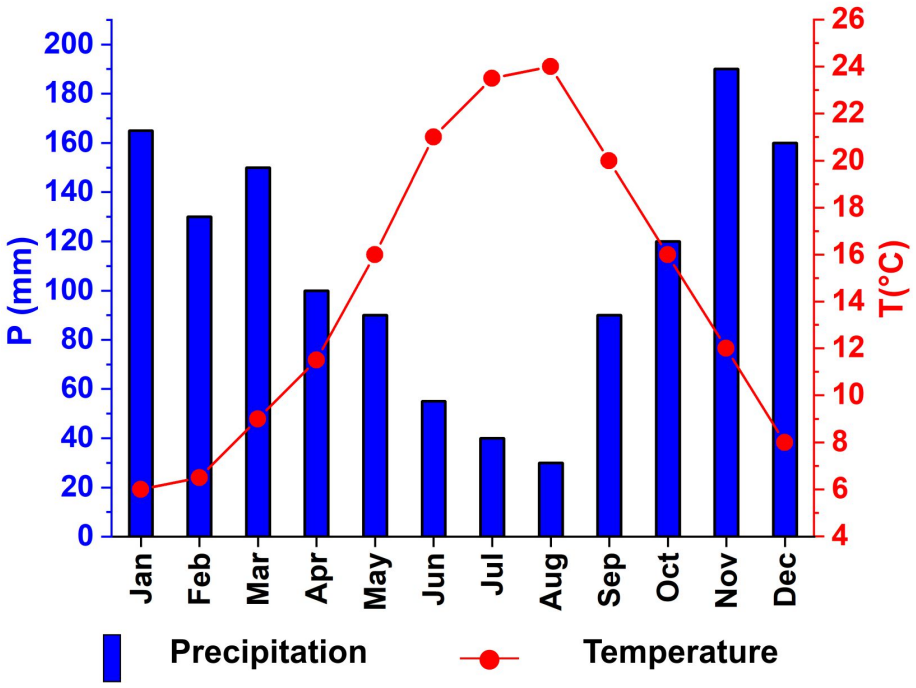


Figure 5 – Monthly rainfall and air temperature regime.

Groundwater management

The regional ecological importance of the Avella karst aquifer is confirmed by the wide geo - and biodiversity, reflected in different natural ecosystems, including forests, grasslands, springs, rivers and karst landforms (Fig. 6a). Further evidence of these environmental assets is the presence of two Regional Parks (Partenio and Sarno) and three Site of Community Importance (SCI – Partenio Mts., Pietra Maula and Lauro Mts.). In addition, the hydro-ecological regime of the Sarno, Regi Lagni, Isclero and Sabato rivers is regulated by its surface and groundwater resources.

The aquifer is a vital source for the Campania region, but its management is particularly complex as it is a representative example of a Local Transboundary Aquifer (LTBA). This means that the aquifer is shared by all five provinces of Campania region (Avellino, Salerno, Naples, Caserta, and Benevento) in which the recharge and outflows area are not uniformly distributed (Fig. 6b). About 63% of the recharge area falls in the Avellino province, while 14%, 13.8%, 5.7% and 3.5% are in the provinces of Salerno, Naples, Caserta, and

Benevento, respectively. In contrast, about 85% of the main natural outflow discharges through basal springs in the Salerno province, while only 12% and 3% in the Caserta and Naples provinces, respectively. Due to the geographical and hydrological configuration of the aquifer careful and coordinated management strategies are required, as over-exploitation or poorly coordinated policies in one province can negatively affect the others. Today, the groundwater is exploited by four major regional and provincial waterworks (GORI SpA, Acquedotto Campano, ABC Napoli, Alto Calore Servizi SpA) as well as by several municipal aqueducts. These entities provide drinking water to a vast area of the Campania region, feeding a population of around four million people. In addition, private wells have been increasingly drilled since the 1990s and 2000s for agricultural, industrial, and domestic use, further challenging groundwater management.

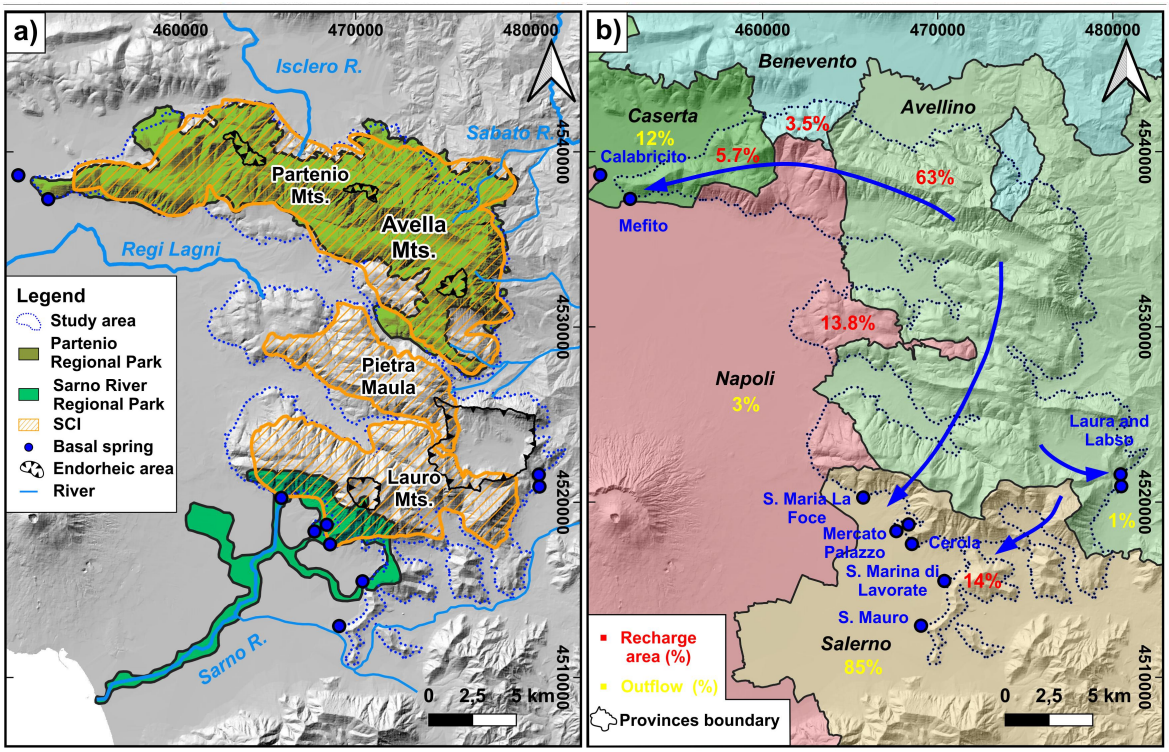


Figure 6 - a) Groundwater-dependent ecosystems of Avella Mts.; b) Recharge and outflow areas for the provinces of Campania region.

2.2 Baiano District piedmont karst aquifer

At sectoral scale, the Ph.D. study focuses on the Baiano District, situated in the north-western sector of the Avella Mts (Fig. 7a). The District covers an area of approximately 100 km^2 and falls within the administrative boundaries of the municipalities of Avella, Baiano,

Mugnano del Cardinale, Quadrelle, Sirignano and Sperone, commonly referred to as the "Mandamento of Baiano". Its current geo-morphological setting is strongly affected by the volcanic, sedimentary and tectonic phenomena occurred during the Quaternary in the sector between Nola plain and Avella carbonate slopes (Fig. 7b). The latter are mainly composed of Meso-Cenozoic carbonate rocks (Pescatore and Ortolani, 1973; Pescatore and Sgrosso, 1973) and due to high degree of fracturing and karstification are highly permeable allowing a significant groundwater circulation. Carbonate slopes are covered by pyroclastic and eluvial-colluvial deposits, with thicknesses of up to 6-8 metres (De Vita et al., 2006b; Fusco et al., 2017). Locally, there are NE-SW, SW-NE and N-S orientation faults that dislocate the carbonate substrate below the Nola plain deposits. This plain is located in the northeastern sector of the Campania Plain, about 16 km northward of the Somma-Vesuvius volcano, to the north of Cancello hill and to the east of Avella Mts. (Petrone et al., 2023). The latter consists of Quaternary deposits, including marine-transitional facies linked to positive glacio-eustatic fluctuations during the Middle-Upper Pleistocene, as well as ash-fall/ash-flow pyroclastic deposits (Putignano et al. 2007; Santangelo et al. 2010), erupted by the intense volcanic activity dating back to 116 k-yrs (Campania Grey Tuff; De Vivo et al. 2001) and 15 k-yrs (Neapolitan Yellow Tuff; Deino et al. 2004).

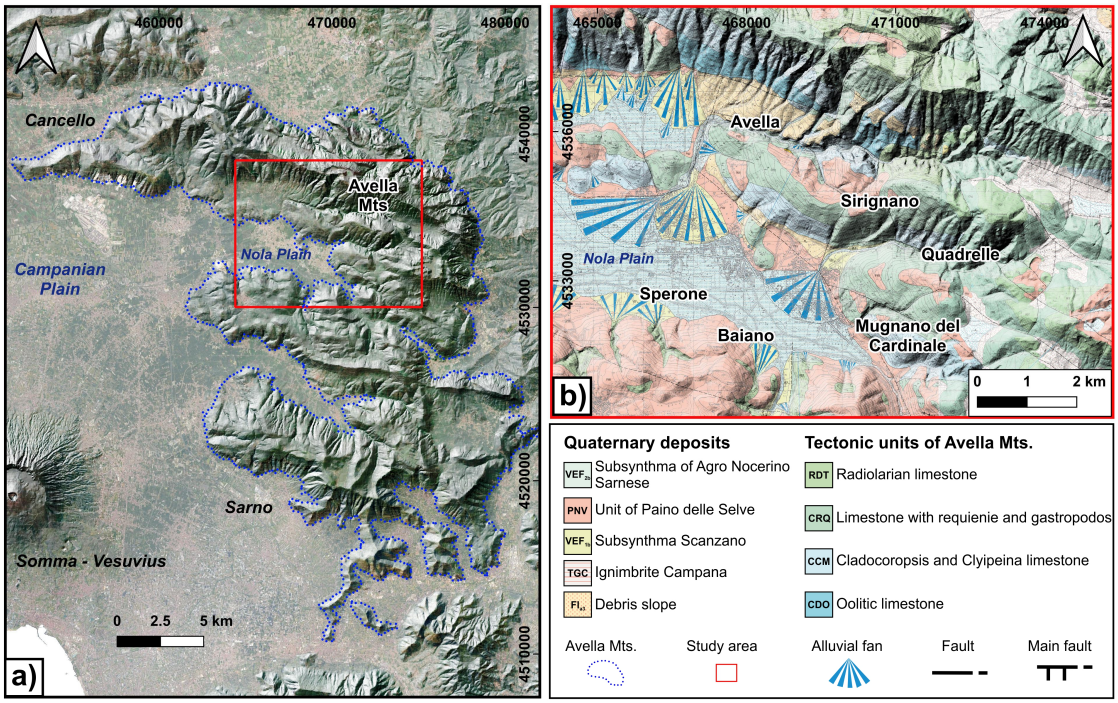


Figure 7 - a) Study area location.; b) Excerpt from the geological map of Italy at 1:50.000 scale (from ISPRA, modified), Ercolano (N. 448) and Avellino (N. 449) sheets.

Baiano District is situated precisely in the transitional sector between the carbonate slopes and the Quaternary deposits of the Nola plain. This morphological link is represented by wide debris fans derives from the intense erosion of the carbonate bedrock (Di Vito et al., 1997), whose stratigraphy is reported in detail by Di Vito et al. (1998) (Fig. 8). The fans are composed of gravels and carbonate blocks with a matrix rich in reworked pyroclastic materials. At the top, palaeosols are intercalated with volcanic deposits.

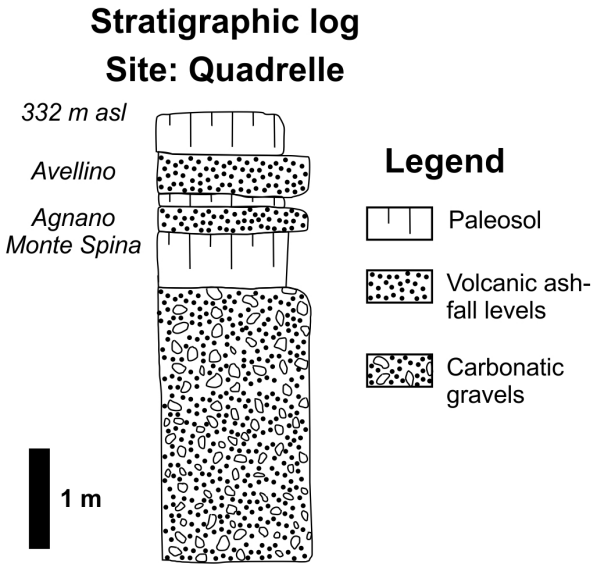


Figure 8 – Example of stratigraphic log representative of the depositional sequence exposed in the highest portion of the alluvial fans (De Vito et al., 1998, modified).

From a hydrogeological point of view, the piedmont area hosts a strategic karstic aquifer, whose basal groundwater table reaches depths of several hundred metres above ground level. This aquifer represents a local expression of karst aquifer of the Avella Mts. which feds Sarno springs. According to the basin-scale model, groundwater follows a main south-west direction. During this path, part of the flows moves into the pyroclastic and alluvial deposits of the Nola plain, while another part flows towards the Sarno spring group. In the Baiano district there are numerous withdrawals that capture the deep aquifer water by wells. Manly the groundwater is used for drinking purpose by companies such as Alto Calore Servizi SpA and the municipal aqueducts, but also for industrial and, subordinately, irrigation.

2.3 Foce hydrogeological karst observatory

A site-specific study was carried out in the Foce locality, where a hydrogeological karst observatory was designed and constructed as part of Ph.D. research program (Fig. 9c). From a geomorphological point of view, the study area is identified with a hydrogeological catchment area, extended about 0.90 km^2, of the southern slope of Torre Savaio Mt. which rises to 847 m above sea level and belongs to Sarno Mts. ridge, in south of the Avella Mts. system (Fig. 9a).

The carbonate structure of Sarno Mts. is bordered by the Nola plain (west), the Sarno plain (south), the Solofrana (east) and the Lauro valleys (north) (Fig. 9b). It consists of Mesozoic carbonate platform series fractured and karstified that were thrust over the external palaeogeographic units, characterised by the sedimentation of oceanic basins, during the Miocene compressive tectonic phases (D'Argenio et al., 1973; Mostardini and Merlini, 1986; Patacca and Scandone, 2007).

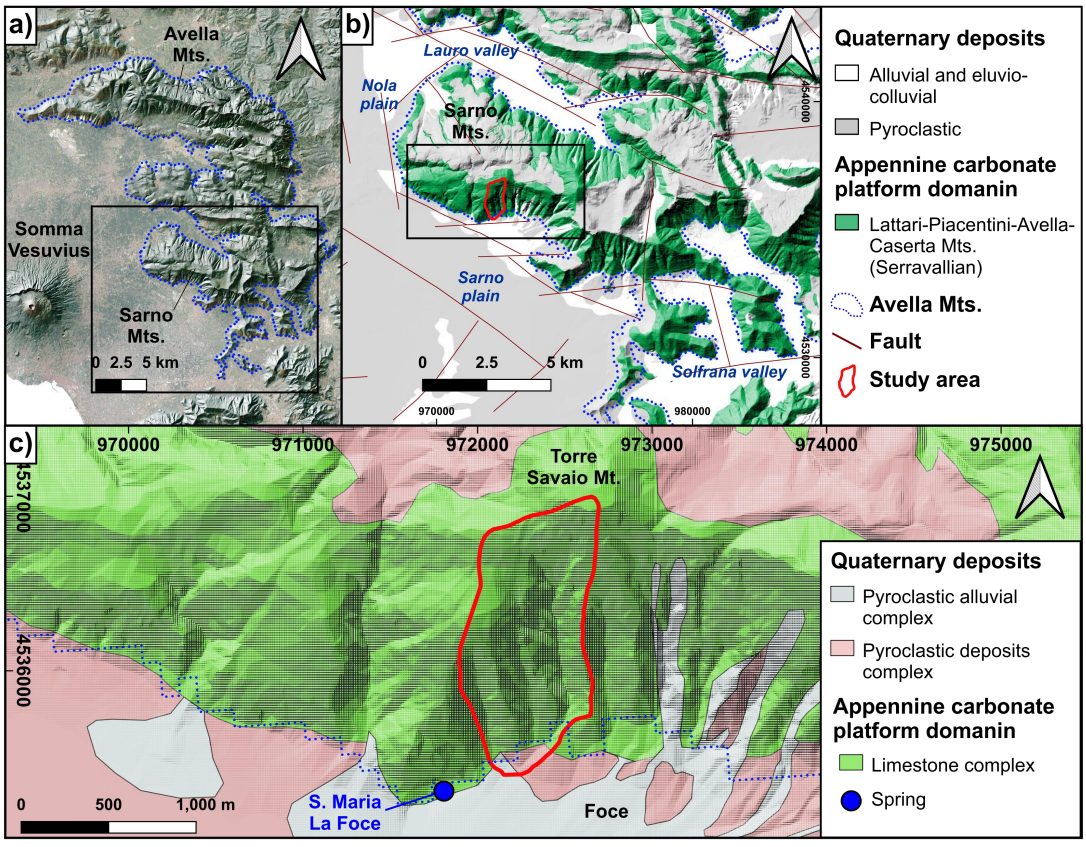


Figure 9 – a) Sarno Mts. location; b) Excerpt from geological map (Vitale and Ciarcia, 2018, modified); c) Excerpt of Foce experimental hydrogeological basin from hydrogeological map of Avella Mts.

Successive Pliocene and Pleistocene tectonic activity shaped the landscape, forming the steep structural slopes that define the current morphology of these mountain ranges (Patacca and Scandone 2007; Vitale and Ciarcia 2018). The slopes have straight profiles with an inclination of about 35° (Brancaccio et al., 2000). This allows the flow of meteoric water in well-defined paths, which contributes to the development of impluvium areas. In addition, sub-vertical morphological discontinuities cause irregular accumulation of ash-fall pyroclastic deposits came from the volcanic centres of the Phlegraean Fields and Somma Vesuvius (Di Crescenzo and Santo, 2005), accelerating drainage channel formation. This geomorphological configuration produces a discontinuous hydrographic network with non-permanent streams, deep second- and third-order basins and hollows located where the slope not yet involved in flow channelling processes.

The carbonate bedrock of Foce experimental hydrogeological basin (Fig. 9c) hosts a local aquifer that is part of the huge basal groundwater circulation of the Avella Mts. In the experimental site the groundwater flow is oriented towards the S. Maria La Foce basal spring (32 m a.s.l.) captured since 1962 by a drainage tunnel.

Along the altitudinal profile, the study area has a diversified land use distribution. Upstream area is mainly characterised by forests and transitional woodland-shrub, with deciduous forest of chestnut (Castanea sativa) dominating. In downstream area land use is more diversified with oak forests alternating with natural grassland and agricultural areas.

The carbonate bedrock of the basin is mantled by a discontinue ash-fall pyroclastic deposits (Fig. 10). which exert a very relevant role on groundwater recharge, infiltration processes and rainfall-induced landslides.

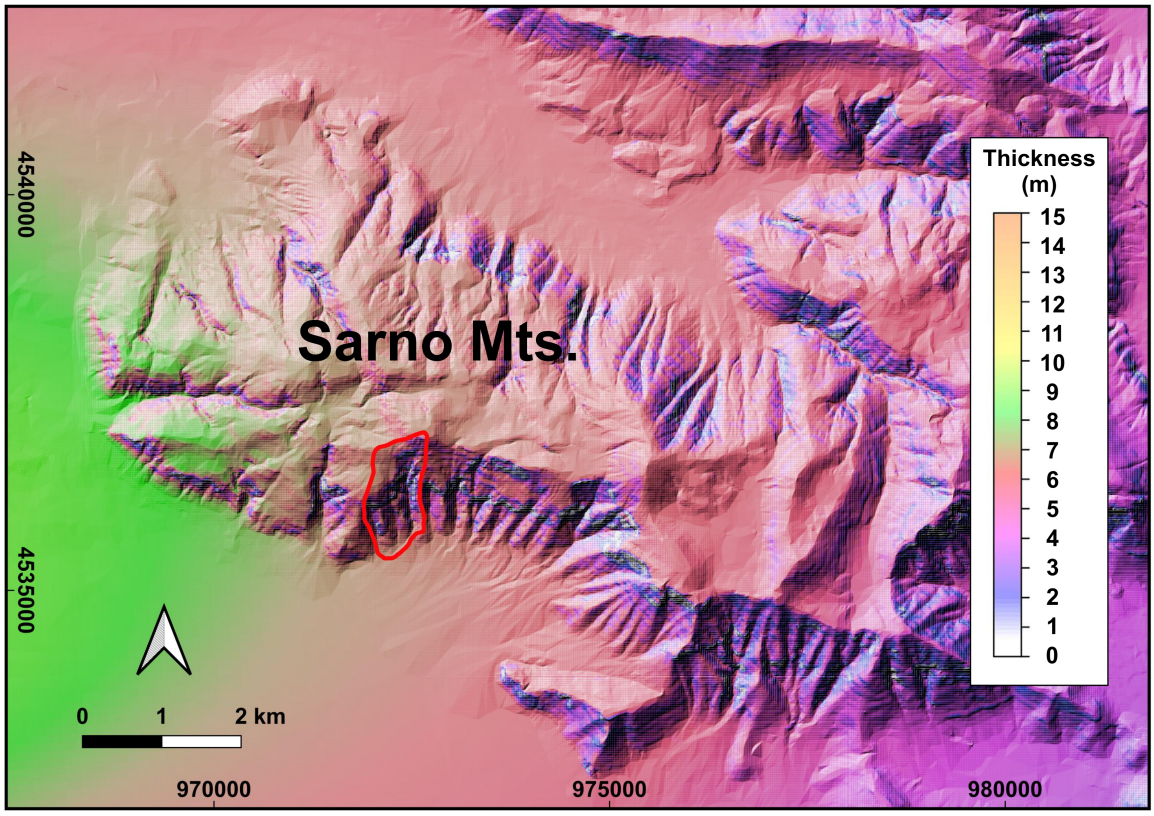


Figure 10 - Distribution model of ash-fall soil pyroclastic deposits in Sarno Mts. (Fusco et al., 2017, modified)

The volcanoclastic sequence was denuded by erosive and gravitational phenomena, depending on the morphological characteristics of the slopes. As a result, the stratigraphic sequence is incomplete in many places.

Rolandi et al. (1998, 2000) identify a representative complete pyroclastic series in the southwestern footslope of Sarno Mts., which are divided in two complexes, as follows:

- the Ancient Pyroclastic Complex (APC), mainly consisting of Ignimbrite Campana flow deposits (dated 39 k-year) and other products of the eruptions of Phlegrean Fields and the Ischia island;
- the Recent Pyroclastic Complex (RPC), coming from the Somma-Vesuvius eruptions;

The eruptions that produced the RPC deposits include: Codola (dated 17 k-year - Rolandi et al., 2000), Sarno (dated 17 k-year - Rolandi et al., 2000), Ottaviano (dated 8 k-year - Rolandi et al., 1993a) and Avellino (dated 3.8 k-year – Rolandi et al., 1993b). Products of RPC are also the most recent eruptions of Vesuvius: 79 AD (Rolandi et al, 2007), 472 AD (Rolandi et

al, 2004) and 1631 AD (Rosi et al, 1993) as well as the successive eruptions of minor importance for the amount of material erupted, the last in 1944. The dispersion axes of the RPC eruptions were oriented towards the east, mainly involving the carbonate ridge of the Sarno Mts., except for the 79 AD eruption, whose dispersion axis was oriented towards the south (De Vita et al., 2006a).

De Vita et al. (2006b) carried out geological surveys, artificial cuts and exploratory trenches to describe the stratigraphic and pedological setting of the pyroclastic deposits in morphological conservative areas, with slope angle lower than 28°. For slope angle greater than 28° there is a thinning of the pyroclastic soil mantle up to its nearly disappearance for values greater than 50°. The investigation was conducted to the north-east of the Pizzo d'Alvano relief (1,133 m a.s.l.), where the landslides occurred between 5 and 6 May 1998. Seven pedogenetic horizons were recognized (Fig. 11) and classified according to the Terribile et al. (2000), USDA (2014) and the USCS criteria as follows:

- A horizon, characterised by an abundance of organic material with a few pumiceous clasts, classified as highly organic soil (Pt);
- B horizon, characterised by pumiceous clasts ranging from coarse to fine ash, classified as sand with silt (SM);
- C horizon, constituted of pumiceous clasts with maximum dimension of 30 mm, classified as gravels and sands from poor to well graded (GW or GP);
- Bb horizon, corresponding to a B horizon buried by the succesive depositional event and therefore considered as a palaeosol, classified as sand with silt (SM);
- Cb horizon, representative of a buried C horizon, classifiable as the C horizon (GW or GP) even if in some cases the lower is characterised by the relative abundance of the sandy fraction (SW or SP);
- Bb_{basal} horizon, corresponding to a residual pyroclastic deposit, highly pedogenised, representative of products of previous eruptions classified as sand with silt (SM);
- R horizon, corresponding to the carbonate bedrock whose discontinuities are filled by the finest grain size fraction of the overlying pyroclastic deposit.

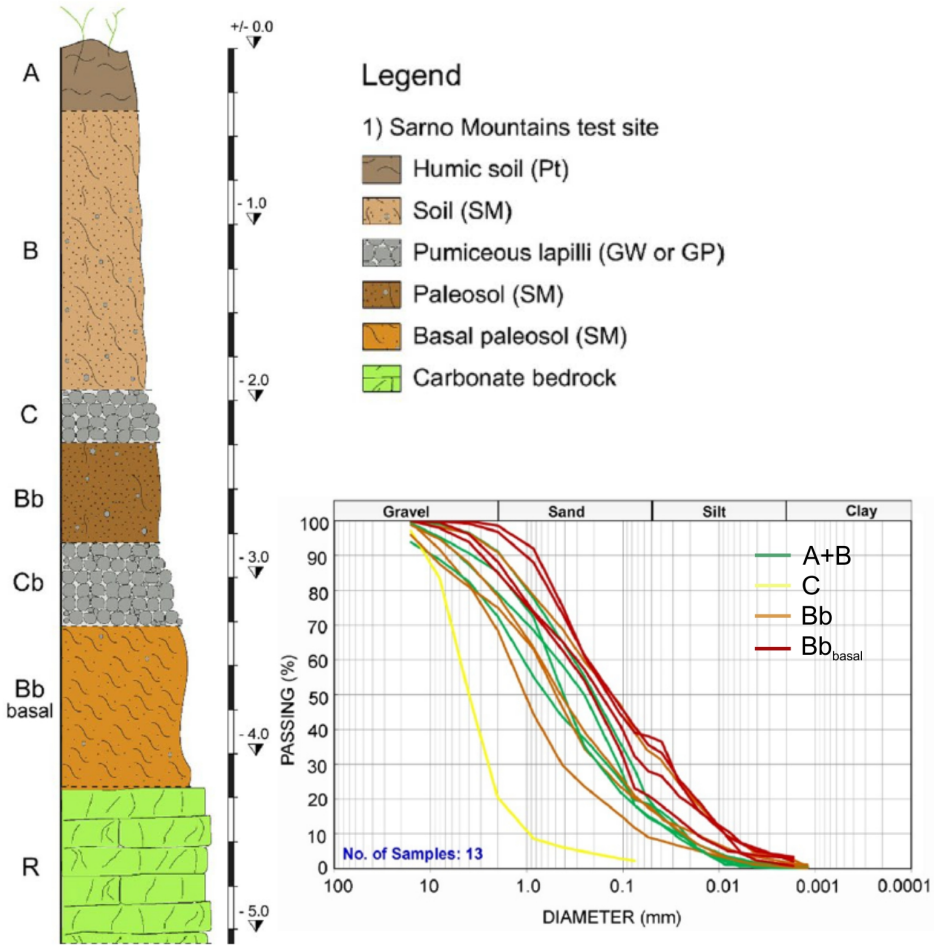


Figure 11 - Representative stratigraphic setting of soil covers mantling (Fusco et al., 2022, modified).

The groundwater recharge of the underlying karst aquifers is influenced by the hydrological regime of the pyroclastic mantle (Fusco et al., 2017) that determines the amounts of water lost to the atmosphere through evapotranspiration and percolation to the groundwater table. This process is mainly governed by the high water retention capacity of pyroclastic soils (Napolitano et al., 2016), which permits a high storage of soil water. For the Sarno Mountains, the specific hydraulic properties of the pyroclastic deposits were investigated through field surveys and laboratory tests. De Vita et al. (2013) developed water retention curves (SWRC) at the different depths in the pyroclastic cover, showing differences in residual water content for each horizon. Although the pedogenised levels (B, Bb, Bbbasal) exhibit similar hydraulic behaviour, the pumiceous horizons show an unusual water retention capacity, attributable to the high specific surface area of the voids and inter-particle connections.

To improve understanding of the temporal and spatial variability of the hydrological conditions in the ash-fall pyroclastic soil, Fusco et al. (2017) developed a hydro-geomorphological model of the pyroclastic mantle, based on pressure head monitoring lasted 4 years (2010-2014). This model shows that during wet periods (November to March), despite higher pressure heads, conditions of total saturation are never reached and only in the shallower B horizon values are near saturation. During late spring and summer, pressure head drops significantly, especially in August and September due to increased evapotranspiration and reduced rainfall. This decrease occurs progressively, starting from the B horizon and propagating towards the Bb and Bb_{basal} deeper layers. Pressure head values were transformed in the correspondent volumetric water content values by the Soil Water Retention Curvers (SWRCs - van Genuchten et al.,1980), allowing calculating the total Soil Water Depth (SWD - Kutilek and Nielsen, 1994) time series stored in the ash-fall pyroclastic soil cover (Fig. 12). The SWD seasonal fluctuations were also compared with the SWD levels corresponding to Saturation (SAT), Field capacity (FC) and Permanent Wilting Point (PWP), estimated equal to 2084 mm, 1121 mm and 507 mm respectively. The SWD shows fluctuations around the FC level, identifying periods during the rainy season when the water content exceeds this level and the available water allows percolation into the underlying karst aquifer. Gravity drainage varies with depth as the B horizon drains during the whole year, while the Bb_{basal} only in spring and summer. Since the Bb_{basal} is in contact with the carbonate bedrock, it is likely to influence the recharge of the aquifer, unless preferential flows are present (Mirus and Nimmo, 2013).

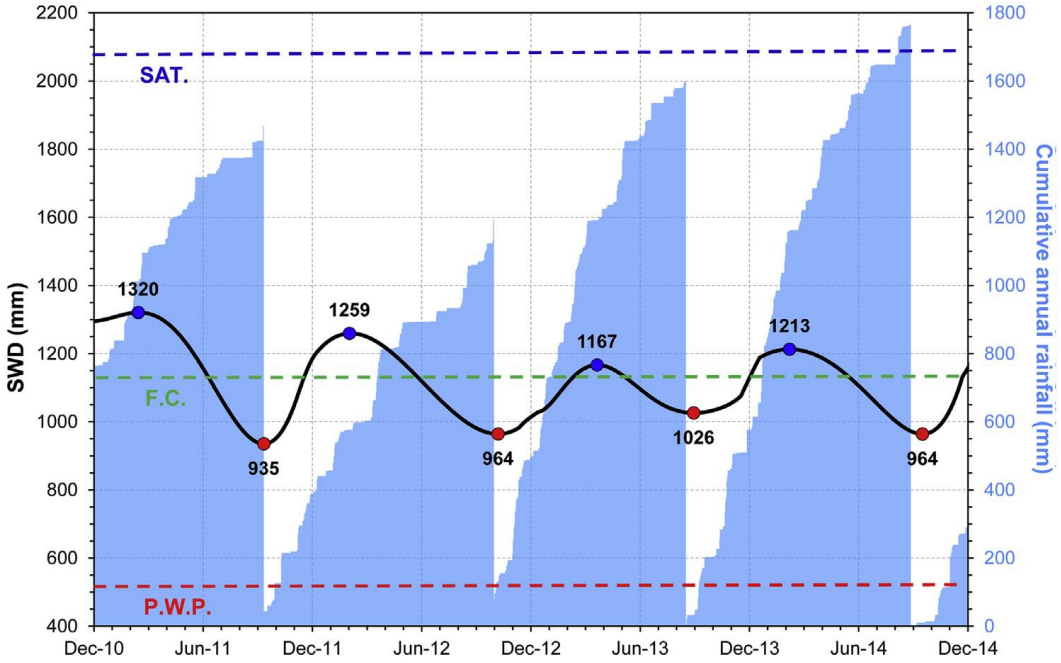


Figure 12 - Estimated time series of SWD in comparison with the annual rainfall cumulative curves with yearly maximum (red dots) and minimum values (blue dots). Dashed horizontal lines represent SAT (blue), FC (green) and PWP (red) (Fusco et al., 2017).

3. Data and methodologies

This chapter provides an overview of the data and methods used in this research. Detailed discussions are presented in the results chapters, which are structured as five manuscripts, each dealing with a specific aspect of the hydrogeological study at different scales of analysis. The following sections briefly outline the datasets and methods applied and refer to the respective manuscripts for further details.

3.1 Cartographic and hydrogeological database

A GIS-based approach was applied to develop a novel hydrogeological conceptual model for the Avella karst aquifer. Geological, piezometric and stratigraphic data from institutional archives and field measurements were digitised and implemented in a hydrogeological geodatabase (see section 4.1, p. 59 for details).

3.2 Water balance by empirical approach and numerical code

Three methods were used to estimate groundwater recharge. Two were based on an empirical approach and aimed to estimate the mean annual groundwater recharge at the aquifer scale by ground-based hydrological and remote sensing data referred to the period 2000-2019 (see section 4.1, p. 60 for details). The third method used the Soil Water Balance (SWB) numerical code to estimate groundwater recharge at different time scales (mean annual, annual, monthly and daily) for the period 2010-2021 and both for the aquifer and its groundwater basins (see section 4.2, p. 92 for details). The SWB model was also used to estimate the mean annual groundwater recharge at the sectoral scale of the Baiano district (see section 4.4, p. 138 for details) for the period 2008-2022. Unlike empirical approaches, SWB required not only climate data but also inputs on land use, soil texture and hydrological properties.

3.3 Spring inventory map and wells registry

A spring inventory map and a well register were developed, based on a database that collects information on water points (wells and springs). The database includes the geographical coordinates, spring discharges, authorised withdrawals from wells and piezometric levels collected from institutional databases and scientific literature and contributed to the

validation of water balance models at the aquifer and groundwater basin scale (see section 4.2, p. 94 for details).

3.4 Regional Climate Models (RCMs)

To analyse the potential impact of climate variability on groundwater recharge at the aquifer scale, historical (1950-2005) and future (2006-2100) precipitation and air temperature datasets from the EURO-CORDEX RCM ensemble were used (see section 4.3, p. 116 for details). These datasets were bias-corrected using observed historical measurements and an empirical approach was applied to estimate groundwater recharge under two representative IPCC concentration pathways (RCP4.5 and RCP8.5).

3.5 Pumping tests and groundwater quality

Data from pumping tests and chemical-physical and microbiological analyses were used to assess the groundwater potential and quality of the piedmont aquifer sector corresponding to the Baiano district (see section 4.4, p. 140 for details).

3.6 Characterization of Foce hydrogeological karst observatory

A stratigraphic characterisation and determination of the physical-volumetric, index and hydraulic properties of the ash-fall pyroclastic soil cover at the site-specific scale of the Foce experimental hydrogeological basin were carried out through laboratory and field tests (see section 4.5, p. 157 for details). The data acquired were used to implement a numerical model to simulate hydrogeological processes in the unsaturated zone.

3.7 Hydrological monitoring system

A hydrogeological observatory was established in the Foce basin to provide continuous and real-time monitoring of all parameters of the water balance. Detailed descriptions of the observation stations can be found in Section 4.5 (see page 158), whose collected data were used to implement and calibrate the numerical model.

3.8 Numerical modelling of water balance

The numerical model HYDRUS-1D, implemented and calibrated with data from the Foce hydrogeological karst observatory, was used to simulate the water infiltration processes in the pyroclastic soil over a period of about three years (see section 4.5, p. 161 for details).

4. Results

4.1 Hydrogeological conceptual model and groundwater recharge of Avella Mts. karst aquifer (southern Italy): A literature review and update

Paola Petrone[1], Pantaleone De Vita[1], Palmira Marsiglia[1], Pasquale Allocca[1], Silvio Coda[1*], Delia Cusano[1], Daniele Lepore[1], Vincenzo Allocca[1*]

[1] Department of Earth Sciences, Environment and Resources, University of Naples Federico II, Monte S. Angelo Campus, 21 Cinthia Street, Building 10, 80126, Naples, Italy.

Corresponding authors: vincenzo.allocca@unina.it; silvio.coda@unina.it

Abstract

Study Region: Avella Mts., southern Italy.

Study Focus: The paper is focused on groundwater of Avella Mts.. This aquifer has been experiencing an increasing human pressure due to periods of drought and growth in groundwater extraction. A novel hydrogeological conceptual model was developed, and groundwater recharge was estimated by two approaches. The study was carried out by an in-depth literature review and a GIS-based analysis of geological and piezometric data, ground-based meteorological and remotely sensed data.

New Hydrological Insights for the Region: The new hydrogeological conceptual model allowed to reconstruct the aquifer lithology, its deep geometry, and, for the first time, groundwater flow scheme. Five groundwater basins were recognized with distinct outlets and subsurface outflows, suggesting a new aquifer compartmentalization in-series groundwater basins. Some basal springs are fed by autonomous basins with smaller extension, while other springs have dried up completely. The groundwater recharge varies from 7.30 to 6.90 m^3/s as estimated by Turc formula and MODIS data, respectively; the values are comparable among them, confirming mutually the validity of approaches used. The comparison with previous studies highlights variations and changes for both the hydrogeological conceptual model and water balance, linked to natural and anthropogenic factors.

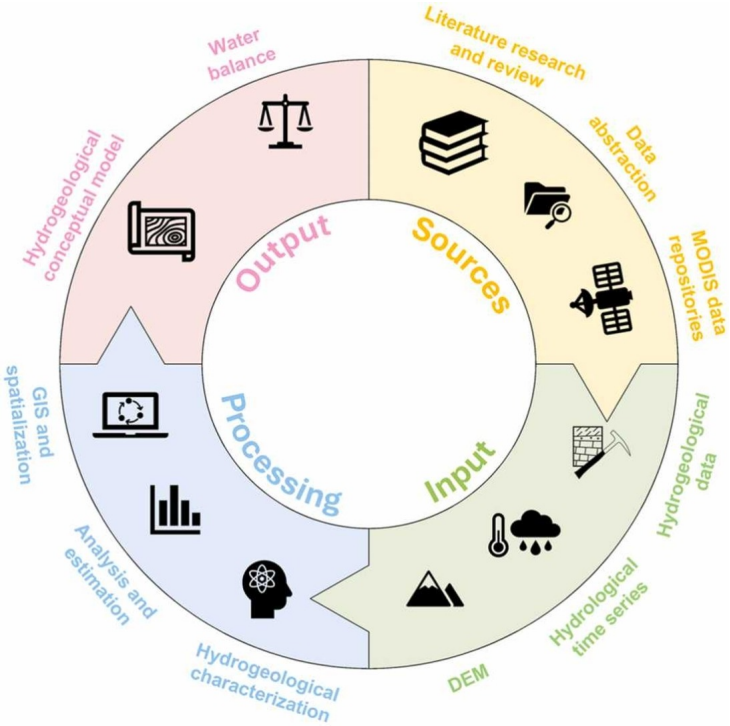
The results obtained represent a way for supporting sustainable management of groundwater, waterwork systems security and groundwater-dependent ecosystems protection of a large sector of Campania region.

Keywords: karst aquifer, hydrogeological conceptual model, groundwater recharge, groundwater management.

Highlights

- An in-depth literature review of Avella Mts. karst aquifer was performed.
- A novel GIS-based hydrogeological conceptual model and a multi-approach groundwater recharge estimation were developed.
- Reconstructing the aquifer structure and groundwater flow allowed to define new groundwater basins.
- The approach and results can support decisions for sustainable groundwater management.

Graphical abstract



Introduction

Globally 15.2% of the Earth's land surface is characterized by carbonate rocks and contain abundant groundwater resources (Goldscheider et al., 2020). Approximately about 25% of the global population depends on karst groundwater (Ford and Williams, 2007). In many countries and regions of the world such as USA (e.g., Texas, Florida), Europe (e.g., Austria, Italy, Dinaric region) and Asia (e.g., China, Lebanon, Syria), karst aquifers massively contribute to the freshwater supply; several large cities, e.g. the city of San Antonio, Miami, Vienna, Rome, Naples, Taiyuan, Beirut, and Damascus entirely depend on karst groundwater (Sun et al., 2020; Chen et al., 2017; Allocca et al., 2014). Karst aquifers hosts important groundwater resources for human consumption, agriculture, industry, cattle farming, energy production, tourism and include cultural heritages, natural landscapes, and ecosystems with great geo- and bio-diversity (Allocca et al., 2018; Goldscheider et al., 2020).

In Campania region, southern Italy, about 25% of the land surface is characterized by karst aquifers forming the highest mountain ridges with altitudes up to 1898 m a.s.l..

These aquifers represent the main source for drinking water, agriculture, and industry, and play a vital role for environmental protection and groundwater-dependent ecosystems as Garigliano, Volturno, Sarno and Sele rivers. Historically these aquifers have represented a strategic resource for economic growth and development (Allocca et al., 2014; 2015). In Roman times, some karst springs were captured to feed by Augustan aqueduct (33 − 12 BC) cities such as *Neapolis*, *Puteoli*, *Pompeii*, *Cumae* and *Beneventum* (Cusano et al., 2023). In the post-Second World War period, karst groundwater has certainly favored the economic growth, industrialization, infrastructure development and improvement of living conditions of the Campanian population. This was possible thanks to mean annual specific groundwater recharge (up to 0,040 $m^3/s/km^2$) among the highest in Italy, being linked to high permeability of karst rocks, high rates of precipitation, endorheic areas, and permeable pyroclastic soils covered by dense deciduous forest that favour groundwater recharge (Allocca et al., 2014; 2015; Fusco et al., 2017; De Vita et al., 2018; Cusano et al., 2024). Huge basal springs have a high average annual flow rate (up to about 6 m^3/s) and excellent hydrochemical quality, feeding rivers, lakes, wetlands, and coastal areas. However, these karst aquifers are particularly vulnerable to pollution and human impacts (Tufano et al., 2020; Cusano et al., 2023) and, in some cases, it is difficult to implement effective protection strategies that involve strong restrictions on both land use and anthropogenic activities (Allocca et al.,

2018; Cusano et al., 2023). The strongly space-time climatic variability of Campania region related to the North Atlantic Oscillation (De Vita et al., 2012) determine a significant inter-annual variation of groundwater recharge and spring discharges, and consequently a reduction in groundwater availability for regional and local waterwork systems.

For these reasons, the risk to unbalance between groundwater supply and demand is high, as already experienced in water-emergencies occurred in 2000, 2011, 2017 and 2020 in the Naples metropolitan area, where highest drinking-water demand occurs. In this densely populated area (total inhabitants about 3.2 million) of Campania region, during the last decades, the human pressure and aquifer exploitation rate are strongly increasing as resulting from inter-annual meteorological drought periods. Thus, in addition to the large basal springs captured for drinking water use, numerous private wells (in some cases even unauthorized) and well-fields were drilled for drinking, agriculture, industry, and other water supplies (Allocca et al., 2007).

Moreover, the water withdrawals from these wells occur through an uncoordinated management among the regional and provincial public bodies, in charge to give permissions to groundwater exploitation, and above all not based on an updated conceptual hydrogeological model and water balance.

In a such complex hydrogeological scenario, the need of a revisited hydrogeological conceptual model and updated water balance is an urgent issue to be addressed to prevent overexploitation of aquifers (Lancia et al., 2020; Ben Saad et al., 2023), in agreement with water policies of the UN 2030 Agenda for Sustainable Development and Water Framework Directive 2000/60/EC.

The Avella Mts. karst aquifer was selected among the others of the Campania region because supplying numerous urban centers of Naples, Caserta, Avellino, Salerno and Benevento provinces and the human pressure and aquifer exploitation rate are strongly increased in the last decades. Based on an in-depth literature review, the aim of this study was to reconstruct a novel hydrogeological conceptual model of Avella Mts. by new geological and hydrogeological data and estimate groundwater recharge by a water balance based on both ground-based meteorological observations and remotely sensed data.

The remaining of the paper is organized as follows: Section 2 describes the geological and hydrogeological characteristics of the study area, as well as spring tapping works, waterworks, and groundwater use; Section 3 provides a literature review regarding previous

hydrogeological schemes and water balances; Section 4 shows the data and methodological approaches used; Sections 5 and 6 comment the obtained results and provide their discussion, while Section 7 reports the concluding remarks.

Study area description

Geological and hydrogeological setting

The Avella Mts. extending approximately 370 km^2 are located within of Partenio and Sarno River Regional Parks and shared by all five provinces of the Campania region (Figs. 13a and 13b).

This large carbonate ridge hosts a karst aquifer system with a mean annual specific groundwater recharge (up to 0.037 $m^3/s/km^2$) among the highest in the southern Apennine and sustaining a series of ecosystem services. A large Site of Community Importance (https://www.mase.gov.it/pagina/rete-natura-2000) and numerous environments and ecosystems, e.g., forests, grasslands, springs, rivers, poljes and other karst landforms contribute to its variegated and wide geo - and biodiversity. Surface and groundwater resources play a primary role in the regulation of the hydro-ecological regime of Sarno, Regi Lagni and Sabato rivers (Fig. 13a).

From a hydrogeological point of view, the Avella Mts. are a well-defined karst aquifer (Celico, 1983), delimited to the west by the Campanian plain, to the north and south by the alluvial plains of Isclero and Solofrana rivers, respectively (Fig. 1b). The massif is constituted mainly by a fractured and karstified Mesozoic-Cenozoic carbonate series of the Apennine platform domain belonging to the "*Monti Picentini and Lattari*" and "*Monti di Avella*" tectonic units (ISPRA, 2017), characterized from bottom to top by Norian-Hettangian dolomites, Jurassic-Lower Cretaceous dolomitic limestones, and Cretaceous limestones, faulted and fractured by a complex network of discontinuity NW-SE and SW-NE oriented (Vitale and Ciarcia, 2018). The carbonate hydrostructure is hydraulically confined by low permeability terrigenous units belonging to synorogenic wedge-top basin deposits laterally juxtaposed by thrust, and alluvial deposits and Vesuvian and Phlegraean ash-fall and ash-flow pyroclastic deposits in tectonic contact by normal faults (Fig. 13b).

In such a hydrogeological framework, Avella Mts. are characterized by a basal groundwater flow orientated towards three main spring groups (Fig. 13a): i) Cancello spring group located in the north-western sector, originally was characterized by Calabricito and Mefito springs

(30 and 28 m a.s.l.); ii) Sarno spring group located in the southern sector, originally represented by S. Maria La Foce (32 m a.s.l.), Mercato, Palazzo (26 and 24 m a.s.l.), Cerola (28 m a.s.l.), S. Marina di Lavorate (28 m a.s.l.) and S. Mauro springs (27 m a.s.l.); iii) Laura and Labso springs (185 and 199 m a.s.l.) located in the south-eastern sector.

Systematic flow measurements carried out in the 1960s and 1970s by National Hydrological Service - Department of Naples (Celico, 1983; Allocca et al., 2007) allowed to estimate the following average spring discharges: 1.20 m^3/s for the Calabricito and Mefito springs; 2.60 m^3/s for the S. Maria La Foce spring; 3.00 m^3/s for the Mercato and Palazzo springs; 0.60 m^3/s for the Cerola spring; 1.80 m^3/s for the Santa Maria di Lavorate spring; 0.40 m^3/s for the San Mauro spring; 0.25 m^3/s for the Laura and Labso springs.

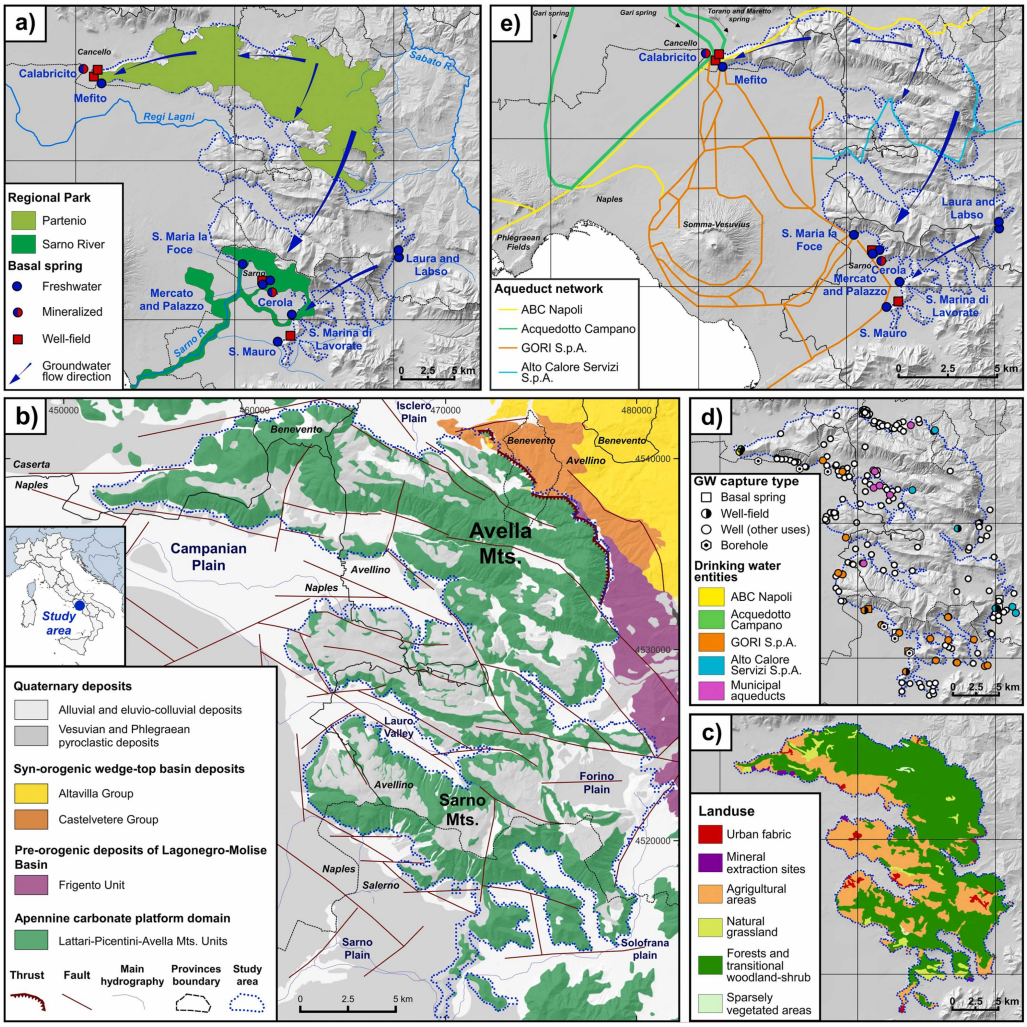


Figure 13 – Location of the study area. a) Avella Mts., Partenio and Sarno River Regional Parks, and groundwater-dependent ecosystems (https://www.sciencedirect.com/topics/earth-and-planetary-sciences/groundwater-dependent-ecosystem) of Sarno, Sabato and Regi Lagni rivers; b) Geological

map (from Vitale and Ciarcia, 2018, modified); c) Corine Land Cover (2018) simplified; d) Well-fields, wells, boreholes, and basal springs used for drinking water supply by public bodies, companies and private users; **e)** Tapped basal springs and aqueduct systems.

These basal springs are characterized by freshwater (electrical conductivity between 670 and 1020 μS/cm) with an excellent hydrochemical quality and a typically bicarbonate-calcium composition that reflects the aquifer lithology (Celico et al., 1980). High content of endogenous CO_2 (up to 330 ppm) that characterizes the Calabricito and Cerola highly mineralized springs (electrical conductivity up to 2130 μS/cm) (Fig. 13a) are linked to gas rise through deep normal faults which interacts locally with deep and shallow groundwater of the karst aquifer (Celico et al., 1980).

Given the proximity to the volcanic centers of Somma-Vesuvius and Phlegraean Fields, the karst aquifer is singularly covered (Figs. 13b and 13e) by alkali-potassic ash-fall pyroclastic deposits with thickness up to about 8 m along slopes, where the slope angle is greater (up to 40°), and about 50 m, in summit flat and endorheic areas (Fusco et al., 2017). Along the steep slopes, dense deciduous forests and transitional woodlands constitute the predominant types of land use and vegetation cover, while in the endorheic karst areas and in the piedmont sectors, agricultural areas (chestnuts and hazelnuts), natural grassland and subordinately urban areas are prevalent (Fig. 13c).

The climate is Mediterranean-mild type (CSb) (Beck et al., 2018), whereas mean annual rainfall and air temperature are equal to 1700 mm/y and 13,4 °C, respectively (Allocca et al., 2014; Ruggieri et al., 2021).

Groundwater development growth

Since the 1960s groundwater of Avella Mts. (Fig. 1d) has played a strategic role in socioeconomic growth and development of the Campania region. In the post-Second World War period, water demands of the Naples metropolitan area has significantly increased, due to industrialization, urbanization, and population growth. Given the excellent hydrochemical quality of the groundwater, some basal springs originally used by local farmers for irrigation were tapped and exploited for drinking water supply (Fig. 14). Thus, in the framework the Special Project 29 the Cassa per il Mezzogiorno Italian Government Agency were financed and constructed the Campanian aqueduct (Acquedotto Campano; Fig. 13e) and the so-called

Sarno aqueduct (GORI SpA; Fig. 13e) for the water supply of Naples metropolitan district, including the peri-vesuvian area.

In 1962 and 1972 two drainage tunnels were constructed (Figs. 14a and 14b) each with a total length of about 0.30 km, to tap water of S. Maria La Foce and S. Marina di Lavorate springs (Civita et al., 1969a; 1969b). Both tunnels were excavated with sub horizontal inclination, about 28 and 26 m a.s.l., respectively, i.e., few meters below the natural altitude of basal springs (32 and 28 m a.s.l.). In the summer of 2001, after a meteorological drought period the drainage tunnel of S. Maria La Foce spring dried up totally; thus, eleven wells were drilled inside the tunnel (Fig. 14a) to compensate the flow rate during periods of drought such as those occurred again in 2011, 2017, and 2020.

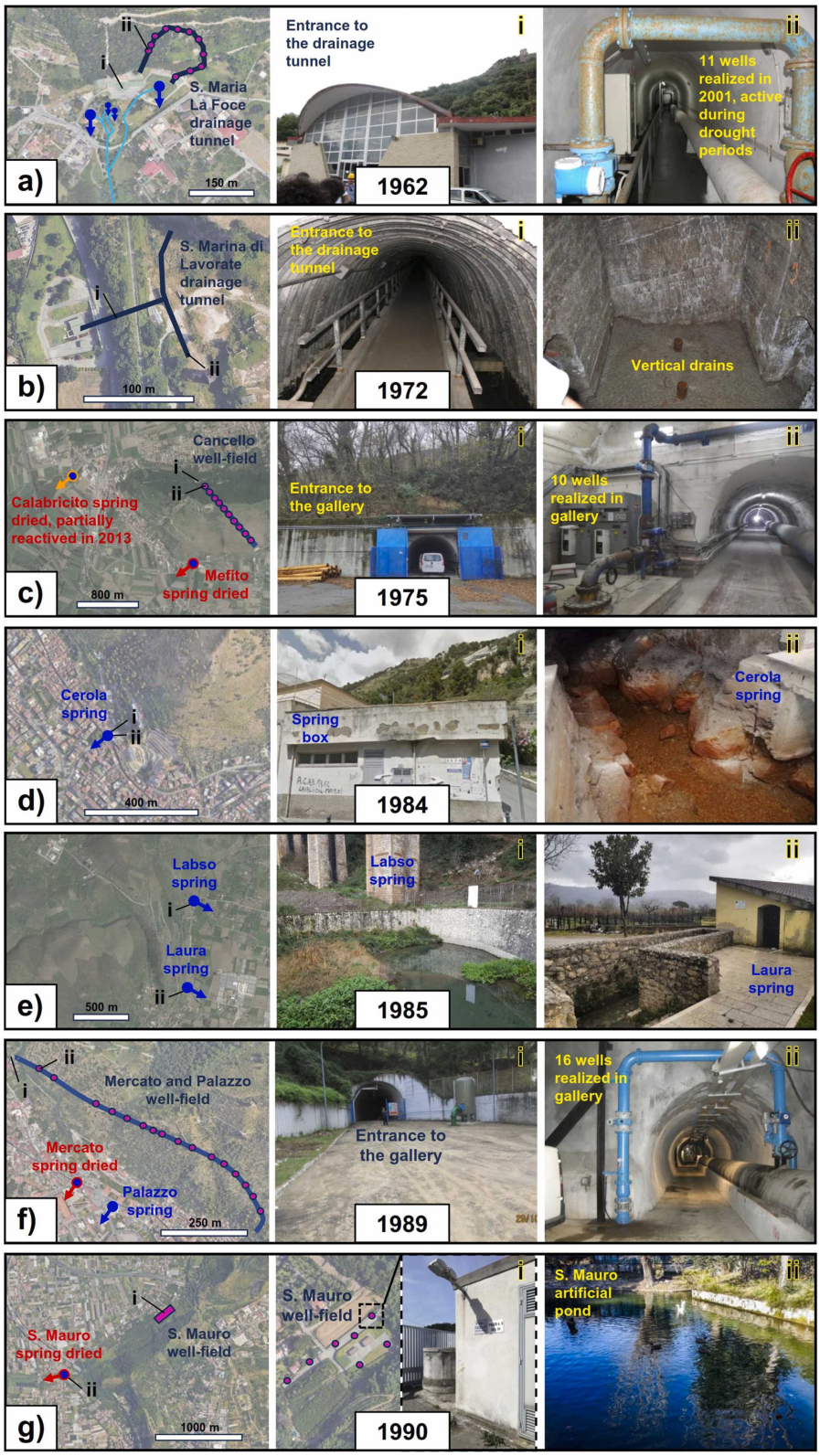


Figure 14 – Location sketch, date of construction, and characteristics of basal spring tapping works. a) S. Maria La Foce spring; b) S. Marina di Lavorate spring; c) Mefito and Calabricito springs; d) Cerola spring; e) Laura e Labso springs; f) Mercato and Palazzo springs; g) S. Mauro spring.

In the meantime, three well-fields were drilled upstream of Mefito, Calabricito, Mercato, Palazzo and S. Mauro springs in the 1975, 1989 and 1990, respectively (Figs. 14c, 14f and 14g). The activation of these well-fields led to the drying up of Mefito, Calabricito, Mercato and S. Mauro springs. Instead, the Cerola, Laura and Labso springs were tapped in the first half of the 1980s for agricultural use by gravity intake systems (Figs. 14d and 14e).

Starting from the 1990s and 2000s further wells and well-fields were drilled by public agencies and joint-stock companies for drinking water supply (Fig. 13d). Today, the entire volume of groundwater exploited for drinking water supply, totaling about 198×10^6 m^3/y, is distributed by four main regional and provincial waterworks (Fig. 13e; GORI SpA, Acquedotto Campano, ABC Napoli, Alto Calore Servizi SpA) and some municipal aqueducts (Fig. 13d) to feed a large area of the Campania region with a population of approximately four million inhabitants.

Contextually, starting from the 1990s and 2000s numerous private wells have drilled in the piedmont karst areas for agriculture, industry, domestic and other private uses (Fig. 13d) of whose withdrawal rates are not known. All these wells have resulted in strong increase of groundwater exploitation whose critical effects were enhanced by drought periods and an uncontrolled and uncoordinated groundwater management.

Literature research and review

Previous hydrogeological maps

Starting from the 1970s some conceptual hydrogeological model and groundwater circulation schemes of Avella Mts. were published with different hydrogeological information.

The first scheme at the 1:100,000 scale (Fig. 15a) is shown on the hydrogeological map of north-western Campania region (Civita et al., 1973), in which three hydrogeological complexes were identified, i.e., limestone, pyroclastic and debris slope complexes. Based on a geomorphological criterion, the hydrogeological scheme shows a local correspondence between watershed and hydrogeological boundaries. In addition to the hydrogeological limits of groundwater basins of Cancello and Sarno springs, the occurrence of other small groundwater basins was hypothesized, in the north-eastern sector where historically the basal springs have never recognized.

Subsequently, in the framework of the hydrogeological map of the central-southern carbonate Apennine (Celico, 1978) a new scheme is proposed at the 1:400,000 scale (Fig.

15b) based on a hydrogeological and hydrostructural criterion coupled with magnitude of spring discharges (Celico, 1983). Although characterized by lesser geological information (a unique carbonate complex is mapped), two main large groundwater basins were identified and no correspondence among hydrographic and hydrogeological boundaries is proposed. The basal groundwater flow is split into two main directions (Fig. 15b); the first N-W oriented, towards the Cancello spring group, and the second southward directed, towards the Sarno spring group, and subordinately Laura and Labso springs. Conversely, the thrust occurring along north-eastern edge of massif was interpreted as a no-flow boundary as well as inverse faults within the carbonate ridge were considered as probable limit of groundwater basins feeding springs.

In the two subsequent schemes (Figs. 15c and 15d) implemented at the 1:400,000 (Celico, 1983) and the 1:200,000 scale (Budetta et al., 1994), respectively, the previous hydrogeological scheme (Celico, 1978) is confirmed, and some information about outflow from carbonate to alluvial-pyroclastic complex are indicated. Moreover, based on hydrochemical and isotopic spring data (Celico et al., 1980) a possible outflow from the Solofrana plain to the carbonate complex has been also hypothesized.

A partial scheme at the 1:100,000 scale (Fig. 15e) is proposed within of the hydrogeological map of Avellino province (Allocca et al., 2008). In addition to hydrogeological complexes and groundwater flow scheme, the high-altitude springs and main drinking, agricultural, and industrial wells are also reported.

Recently, a scheme at the 1:300,000 scale (Fig. 15f) was realized in the framework of the hydrogeological map of continental southern Italy (Allocca et al., 2007; De Vita et al., 2018), which provided an update of the basal and perched spring discharges, as well as location of main drinking well-fields.

In all hydrogeological schemes there is missing data about the morphology of the piezometric surface of basal water table, as well as information on hydraulic gradients, extension of groundwater basins feeding basal springs, based on piezometric data and groundwater flow path. This represents a lack of information affecting generally the karst aquifers of southern Italy, whose impervious mountain morphology prevents the drilling of very deep water wells.

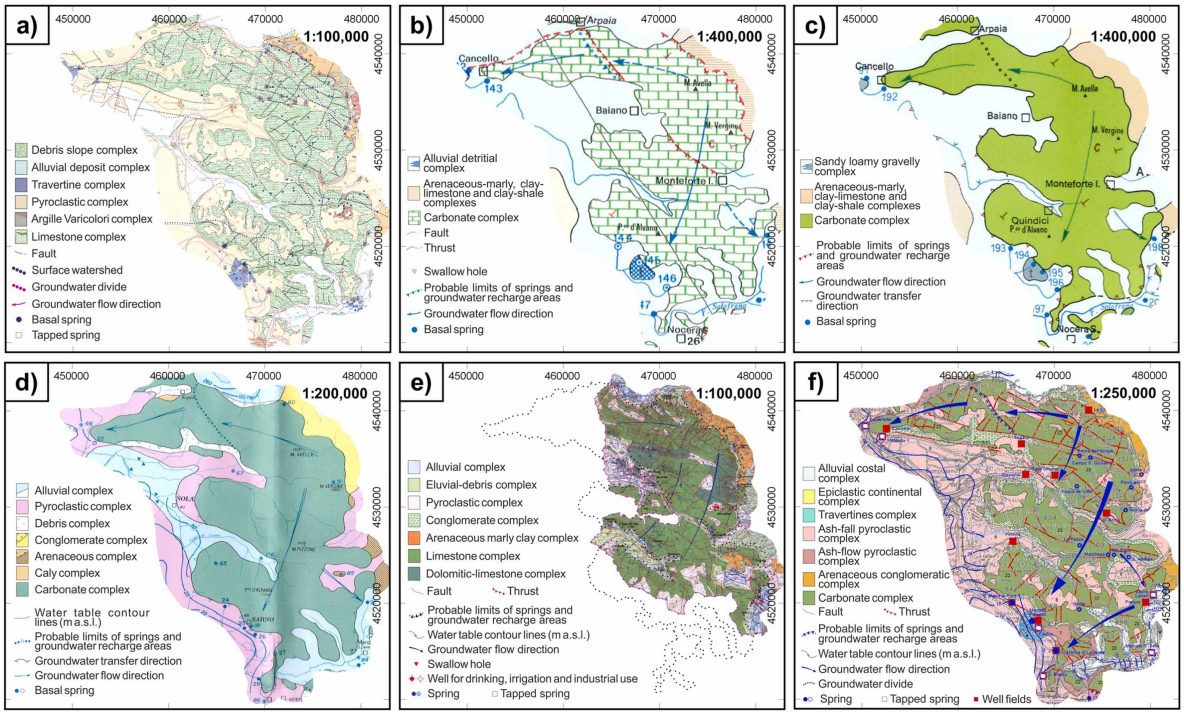


Figure 15 - Previous hydrogeological schemes of Avella Mts.: a) from Civita et al. (1973) modified; b) from Celico (1978) modified; c) from Celico (1983) modified; d) from Budetta et al. (1994) modified; e) from Allocca et al. (2008) modified; f) from De Vita et al (2018) modified.

Previous water balances

In the last 60 years, starting from the preparatory surveys aimed at the design of tapping works of basal springs (Nicotera and Civita, 1969a; 1969b; Civita et al., 1970; Civita et al., 1973), the groundwater recharge (GR) of Avella Mts. was estimated by different dataset and methodologies, as well as different periods and scale of analysis (Tab. 1). The previous estimates of GR were carried out by an empirical method based on the multiplication of actual precipitation, namely precipitation minus actual evapotranspiration, by a Groundwater Recharge Coefficient (GRC), whose complement represent the runoff coefficient.

Civita et al. (1970) estimates the GR for 1968÷1969 hydrologic year. Using ground-based hydrological data of 11 precipitation gauges and 7 air temperature stations, and by application of Thiessen method and Turc's (1954) formula, the GR was evaluated in 13.30 m^3/s by the estimate of effective precipitation and GRC equal to 1, thus considering the runoff as null (Tab. 1).

Celico and de Riso (1978) estimated the mean annual GR for the period 1921÷1955 by rainfall and air temperature data of 15 meteorological stations and applying Thiessen and isohyetal methods, and Turc's formula. The mean annual GR was estimated varying between 8.50 and 9.20 m^3/s, depending on the spatialization technique used and considering negligible the runoff (i.e., GRC equal to 1).

Allocca et al. (2014) estimate the mean annual GR for the period 1926÷2012 using for first time a GIS-based procedure and a methodological approach that considers the role of the aquifer lithology, cover soil type, land use, and endorheic areas. By a large dataset of meteorological stations and regional distributed models of precipitation and air temperature, the GR was estimated equal to 6.38 m^3/s, by the calculation of actual evapotranspiration by Turc's empirical formula and considering a GRC equal to 1 and 0.57 for endorheic and open slope areas, respectively (Tab. 1).

Ruggieri et al. (2021) estimate the mean annual GR for the period 2000÷2014 by ground-based hydrological and satellite data. By a GIS-based procedure and regional regression models of precipitation and air temperature, the GR was estimated equal to 6.74, 5.97, 5.46, and 5.53 m^3/s by means of the empirical formulas of Coutagne (1954), Turc (1954), Thornthwaite and Mater (1955) and MODIS data, respectively, and considering a GRC equal to 1 and 0.57 for endorheic and open slope areas as described in Allocca et al. (2014).

Based on these estimates, the mean annual Specific Groundwater Recharge (SGR) of Avella Mts. varies from 0.016 to 0.037 $m^3/s/km^2$ (Tab. 1).

All other hydrological data and relative scale of analysis, different methods and results of water balances have been summarized in Table 1.

References	Water balance	Area (km^2)	Scale of analysis	Period	No. of stations		P (mm)	T (°C)	AET (mm)	GR (mm)	GRC	GR (m^3/s)	SGR ($m^3/s/km^2$)
					P	T							
Civita et al. (1970)	1	361	1:200,000	1968÷1969	11	7	1,842	14.3	740	1,161	1	13.30	0.037
Celico and de Riso (1978)	2	360	1:300,000	1921÷1955	15	7	1,339÷1,477 (1,408**)	13.5	590÷638 (614**)	790	1	8.50÷9.20 (8.85**)	0.024÷0.026 (0,025**)
Allocca et al. (2014)	3	334	1:250,000	1921÷2012	387*	228*	1,437	12.7	454	602	1÷0.57	6.38	0.019
Ruggieri et al. (2021)	4	334	1:250,000	2000÷2014	266*	150*	1,476	13.6	660 (C) 692 (T) 747 (TM) 711 (M) (703**)	636 (C) 564 (T) 515 (TM) 522 (M) (559**)	1÷0.57	6.74 (C) 5.97 (T) 5.46 (TM) 5.53 (M) (5.93**)	0.020 (C) 0.018 (T) 0.016 (TM) 0.017 (M) (0.018**)

Table 1 - Summary table of previous water balances of Avella Mts.. P, mean annual precipitation; T, mean annual air temperature; AET, mean annual actual evapotranspiration; GR, mean annual groundwater recharge; GRC, Groundwater Recharge Coefficient; SGR, mean annual Specific Groundwater Recharge (mean annual groundwater recharge for unit area); * No. of stations used to reconstruct distributed models of P and T at the regional scale; (C) Coutagne; (T) Turc; (TM) Thornthwaite-Mather; (M) MODIS; (**) average value

Data and methodology

In the Figure 16 is shown a flowchart containing the sources, input data, processing, and outputs to develop the novel conceptual hydrogeological model and the twofold water balance.

All data and each step of performed procedures are described in the following paragraphs.

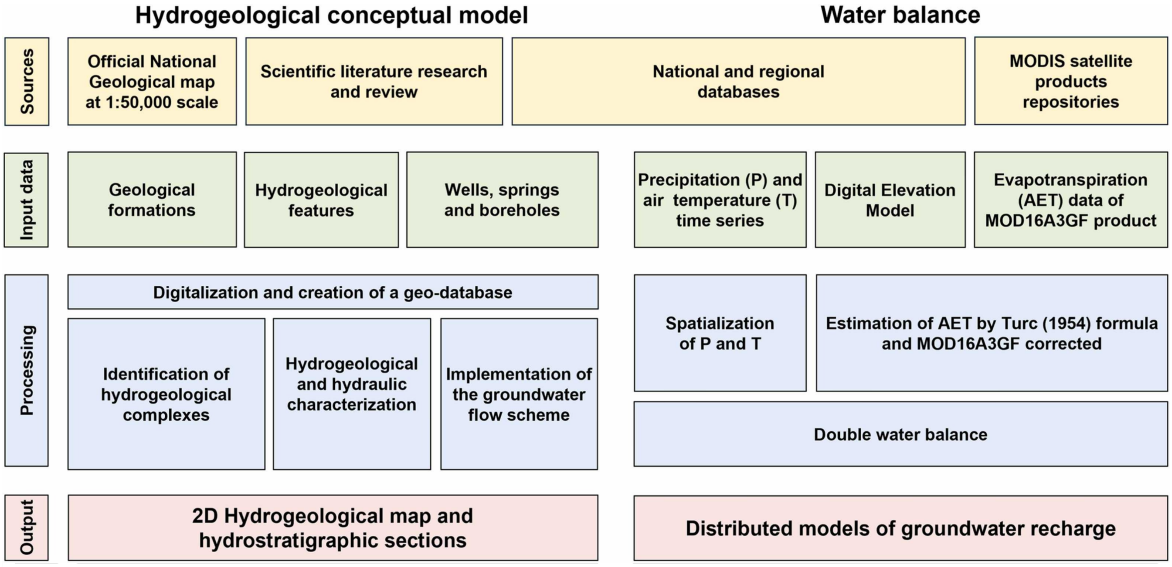


Figure 16 – Flow chart showing the workflow developed for the definition of the hydrogeological conceptual model and water balance of Avella Mts.

Geological and hydrogeological data

By a GIS-based procedure, a novel hydrogeological conceptual model of Avella Mts. was implemented using new and open-sources geological data of the CARG project (Sheets No. 431, 432, 448, 449, 466, 467, 485; ISPRA, 2017), literature data, field measurements, as well as unpublished stratigraphic, spring and piezometric data contained in institutional archives and national databases.

All sources and data collected (Tab. 2) was stored in a hydrogeological geospatial database. Using a WGS84-UTM33N projected coordinate system during the processing phase (Fig. 16), all geological data were digitized in a CAD environment, assigning an ID code to each geological formation. In accordance with the method described in De Vita et al. (2018), the geological formations were divided based on sedimentation domain, lithology, structural and hydrogeological characteristics, age, and merged into hydrostratigraphic units (Maxey, 1964; Seaber, 1988). These hydrostratigraphic units, also referred to as hydrogeological

complexes (Celico, 1986), are defined as a series of lithotypes or formations with a proved spatial and structural unity, an analogous type of relative permeability and a permeability grade ranging in a restricted interval. Thus, to each hydrogeological complex a type and grade of porosity and relative permeability, range of hydraulic conductivity (Freeze and Cherry, 1979; Civita, 2005) and hydrogeological role were assigned.

For the first time, an unreleased groundwater flow scheme was implemented by a piezometric contour map of the basal water table. This represents a novelty for the Avella Mts. and, in general, for southern Italy, if considering the lack of piezometric data in the inner part of mountainous karst aquifers. In total, hydraulic heads data of eight basal springs and two hundred and twelve wells and boreholes (Fig. 13d) were acquired during a new census and piezometric investigations carried out in the period 2019÷2020, measuring: i) geographic coordinates and elevation of springs and wells (m a.s.l.) by a portable differential GPS (K9 Series RTK, KOLIDA Instrument, China), and ii) depth of piezometric levels (m b.g.l.) in public and private wells using a water level indicator (BFK-100 model, PASI, Italy). The field measurements were integrated with available data from online national database (http://portalesgi.isprambiente.it/), institutional archives and literature data. All piezometric data (Figs. 13b and 13d) were interpolated and spatialized through the Triangulated Irregular Network method, using SURFER software.

Moreover, an in-depth census of the high-altitude springs and a mapping of surface karst landforms was carried out, by an analysis of digital regional technical cartography at the scale 1:5,000, supported by field survey and uploading the literature data and inventory of karst caves of Campania region (http://www.fscampania.it/catasto-2/catasto/).

All geological and hydrogeological data were merged into a novel hydrogeologic conceptual model (Fig. 17), represented by a hydrogeological map at the scale 1:50,000 and two hydrostratigraphic sections reconstructed based on literature data and new boreholes.

Updated water balance

The mean annual GR was estimated by an updated water balance for the 2000÷2019 period, starting from the following equation (Eq. 1):

$$P = AET + R + GR \pm \Delta Wr \quad (1)$$

where P (mm/y) is mean annual precipitation, AET (mm/y) is the mean annual actual evapotranspiration, R (mm/y) is the mean annual runoff, GR (mm/y) is the mean annual GR, and $\pm\Delta Wr$ (m^3) is the inter-annual variation of groundwater reserves, the latter considered negligible in the long-term timescale.

Time series of precipitation and air temperature of 23 rain gauges and 11 air temperature stations (Fig. 18) were acquired from regional hydro-meteorological monitoring network of the Civil Protection of Campania Region. All sources and input data collected (Tab. 2) were stored in a hydrogeological database.

Two linear models for rainfall-altitude and air temperature-altitude relationship were reconstructed (Fig. 18) by a linear regression methodology, and applied on a DEM with a resolution of 10 m. Subsequently, the distributed models of mean annual precipitation and mean annual air temperature were upscaled at a resolution of about 500 m, likewise the actual evapotranspiration and groundwater recharge.

In order to make a comparison between previous and new results, the AET has been estimated empirically by Turc's (1954) formula (Eq. 2):

$$AET = \frac{P}{\sqrt{0.9+\left(\frac{P}{300+25T+0.05T^3}\right)^2}} \quad (2)$$

where P (mm/y) and T (°C) are the mean annual precipitation and mean annual air temperature, respectively. A value of AET equal to 0 was assigned to non-vegetated areas, identified by the Corine Land Cover (2018) dataset at the 1:250,000 scale of the Copernicus Land Monitoring Service (https://land.copernicus.eu/en) and verified through satellite images from Google Earth.

Moreover, the AET was evaluated by the Terra Moderate Resolution Imaging Spectroradiometer (MODIS) dataset which includes meteorological variables, land cover and soil type. The product employed was MOD16A3GF v061 (Running et al., 2021) available at native resolution of 500 m, which provides data generated by an algorithm based on the Penman-Monteith equation (Monteith, 1965). The yearly AET maps were downloaded, converted to tiff format, and reprojected to WGS84-UTM33N system, using a R package named MODIStsp (Busetto and Ranghetti, 2016). Each raster underwent processing in according to the user's guideline of the MOD16A3GF product (Running et al.,

2021), assigning a value equal to 0 for non-vegetated areas or with low-quality acquisition, and converting the unit of measure from kg/m^2/y to mm/y. The mean annual AET raster was computed as arithmetic average of yearly AETs.

Lastly, starting from the general water balance equation (1), the mean annual GR has been estimated empirically by following formula (Eq. 3):

$$GR = (P - AET) \times GRC \quad (3)$$

where GRC (dimensionless) is groundwater recharge coefficient, equal to 0.57 to open slopes with a slope angle greater than 5° (Allocca et al., 2014), while equal to 1 and 0 to endorheic and urban *impervious* areas, respectively. The outputs were two distributed models of mean annual GR calculated by both AET estimations (Fig. 16). Coupled use of terrestrial and satellite data was found to be an attractive approach, reducing uncertainties, and having a mutual control in the estimate of groundwater recharge.

Results

Hydrogeological conceptual model

In Table 2 and Figure 17 the summary of the novel hydrogeological conceptual model is presented.

At the 1:50,000 scale, it was possible to recognize 15 hydrogeological complexes belonging to four hydrogeological domains, 13 of which are outcropping and two buried (see section A-A', B-B' and C-C' in Fig. 17). In chrono-stratigraphic order, Table 2 provides a description of the lithology, age, grade and type of relative permeability, literature hydraulic conductivity, role, extension of each hydrogeological complex and, in simple form, the type of groundwater. Among the outcropping complexes, limestone-dolomite complex (ID 12) of the Mesozoic-Cenozoic Apennine platform domain is the most representative, covering 33.3% of the area. It is followed by the pyroclastic deposits (ID 6), limestone (ID 10), detrital (ID 4) and pyroclastic-alluvial complex with extensions of 27.6%, 19.5%, 9.0% and 4.6%, respectively. The hydrogeological complexes with the smallest extensions include eluvial-colluvial (ID 1), lacustrine and marshy (ID 2), sandstone (ID 8), dolomite (ID 13) and marly limestone (ID 14) complexes, with coverages 2.7%, 1.3%, 0,9%, 0,3% and 0,3%, respectively. In relation to the total surface (approximately 370 km^2), the hydrogeological complexes characterized by high (52.8%), medium (45.5%) and low (1.3%) degrees of

relative permeability occupy areas of about 195, 168, and 4.80 km^2, respectively. Among the outcropping hydrogeological complexes, the aquifers (94.4%), aquitards (1.5%), and aquicludes (1.2%) occupy areas of about 349.3, 5.5, and 4.4 km^2, respectively.

The Mesozoic-Cenozoic carbonate domain constitutes the basal aquifer, the turbiditic pre- and syn-orogenic deposits and Quaternary pyroclastic-alluvial deposits represent the lateral aquiclude and aquitard, respectively. The three hydrostratigraphic sections (see A-A', B-B' and C-C' in Fig. 17) show a thickness of about 2800 m and the deep geometry of the carbonate succession, tectonically juxtaposed with lower permeability units belonging to the domains of Lagonegro-Molise Basin and turbiditic pre- and syn-orogenic deposits.

Locally, some direct and inverse fault systems in north-eastern sector act as semipermeable barriers to groundwater flow directed towards the springs, establishing a typically basins-in-series system.

The piezometric contour lines of the groundwater model (Fig. 17) shows an unconfined basal flow oriented towards the north-western, southern, and south-eastern edges. The water table is very deep, reaching up to about 1300 m b.g.l., with values variable approximately between about 350 and just below 30 m a.s.l.. Hydraulic gradients range from 6.32×10^{-4} to 1.03×10^{-1} with an average value of 2.01×10^{-2}; the highest values correspond to a groundwater drainage zone located in the central sector of the massif.

Due to the occurrence of groundwater divides, which partially coincide with a synclinal and anticlinal fold system (Fig. 17), five groundwater basins are delineated with distinct natural groundwater outlets. In addition to the groundwater basins of the Cancello, S. Maria La Foce, Mercato, Palazzo, S. Marina di Lavorate and S. Mauro springs, two new groundwater basins were recognized. Their subsurface outflow is directed towards the pyroclastic-alluvial deposits of the Campanian plain through the locally highly transmissive piedmont karst aquifer of the Baiano valley (Fig. 17). Moreover, in the southern sector an interaction between the groundwater of the Solofrana plain and karst aquifer is certainly possible, in agreement with previous studies (Celico, 1983; Celico et al., 1980).

Currently, the active basal springs are S. Maria La Foce, Palazzo, Cerola, S. Marina di Lavorate, Laura and Labso springs, while those continuously monitored since 2021 by GORI SpA are only S. Maria La Foce and S. Marina di Lavorate, whose average discharge is equal to 1.70 m^3/s and 1.80 m^3/s, respectively.

In contrast, Mefito, Calabricito, Mercato and S. Mauro springs have been completely dry since the 1980s and 1990s, although Calabricito spring has been partially and temporarily reactivated in 2013 with a flow rate up to about 0.01 m^3/s. In accordance with Meinzer's classification (Meinzer, 1923; 1927) these basal springs are classified as "cold gravity springs" of second and third magnitude, being the average discharge rate variables from 0.1 to 10 m^3/s. Within the spring groundwater basins, a sub horizontal and laminar flow is present, that near springs is slightly ascending and oriented towards the Quaternary alluvial-pyroclastic deposits (see sections in Fig. 17). Due to their deep reservoir geometry, these spring basins contain significant volumes of groundwater reserves, in addition to the dynamic groundwater resources annually discharged by the springs.

In addition to basal springs, 137 high-altitude springs were censused, mainly located in the central and northern sectors (Fig. 17) at altitudes ranging from 160 and 1300 m a.s.l. and characterized by maximum discharges up to 0.040 m^3/s and seasonal and perennial regimes. Based on Springer and Stevens (2009) classification, these are hanging and multi-habitat springs emerging from perched and unconfined aquifers in the limestone and limestone-dolomite complexes, and subordinately in detrital and pyroclastic deposits. Fed by a gravity-driven laminar flow, these springs are characterized by restricted dynamic groundwater resources, while the static deep reserves are not available. The genesis of these perched springs is controlled by stratigraphic and structural contacts within carbonate bedrock (e.g., the layer of Orbitolina marly limestone, and faults), as well as vertical variations of hydraulic conductivity within of the "pyroclastic soil-epikarst-carbonate bedrock" system (De Vita et al., 2003; Celico et al., 2010). This surficial heterogeneous system, acting as a temporary water storage tank, regulates the infiltration and evapotranspiration processes in the soil-plant-atmosphere system.

Well-developed karst landforms, such as endorheic areas, sinkholes, caves, and swallow holes, are mainly located in the southern sector. These karst forms exert significant control over groundwater recharge and transport of pollutants towards the springs; additionally, they influence ground instabilities, locally representing a new geohazard (e.g., flooding, soil collapse phenomena) in a karst environment already known for a high risk of landslide, sinkhole, and subsidence (Santo et al., 2018; 2019; Valente et al., 2021).

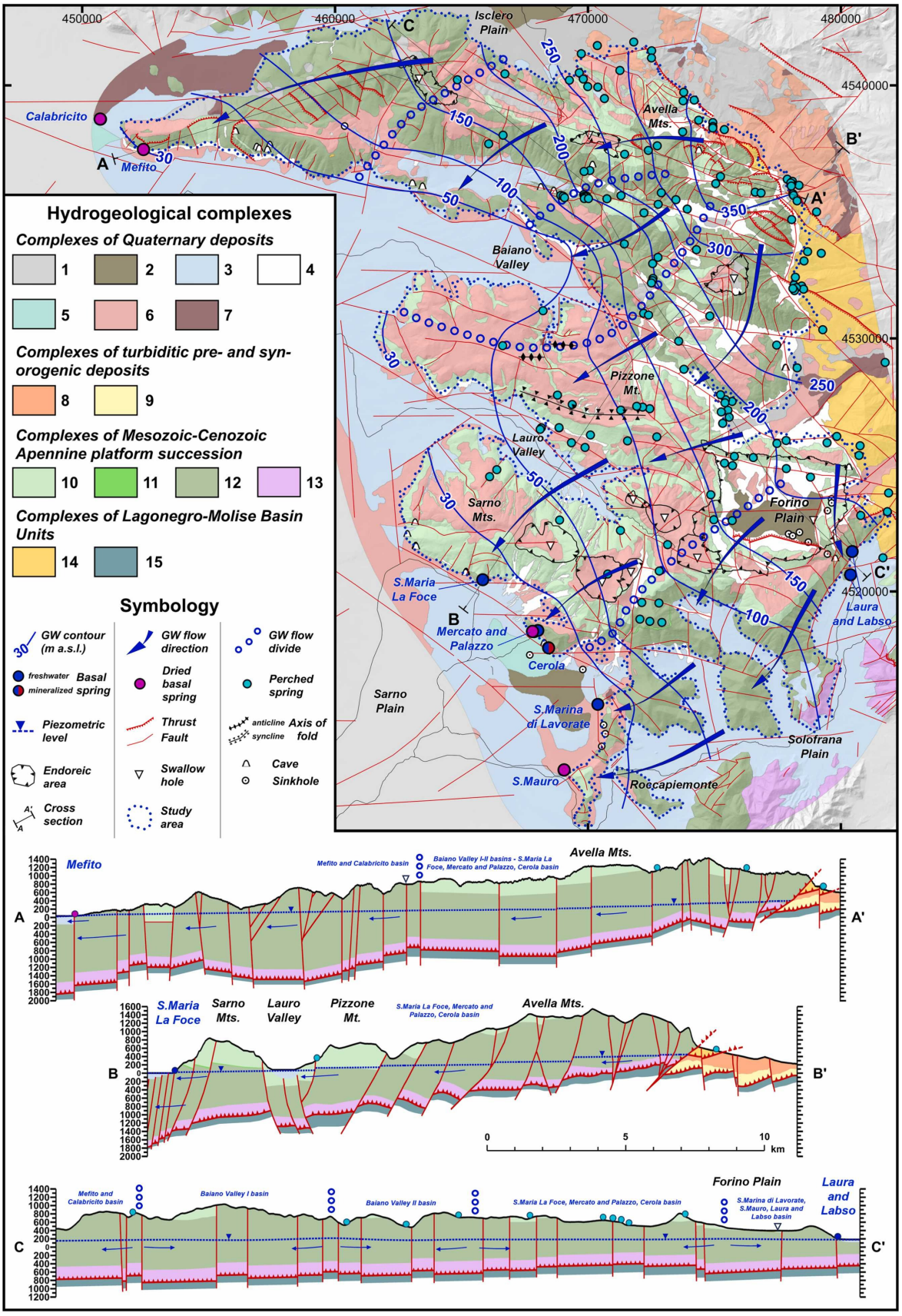


Figure 17 – Novel hydrogeological conceptual model of Avella Mts.

Hydrogeological domain	Hydrostratigraphic unit/ Hydrogeological complex			Degree and type of relative permeability	Hydraulic conductivity (m/s)	Hydrogeological role	GW type	Area (% of total)
	ID	Litology	Age					
Quaternary deposits	1	Eluvial-colluvial	Holocene-Present	Medium (P)	$10^{-9}\div10^{-5}$	Aquitard	F_W	2.7
	2	Lacustrine and marshy	Early Pleistocene-Present	Medium (P)	$10^{-9}\div10^{-4}$	Aquifer/aquitard	F_W	1.3
	3	Pyroclastic-alluvial	Late Pliocene-Present	Medium (P)	$10^{-6}\div10^{-3}$	Aquifer	F_W	4.6
	4	Detrital	Late Pleistocene-Present	Medium (P)	$10^{-6}\div10^{-3}$	Aquifer	F_W	9.0
	5	Travertine	Holocene	Medium (P)	$10^{-6}\div10^{-3}$	Aquifer	F_W , locally M_W	< 0.1
	6	Pyroclastic deposits	Late Pleistocene-Holocene	Medium (P)	$10^{-9}\div10^{-3}$	Aquifer/aquitard	F_W	27.6
	7	Tuff	Late Pleistocene-Holocene	Low (P and F)	$10^{-9}\div10^{-4}$	Aquitard	F_W	0.1
Turbiditic pre- and syn-orogenic deposits	8	Sandstone	Late Miocene-Late Pliocene	Low (P and F)	$10^{-9}\div10^{-6}$	Aquiclude	\	0.9
	9	Argille Varicolori	Oligocene-Early Miocene	Low (P and F)	$10^{-10}\div10^{-7}$	Aquiclude	\	-
Mesozoic-Cenozoic carbonate platform succession	10	Limestone	Middle Jurassic-Early Miocene	Very high (F and K)	$10^{-3}\div1$	Aquifer	F_W , locally M_W	19.5
	11	Orbitolina limestone and marl	Early Cretaceous	Low (F)	$10^{-9}\div10^{-6}$	Aquitard	F_W	< 0.1
	12	Limestone-dolomite	Late Triassic-Late Cretaceous	Very high (F and K)	$10^{-3}\div1$	Aquifer	F_W , locally M_W	33.3
	13	Dolomite	Late Triassic-Early Jurassic	Medium (P and F)	$10^{-6}\div10^{-3}$	Aquifer	F_W , locally M_W	0.3
Lagonegro-Molise Basin Units	14	Marly limestone	Eocene-Early Miocene	Low (P and F)	$10^{-9}\div10^{-6}$	Aquiclude	\	0.3
	15	Siliceous-marly	Middle Triassic-Early Cretaceous	Low (P and F)	$10^{-10}\div10^{-7}$	Aquiclude	\	-

Table 2 – Hydrogeological domains, characteristics, and hydraulic properties of hydrogeological complexes of Avella Mts.. (P) Porosity; (F) Fracturing; (K) Karst; (FW) Freshwater; (MW) Mineralized water.

Updated water balance

At the aquifer scale, the study area is characterized by a homogeneous planimetric distribution of thermo-pluviometric stations (Fig. 18a). Conversely, an uneven altitude distribution was observed, as there is a lack of stations at altitudes higher than 800 m a.s.l. (Fig. 18b). The comparison between the hypsometric curve and the distribution of monitoring stations altitude shows that about 30% of the recharge area with altitudes ranging from 800 and 1600 m a.s.l., lacks rain gauges and air temperature stations. Notwithstanding this structural gap in the regional basic climate network, also observed in other carbonate areas of the southern Apennine (Allocca et al., 2014), two linear regression models were implemented for precipitation and air temperature with altitude (Figs. 6c and 6d), by the following equations with high statistical significance:

P (mm) =1,286×h (m a.s.l.) + 960.96 (R^2 = 0,85; Prob. F-Fisher<0.1 %), and

T (°C) = −0.0059×h (m a.s.l.) +16.871 (R^2 = 0.86 Prob. F-Fisher<0.1 %).

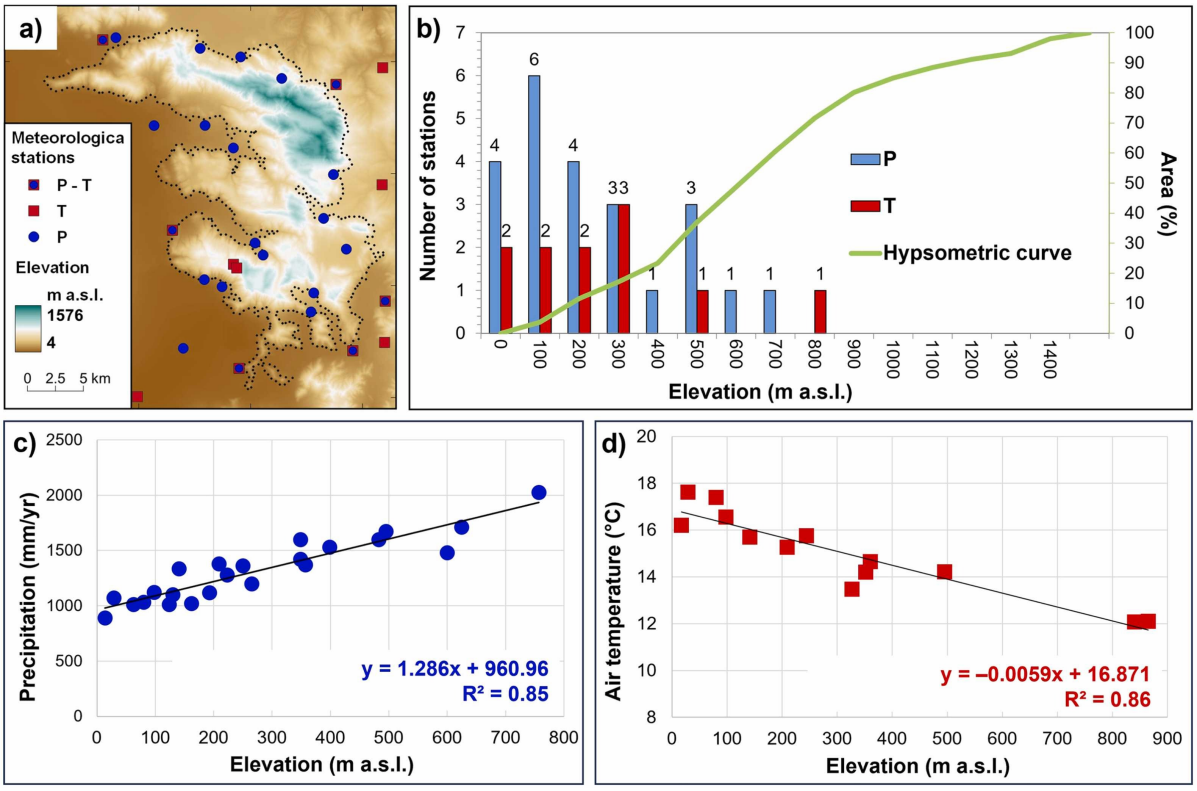


Figure 18 – a) Planimetric distribution of the meteorological stations network; b) Hypsometric curve and distribution of gauges with altitude; c) Linear regression model of mean annual precipitation (2000-2019 period); d) Linear regression model of mean annual air temperature (2000-2019 period).

The equations were applied to develop distributed models of the precipitation, air temperature (Fig. 19a and 19b), and AET by application of Turc (1954) formula (Fig. 19c).
The distributed models (Figs. 19a and 19b) show a variation of precipitation from a minimum value of 993 mm/y to a maximum of about 2970 mm/y, with a mean value about 1702 mm/y (Fig. 19a; Tab. 3), while air temperature ranges from 7,6 to 16,7 °C, with a mean annual value about 13,4 °C (Fig. 19b; Tab. 3).
In Figure 7c and 7d are reported both distributed models of AET estimated by Turc (1954) and MODIS satellite data. AET calculated by Turc (1954) formula varies from a minimum of 507 mm/y to a maximum of about 730 mm/y, with a mean value about 660 mm/y (Fig. 19c; Tab. 3), whereas estimated with MODIS satellite data varies from a minimum of 380 mm/y to a maximum of about 1100 mm, with a mean value about 725 mm/y (Fig. 19d; Tab. 3); in both cases, an AET value equal to 0 mm was assigned to urban areas or with absent vegetation. The variation ranges of AET with altitude and the differences in mean annual values depend on the approaches employed and spatial variability of air temperature, precipitation, and land use.
The GR values varies from 0 mm to 2449 mm (with a mean value about 622 mm), and from 0 mm to 2265 mm (with a mean value about 588 mm) with Turc (1954) formula and MODIS satellite data, respectively. The highest GR values are at the highest altitudes, endorheic areas or with lower soil thickness or absent, whereas the lowest values generally are in the piedmont or urbanized areas. Overall, for the entire karst aquifer was estimated a GR variable from about 7,30 m^3/s to 6,90 m^3/s, respectively by AET Turc (1954) formula and MODIS data, corresponding to mean annual SGR equal to about 0.020 $m^3/s/km^2$ for the period 2000-2019 (Tab. 3). The results of water balance obtained by both approaches are mutually comparable, thus confirming the validity of dataset and approaches used. The very slightly difference among the values is probably linked to the different structure of the satellite data, which in urban areas estimates locally a higher actual evapotranspiration rate (Figs. 19a and 19b) for the small public and private green areas.
The new estimate of GR is certainly reliable because carried out by a more detailed hydrogeological conceptual model and a data-based ground and satellite integrated approach, considering the land use, soil type and other geomorphological factors that control groundwater recharge.

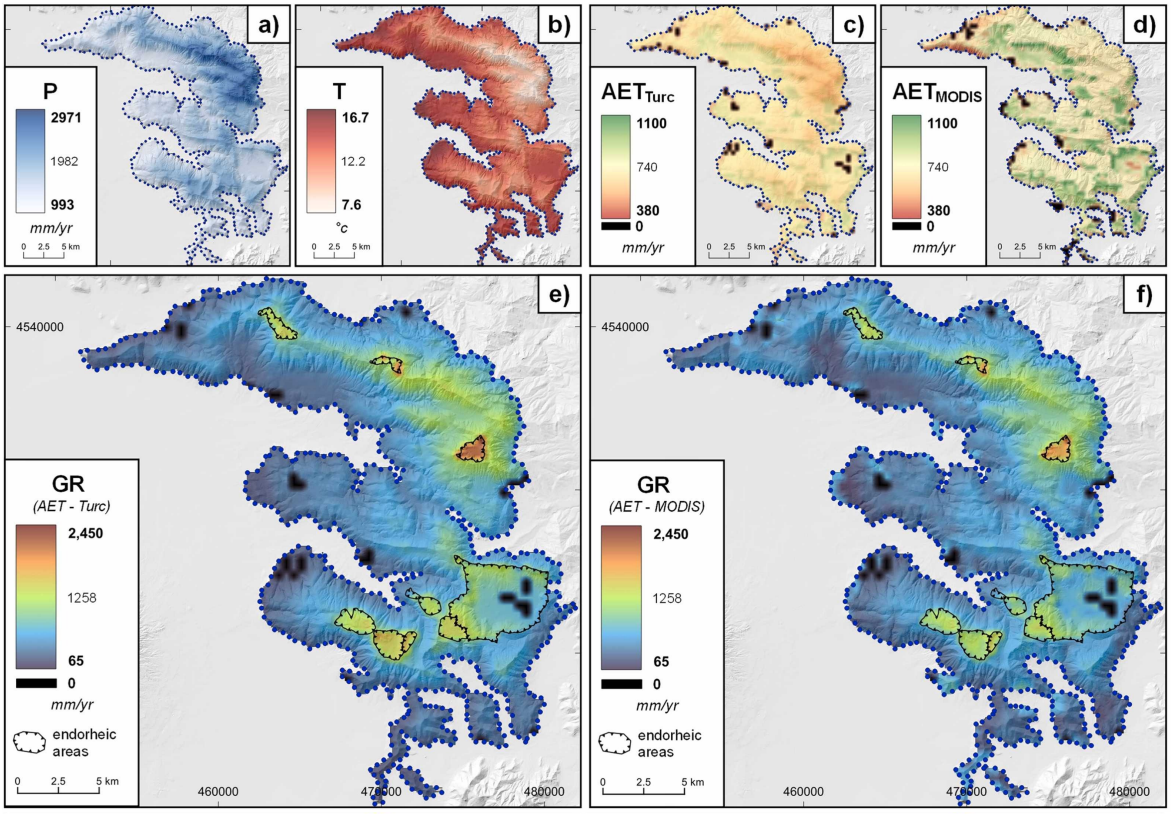


Figure 19 – Distributed models of: a) mean annual precipitation; b) mean annual air temperature; c) mean annual AET (Turc, 1954); d) mean annual AET (MODIS); e) mean annual GR (calculated by AET Turc); f) mean annual GR (calculated by AET MODIS).

Water balance	Method for EAT	Area (km^2)	Scale of analisys	Period	No. of meteorological stations		P (mm)	T (°C)	AET (mm)		GRC	GR (mm)		GR (m^3/s)		SGR ($m^3/s/km^2$)	
					P	T											
1	Turc (1954)	370	~ 500 m	2000÷ 2019	23	11	1,702	13.4	660	(693*)	0, 0.57 and 1	622	(605*)	7.30	(7.10*)	0.020	(0,020*)
2	MODIS data	370	~ 500 m	2000÷ 2019	23	11	1,702	13.4	725		0, 0.57 and 1	588		6.90		0.019	

Table 3 – Updated water balances of Avella Mts.. P, mean annual precipitation; T, mean annual air temperature; AET, mean annual actual evapotranspiration; GRC, groundwater recharge coefficient; GR, groundwater recharge; SGR, mean annual Specific Groundwater Recharge; (*) average value.

Discussion

The comparison between the preceding literature and new hydrogeological schemes (Figs. 20a, 20b and 20c) shows substantial differences and changes. The differences are linked not only to the more detailed analysis scale, but also to a new geological and hydrogeological dataset that allowed to define groundwater flow path and extension of groundwater basins of springs.

In disagreement with Civita et al. (1973), along the north-eastern edge the basal springs are absent, because the water table is very deep and barred by tectonic contact with turbiditic pre- and syn-orogenic deposits. The springs incorrectly interpreted as basal springs are fed by shallow lateral outflow within both Mesozoic-Cenozoic carbonate sequence and permeable detrital deposits overlying the turbiditic pre- and syn-orogenic units.

Unlike previous schemes, the carbonate hydrostructure is divided into five groundwater basins (Fig. 20c). This new aquifer compartmentalization highlights that Cancello spring group, S. Maria La Foce and Palazzo springs have dimensionally smaller groundwater basins (Fig. 20c) as well as S. Marina di Lavorate and S. Mauro springs fed by an autonomous groundwater basin which includes the small limestone relief near the town of Roccapiemonte (Figs. 17 and 20c). Instead, it is quite clear that the total disappearance of some basal springs (e.g. Mefito, Calabricito, Mercato and S. Mauro springs) is due to mainly anthropogenic factors linked to excessive exploitation of the aquifer at the local scale (Figs. 13d, 14 and 20c), as probably also the decrease in the average flow rate of the S. Maria La Foce spring, from 2.60 m^3/s measured in the 1960s÷1970s (Celico, 1983; Allocca et al., 2007) to 1.70 m^3/s, recorded currently.

The comparison between the previous and new water balance (Fig. 20d) highlights significant differences and changes linked in addition to the scale of analysis, method and dataset used, also reduction in the precipitation and recharge, as well as increase of air temperature and actual evapotranspiration. The new estimate of GR variable between about 622 and 588 mm/y (mean value 605 mm/y) (Tab. 3; Figs. 19d and 20d), while the GR calculated by Civita et al. (1970) equal to 1200 mm/y (Tab. 13 e Fig. 20d) is probably overestimated, having used a maximum value of the GRC (equal to 1) and recorded a peak of annual precipitation in the 1968÷1969 hydrological year (Fig. 20d). More contained are the differences with other previous estimates carried out by Celico and de Riso (1978), Allocca et al. (2014) and Ruggieri et al. (2021) equal to about 790, 602 and 559 mm/y, respectively (Tab. 1; Fig. 20d). However, on the long term a decreasing trend of the mean

GR (from 1200, 790 mm to 605 mm/y) and mean annual SGR (from 0.037, 0.025 to 0.020 $m^3/s/km^2$) is observed (Fig. 20d). These trends are probably due to decadal and inter-annual variability of precipitation, teleconnected with the North Atlantic Oscillation (De Vita et al., 2012; Longobardi and Boulariah, 2022), and a change in rainfall regime, as well as increase in extreme rainfall events observed at the national and regional scale (e.g., Brunetti et al., 2004; Caporali et al., 2020; Capozzi et al., 2023; Avino et al., 2024) which certainly does not favor groundwater recharge processes.

The differences and changes found in the new conceptual model and water balance have important implications for current and future groundwater management, as well as waterwork systems security and groundwater-dependent ecosystems. In this new hydrogeological scenario under climate change (e.g., Bucchignani et al., 2016; Bonanno and Faggian, 2018; Faggian, 2021) and increasing human pressure, a change in groundwater management is fundamental to prevent further environmental changes for the springs, groundwater-dependent ecosystems and groundwater quality (Gleeson et al., 2012).

The current management is lacking in coordination between public bodies and private subjects. Moreover, is a priority to implement by local authorities the water user register or inventory which is currently missing or incomplete. Some next steps of the study were planned to assess of the current exploitation status of the aquifer. Automatic multiparametric (e.g., piezometric level, spring discharge, water temperature) monitoring stations were installed into the main springs tapping works, wells and well fields used for drinking water. Withdrawals data for private uses, partially collected from local authorities, will be integrated with new field surveys. This will allow validate the water balance and reduce uncertainty of the multi-approach estimations (Guardiola-Albert et al., 2015; Zekri et al., 2015) as well as to quantify the water stress degree of karst aquifer. In addition, numerical models in steady and transient state (e.g., SWB and SWAT) are in phase of implementation for the simulation of future scenarios considering different natural and anthropogenic forcings (e.g., decrease of rainfall and recharge, increase of groundwater abstractions, environmental needs).

A comprehensive hydrogeological conceptual model and the integration of regional climate models and numerical simulation could support decision-makers in groundwater management (Nayak et al., 2015; Mamo et al., 2021; Singh et al., 2019; Brussolo et al.,

2022), also to predict possible water crisis scenarios and establish a multiscale aquifer exploitation threshold.

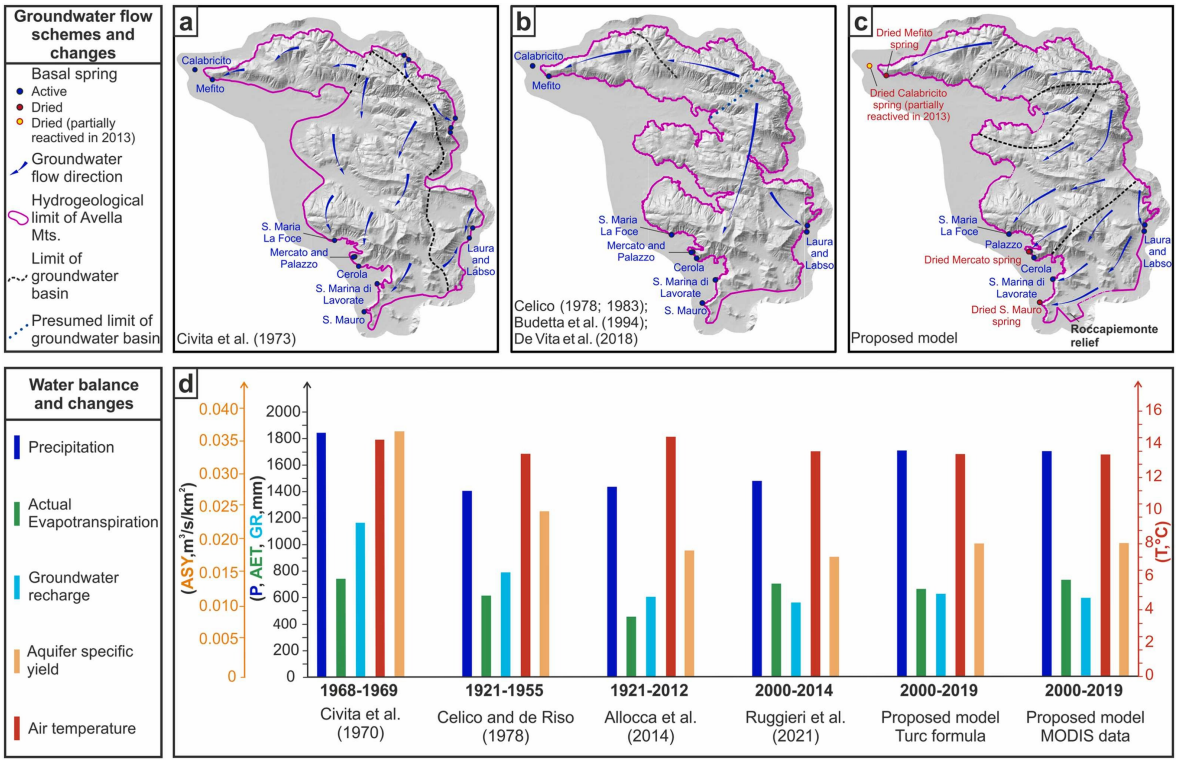


Figure 20 – Comparison between previous schemes a) Civita et al. (1973); b) Celico (1978; 1983); Budetta et al. (1994); De Vita et al. (2018); and c) proposed hydrogeological model; d) Comparison between previous and proposed water balances.

Conclusions

Based on a systematic literature review and new geological and piezometric data, in this study we propose a novel hydrogeological conceptual model of Avella Mts. at the 1:50,000 scale, and a double estimate of groundwater recharge carried out by ground-based hydrological and remote sensing data referred to the period 2000÷2019.

The main results related to the new hydrogeological conceptual model and the updated water balance are summarized as follows:

- 15 hydrogeological complexes belonging to 4 hydrogeological domains have been identified.
- Limestone-dolomite complex (ID 12) of the Mesozoic-Cenozoic Apennine platform domain is the most representative (33.3% of the area).

- Hydrogeological complexes (ID 10, 12 and 13) of the Mesozoic-Cenozoic carbonate domain constitutes the basal aquifer, while the turbiditic pre- and syn-orogenic deposits and Quaternary pyroclastic-alluvial deposits represent the lateral aquiclude and aquitard, respectively.
- The local pattern of the tectonic discontinuities determines a typically basins-in-series system for the deep structure of the aquifer, also influencing the basal groundwater flow which is mostly oriented towards the north-western, southern, and south-eastern edges of the massif.
- groundwater basins are recognized and 3 of them feed basal springs tapped for drinking water demand by different aqueduct systems; these basal springs are affected by a decrease in discharge rate comparing to historical data due to natural and anthropogenic factors.
- In addition to basal springs, 137 high-altitude springs are mainly located in the central and northern sectors of the massif fed by local perched (epikarst, detrital and pyroclastic) aquifers.
- The estimated groundwater recharge of the whole aquifer is variable from about 7,30 m^3/s to 6,90 m^3/s corresponding to a mean annual SGR equal to 0.020 $m^3/s/km^2$; the highest values of infiltration are at the highest altitudes, endorheic areas or with lower soil thickness or absent.

The new hydrogeological conceptual model, along with the updated estimation of groundwater recharge, provide a fundamental basis for: (i) supporting regional and local water authorities in the sustainable management of this strategic aquifer for health, economy, and environment of a large area of Campania region, and (ii) evaluating of the effects of climate change on groundwater recharge, and increasing human pressure on groundwater resource.

CRediT authorship contribution statement

Paola Petrone: Data curation, Formal analysis, Methodology, Software, Validation, Writing – original draft; **Silvio Coda:** Data curation, Formal analysis, Methodology, Software, Validation, Writing – original draft; **Palmira Marsiglia**: Data curation, Formal analysis, Methodology, Software, Validation, Writing – original draft; **Pasquale Allocca:** Data curation, Formal analysis, Methodology, Software, Validation; **Delia Cusano:** Data curation,

Formal analysis, Methodology, Software, Validation; **Pantaleone De Vita:** Resources, Data curation, Formal analysis, Investigation, Methodology, Validation, Supervision, Writing – original draft, Writing – review & editing**; Daniele Lepore:** Data curation, Software, Methodology**; Vincenzo Allocca:** Resources, Conceptualization, Data curation, Formal analysis, Investigation, Methodology, Supervision, Validation, Writing – original draft, Writing – review & editing, Project administration.

Declaration of Competing Interest

The authors declare that they have no known competing financial interests or personal relationships that could have appeared to influence the work reported in this paper.

Data availability

Data will be made available on request.

Acknowledgements

The research was undertaken and funded within Research Agreement entitled "*Convenzione di Studio, Ricerca e Supporto tecnico-scientifico relativa alle Sorgenti e opera di captazione di S. Maria la Foce, Mercato-Palazzo, S. Marina di Lavorate e San Mauro (Sarno e Nocera Inferiore – SA) e di Suppezzo (Castellammare di Stabia – NA)*" (Scientific Coordinator: V. Allocca; D. Calcaterra; P. De Vita) signed in July, 2019 (Prot. 2019/0081394 del 30/07/2019, Dipartimento di Scienze della Terra, dell'Ambiente e delle Risorse) between the Department of Earth Sciences, Environment and Resources, University of Naples Federico II and the GORI SpA. This research was also supported by the Earth Science, Environment and Resources, PhD Program of the University of Naples Federico II (XXXIV and XXXVII cycle). The authors thank the Editor and three anonymous reviewers for their precious comments and suggestions.

References

Allocca, V., Celico, F., Celico, P., De Vita, P., Fabbrocino, S., Mattia, S., Monacelli, G., Musilli, I., Piscopo, V., Scalise, A. R., Summa, G., and Tranfaglia, G., 2007. Illustrative Notes of the Hydrogeological Map of Southern Italy. Istituto Poligrafico e Zecca dello Stato, Rome, 1–211, ISBN 88-448-0223-6.

Allocca, V., Aquino, S., Esposito, L., Celico, P., 2008. The groundwater of the Irpinia area (Southern Italy). Current Knowledge and Future Perspectives. L'ACQUA, 6/2008-39-66.

Allocca, V., Manna, F., De Vita, P., 2014. Estimating annual groundwater recharge coefficient for karst aquifers of the southern Apennines (Italy). Hydrology and Earth System Sciences, 18(2), 803–817.

Allocca, V., De Vita, P., Manna, F., Nimmo, J. R., 2015. Groundwater recharge assessment at local and episodic scale in a soil mantled perched karst aquifer in southern Italy. Journal of Hydrology, 529, 843–853.

Allocca, V., Marzano, E., Tramontano, M., Celico, F., 2018. Environmental impact of cattle grazing on a karst aquifer in the southern Apennines (Italy): Quantification through the grey water footprint. Ecological Indicators, 93 (2018) 830-837.

Avino, A., Cimorelli, L., Furcolo, P., Noto, L.V., Pelosi, A., Pianese, D., Villani, P., Manfreda, S., 2024. Are rainfall exstremes intensifying in Southern Italy? Journal of Hydrology, https://doi.org/10.1016/j.jhydrol.2024.130684.

Beck, H. E., Zimmermann, N. E., McVicar, T. R., Vergopolan, N., Berg, A., Wood, E. F., 2018. Present and future Köppen-Geiger climate classification maps at 1-km resolution. Scientific Data, 5, Article 180214. https://doi.org/10.1038/sdata.2018.214.

Ben Saad, E., Ben Alaya, M., Taupin, J.D., Patris, N., Chaabane, N., Souissi, R., 2018. A Hydrogeological Conceptual Model Refines the Behavior of a Mediterranean Coastal Aquifer System: A Key to Sustainable Groundwater Management (Grombalia, NE Tunisia). Hydrology 2023, 10, 180. https://doi.org/10.3390/hydrology10090180.

Bonanno, R., Faggian, P., 2018. Changes in the precipitation regime over the Italian Peninsula and their possible impacts on the electric system. Tethys J. Mediterr. Meteorol. Climatol. 2018, 15, 18–30.

Brunetti, M., Maugeri, M., Monti, F., Nanni, T., 2004. Changes in daily precipitation frequency and distribution in Italy over the last 120 years. J. Geophys. Res. 2004, 109, D05102.

Brussolo, E., Palazzi, E., von Hardenberg, J., Masetti, G., Vivaldo, G., Previati, M., Canone, D., Gisolo, D., Bevilacqua, I., Provenzale, A., & Ferraris, S., 2022. Aquifer recharge in the Piedmont Alpine zone: Historical trends and future scenarios. Hydrology and Earth System Sciences, 26(2), 407–427. https://doi.org/10.5194/hess-26-407-2022

Budetta, P., Celico, P., Corniello, A., de Riso, R., Ducci, D., Nicotera, P., 1994. Carta idrogeologica della Campania 1: 200.000 – Memoria illustrativa. Atti Convegno Int. Geoingegneria: "Difesa e Valorizzazione dei suoli e degli Acquiferi", 1994, 565-586, Torino.

Bucchignani, E., Montesarchio, M., Zollo, A.L., Mercogliano, P., 2016. High-resolution climate simulations with COSMO-CLM over Italy: Performance evaluation and climate projections for the 21st century. Int. J. Climatol. 2016, 36, 735–756.

Busetto, L., Ranghetti, L., 2016. MODIStsp: An R package for automatic preprocessing of MODIS Land Products time series. Computers & Geosciences, 97, 40-48, https://doi.org/10.1016/j.cageo.2016.08.020.

Caporali, E., Lompi, M., Pacetti, T., Chiarello, V., Fatichi, S., 2020. A review of studies on observed precipitation trends in Italy. Int. J. Climatol. 2021;41 (Suppl. 1):E1-E25, DOI: 10.1002/joc.6741.

Capozzi, V., Rocco, A., Annella, C., Cretella, V., Fusco, G., Budillon, G., 2023. Signals of change in the Campania region rainfall regime: An analysis of extreme precipitation indices (2002–2021). Meteorol. Appl., 2023, 30:e2168. https://doi.org/10.1002/met.2168.

Celico F., Naclerio G., Bucci A., Nerone V., Capuano P., Carcione M., Allocca V., Celico P., 2010. Influence of pyroclastic soil on epikarst formation: a test study in southern Italy. Terra Nova, 22, 110-115.

Celico, P., 1978. Schema idrogeologico dell'Appennino carbonatico centromeridionale. Memorie e Note Istituto di Geologia Applicata, Napoli 14, 1–97.

Celico, P., 1983. Idrogeologia dei massicci carbonatici, delle piane quaternarie e delle aree vulcaniche dell'Italia centromeridionale (Marche e Lazio meridionale, Abruzzo, Molise e Campania). Quaderni della Cassa per il Mezzogiorno 4 (2), 1–203, Roma.

Celico, P., 1986. Prospezioni idrogeologiche. Vol. I, 1-735. Liguori Editore, Napoli, Italia. ISBN 88-207-1331-4.

Celico, P., de Riso, R., 1978. Il ruolo della Valle Caudina nella idrogeologia del Casertano e del Sarnese (Campania). Mem. e Note Ist. Geol. Appl, 14, 1–24.

Celico P., De Gennaro M., Ferreri M., Ghiara M., Russo D., Stanzione D., Zenone F., 1980. Il margine orientale della Piana Campana: indagini idrogeologiche e geochimiche. Period. Miner. 49, 241–270.

Chen, Z., Auler, A.S., Bakalowicz, M., Drew, D., Griger, F., Hartmann J., Jiang, G., Moosdorf, N., Richts, A., Stevanovic, Z., Veni, G., Goldscheider, N., 2017. The world karst aquifer mapping project: concept, mapping procedure and map of Europe. Hydrogeol J. 25(3):771–785.

Civita M., 2005. Idrogeologia applicata e ambientale. Casa Editrice Ambrosiana, 1-800. ISBN: 8808087417.

Civita M., de Riso R., Nicotera P., 1970. Sulla struttura idrogeologica alimentante le sorgenti del F. Sarno e le falde pedemontane profonde della parte sud-orientale della Conca Campana. Atti I Convegno Internazionale sulle Acque Sotterranee, IAH, 1-24. Palermo, 6-8 Dicembre 1970.

Civita M., dè Medici G.B., de Riso R., Nicotera P., Nota d'Elogio E., 1973. Memoria descrittiva della carta idrogeologica della Campania nord-occidentale. Atti II Convegno Internazionale sulle Acque Sotterranee, IAH, 1–39. Palermo, 28 Aprile-2 Maggio 1970.

Coutagne, A., 1954. Quelques considérations sur le pouvoir évaporant de l'atmosphere, le déficit d'écoulement effectif et le déficit d'écoulement maximum. La Houille Blanche 1954, 360–374.

Cusano, D., Coda, S., De Vita, P., Fabbrocino, S., Fusco, F., Lepore D., Nicodemo, F., Pizzolante, A., Tufano, R., Allocca V., 2023. Comparison of methods for assessing groundwater vulnerability in karst aquifers: the case study of Terminio Mt. aquifer (Southern Italy). Sustainable Environment Research (2023) 33:42. https://doi.org/10.1186/s42834-023-00204-8.

Cusano, D., Lepore, D., Allocca, V., De Vita, P., 2024. Control of soil mantle thickness and land cover types on groundwater recharge of karst aquifers in Mediterranean areas. Journal of Hydrology, 630 (2024) 130770.

De Vita, P., Agrello, D., Ambrosino, F., De Luzio, E., 2003. Caratterizzazione del sistema idrogeologico superficiale coltre piroclastica-substrato carbonatico nella dorsale dei Monti di Sarno (Campania). Quaderni di Geologia Applicata, 2/2003, 49-69.

De Vita, P., Allocca, V., Manna, F., Fabbrocino, S., 2012. Coupled decadal variability of the North Atlantic Oscillation, regional rainfall and karst spring discharges in the Campania region (southern Italy). Hydrology and Earth System Sciences, 16(5), 1389–1399.

De Vita, P., Allocca, V., Celico, F., Fabbrocino, S., Mattia, C., Monacelli, G., Musilli, I., Piscopo, V., Scalise, A.R., Summa, G., Tranfaglia G., Celico, P., 2018. Hydrogeology of continental southern Italy. Journal of Maps, 14:2, 230–241.

Faggian, P., 2021. Future Precipitation Scenarios over Italy. Water 2021, 13, 1335. https://doi.org/10.3390/w13101335.

Ford, D., Williams, P., 2007. Karst hydrogeology and geomorphology. John Wiley & Sons Ltd, Chichester, UK, 1-576, ISBN:9780470849965, DOI:10.1002/9781118684986.

Freeze, R.A., Cherry, J.A., 1979. Groundwater. Englewood Cliffs, New Jersey 07632: Prentice-Hall, Inc. ISBN 0-13-365312-9.

Fusco, F., Allocca, V., De Vita, P., 2017. Hydro-geomorphological modelling of ash-fall pyroclastic soils for debris flow initiation and groundwater recharge in Campania (southern Italy). Catena 2017, 158, 235–249.

Gleeson, T., Wada, Y., Bierkens, M. F. P., & van Beek, L. P. H., 2012. Water balance of global aquifers revealed by groundwater footprint. Nature, 488(7410), Article 7410. https://doi.org/10.1038/nature11295

Goldscheider, N., 2019. A holistic approach to groundwater protection and ecosystem services in karst terrains. Carbonates and Evaporites, 34(4), 1241–1249.

Goldscheider, N., Chen, Z., Auler, A.S., Bakalowicz, M., Broda, S., Drew, D., Hartmann, J., Jiang G., Moosdorf, N., Stevanovic, Z., Veni, G., 2020. Global distribution of carbonate rocks and karst water resources. Hydrogeology Journal (2020) 28:1661–1677.

Guardiola-Albert, C., Martos-Rosillo, S., Pardo-Igúzquiza, E., Durán Valsero, J. J., Pedrera, A., Jiménez-Gavilán, P., & Liñán Baena, C., 2015. Comparison of Recharge Estimation Methods During a Wet Period in a Karst Aquifer. Groundwater, 53(6), 885–895. https://doi.org/10.1111/gwat.12310

ISPRA, 2017. Geological maps of Italy, scale 1:50,000. Sheets 431, 432, 448, 449, 466, 467, 485. ISPRA – Istituto Superiore per la Protezione e la Ricerca Ambientale, Servizio Geologico d'Italia. Retrieved from http://www.isprambiente.gov.it/Media/carg/campania.html.

Lancia, M., Petitta, M., Zheng, C., Saroli, M., 2020. Hydrogeological insights and modelling for sustainable use of a stressed carbonate aquifer in the Mediterranean area: From passive withdrawals to active management. Journal of Hydrology: Regional Studies 32 (2020) 100749.

Longobardi, A., Boulariah, O., 2022. Long-term regional changes in inter-annual precipitation variability in the Campania Region, Southern Italy. Theoretical and Applied Climatology (2022) 148:869-879.

Mamo, S., Birhanu, B., Ayenew, T., & Taye, G., 2021. Three-dimensional groundwater flow modeling to assess the impacts of the increase in abstraction and recharge reduction on the groundwater, groundwater availability and groundwater-surface waters interaction: A case of the rib catchment in the Lake Tana sub-basin of the Upper Blue Nile River, Ethiopia. Journal of Hydrology: Regional Studies, 35, 100831. https://doi.org/10.1016/j.ejrh.2021.100831

Maxey, G.B., 1964. Hydrostratigraphic units. Journal of Hydrology, 1964, 2, 124-129.

Meinzer, O.E., 1923. Outline of ground-water hydrology, with definitions. U.S. Geological Survey Water-Supply Paper 494, 1-71, Washington DC.

Meinzer, O.E., 1927. Large springs in the United States. U.S. Geological Water-Supply Paper 557, 1-94, Washington DC.

Monteith, J.L., 1965. Evaporation and environment. Symposia of the Society for Experimental Biology, 19, 205–234.

Mu, Q., Zhao, M., Running, S.W., 2011. Improvements to a MODIS global terrestrial evapotranspiration algorithm. Remote Sensing of Environment, 115(8), 1781–1800.

Nayak, P. C., Wardlaw, R., & Kharya, A. K., 2015. Water balance approach to study the effect of climate change on groundwater storage for Sirhind command area in India. International Journal of River Basin Management, 13(2), 243–261. https://doi.org/10.1080/15715124.2015.1012206

Nicotera, P., Civita, M., 1969a. Ricerche idrogeologiche per la realizzazione delle opere di presa delle sorgenti Mercato e Palazzo in Sarno (Campania). Mem. e Note Ist. Geol. Appl. (1969), Vol. 11, 1-59, Napoli.

Nicotera, P., Civita, M., 1969b. Indagini idrogeologiche per la captazione delle sorgenti S. Marina di Lavorate (Sarno). Mem. e Note Ist. Geol. Appl. (1969), Vol. 11, 1-50, Napoli.

Penman, H. L., 1948. Natural evaporation from open water, bare soil and grass. Proceedings of the Royal Society of London. Series A. Mathematical and Physical Sciences, 193(1032), 120–145.

Running, S., Mu, Q., Zhao, M., Moreno, A., 2021. MODIS/Terra Net Evapotranspiration Gap-Filled Yearly L4 Global 500m SIN Grid V061 [Data set]. NASA EOSDIS Land Processes Distributed Active Archive Center. Accessed 2023-12-01 from https://doi.org/10.5067/MODIS/MOD16A3GF.061

Ruggieri, G., Allocca, V., Borfecchia, F., Cusano, D., Marsiglia, P., and De Vita, P., 2021. Testing Evapotranspiration Estimates Based on MODIS Satellite Data in the Assessment of the Groundwater Recharge of Karst Aquifers in Southern Italy. Water, 13(2), 118, 2021.

Springer, A.E., Stevens, L.E., 2009. Spheres of discharge of springs. Hydrogeology Journal (2009) 17: 83–93, DOI 10.1007/s10040-008-0341-y.

Santo, A., Prete, S., Giulivo, I., 2008. Nuove ipotesi sulla formazione dei piping sinkhole in aree alluvionali: il caso della piana di Forino (Avellino, Campania). Italian Journal of Quaternary Sciences, 21(2), 2008, 395-408.

Santo, A., Santangelo, N., De Falco, M., Forte, G., Valente, E., 2019. Cover collapse sinkhole over a deep buried carbonate bedrock: The case study of Fossa San Vito (Sarno - Southern Italy). Geomorphology 345 (2019) 106838, https://doi.org/10.1016/j.geomorph.2019.106838.

Seaber, P.R., 1988. Hydrostratigraphic units. In, Back, W., Rosenschein, J.R., Seaber, P.R., Hydrogeology: The Geology of North America. Geological Society of America, Volume O-2, ISBN 081375206X, DOI: https://doi.org/10.1130/DNAG-GNA-O2.

Singh, A., Panda, S. N., Uzokwe, V. N. E., & Krause, P., 2019. An assessment of groundwater recharge estimation techniques for sustainable resource management. Groundwater for Sustainable Development, 9, 100218. https://doi.org/10.1016/j.gsd.2019.100218

Sun, W., Song, J., Yang, W., Zheng, Y., Li, C., Kuang, D., 2020. Distribution of carbonate rocks and variation analysis of karst water resources in China. Carbonates and Evaporites (2020) 35:121 https://doi.org/10.1007/s13146-020-00657-7.

Thornthwaite, C.W., Mather, J.R., 1955. The Water Balance. Publ. Climatol., 1955, 8, 1–104.

Turc, L., 1954. Le bilan d'eau des sols: Relations entre les précipitations, l'évaporation et l'éecolument. Ann. Agron. 1954, 5, 491–595.

Tufano, R., Allocca, V., Coda, S., Cusano, D., Fusco, F., Nicodemo, F., Pizzolante, A., De Vita, P., 2020. Groundwater vulnerability of principal aquifers of the Campania region (southern Italy). Journal of Maps, 2020, 16:2, 565-576.

Valente, E., Allocca, V., Riccardi, U., Camanni, G., Di Martire, D., 2021. Studying a Subsiding Urbanized Area from a Multidisciplinary Perspective: The Inner Sector of the Sarno Plain (Southern Apennines, Italy). Remote Sens. 2021, 13, 3323. https://doi.org/10.3390/rs13163323.

Vitale, S., Ciarcia, S., 2018. Tectono-stratigraphic setting of the Campania region (southern Italy). Journal of Maps, 2018, 14(2), 9-21.

Zekri, S., Triki, C., Al-Maktoumi, A., & Bazargan-Lari, M. R., 2015. An Optimization-Simulation Approach for Groundwater Abstraction under Recharge Uncertainty. Water Resources Management, 29(10), 3681–3695. https://doi.org/10.1007/s11269-015-1023-x

4.2 A multiscale soil water balance for sustainable groundwater management of a local transboundary karst aquifer

Paola Petrone[1], Pantaleone De Vita[1], Pasquale Allocca[1], Silvio Coda[1*], Delia Cusano[1], Radka Kodešová[2], Daniele Lepore[1], Vincenzo Allocca[1*]

[1] Department of Earth, Environmental and Resources Sciences, Federico II University of Naples, Monte S. Angelo Campus, 21 Cinthia Street, Building 10, 80126, Naples, Italy.

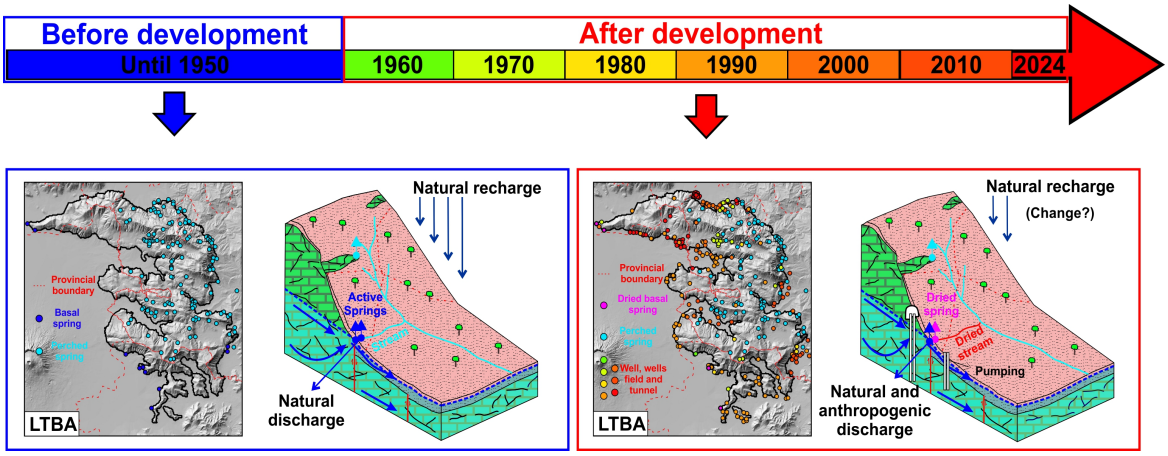
[2] Department of Soil Science and Soil Protection, Faculty of Agrobiology, Food and Natural Resources, Czech University of Life Sciences, Prague, Czech Republic.

[*] Corresponding authors: silvio.coda@unina.it; vincenzo.allocca@unina.it.

Abstract

Sustainable groundwater management of transboundary aquifers (TBAs) remains a major global and regional challenge that requires necessitating enhanced, coordination and cooperation among neighbouring countries and institutions. The Avella Mts. are a vital karst groundwater resource of the Campania region (Italy) and host a local TBA whose water balance equilibrium is increasingly threatened by uncontrolled growth in groundwater extraction and prolonged drought periods. A multiscale soil water balance was performed for the period 2010-2021 to assess the sustainability of current water withdrawals. The findings reveal a high spatio-temporal variability of recharge. At the aquifer scale, recharge average equal to 244.40 Mm^3/y, with interannual variability of about –45% and +73%. At the basin scale, recharge on average varies between 29.64 Mm^3/y and 100.28 Mm^3/y. The springs inventory map and authorised well registry highlight an outgoing groundwater volume of 252.30 Mm^3/y, at the aquifer scale, while at the basin scale, it varies between 6.30 Mm^3/y and 97.76 Mm^3/y, exceeding the recharge in certain basins. Consequently, there is a budgetary disequilibrium within the aquifer, which is particularly pronounced during drought years, as evidenced by the drying of springs and streams. These results highlight significant groundwater stress, which is projected to worsen in the future due to climate change. They demonstrate the urgent need to adopt sustainable groundwater management strategies and reform existing water governance model in the Campania region, as well as in other parts of Italy and Europe.

Graphical abstract



Highlights

1. A multiscale estimation of recharge was performed using the soil water balance code.
2. A first inventory of springs and a registry of authorised wells were implemented.
3. A multiscale comparison between recharge and discharge was carried out.
4. Results offer insights to support decision-makers in developing sustainable groundwater management policies.

Keywords: local transboundary aquifer, groundwater recharge, aquifer overexploitation, groundwater management.

Introduction

Transboundary aquifers (TBAs) are large groundwater basins (GBs) that cross national administrative boundaries, involving two or more states (IGRAC, 2021). Over 40% of the water resources worldwide are transboundary (Fig. 21a) crossing at least a binational border (IGRAC, 2021; Matherne and Megdal, 2023). Management of TBAs involves the cooperation of multiple and distinct jurisdictions with different languages, cultures, and traditions (Matherne and Megdal, 2023). Neighbouring states need deep knowledge of shared GBs and a strong sense of peaceful cooperation because changes in the quality and quantity of water resources can have transboundary effects, and lead to economic imbalances and international geopolitical issues (e.g., Tayia, 2019). While the delimitation and characterisation of shared river basins is relatively less complicated, TBAs require greater effort, making their governance more challenging due to the invisible nature of groundwater. In recent decades, significant progress (IGRAC, 2021; Matherne and Megdal, 2023) has been made in the occurrence, extent, description, and characterisation of TBAs in Africa, South America, Asia, and East Europe (Fig. 21a). However, data and information about TBAs for central-southern Europe, including Italy, are absent (Fig. 21b). In the Alps and along the entire border between Italy and neighbouring countries such as France, Switzerland, Austria, and Slovenia there are potentially transboundary groundwater bodies and shared water basins (e.g., Ticino, Adda and Isonzo rivers, and Maggiore and Lugano Lakes) that are currently unmapped and uncharacterised (Fig. 21c).

Based on European directives (e.g., Directive 2000/60/EC), the Italian institutional and normative framework of water governance (e.g., Law 183/1989; Legislative Decree no. 152/2006) states a management system based on river basins and divided into River Basin District Authorities. Water concessions, usually for a period of approximately 30 years, are provided independently by individual regional and sub-regional authorities (Royal Decree no. 1775/1933; Law no. 36/1994), upon obtaining the opinion of the district authority (Legislative Decree no. 152/2006). The provincial institutions have administrative competence for issuing water concessions for 'small volume derivations' (e.g., for irrigation < 1.0 m^3/s, others use < 0.1 m^3/s), while regional authorities are responsible for issuing concessions for 'large volume derivations' (e.g., for irrigation > 1.0 m^3/s, others use > 0.1 m^3/s), yet, the major Italian groundwater bodies are hosted in the large karst aquifers (e.g., maritime and southern Alps, central-southern Apennine) and in multi-layered porous

aquifers of extensive alluvial plains (e.g., Po river flood plain), whose hydrogeological boundaries extend beyond hydrographic boundaries and administrative borders of regional and provincial authorities (Figs. 21c and 21d). Consequently, due to this extremely fragmented water governance model based on administrative/hydrographic limits and non-hydrogeological boundaries, numerous regional transboundary aquifers (RTBAs) and local (provincial) transboundary aquifers (LTBAs) are present in Italy and elsewhere (Figs. 21c and 21d). In addition, the management of these RTBAs and LTBAs would require a concrete cooperation and coordination among regional and sub-regional authorities, comprehensive censuses and adequate controls of the number and characteristics of water abstraction licenses, which are currently not available, as well as an updated water balances. The lack of these prerequisites can easily favour the overexploitation of shared aquifers, causing effects on downstream ecosystems and leading to water crises for water supply systems. Considering that the central-southern Apennine is characterised by numerous RTBAs and LTBAs (Figs. 21c and 21d) and that the karst groundwater resources are a vital source for human consumption, the economy and the environment, increasing attention is needed to ensure water security and a good governance of shared groundwater.

By using the soil water balance code (Westenbroek et al., 2010), the aim of this study was to estimate the multiscale recharge of Avella Mts. for the 2010-2021 period and compare it with current water withdrawals to assess their sustainability. The Avella Mts. was selected as a representative case study of LTBA (Figs. 21d and 22) for the southern Apennine, whose groundwater resources provide drinking water supply for a significant part of the Campanian population.

The remaining part of the paper is structured as follows: Section 2 provides a description of the hydrogeological and climatic characteristics and groundwater development of the LTBA. Section 3 describes the methodology and input data used for soil water balance and water withdrawal estimation. Sections 4 and 5, respectively, comment on the results and provide their discussion. Finally, Section 6 reports the concluding remarks and recommendations.

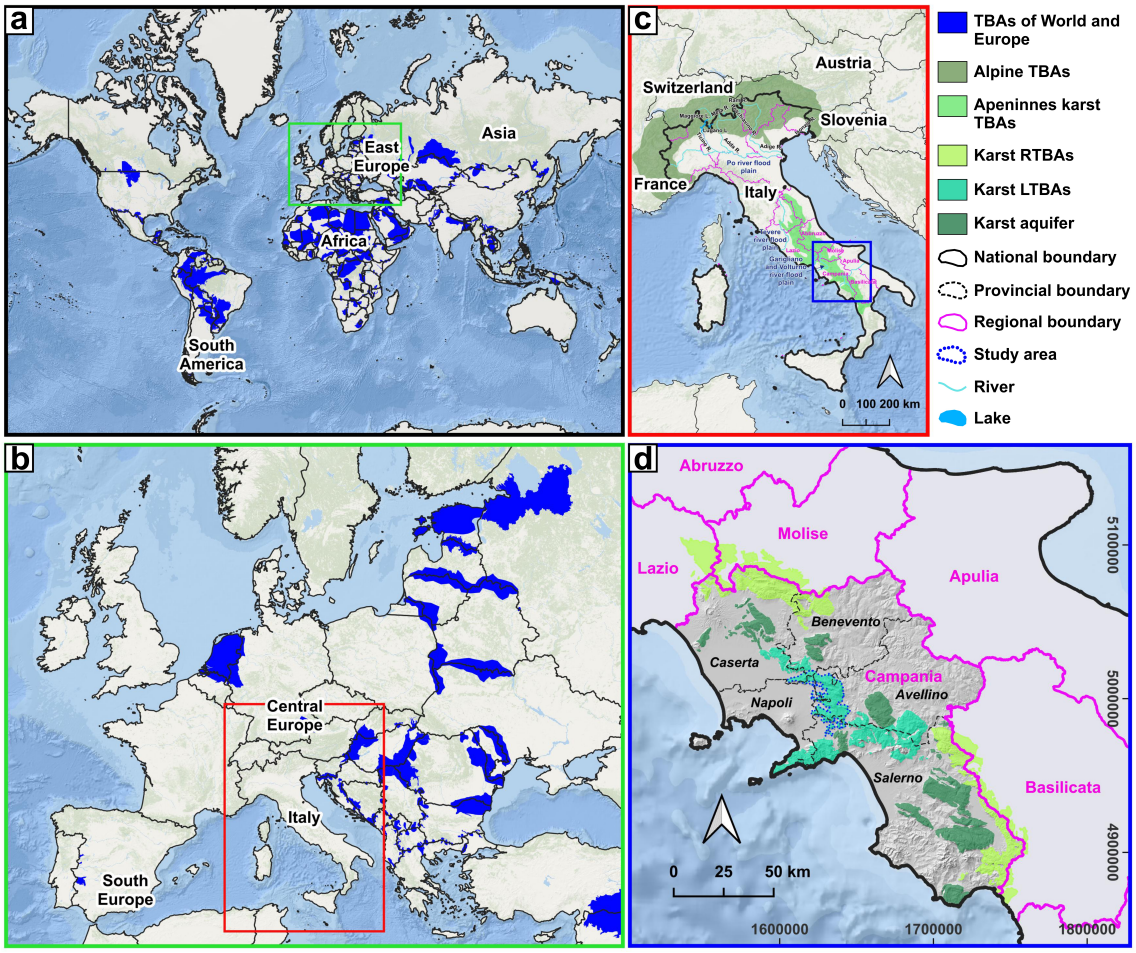


Figure 21 – a) Map of TBAs in the world (IGRAC, 2021, modified); b) Map of TBAs in Europe (IGRAC, 2021, modified); c) Map of potential Italian Alpine and Apennines TBAs; d) Map of karst RTBAs and LTBAs in Campania region.

The LTBA description

Hydrogeological and climatic characteristics

The Avella Mountains, extending approximately 370 km^2, are a large karst groundwater basin and host a LTBA whose hydrogeological limits cross the administrative boundaries of all five provinces of the Campania region (Fig. 22a).

Approximately 63% of the karst recharge area falls within the Avellino province, while 14%, 13.8%, 5.7% and 3.5% are distributed among the provinces of Salerno, Naples, Caserta, and Benevento, respectively (Fig. 22a). Conversely, approximately 85% of the main natural outflow, measured in the 1960s at approximately 9.50 m^3/s (Celico and de Riso, 1978; Celico, 1983; Allocca et al., 2007), emerges from basal springs located in the Salerno province, while 12% and 3% emerge in the Caserta and Naples provinces, respectively.

This large mountain system sustains a series of ecosystem services and regulates the hydrological regime of the Sarno, Regi Lagni, Isclero and Sabato rivers (Fig. 22a). A large site of community importance, two regional parks and natural ecosystems (e.g., forests, grasslands, springs, rivers and poljes) represent its diverse and extensive geo-and biodiversity (Petrone et al., 2024).

The aquifer is constituted by a Mesozoic-Cenozoic carbonate series of the Apennine platform domain belonging to the Lattari-Picentini-Avella Mts. units (Fig. 22a), while the turbiditic pre- and syn-orogenic deposits and Quaternary pyroclastic-alluvial deposits represent the lateral aquiclude and aquitard, respectively. Given the proximity to the Somma-Vesuvius volcano, the aquifer is covered (Fig. 22b) by alkali-potassic ash-fall pyroclastic deposits with a thickness of up to approximately 8 m where the slope angle is lower (up to 40°) and up to 50 m in endorheic areas (Fusco et al., 2017). Along the steep slopes, dense deciduous forests and transitional woodlands constitute the predominant types of land use and vegetation cover, while in the endorheic karst areas and in the piedmont sectors, agricultural areas (chestnuts and hazelnuts), natural grassland and subordinately urban areas are prevalent (Fig. 23d).

Direct and inverse faults, synclinal and anticlinal fold systems cause the horizontal compartmentalisation of the basal groundwater circulation in a typical basin-in-series system. Based on a detailed conceptual hydrogeological model (Petrone et al., 2024), five groundwater basins (GB) are identified (Fig. 22a): i) GB1 feeds the Cancello spring group, originally represented by Calabricito and Mefito springs (30 and 28 m a.s.l.); ii) GB2 and GB3 feed the pyroclastic-alluvial deposits of the Campanian plain and of the Baiano valley; iii) GB4 feeds the Sarno spring group, originally constituted by S. Maria La Foce (32 m a.s.l.), Mercato, Palazzo (26 and 24 m a.s.l.) and Cerola (28 m a.s.l.) springs; iv) GB5 feeds the S. Marina di Lavorate (28 m a.s.l.), S. Mauro (27 m a.s.l.) and Laura and Labso springs (185 and 199 m a.s.l.).

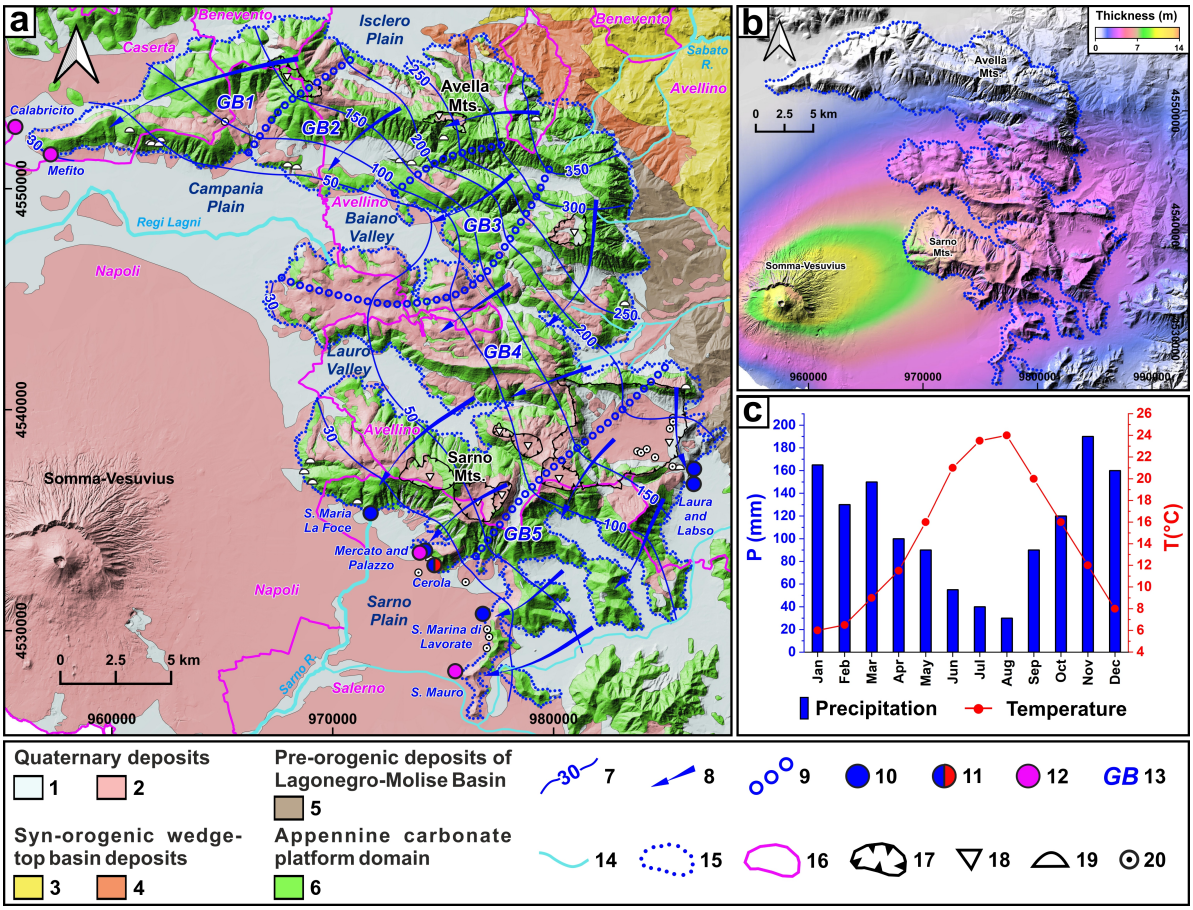


Figure 22 – a) Hydrogeological map of Avella Mts (Petrone et al., 2024, modified). Hydrogeological complexes: 1. Pyroclastic-alluvial; 2. Pyroclastic deposits; 3. Sandstone; 4. Argille Varicolori; 5. Marly limestone; 6. Limestone; 7. Groundwater contour (m a.s.l.); 8. Groundwater flow direction; 9. Groundwater flow divide; 10. Freshwater basal spring; 11. Mineralized basal spring; 12. Dried basal spring; 13. Groundwater basin; 14. River; 15. Study area; 16. Provincial boundary; 17. Endoreic area; 18. Swallow hole; 19. Cave; 20. Sinkhole; b) Total thickness (isopach) map of ash-fall deposits in the area surroundings the Somma-Vesuvius volcano (De Vita et al., 2006; De Vita and Nappi, 2013, modified); c) Seasonal rainfall and air temperature regime.

From the 1920s to 1950s, flow measurements were conducted by the National Hydrological Service-Department of Naples and the Cassa per il Mezzogiorno Italian Government Agency (Celico, 1983; Allocca et al., 2007). These measurements, taken before the tapping works, allowed for the estimation of the following mean spring discharges: 1.20 m^3/s for the Calabricito and Mefito springs; 2.60 m^3/s for the S. Maria La Foce spring; 3.00 m^3/s for the Mercato and Palazzo springs; 0.60 m^3/s for the Cerola spring; 1.80 m^3/s for the Santa Maria di Lavorate spring; 0.40 m^3/s for the San Mauro spring and 0.15 m^3/s for the Laura and Labso

springs. Currently, the active springs are S. Maria La Foce, Palazzo, Cerola, S. Marina di Lavorate, Laura and Labso springs. In contrast, Mefito, Calabricito, Mercato and S. Mauro springs have been completely dry since the 1980s and 1990s, although Calabricito spring was partially and temporarily reactivated in 2013 with a flow rate of up to approximately 0.01 m^3/s (Petrone et al., 2024).

Hydrostratigraphic contacts within the carbonate succession locally determine a vertical compartmentalisation of shallow groundwater circulation into karst, detrital and pyroclastic perched aquifers that feed numerous high-altitude springs with seasonal or perennial regimes. Well-developed karst landforms (e.g., endorheic areas, sinkholes, caves, and swallow holes; Fig. 22a) exert significant control over recharge and influence ground instabilities (Valente et al., 2021; Santo et al., 2019). The climate is Mediterranean-mild type (CSb) (Beck et al., 2018). Average monthly air temperature reaches 25 °C in August and 7 °C in January (Fig. 22c), while mean monthly rainfall varies between 190 mm, in November, and 30 mm, in August (Fig. 22c). According to Allocca et al. (2014) and Ruggieri et al. (2021), the mean annual cumulative rainfall and air temperature are equal to 1,320 mm and 14.4 °C, respectively.

Groundwater development

The groundwater of the Avella Mts. still plays a strategic role in the socioeconomic growth and development of the Campania region. Excluding the Conte of Sarno channel (Fig. 23b), built at the end of the 1500s to supply Torre Annunziata village with water from the S. Maria La Foce spring, there were no groundwater capture structures at the Avella Mts. until the 1950s. Since the 1960s, the groundwater has been exploited for drinking water supply by a single regional water manager, the Acquedotto Campano. Subsequently, in the 1980s and 1990s, industrial, irrigation and domestic self-supply water uses were developed by companies, irrigation consortia, and many private users. The exponential growth in the number of capture structures and increase in water withdrawals are based on the population growth of the Campania region (Fig. 23a). In 1962 and 1972, two drainage tunnels were constructed to tap gravity groundwater in S. Maria La Foce and S. Marina di Lavorate springs, respectively (Nicotera and Civita, 1969a; 1969b; Petrone et al., 2024), to supply the Sarnese aqueduct, which is managed today by GORI SpA (Figs. 22a and 23b). In the 1970s, some spring boxes were built to supply municipal aqueducts with water from high-altitude

springs (Fig. 23b). Subsequently, in 1975, 1989 and 1990 three well-fields for drinking water purposes were drilled upstream of Mefito-Calabricito, Mercato-Palazzo and S. Mauro springs, respectively (Fig. 23b), to supply the regional Campanian aqueduct, causing the progressive drying up of these springs (Fig. 22a). Instead, the Cerola, Laura and Labso springs (Figs. 22a and 23b) were tapped in the first half of the 1980s for agricultural use by gravity intake systems. From the 1990s, additional single wells and wells-fields were drilled by public agencies and joint-stock companies for drinking water use and to supply the regional and interprovincial aqueducts, such as Alto Calore Servizi SpA (Fig. 23b). In the summer of 2001, 11 wells were drilled inside the tunnel of S. Maria La Foce spring after a meteorological drought period and the total drying up of gallery. In 2006, another well-field for drinking water use was drilled upstream of Mefito-Calabricito springs to supply the ABC Napoli aqueduct (Fig. 23b). Starting in the 1990s, numerous private wells were authorised and drilled in the piedmont karst areas for agriculture, industry, mining, domestic and other living uses (Fig. 23a). Due to the lack of concrete coordination between local governments on issuing permits to public and private water users, based on updated water balance, this resulted in a significant increase in groundwater exploitation, with negative effects on the karst aquifer enhanced by cyclic drought periods. Unfortunately, today there is a multitude of public entities and private users that use the same aquifer for multiple purposes in an uncoordinated way. The supply of drinking water is provided by four regional waterworks (Acquedotto Campano, GORI SpA, ABC Napoli, and Alto Calore Servizi SpA) and two municipal aqueducts to feed a large area of the Campania region, with a population of approximately 5 million inhabitants (Figs. 23a and 23b).

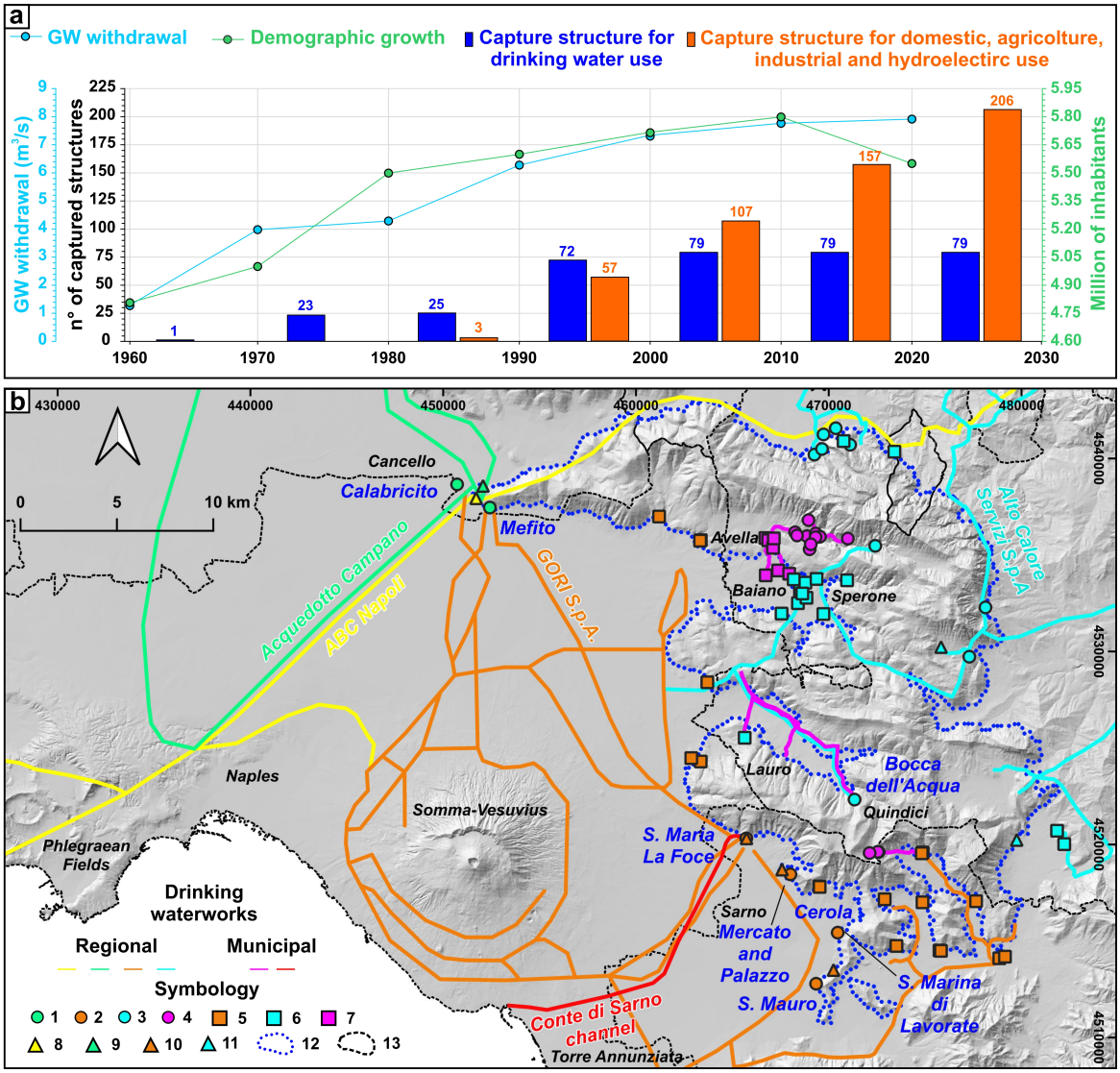


Figure 23 – a) Comparison between demographic growth, withdrawals, and no. of capture structures. b) Waterwork for drinking use. 1. Spring captured by Acquedotto Campano; 2. Spring captured by GORI SpA; 3. Spring captured by Alto Calore Servizi SpA; 4. Spring captured by municipal waterwork; 5. Well used for drinking water supply by GORI; 6. GORI SpA well; Alto Calore Servizi SpA well; 7. municipal waterwork well; 8. ABC Napoli wells field; 9. Acquedotto Campano wells Field; 10. GORI SpA wells field; 11. Alto Calore Servizi SpA wells field; 12. Study area; 13. Provincial boundary.

Methodology, input data and validation

Soil Water Balance model and input data

The Soil Water Balance (SWB, version 1.2) code developed by the United States Geological Survey (Westenbroek et al., 2010) was employed to estimate the spatial and temporal

variations in groundwater recharge for the period 2010-2021. The SWB code implementation followed the procedure shown in the Figure 24. The computational domain, extending of approximately 370 km² was discretized into square cells with a spatial resolution of 20 m. The code applied was based on a modified Thornthwaite-Mather soil-water-balance approach (Westenbroek et al., 2010) to compute potential recharge on a daily timestep for each cell in the model. Groundwater recharge is quantified using the following empirical formula (Eq. 4):

$$GR = (P + Sn + F) - (O + ET + In) - \Delta\theta \quad (4)$$

where:

GR (inches) is the groundwater recharge; *P* (inches) is the precipitation; *Sn* (inches) is the amount of water on the ground surface as a result of snow melt; *F* (inches) is the surface water from upslope grid cells; *O* (inches) is the surface runoff calculated using the Curve Number method (USDA, 1972); *ET* (inches) is the actual evapotranspiration estimated by the Thornthwaite-Mather method; *In* (inches) is the interception, the amount of rainfall caught by vegetation and evaporated or transpired from plant surface; and $\Delta\theta$ (inches) is the temporal variation in soil moisture.

The SWB code calculates recharge using grid and tabular input data (Figs. 24a, 24b, 24c, 24d and 24e), in a GIS environment. The followings input gridded data layers were collected and reconstructed: i) flow direction (Fig. 24b); ii) available soil water content map (Fig. 24c); iii) land use map (Fig. 24d); iv) hydrologic soil group map (Fig. 24e) and v) daily rainfall and minimum and maximum air temperatures maps (Fig. 24a) acquired by the regional hydro-meteorological monitoring network of the Civil Protection of the Campania region.

The study period was selected based on the continuous working of monitoring stations, ensuring reliable estimates of daily precipitation and air temperature data. These were interpolated using the Inverse Distance Weighted algorithm in the GIS environment. Additionally, the land use lookup table was implemented in the SWB model contained parameters such as values of interception, root zone depth and maximum net infiltration rates for each land use and hydrologic soil group combination.

The SWB code generated groundwater recharge output as daily, monthly, and annual values. Finally, the groundwater recharge coefficient (GRC, %) and specific groundwater recharge yield (GRY, $Mm^3/y/km^2$) were estimated as the ratio between recharge and the precipitation minus actual evapotranspiration, and the ratio between recharge and karst recharge area, respectively.

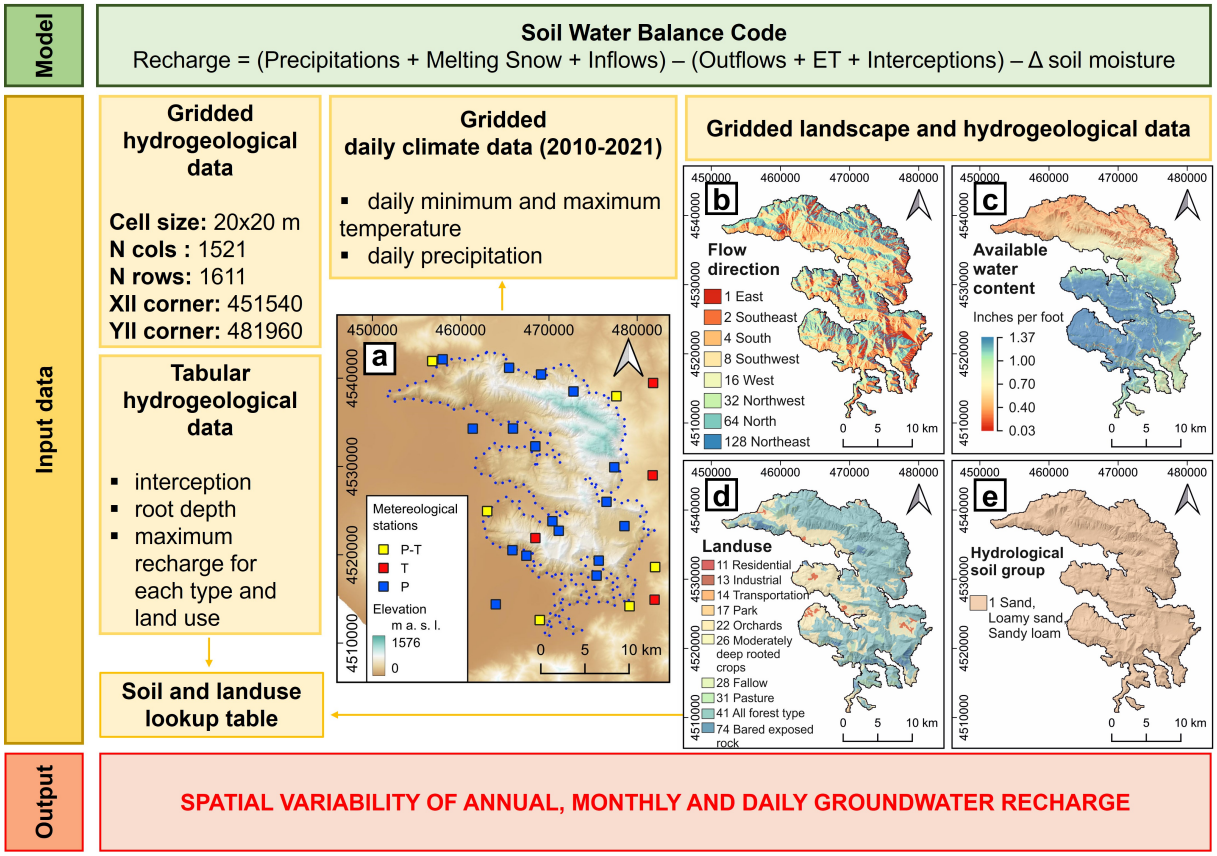


Figure 24 – Procedure used to implementation of the SWB code. a) Elevation map with the location of the meteorological stations; b) Flow direction map; c) Available water content map; d) Land use map; e) Hydrological soil group map.

Water withdrawals and spring discharge

To compare and validate the water balance, data on spring discharge data and authorised water withdrawals were assessed. Data on springs, wells and other capture structures were collected from four main sources: i) published data including scientific articles (e.g., Civita et al., 1973; Celico, 1983; Allocca et al., 2007; Allocca et al., 2008; Cusano et al., 2022; Petrone et al., 2024), ii) public databases from national (http://sgi2.isprambiente.it/mapviewer/) and regional hydrological services and provincial

authorities, iii) private databases of water companies, water suppliers and users and iv) cartographic, geological, and hydrogeological maps. A map-based survey was conducted for basal and high-altitude springs by consulting the i) Regional Technical Map of the Campania region (at 1:5,000 scale), ii) Topographic Map of Italy of the Military Geographic Institute (at 1:25,000 scale) (https://www.igmi.org/), iii) geological sheets of the CARG project (at 1:50,000) (https://www.isprambiente.gov.it/Media/carg/) and iv) high-resolution satellite images from Google Earth (https://www.google.it/intl/it/earth/). A census of wells and water abstraction licenses was carried out at regional and sub-regional authorities. Since the data and information on the number and characteristics of water licenses are not publicly accessible and available, much of the collected data was disaggregated and non-computerised data and organized at the municipal level. Each groundwater source has been assigned with an ID code, geographical coordinates, altitude, well depth, type of capture structure, discharge, authorised withdrawal, piezometric levels, water use, status of licence, province and municipality. The spring and well data were temporally discontinuous and non-homogeneous, with some relying on literature sources. The basal spring data and withdrawals from wells and well-fields for drinking purposes were recorded at daily and annual timescale, covering different timespans. The extracted discharge from authorised and regular private wells for industrial, domestic and agricultural uses were reported in absolute terms as the average or maximum authorised volume. However, no data was available for unknown or irregular private wells, which are known to exist. The withdrawal period typically spanned the entire solar year for drinking, industrial and domestic uses, but were concentrated mainly in the spring and summer seasons for agricultural use. The discharge data for high-altitude springs relied on literature, while additional data on withdrawals and basal springs was collected through field surveys conducted since 2019.

All collected data summarized in Table 4 were checked and stored in a hydrogeological geospatial database, implementing an inventory of springs and an authorised well registry, along with other capture structures.

Type	Total number	Depth range (m)	Use	Source
Well-fields	7 (with 63 wells)	51.8-234	Drinking water	ABC Napoli; Acquedotto Campano; Alto Calore Servizi SpA; GORI SpA; Allocca et al. (2008).
Wells	241	14-362	Agricultural, domestic, drinking water, industrial	Alto Calore Servizi SpA; GORI SpA; Allocca et al. (2008); Civita et al. (1970); Metropolitan City of Naples; Avellino Province.
Basal springs	10	-	Agricultural, drinking water, hydroelectric	Alto Calore Servizi SpA; GORI SpA; Civita et al. (1973); Allocca et al. (2008).
Perched springs	141	-	Drinking water, uncaptured	Alto Calore Servizi SpA; GORI SpA; Civita et al. (1973); Celico et al. (2000); Allocca et al. (2008).

Table 4 - Summary of water point types, total count, depth range (min–max) for wells, use, and data sources.

Results

Spatial and temporal variations of groundwater recharge

From aquifer to basin scale, the results demonstrate a high spatio-temporal variability of recharge in the studied period. Spatially, the annual and monthly recharge maps reveal a strong influence on the hydrological and physical surface characteristics of the aquifer (Figs. 25a and 25b). Higher values of annual and monthly recharge were observed in high-altitude zones along the open slopes, where the precipitation rate reach up to 3,147 mm, and in regions with closed morphological depressions. These endorheic depressions (Fig. 22) collect most of the surface runoff, and locally favour conditions for point groundwater recharge into karst aquifer (Allocca et al., 2014; Allocca et al., 2015; Cusano et al., 2024a). For areas with similar vegetation cover and slope (Fig. 24d), the recharge tends to be greater in zones with small or absent pyroclastic soil layers, due to the decreased available water content for evapotranspiration (Fig.24c) (Cusano et al., 2024b).

Temporally, the average annual recharge was found to be 660.55 mm (corresponding to 50% of the mean annual precipitation), equal to 244.40 Mm^3/y, although individual values span over two orders of magnitude, from 35.56 to 2,530 mm/y (Figs. 25a, 25b and 25c). These values agree with mean groundwater recharge recently estimated (Allocca et al., 2014; Ruggieri et al., 2021; Petrone et al., 2024) by empirical approaches (Turc, 1954; Thornthwaite and Mather, 1955) and MODIS satellite data. For this time span, a high

interannual variability of recharge was observed (Figs. 25b and 25c) compared to the average value. Dry and wet years occurs due to decadal and multidecadal variability of rainfall (De Vita al., 2012; Longobardi and Boulariah, 2022) with the recharge varies between –45% (equal to 167,10 Mm^3/y) and +73% (equal to 423.84 Mm^3/y) if compared to the average value. Consequently, also an interannual variability of both GRC and GRY (Figs. 25d and 25e) was observed, ranging from 79% to 66% and from 1.15 $Mm^3/y/km^2$ to 0.45 Mm^3/y per km^2, respectively.

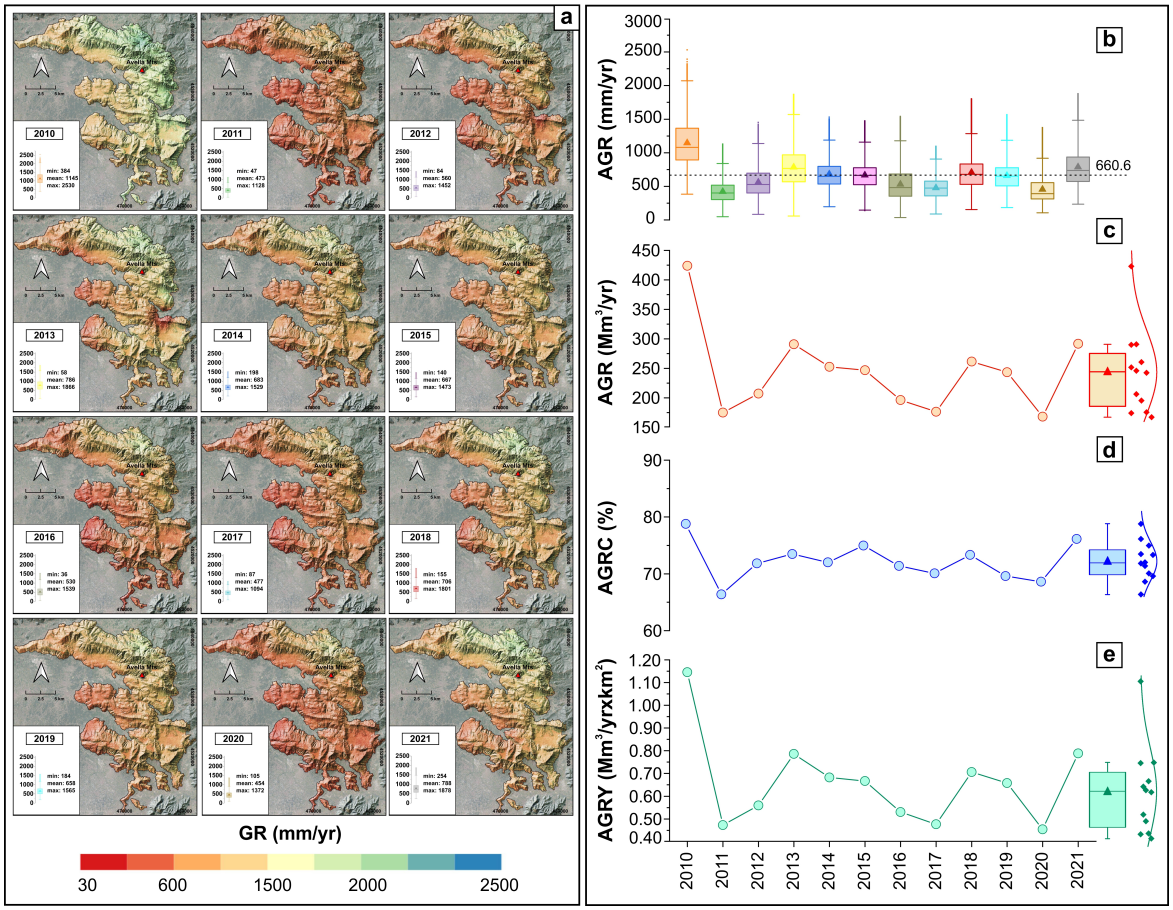


Figure 25 – Spatial (a) and temporal distribution of annual GR (b and c), annual GRC (d) and annual GRY (e).

At the monthly scale, an average recharge value of approximately 56.30 mm (equal to 20.85 Mm^3/month) was estimated (Figs. 26a, 26b and 26c). Groundwater recharge is higher during October to March, consistent with the seasonal rainfall regime (Fig. 22c) and lower during May-September (Figs. 26b and 26c). Consequently, an intermonthly variability of GRC and

GRY (Fig. 26d and 26e) was observed, ranging from 100% to 21% and from 0.14 $Mm^3/month/km^2$ to 0.001 $Mm^3/month/km^2$, respectively.

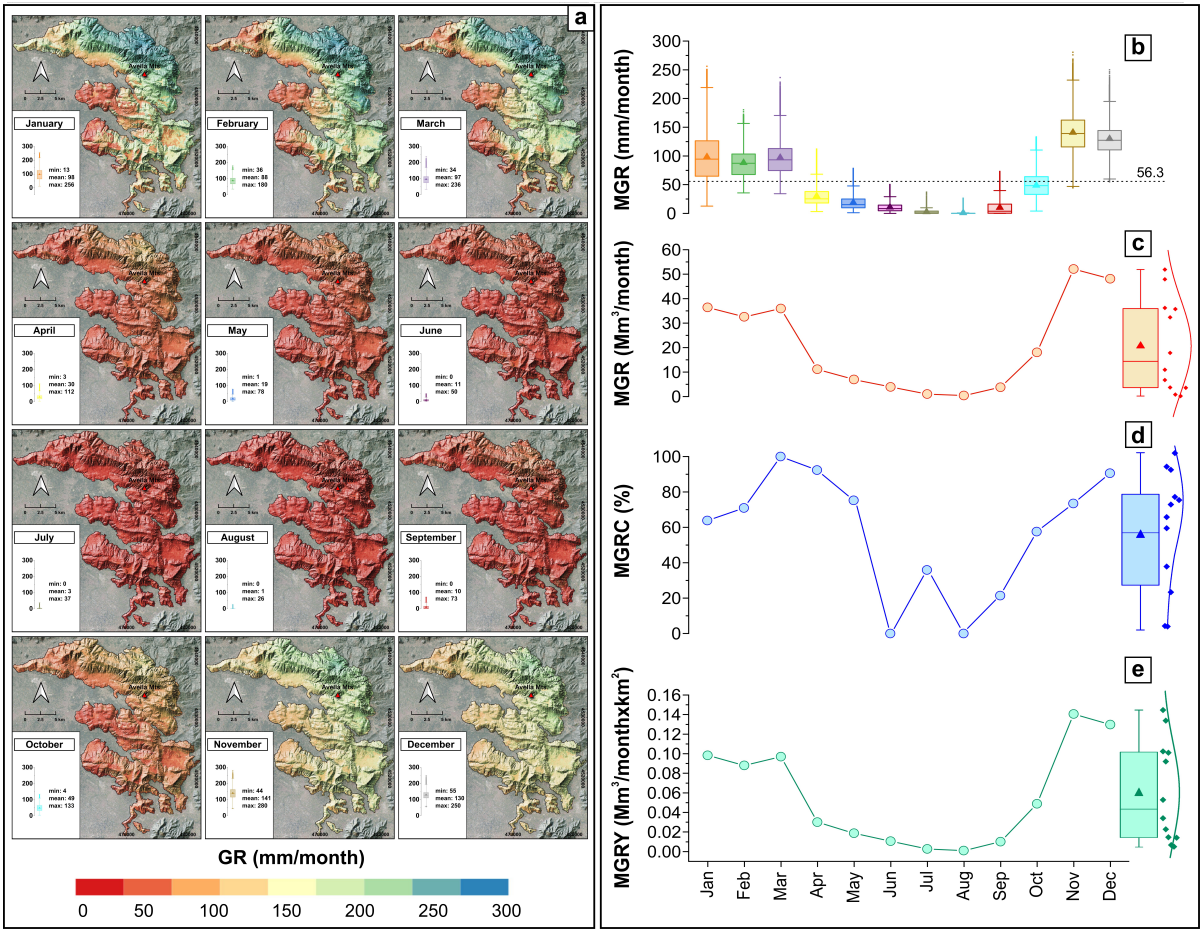


Figure 26 – Spatial (a) and temporal distribution of monthly GR (b and c), monthly GRC (d) and monthly GRY (e).

At the daily scale, an average recharge value of approximately 1.80 mm (equal to 0.67 Mm^3/day) was estimated. The groundwater recharge is relatively greater in the days of November (Figs. 27a and 27b), while it is zero in the summer months (Figs. 27a and 27b). Consequently, a daily variability of GRC and GRY (Fig. 27c and 27d) was observed, ranging from 100% to 0.01% and from 0.01 m^3/s to 0.00 $m^3/s/km^2$, respectively.

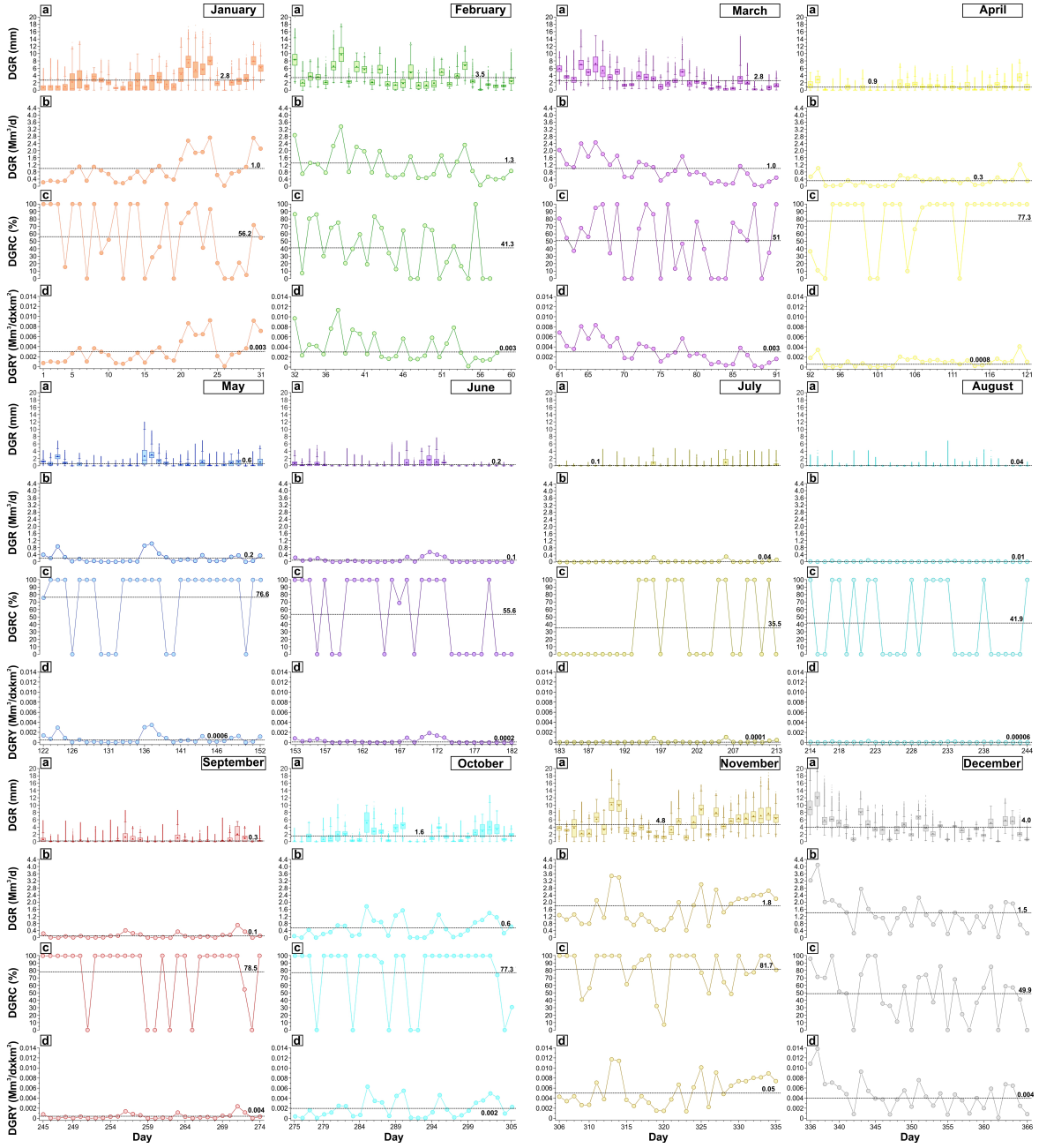


Figure 27 – Temporal variations of the daily GR (a and b), daily GRC (c) and daily GRY (d). The colors indicate the days of the month; each month is divided into four boxes (a, b, c, and d).

Spring inventory map and authorised well registry

Figure 28a presents the first springs inventory and authorised well map of Avella Mts., showing a groundwater points density of no less than 1.22/km^2. This map illustrates the distribution pattern of basal and perched springs, groundwater capture sites and authorised well registry.

A total of 151 springs were censused and detected (Fig. 28b) of which 10 are basal springs and 141 are high-altitude springs, accounting for 6.6% and 93.4%, respectively.

The basal springs are located along the western and southern boundaries of the aquifer, at altitudes ranging from 23 to 199 m a.s.l., whereas the high-altitude springs are predominantly situated in the central and northern sectors of the Avella Mts. (Fig. 28a), at altitudes ranging from 160 and 1300 m a.s.l.. Approximately 21% of springs are captured by spring boxes, drainage tunnels and upstream well-fields of springs, while approximately 79% correspond to high-altitude springs remain untapped (Fig. 28b). Five basal springs (i.e., Calabricito, Mefito, Mercato, Palazzo and S. Mauro springs) are captured by well-fields, with four were nearly dried up (Fig. 28a). Other springs, such as S. Maria La Foce and S. Marina di Lavorate are captured via tunnels, and Laura, Labso and Cerola springs through intake systems (Fig. 27a). Among the captured springs, approximately 17% are used for drinking water, 2% agriculture and 1% hydroelectric purposes (Fig. 28b).

Overall, a total number of 304 wells and well-fields was censused (Figs. 28a and 28d) and authorised for small and large volume groundwater extractions. Approximately 35% was used for drinking water, while 47%, 12% and 6% were used for domestic, agricultural, and industrial purposes, respectively (Fig. 28d). These wells and well-fields are largely concentrated around the periphery and some internal sectors of the massif (Fig. 28a) and explore the basal aquifer with diameters and depths up to 500 mm and 200-300 m b.g.s., respectively, and with screened intervals up to −10 m b.s.l..

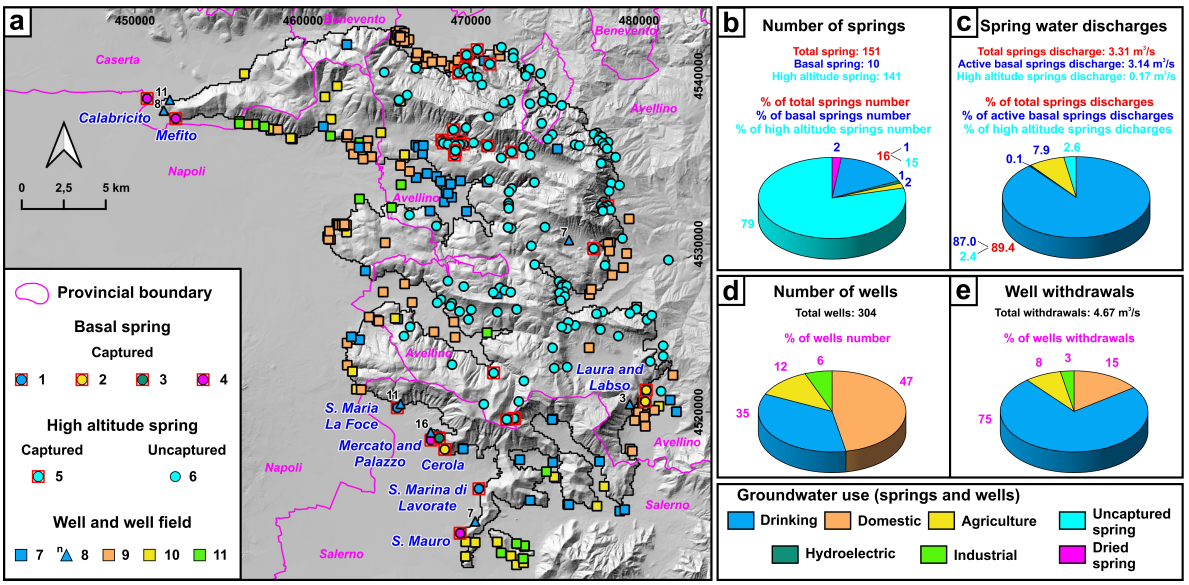


Figure 28 – a) Springs inventory map and registry of authorized wells. 1. Basal spring captured by drinking use; 2. Basal spring captured by agriculture use; 3. Basal spring captured by hydroelectric use; 4. Dried basal spring captured by drinking use; 5. High-altitude spring captured by drinking use; 6. Uncaptured high-altitude spring. 7. Well for drinking use; 8. Wells field for drinking use; 9. Well for domestic use; 10. Well for agriculture use; 11. Well for industrial use; b) Number and percentage of basal and high-altitude springs for different use; c) Spring water discharge in m^3/s and percentage of total springs, including basal and high-altitude springs for different use; d) Number and percentage of wells for different use; e) Well withdrawals in m^3/s and percentage for different use.

At the aquifer scale, the outgoing groundwater volume is overall equal to 7.98 m^3/s (Figs. 28c and 28e), corresponding to 252.30 Mm^3/y. The spring discharge drained via tunnels and intake systems is on average equal to 3.31 m^3/s, of which 89.4%, 7.9% and 0.1% are used for drinking water, agriculture, and hydroelectric purposes, respectively (Fig. 28c). Instead, the extracted groundwater volume by pumping is overall equal to 4.67 m^3/s, of which 75%, 15%, 8% and 3% are for drinking water, domestic, agriculture and industrial use, respectively (Fig. 28e).

Discussion

This section presents a multiscale comparison between potential groundwater recharge and water withdrawals to assess the groundwater sustainability of the Avella Mts. karst aquifers, which strongly depends on the equilibrium between the renewable groundwater resources and groundwater demand, from aquifer to basin, down to the local scale.

At the aquifer scale (Figs. 29a and 29b), the average annual recharge is equal to 7.75 m^3/s (corresponding to 244.40 Mm^3/y), whereas the total outgoing groundwater volume is equal to 7.98 m^3/s (corresponding to 252.30 Mm^3/y). Although the outgoing groundwater volume overall exceeds the mean annual recharge by approximately +3.2%, a significant portion (approximately 41%) of this outflow is drained by gravity and passive structures (e.g., spring boxes and drainage galleries) through basal (approximately 95%, equal to 3.14 m^3/s) and tapped and untapped high-altitude springs (approximately 5%, equal to 0.17 m^3/s) (Fig. 29b). The budgetary recharge-discharge imbalance (Figs. 29a and 29b) becomes more pronounced during drought years (Figs. 25b and 25c), where annual recharge decreased up to 5.30 m^3/s (equal to 167.10 Mm^3/y).

At the basin scale, the spatial distribution of recharge and groundwater demand is uneven (Fig. 29c and 29d). A comparison between the average annual recharge (Fig. 29c) and the water withdrawals (Fig. 29d) reveals that GB1 and GB5 experience a water deficit of 0.69 m^3/s and 1.10 m^3/s, respectively. Groundwater in GB1 is entirely captured by pumping, while in GB5, 65% is drained by gravity and 35% by pumping (Fig. 29d). GB2 and GB3 exhibit a water surplus of approximately 1.56 m^3/s and 0.77 m^3/s, respectively. In GB2, groundwater is drained by gravity (16%) and pumping (84%), while in GB3 gravity accounts for 64% and pumping for 36%. In GB4, an equilibrium condition exists with a perfectly balanced budget (Fig. 29c and 29d), with 40% of groundwater drained by gravity and 58% by pumping.

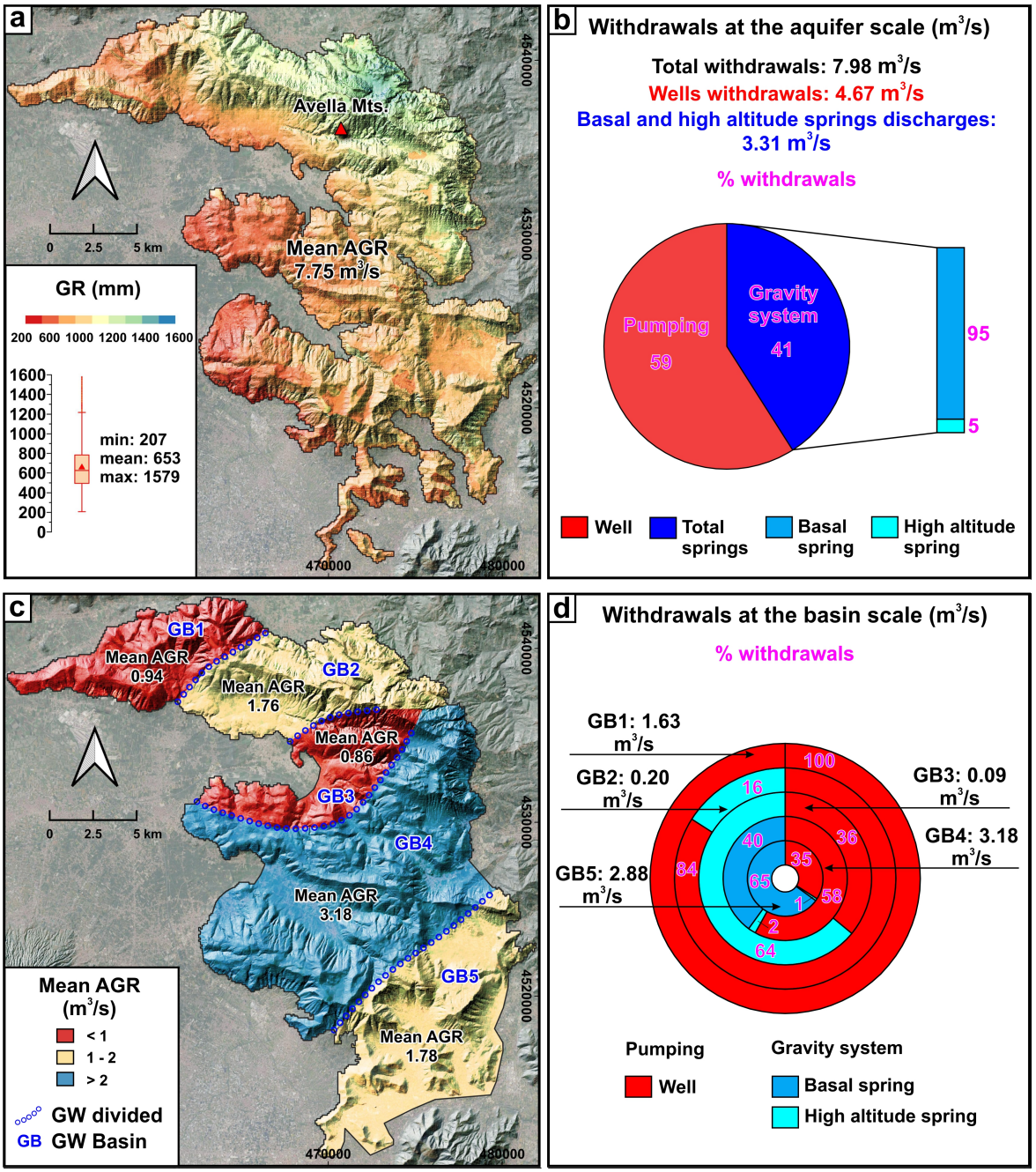


Figure 29 – Comparison between groundwater recharge and withdrawal at the aquifer (a and b) and basin scale (c and d)

At the local scale, multiple comparison between spring discharge, withdrawals and conceptual models reveals the impacts on spring-stream systems. For S. Maria La Foce, S. Marina di Lavorate, Cerola, Laura and Labso springs (Figs. 30a, 30e, 30h and 30k), drainage tunnels and spring boxes, being passive capture works, have not changed the natural regime of the springs and have only partially affected the local downstream flow. Temporal

variations in spring discharge (Figs. 30a and 30d) observed after groundwater development are likely attributed to natural factors. In contrast, springs like Mefito, Calabricito and San Mauro (Figs. 30n and 30t) show negative impacts from pumping evidenced by spring drying and outflow downstream. For Mercato spring (Fig. 30q), the disappearance of the downstream flow appears more related to urban developments such as constructing a public car park (Fig. 30r) rather than withdrawals from the well-field. This was supported by the nearby Palazzo spring, which remains active with a discharge of a few m^3/s (Fig. 30p).

These results suggest that the Avella Mts. are affected by groundwater stress conditions and that the current withdrawal rates are unsustainable in the medium to long term. A lack of an updated water balance, well registry, as well as a reciprocal and concrete coordination among regional and sub-regional authorities in the issuing of water concessions, has led to the uncontrolled development of wells, exacerbating the imbalance between water availability and demand.

In the future, climate changes (Lepore et al., 2024) and human activities could further deplete springs, degrade water quality (e.g., Schuch et al., 2023; Lancia et al., 2020) and cause ground instabilities (e.g., Cascini and Di Maio, 1994; Valente et al., 2021), leading to adverse effects on the environment, economy, and health. The hydrogeological scenario needs to be mitigated by actions to reduce the withdrawal rate and change the current regional water governance model.

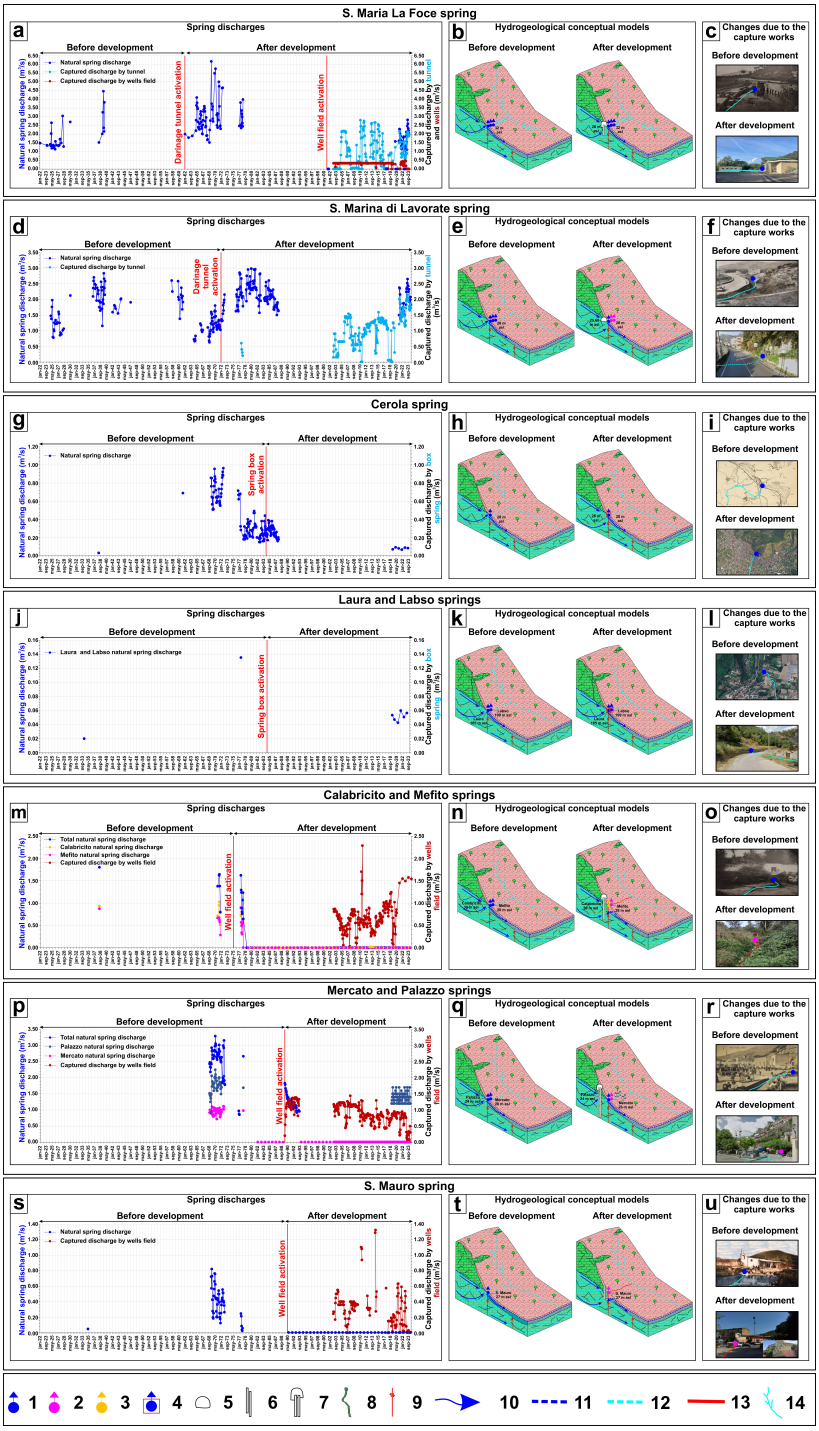


Figure 30 – Multiple comparison between spring discharges, withdrawals (a, d, g, j, m, p and, s), simplified hydrogeological conceptual models (b, e, h, k, n, q, t, l, o, r and, u) and changes before and after development (c, f, i, l, o, r and, u). 1. Active spring; 2. Dried spring; 3. Dried spring partially reactived; 4. Spring box; 5. Drainage tunnel; 6. Wells; 7. Drainage tunnel with wells; 8. Karstic conduit; 9. Normal fault; 10. Groundwater flow direction; 11. Piezometric level; 12. Buried stream; 13. Dried stream; 14. River.

Conclusions

The groundwater of the Avella Mts. plays a vital role in suppling water to a significant portion of the Campanian population. Hydrogeologically, the karst massif is divided into a basins-in-series system, hosting a locally TBA whose groundwater knows no hydrographic and provincial borders and are affected to varying degrees by both anthropogenic and climatic impacts.

This study conducted a multitemporal assessment of natural recharge and a multiscale comparison with spring discharges and water withdrawals to evaluate groundwater sustainability.

The main findings are summarised as follows:

- A high spatio-temporal variability of recharge is observed, influenced by hydrological and physical surface characteristics of the aquifer.
- At the aquifer scale, the average recharge is equal to 244.40 Mm^3/y, with marked interannual variability of approximately –45% and +73%, while at the basin scale, it varies on average between 29.64 Mm^3/y and 100.28 Mm^3/y;
- At the aquifer scale, the total outgoing groundwater volume is equal to 252.30 Mm^3/y, whereas at the basin scale, it varies between 6.30 Mm^3/y and 97.76 Mm^3/y.
- From aquifer to basin scale, there is a budgetary disequilibrium that is unsustainable in the medium to long term, especially during drought years, as evidenced by drying up of some springs and streams.

The results underscore the urgent need for improved prevention measures and water management policies to mitigate human impacts. Numerical models that simulate the aquifer's response to pumping and meteorological forcing, coupled with a reduction of authorised withdrawals based on prioritisation criteria, are essential. Such measure would be useful to ensure a major active flow towards springs, assess sustainable exploitation thresholds and forecast the effects of climate and anthropogenic pressures. Additionally, there is an urgent need to reform water governance in Campania and other Italian region, shifting from the current model constructed on administrative/hydrographic boundaries to a management system based on the hydrogeological boundaries of groundwater bodies. This shift requires establishing a new water management authority, such as an 'Italian Aquifer Authority', to reform current water governance and water licence regimes not based on the hydrogeological boundaries of aquifers. Effective cooperation and coordination among

institutions and stakeholders involved in groundwater use are critical to ensuring water security and preventing power conflict, competition, and local rivalries. Continuous groundwater monitoring, sharing and exchanging data, regular updates of water budget are necessary to ensure the sustainable use of this shared groundwater resource, which is vital for the economy, environment, and social security in the most-populous area of southern Italy.

CRediT authorship contribution statement

Paola Petrone: Writing - original draft, Validation, Software, Methodology, Formal analysis, Data curation**. Pantaleone De Vita**: Writing - review & editing, Writing - original draft, Validation, Supervision, Resources, Methodology, Investigation, Formal analysis, Data curation.
Pasquale Allocca: Software, Methodology, Formal analysis, Data curation. **Silvio Coda:** Software, Methodology, Formal analysis, Data curation. **Delia Cusano:** Software, Methodology, Formal analysis, Data curation. **Radka Kodešová**: Writing – review & editing, Validation, Supervision. **Daniele Lepore:** Software, Methodology, Formal analysis, Data curation. **Vincenzo Allocca:** Writing – review & editing, Writing – original draft, Validation, Supervision, Resources, Project administration, Methodology, Investigation, Formal analysis, Data curation, Conceptualization.

Declaration of Competing Interest

The authors declare that they have no known competing financial interests or personal relationships that could have appeared to influence the work reported in this paper.

Data availability

Data will be made available on request.

Acknowledgements

This research was also supported by the Earth Sciences, Environment and Resources, PhD Program of the University of Naples Federico II (XXXVII cycle).

References

Allocca, V., Celico, F., Celico, P., De Vita, P., Fabbrocino, S., Mattia, S., Monacelli, G., Musilli, I., Piscopo, V., Scalise, A.R., Summa, G., and Tranfaglia, G., 2007. Illustrative Notes of the Hydrogeological Map of Southern Italy. Istituto Poligrafico e Zecca dello Stato, Rome, 1-211, ISBN 88-448-0223-6.

Allocca, V., Aquino, S., Esposito, L., Celico, P., 2008. The groundwater of the Irpinia area (Southern Italy). Current Knowledge and Future Perspectives. L'ACQUA 6 (2008), 39-66.

Allocca, V., Manna, F., De Vita, P., 2014. Estimating annual groundwater recharge coefficient for karst aquifers of the southern Apennines (Italy). Hydrol. Earth Syst. Sci. 18, 803-817. https://doi.org/10.5194/hess-18-803-2014.

Beck, H.E., Zimmermann, N.E., McVicar, T.R., Vergopolan, N., Berg, A., Wood, E.F., 2018. Present and future Köppen-Geiger climate classification maps at 1-km resolution. Sci. Data 5, 1-12. https://doi.org/10.1038/sdata.2018.214.

Cascini, L., and Di Maio, C., 1994. Emungimento delle acque e cedimenti nell'abitato di Sarno: analisi preliminare. Rivista Italiana di Geotecnica, 28(3), 217-231.

Celico, P., de Riso, R., 1978. Il ruolo della Valle Caudina nella idrogeologia del Casertano e del Sarnese (Campania). Mem. e Note Ist. Geol. Appl., 14, 1-24.

Celico, P., 1983. Idrogeologia dei massicci carbonatici, delle piane quaternarie e delle aree vulcaniche dell'Italia centro-meridionale: Marche e Lazio meridionali, Abruzzo, Molise e Campania. Quaderni della Cassa per il Mezzogiorno 4 (2), 1-203, Roma.

Nicotera, P., Civita, M., 1969a. Ricerche idrogeologiche per la realizzazione delle opere di presa delle sorgenti Mercato e Palazzo in Sarno (Campania). Mem. e Note Ist. Geol. Appl. (1969) Vol. 11, 1-59 (Napoli).

Nicotera, P., Civita, M., 1969b. Indagini idrogeologiche per la captazione delle sorgenti S. Marina di Lavorate (Sarno). Mem. e Note Ist. Geol. Appl. (1969) Vol. 11, 1-50 (Napoli).

Civita, M., de Riso R., Nicotera, P., 1970. Sulla struttura idrogeologica alimentante le sorgenti del F. Sarno e le falde pedemontane profonde della parte sud-orientale della Conca Campana. Atti I Convegno Internazionale sulle Acque Sotterranee, IAH, 1-24. Palermo, 6-8 Dicembre 1970.

Civita, M., de Medici, G.B., de Riso, R., Nicotera, P., Nota d'Elogio E., 1973. Memoria descrittiva della carta idrogeologica della Campania nord-occidentale. Atti II Convegno Internazionale sulle Acque Sotterranee, IAH, 1–39. Palermo, 28 Aprile-2 Maggio 1970.

Cusano, D. Allocca, V., Coda, S., Lepore, D., Vassallo, M., De Vita, P., 2022. The Survey of Italian Springs by the National Hydrographic Service, a Forgotten Database. Structuring and Analysis of a Dataset of Campania Springs (Southern Italy). Acque Sotterranee - Italian Journal of Groundwater, 11, 31-41. https://doi.org/10.3390/w15213756.

Cusano, D., Allocca, V., Coda, S., Di Clemente, E., Fabbrocino, S., Lepore, D., Panza, R., Petrone, P., De Vita P., 2024a. Effects of ash-fall pyroclastic soil mantle on groundwater recharge of Terminio Mt. peri-volcanic karst aquifer. Journal of Hydrology: Regional Studies. 53 (2024) 101844. https://doi.org/10.1016/j.ejrh.2024.101844

Cusano, D., Lepore, D., Allocca, V., De Vita, P., 2024b. Control of soil mantle thickness and land cover types on groundwater recharge of karst aquifers in Mediterranean areas. Journal of Hydrology 630, 130770. https://doi.org/10.1016/j.jhydrol.2024.130770.

De Vita, P., Agrello, D., Ambrosino, F., 2006. Landslide susceptibility assessment in ash-fall pyroclastic deposits surrounding Mount Somma-Vesuvius: Application of geophysical surveys for soil thickness mapping. J. Appl. Geophys. 2, 126-139. https://doi.org/10.1016/j.jappgeo.2005.09.001.

De Vita, P., Allocca, V., Manna, F., Fabbrocino, S., 2012. Coupled decadal variability of the North Atlantic Oscillation, regional rainfall and karst spring discharges in the Campania region (southern Italy). Hydrol. Earth Syst. Sci. 16 (5), 1389-1399. https://doi.org/10.5194/hess-16-1389-2012.

De Vita, P., Nappi, M., 2013. Regional distribution of ash-fall pyroclastic deposits in Campania (southern Italy) for landslide susceptibility assessment. In: Landslide Science and Practice (Margottini C., Canuti P, Sassa K. eds.), 3, Spatial Analysis and Modelling, Springer-Verlang, 103-110. https://doi:10.1007/978-3-642-31310-3_15.

Fusco, F., Allocca, V., De Vita, P., 2017. Hydro-geomorphological modelling of ash-fall pyroclastic soils for debris flow initiation and groundwater recharge in Campania (southern Italy). Catena 158, 235–249. https://doi.org/10.1016/j.catena.2017.07.010.

IGRAC (International Groundwater Resources Assessment Centre), 2021. Transboundary aquifers of the world [map]; Edition 2021, Scale 1: 50,000,000; IGRAC: Delft, The Netherlands, 2021.

Lancia, M., Petitta, M., Zheng, C., Saroli, M., 2020. Hydrogeological insights and modelling for sustainable use of a stressed carbonate aquifer in the Mediterranean area: From passive withdrawals to active management. J. Hydrol. Reg. Stud. 32, 100749. https://doi.org/10.1016/j.ejrh.2020.100749.

Lepore, D., Bucchignani, E., Montesarchio, M., Allocca, V., Coda, S., Cusano, D., De Vita, P., 2024. Impact scenarios on groundwater availability of southern Italy by joint application of regional climate models (RCMs) and meteorological time series. Scientific Reports, 14:20337. 10.1038/s41598-024-70257-1. https://doi.org/10.1038/s41598-024-70257-1.

Longobardi, A., Boulariah, O., 2022. Long-term regional changes in inter-annual precipitation variability in the Campania Region, Southern Italy. Theor. Appl. Climatol. (2022) 148, 869–879. https://doi.org/10.1007/s00704-022-03972-2.

Matherne, A.-M., Megdal, S.B., 2023. Advances in transboundary aquifer assessment. Water 15, 1208. https://doi.org/10.3390/w15061208.

Petrone, P., De Vita, P., Marsiglia, P., Allocca, P., Coda, S., Cusano, D., Lepore, D., Allocca, V., 2024. Hydrogeological conceptual model and groundwater recharge of Avella Mts. karst aquifer (southern Italy): A literature review and update. J. Hydrol. Reg. Stud. 54, 101871. https://doi.org/10.1016/j.ejrh.2024.101871.

Ruggieri, G., Allocca, V., Borfecchia, F., Cusano, D., Marsiglia, P., De Vita, P., 2021. Testing evapotranspiration estimates based on MODIS satellite data in the assessment of the groundwater recharge of karst aquifers in southern Italy. Water 13 (2), 118. https://doi.org/10.3390/w13020118.

Santo, A., Santangelo, N., De Falco, M., Forte, G., Valente, E., 2019. Cover collapse sinkhole over a deep buried carbonate bedrock: The case study of Fossa San Vito (Sarno-Southern Italy). Geomorphology 345, 106838. https://doi.org/10.1016/j.geomorph.2019.106838.

Schuch, C.S., Galvão, P., de Melo, M.C., Pereira, S., 2023. Overexploitation assessment in an urban karst aquifer: The case of Sete Lagoas (MG), Brazil. Environ. Res. 236, 116820. https://doi.org/10.1016/j.envres.2023.116820.

Tayia, A., 2019. Transboundary Water Conflict Resolution Mechanisms: Substitutes or Complements. Water 2019, 11(7), 1337; https://doi.org/10.3390/w11071337

Thornthwaite, C.W., Mather, J.R., 1955. The Water Balance. Publ. Climatol. 1955, 8, 1-104.

Turc, L., 1955. Le bilan d'eau des sols: relations entre les précipitations, l'évaporation et l'écoulement. Ann. Agron. 1954 5, 491-595.

USDA, 1972. SCS National Engineering Handbook, Section 4, Hydrology. Chapter 10, Estimation of Direct Runoff From Storm Rainfall. U.S. Department of Agriculture, Soil Conservation Service, Washington, D.C., 10.1-10.24.

Valente, E., Allocca, V., Riccardi, U., Camanni, G., Di Martire, D., 2021. Studying a subsiding urbanized area from a multidisciplinary perspective: The inner sector of the Sarno Plain (Southern Apennines, Italy). Remote Sens. 13, 3323. https://doi.org/10.3390/rs13163323.

Westenbroek, S.M., Kelson, V., Dripps, W., Hunt, R., Bradbury, K., 2010. SWB-a modified Thornthwaite-Mather Soil-Water-Balance Code for estimating groundwater recharge. US Department of the Interior, US Geological Survey, Ground Resources.

4.3 Impacts of climate change on the groundwater recharge of the Avella Mts. karst aquifer by Regional Climate Models

Keywords: Climate Change, Groundwater Recharge, Karst Aquifer, Regional Climate Models, Southern Italy

Abstract

This study assesses the impacts of climate change on the groundwater recharge of the Avella karst aquifer (Southern Italy) using the ensemble $E15_{Avella}$, derived from the multimodel ensemble of 15 Regional Climate Models (RCMs) developed by Lepore et al. (2024). The analysis employs the time series of precipitation and air temperature of $E15_{Avella}$ for the historical period (1950-2005) and scenario projections (2006-2100), bias-corrected using observed data from the National Hydrographic Service network (45 rain gauges and 28 air temperature stations). Annual hydrological balances were computed using effective evapotranspiration (ETR), estimated by the Turc formula, and effective precipitation (P-ETR) for the historical period and the IPCC Representative Concentration Pathways (RCP4.5 and RCP8.5) scenarios over three consecutive 30-year periods: 2010-2040, 2041-2070 and 2071-2100. The projections indicate a consistent reduction in groundwater recharge compared to the mean value of the historical period (1950-2005). The most significant reduction, equal to 50%, occurs under the RCP8.5 scenario for the long term period (2071–2100), while the RCP4.5 scenario predicts a decrease of 22%. The Mean Annual Groundwater Recharge Index (MAGRI) was calculated to analyse variations in groundwater recharge which for future scenarios (2006–2100) indicate marked inter-annual variability along with decreasing trends. These trends highlight the significant impact of climate change on groundwater availability in the Avella karst aquifer, which may be exacerbated by artificial pumping.

The results of this study emphasise the need for sustainable groundwater management, especially in aquifers with Mediterranean-type climates worldwide and provide essential evidence to help water authorities plan large-scale infrastructure projects for future resilience.

Introduction

Assessing the impacts of climate change on groundwater resources is a critical challenge and fundamental to ensuring sustainable aquifer management (Moeck et al., 2016). This is particularly true for Mediterranean karst aquifers, which are particularly sensitive to hydroclimatic variability. In specific, the Mediterranean region is recognised as a climate change hotspot, with warming rates exceeding the global average (Giorgi, 2006; Sivelle et al., 2021; Todaro et al., 2022). Precipitation and air temperature are key variables controlling groundwater recharge processes and are highly susceptible to the effects of climate change. The estimation of the recharge using these parameters is essential for the quantification of groundwater resources (Freeze and Cherry, 1979; Pulido-Velazquez et al., 2018), especially in southern Italy, where karst aquifers, known for their high mean annual groundwater yield, the highest in Europe (Stevanović, 2018), are the main source of drinking water (Allocca et al., 2007).

One of the most recognised approaches for future climate projections is the use of climate model data derived from different general circulation models (GCMs) and regional climate models (RCMs) that consider different greenhouse gas emission scenarios (D'Oria et al., 2018). Although the impact of climate change on groundwater recharge is less studied compared to surface water, several studies in the Mediterranean used empirical (Lepore et a., 2024; Pardo-Igúzquiza et al., 2019; Pulido-Velazquez et al., 2018; Stigter et al., 2012, 2014) and numerical methods (D'Oria et al., 2019; Nerantzaki et al., 2020; Voulanas et al., 2021) based on GCMs and RCMs. These studies used an ensemble of RCMs from the European Coordinated Regional Downscaling Experiment (EURO-CORDEX) (Giorgi et al., 2009) to better quantify uncertainties, focusing on precipitation and air temperature as key variables for groundwater recharge estimation. Bias adjustment was applied to align GCMs/RCMs data with observations, reducing uncertainty in projections (Teutschbein and Seibert, 2012). Projections considered different greenhouse gas scenarios (Representative Concentration Pathways, RCPs), with RCP4.5 representing intermediate conditions and RCP8.5 the most severe (IPCC, 2014; Van Vuuren et al., 2011).

The aim of this research is to assess the impacts of climate change on groundwater recharge in the Avella Mts., one of the main important karst aquifer in the Campania region (southern Italy). The analysis used data from the $E15_{Avella}$ ensemble, a subset of the ensemble mean of 15 RCMs (E15) derived from Lepore et al. (2024), provided by the EURO-CORDEX (Giorgi

et al., 2009) with a spatial resolution of 0.11° (~12 km) considering the RCP4.5 and RCP8.5 scenarios. To ensure the reliability of the results, the raw data of the RCMs were subjected to a rigorous bias-correction process that adjusted for systematic discrepancies between RCMs and observed data. Observed climatological data from 45 rain gauges and 28 air temperature stations distributed over the study area were used for this purpose. The bias correction was performed over a 30-year period (1954-1984), which provided sufficient overlap between the observed and RCMs data sets. Groundwater recharge was estimated using the hydrological balance equation. The Turc formula is used to calculate effective evapotranspiration (ETR) based on annual precipitation and mean air temperature for each grid cell. Recharge is then determined by multiplying the coefficient of potential infiltration (CIP), specific to the carbonate karst aquifers of southern Italy (CIP = 0.9, Celico et al., 1986), by the effective precipitation (P - ETR). The Mean Annual Groundwater Recharge Index (MAGRI) was calculated to quantify deviations in recharge relative to historical conditions.

The rest of the paper is organised as follows: Section 2 describes the geological, hydrogeological and climatic characteristics of the study area; Section 3 presents the data and methodological approaches used; Sections 4 and 5 comment and discuss the results obtained, and Section 6 presents the concluding remarks.

Study area

The Avella Mts., covering an area of about 370 km^2, host one of the most important karst aquifers in the Mediterranean region with a mean annual specific groundwater of up to 0.037 $m^3/s/km^2$. This aquifer provides groundwater resources mainly for drinking water supply and is also used for industrial and agricultural purposes. It supports natural landscapes and ecosystems (eg. forests, grasslands, springs, rivers, poljes and karst landforms) with great geo- and biodiversity and controls the hydrological regime of Sarno, Regi Lagni, Isclero and Sabato rivers. The basal aquifer consists mainly of limestones, dolomitic limestones and dolomite belonging to the Mesozoic-Cenozoic carbonate domain (Fig. 31a) (Petrone et al., 2024) with a thickness of about 2800 m. The turbiditic pre- and syn-orogenic deposits and Quaternary pyroclastic-alluvial deposits represent the lateral aquiclude and aquitard, respectively. The carbonate domain is highly fractured and karstified due to tectonic activity, with fault and fracture networks NW-SE and SW-NE oriented (Vitale and Ciarcia, 2018). The local tectonic structure, including direct and inverse faults and synclinal-anticlinal folds, creates a basins-in-series system that influences the basal groundwater flow. Five groundwater basins are identified (Petrone et al., 2024): GB1 supplies the Cancello spring group (Calabricito and Mefito springs), GB2 and GB3 feed subsurface flow towards the Campanian plain and Baiano valley, GB4 supplies the Sarno spring group (S. Maria La Foce, Mercato Palazzo and Cerola springs) and GB5 supplies the S. Marina di Lavorate, S. Mauro, Laura and Labso springs. Due to natural and anthropogenic factors, the flow of these springs is decreasing. A recent study conducted by Petrone et al. (2024) provided an updated groundwater balance for the aquifer, in which the estimated groundwater recharge ranges from approximately 7.30 m^3/s to 6.90 m^3/s.

The Avella Mts. are characterized by a Mediterranean-mild climate (CSb), with hot, dry summers and mild, wet winters. The average monthly air temperature reaches 25°C in August and drops to 7°C in January, while monthly rainfall ranges from 190 mm in November to just 30 mm in August (Fig. 31b). The mean annual cumulative rainfall is approximately 1320 mm, and the average air temperature is around 14.4°C (Allocca et al., 2014; Ruggieri et al., 2021).

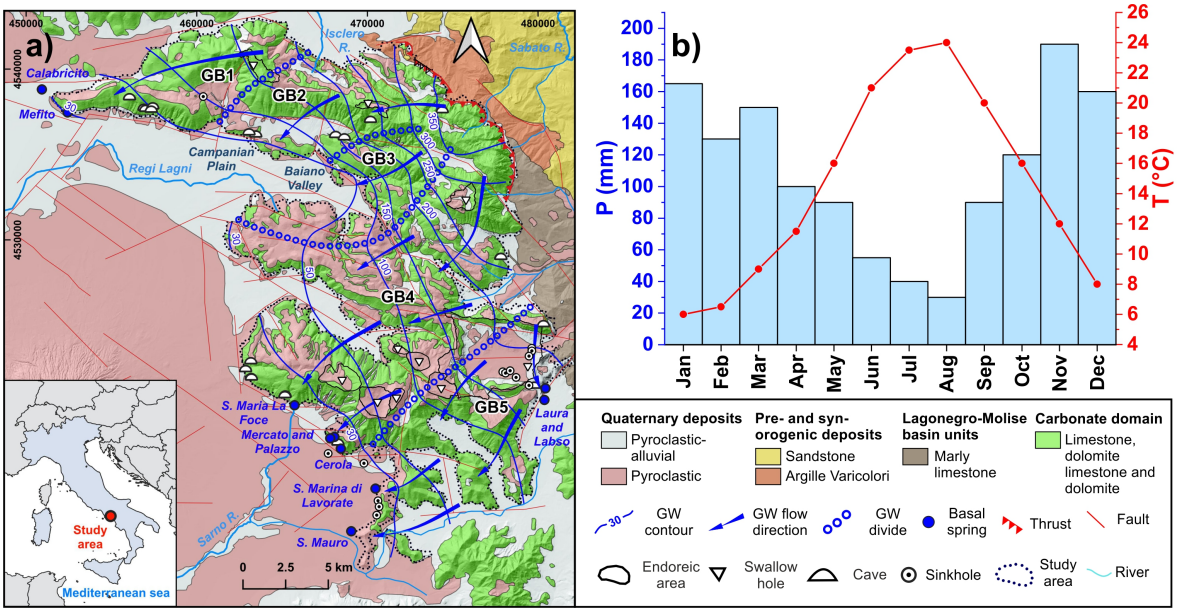


Figure 31 – a) Hydrogeological map of Avella Mts. (Petrone et al., 2024, modified); b) Seasonal rainfall and air temperature regime.

Data and methods

RCMs

To assess historical and future climate projections and their impact on recharge processes in the study area, the multimodel ensemble of 15 RCMs (E15) developed by Lepore et al. (2024) was used. RCMs projections derive from the EURO-CORDEX simulations (Jacob et al., 2014) and belong to the EUR-11 subset with a grid resolution of 0.11° (about 12.5 km). The available data for the historical experiment period (1950-2005) and future simulations (2006-2100) were analysed for RCP4.5 and RCP8.5 scenarios. RCP4.5 is representative of intermediate conditions, while RCP8.5 is the most drastic ("business as usual") and is commonly used because it represents the most extreme conditions, even if they are the least likely (Hausfather and Peters, 2020).

The E15 developed by the authors provides climate projections for the karst aquifers of southern Italy and is re-projected in WGS84-UTM 33N. In this study, the RCMs grid cells covering the Avella Mts. were extracted from E15, resulting in a subset of 12 cells well adapted to the study area, named $E15_{Avella}$.

Observed climatological time series (1950–2005)

In Italy, climatological monitoring began in 1921 when the SIMN governmental agency established a large network of rain gauges and air temperature stations. Climatological data from 1921 to 1999 were published in the SIMN annals after a validation process and aggregation to daily, monthly and annual time scales. The Italian Institute for Environmental Protection and Research (ISPRA) organised the data into a database covering the period from 1950 to 1996, including annual precipitation and mean annual air temperature records. In this study, climatological time series from the ISPRA database were used, specifically from monitoring stations located within the 12 cells of the RCMs grids selected for the study area (Figs. 32a, 32b, 32c, 32d).

To extend the analysis period, the climatological time series from 1997 to 2005, collected by a regional online database (https://centrofunzionale.regione.campania.it), were also included, selecting stations in the same RCMs cells. All climatological stations within the cells were considered observation points (OBS) since they provide climatological time series data observed for the validation period. A total of 45 precipitation OBS were selected, of which only 6 are characterized by continuous time series from 1950 to 2005, 18 from 1997 to 2005 and 21 from 1950 to 1996 (Fig. 32a). 28 temperature OBS were also selected, of which 2 stations provide a continuous time series from 1950 to 2005, 16 from 1950 to 1996 and 9 from 1997 to 2005 (Fig. 32c). Mean OBS precipitation (OBS_P) (Fig. 32e) and OBS air temperature (OBS_T) (Fig. 32g) were calculated for multiple stations in the same grid cell. The OBS_P and OBS_T time series were used for statistical comparison with $E15_{Avella\text{-}P}$ (Fig. 32f) and $E15_{Avella\text{-}T}$ (Fig. 32h) time series, respectively, at the aquifer scale. Missing values for the 1997 - 2005 period were filled with the OBS time series of neighbouring cells to improve data reliability.

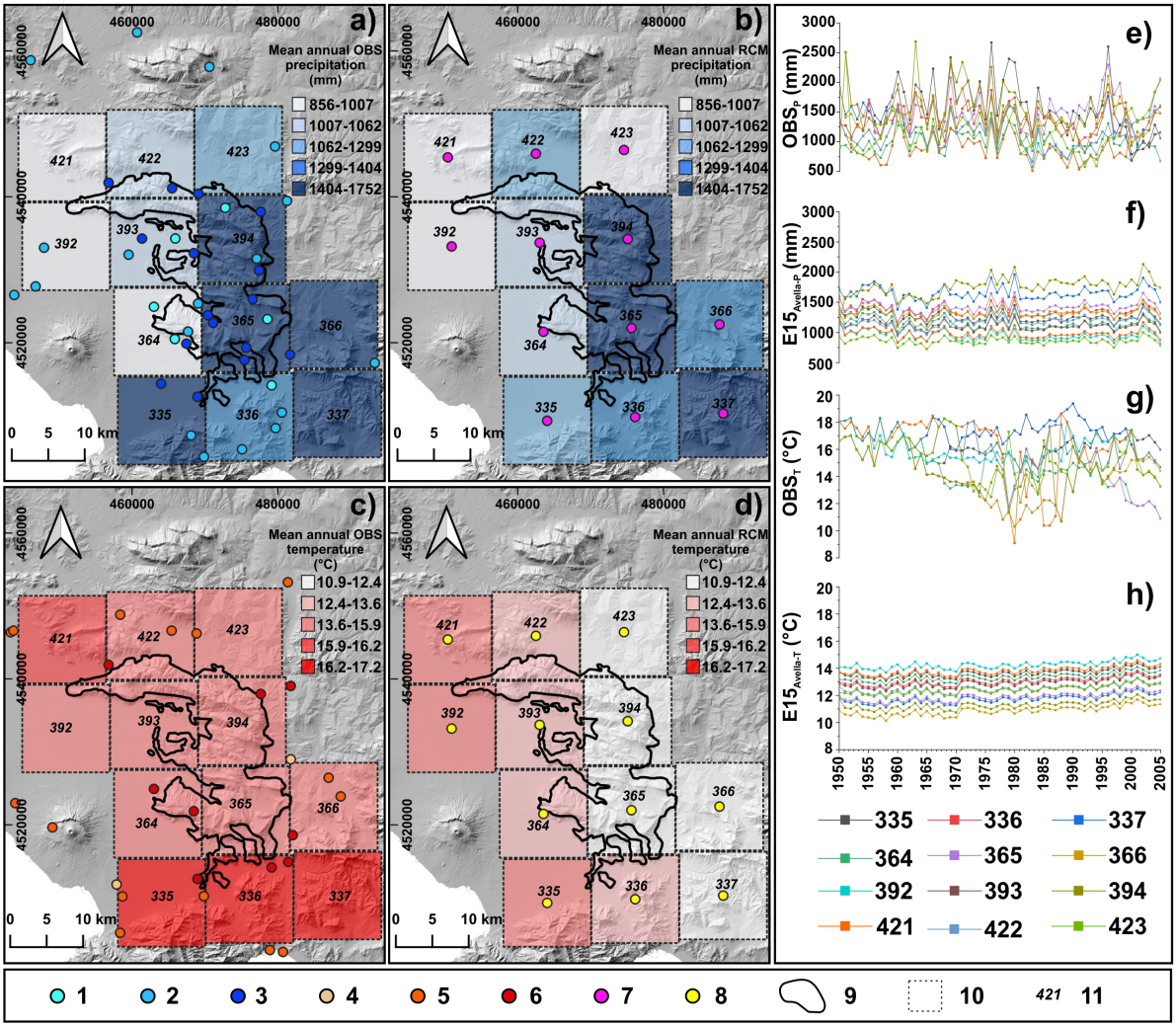


Figure 32 – a) Map of mean annual observed precipitation; b) map of mean annual RCMs precipitation; c) map of mean annual observed temperature; d) map of mean annual RCMs temperature; mean time series graphs extracted from each pixel of e) OBS_P; f) $E15_{Avella\text{-}P}$; g) OBS_T; h) $E15_{Avella\text{-}T}$. Symbology: 1) OBS_P from 1950 to 2005; 2) OBS_P from 1950 to 1996; 3) OBS_P from 1997 to 2005; 4) OBS_T from 1950 to 2005; 5) OBS_T from1950 to 1996; 6) OBS_T from1997 to 2005; 7) $E15_{Avella\text{-}P}$ from 1950 to 2005; 8) $E15_{Avella\text{-}T}$ from 1950 to 2005; 9) study area; 10) RCMs cell; 11) number of RCMs cell.

Bias-correction and validation

A bias correction was applied to the selected RCMs data to remove systematic errors. This method is applied considering a period where observed (OBS) and modelled time series are available and overlap (D'Oria et al., 2018). The bias correction method aims to assess the differences between the RCMs "historical experiment" and the OBS datasets over at least 30 years (Trzaska and Schnarr, 2014). For this study, bias correction was applied from 1954

to 1984. This timeframe was selected because it offers a reliable overlap between observed and modelled data. Additionally, it allows for a robust statistical comparison and covers a sufficiently long duration to account for natural climate variability. Two pairs of datasets were created to compare the $E15_{Avella}$ and OBS data. These datasets were based on identifying the grid cells from the RCMs model that contain available OBS_P and OBS_T data, which were compared with the corresponding $E15_{Avella}$ precipitation ($E15_{Avella\text{-}P}$) and air temperature ($E15_{Avella\text{-}T}$) data for the same grid cell each year. The bias analysis between $E15_P$ and OBS_P and between $E15_T$ and OBS_T was conducted for each grid cell on an annual basis using the equation Eq. (5):

$$Bias_{P,T,t}\,(j) = \frac{(Model_{P,T,t}\,(j) - OBS_{P,T,t}(j))}{OBS_{P,T,t}(j)} \tag{5}$$

where $Model_{P,T,t}\,(j)$ is the value of $E15_{Avella\text{-}P}$ or $E15_{Avella\text{-}T}$ and $OBS_{P,T,t}\,(j)$ is the observed value of precipitation or air temperature for the year t (t = 1954, 1955⋯1984) in the *jth* grid cell.

Next, the mean value of the bias over the generic t_{year} ($Bias_{P,T,t}$) and the entire area was calculated by Eq. (6):

$$\overline{Bias_{P,T,t}} = \frac{\sum_{j=1}^{n} Bias_{P,T}(j)}{\sum_{j=1}^{n} j} \tag{6}$$

in this case, n is the number of grid cells considered. Finally, the bias-corrected annual value of the $E15_{Avella}$ ($Model_{P,T,t}\,(j)$) is then estimated using Eq. (7):

$$Model^{*}_{P,T,t}\,(j) = Model_{P,T,t}(j) \times (1 - \overline{Bias_{P,T,t}}) \tag{7}$$

Groundwater balance

The long-term impact of climate change on hydrological variables affecting groundwater recharge in the Avella karst aquifer was assessed using the $E15_{Avella}$ bias-corrected values of precipitation and air temperature. Considering the whole $E15_{Avella}$ dataset, a time series of mean annual precipitation and air temperature was created for reconstructing a complete time series including both the "historical experiment" period (1950–2005) and scenarios (2006–2100) under both the RCP4.5 and RCP8.5 pathways.

The effects of climate change on groundwater recharge were evaluated using the hydrological budget equation Eq (8):

$$P_{tj} = ETR_{tj} + Ie_{tj} + R_{tj} \quad (8)$$

where P_{tj} is the precipitation, ETR_{tj} is the actual evapotranspiration, Ie_{tj} is the effective infiltration or groundwater recharge, and R_{tj} is the runoff, all related to the t-*year* and j-*cell*.

The empirical Turc formula (Eq. 9) (Turc, 1955; Shaw et al., 2010) was used to estimate the ETR:

$$ETR_{t,j} = \frac{P_{t,j}}{\sqrt{0.9+\left(\frac{P_{t,j}}{300+25*T_{t,j}+0.05*T_{t,j}^3}\right)^2}} \quad (9)$$

where $P_{t,j}$ is the total annual precipitation (mm) and $T_{t,j}$ is the mean annual air temperature (°C), both for the j-*cell*. The Turc formula relies on annual precipitation (P) and mean annual air temperature (T), which naturally accounts for the spatial variability of these two hydrological variables. As a result, the formula was applied to all grid cells where P and T data were reconstructed by the RCMs ensemble for each year in the time series.

The recharge derived by RCMs data is expressed using the Eq (10):

$$Recharge = CIP * (P - ETR)_{t,j} \quad (10)$$

where *P* is precipitation, *ETR* is evapotranspiration, and *CIP* is the *Coefficient of Potential Infiltration* that is constant during the historical and future periods (Pardo-Igúzquia et al. 2019). A CIP value of 0.9, which is typical of carbonate karst aquifers in southern Italy (Celico et al., 1986), was assigned. This choice is supported by the spatial resolution of the RCMs grid cells, approximately 12.5 km, which allows assigning a representative CIP value for carbonate units.

Finally, in order to study the variation of the groundwater recharge with respect to the historical period (1950-2005) and the scenarios (2006-2100), the Mean Annual Groundwater Recharge Index (MAGRI) was calculated for each year of the time series and for the whole area, as follows Eq. (11):

$$MAGRI_t = \frac{GR_t - Hist\ GR}{Hist\ GR} \quad (11)$$

where $MAGRI_t$ is the Mean Annual Groundwater Recharge Index for the t-*year* (%), Gr_t is the Groundwater Recharge for the t-*year* and Hist GR is the Mean Annual Groundwater Recharge of the whole RCM time series, corresponding to the historical period (1950-2005), and the entire area.

Results

RCMs validation

The bias assessment applied over the 30 years (1954 - 1984) allowed for quantifying the accuracy of precipitation and air temperature of the single RCMs compared to the corresponding OBS. The box plots in Figure 33 show distributions of OBS and $E15_{Avella}$ before and after the correction. The application of bias correction significantly reduces systematic error (Tab. 5). Before the correction, $E15_{Avella\text{-}P}$ exhibited an underestimation of 4% compared to OBS_P, whereas, after correction, the model showed an overestimation of only 0.001%. Similarly, a comparison between $E15_{Avella\text{-}T}$ and OBS_T revealed that $E15_{Avella\text{-}T}$ initially underestimated OBS_T by approximately 19%, which was reduced to a 4% underestimation after the correction.

Mean precipitation (mm)				
OBS_P	**$E15_{Avella\text{-}P}$**	**Bias $E15_{Avella\text{-}P}$**	**$E15_{Avella\text{-}P}$ corr**	**Bias $E15_{Avella\text{-}P}$ corr**
1,319.5	1,245.1	-0.04	1,294.9	0.00001
Mean temperature (°C)				
OBS_T	**$E15_{Avella\text{-}T}$**	**Bias $E15_{Avella\text{-}T}$**	**$E15_{Avella\text{-}T}$ corr**	**Bias $E15_{Avella\text{-}T}$ corr**
15.5	12.5	-0.19	14.8	-0.04

Table 5 – Mean annual precipitation and temperature over the period 1954-1984, observed values (OBS_P and OBS_T), Bias $E15_{Avella}$ (Bias $E15_{Avella\text{-}P}$ and Bias $E15_{Avella\text{-}T}$), $E15_{Avella}$ corrected ($E15_{Avella\text{-}P}$ corr and $E15_{Avella\text{-}T}$ corr).

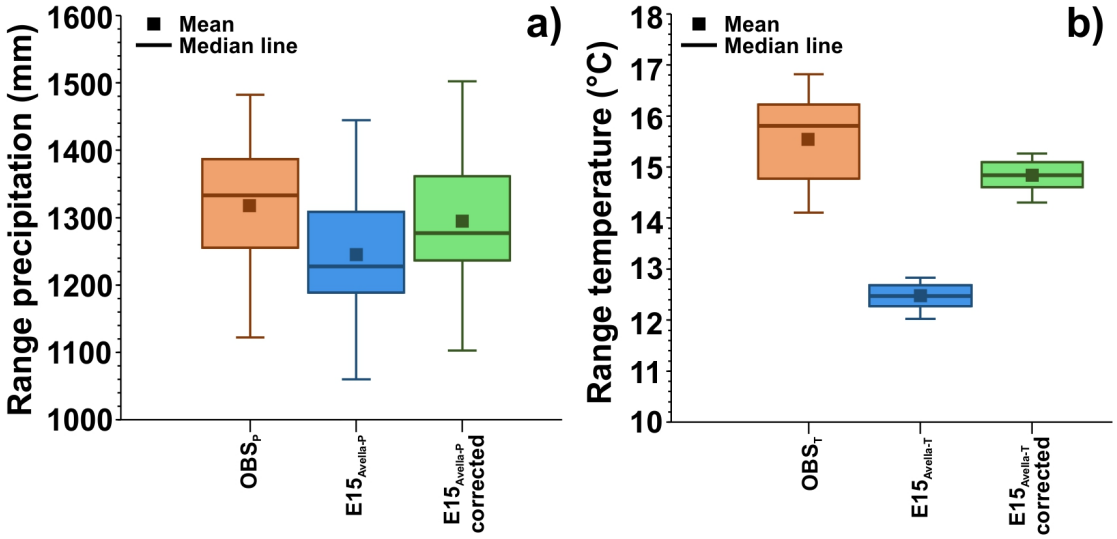


Figure 33 – a) Box plot of OBS_P, $E15_{Avella-P}$ and $E15_{Avella-P}$ corrected; b) Box plot of OBS_T, $E15_{Avella-T}$ and $E15_{Avella-T}$ corrected.

Annual hydro-climatological parameters forecasting

A continuous time series up to 2100 for both RCP 4.5 and RCP 8.5 scenarios was constructed using the annual corrected $E15_{Avella-P}$ and $E15_{Avella-T}$ values for the whole Avella karst aquifer (Figs. 34a, 34b). Precipitation projections show a decreasing trend under both pathways, characterized by significant interannual variations, particularly under the RCP8.5 scenario (Fig. 34a). Both scenarios predict a significant increase in air temperature (Fig. 34b). In particular, the RCP8.5 scenario predicts the most significant increase, with average temperatures rising by around 4°C by the end of the century. On the other hand, the RCP4.5 scenario predicts an increase of about 2°C. The differences between the two scenarios become evident from 2040 onwards when a divergence in the trends of the time series is observed.

The $E15_{Avella-P}$ and $E15_{Avella-T}$ time series of both pathways were used to quantify the ETR and P-ETR scenarios (Figs. 34c, 34d). According to the general increase in air temperature, the ETR scenarios for 2006–2100 show a progressive rise for both RCP pathways (Fig. 34c). Analyzing P-ETR, the time series show a significant decreasing trend for both RCP8.5 and RCP4.5 pathways, with the most severe conditions observed for RCP8.5 (Fig. 34d).

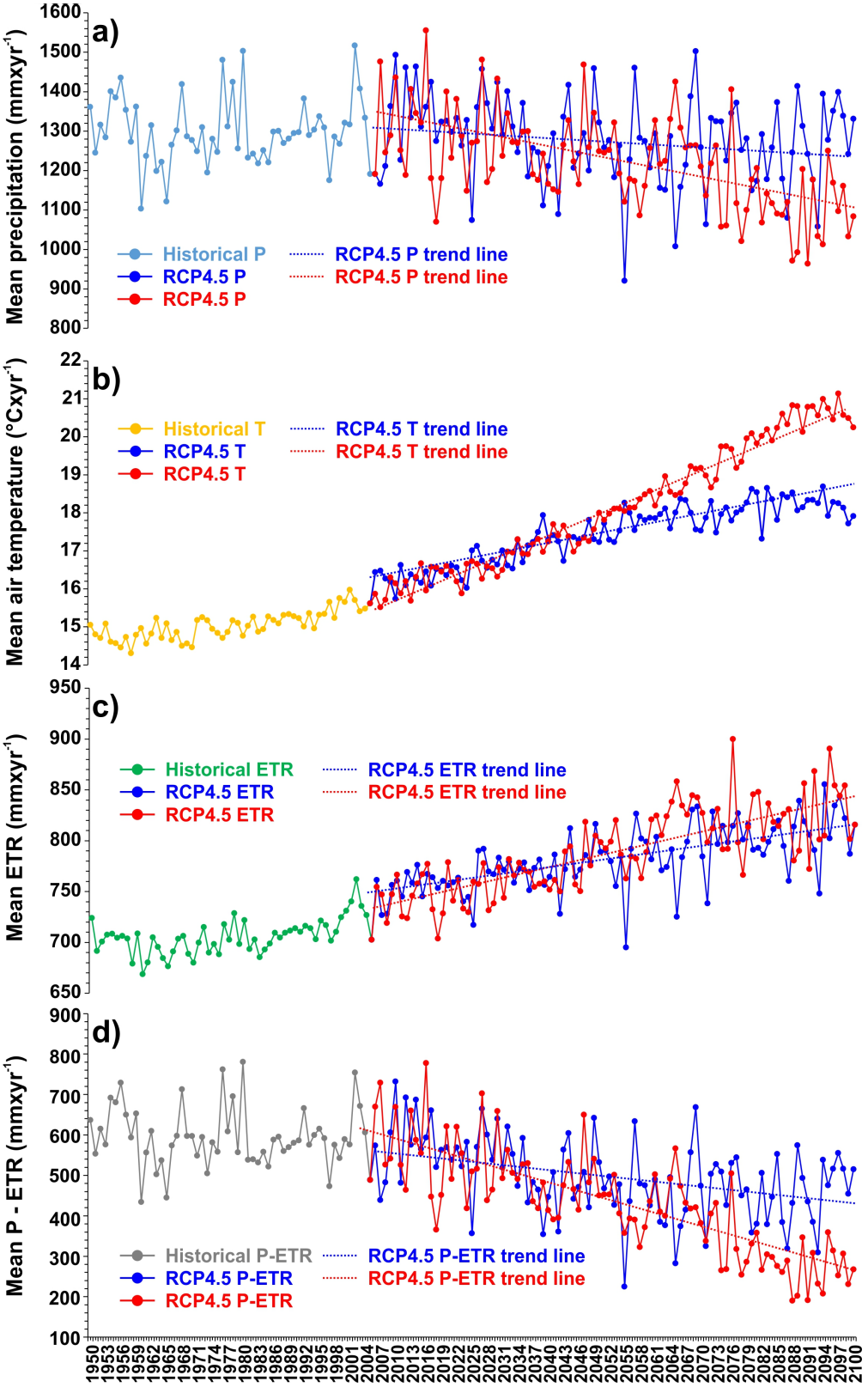


Figure 34 - Time series of the "historical" period (1950–2005) and scenarios (2006–2100) under RCP8.5 and RCP4.5 pathways: a) mean annual precipitation; b) mean annual air temperature; c) mean annual ETR; d) mean annual P-ETR.

Groundwater recharge scenarios

The potential effects of climate change on groundwater recharge in the Avella karst aquifer were evaluated using P-ETR climate projections derived from the RCM ensemble. Recharge was estimated for three consecutive periods: 2010-2040 (short term), 2041-2070 (medium term) and 2071-2100 (long term). Both climate scenarios, RCP4.5 and RCP8.5, were analysed and compared with RCM historical recharge values (212 Mm^3 yr^{-1}) for the reference period 1950-2005 (Fig. 35a).

Groundwater recharge is reduced for both RCP8.5 and RCP4.5 scenarios compared to the historical period, with a decrease more significant for RCP8.5. An overview of the average and total volumes for both RCP and reference periods is summarized in Table 6, while Figures 35b, 35c, 35d, 35e, 35f and 35g show the percentage decrease in recharge over the RCP periods relative to the control period.

Based on the historical recharge values in Table 6 and focusing on the RCP4.5, groundwater recharge is expected to decrease by 7% (insignificant change), 21% and 22% (significant change) in the short (Fig. 35b), medium (Fig. 35c) and long term (Fig. 35d) respectively. Furthermore, the projections for RCP8.5 in Table 6 show a significant reduction in recharge, with an 11% (significant change) reduction in the short term (Fig. 35e), a 25% (significant change) reduction in the medium term (Fig. 35f) and a substantial 50% (major change) reduction in the long term (Fig. 35g).

To assess MAGRI, recharge time series were reconstructed for the historical period (1950-2005) and projected scenarios from 2006 to 2100 for both RCP4.5 and RCP8.5 pathways over the study area (Fig. 35h). During the historical period (1950-2005), MAGRI showed relative stability, averaging around 212 Mm^3 yr^{-1}. MAGRI fluctuated significantly with a minimum of -27% in 1960 and a maximum of +32% in 1980, compared to the average recharge value for the entire historical period. Similarly, MAGRI estimates for the future scenario periods (2006-2100) under both RCP4.5 and RCP8.5 pathways show marked inter-annual fluctuations coinciding with decreasing trends.

Recharge	Historical 1950-2005	RCP 4.5			RCP 8.5		
		short 2011-2040	medium 2041-2070	long 2071-2100	short 2011-2040	medium 2041-2070	long 2071-2100
Mean (Mm^3yr^{-1})	212.00	184.37	156.69	153.26	175.70	148.51	98.39
Variation (%)	-	-0.07	-0.21	-0.22	-0.11	-0.25	-0.50

Table 6 - Mean annual groundwater recharge and variation (%) against the historical period estimated for three consecutive decades: 2011–2040 (short term), 2041–2070 (medium term), and 2071–2100 (long term).

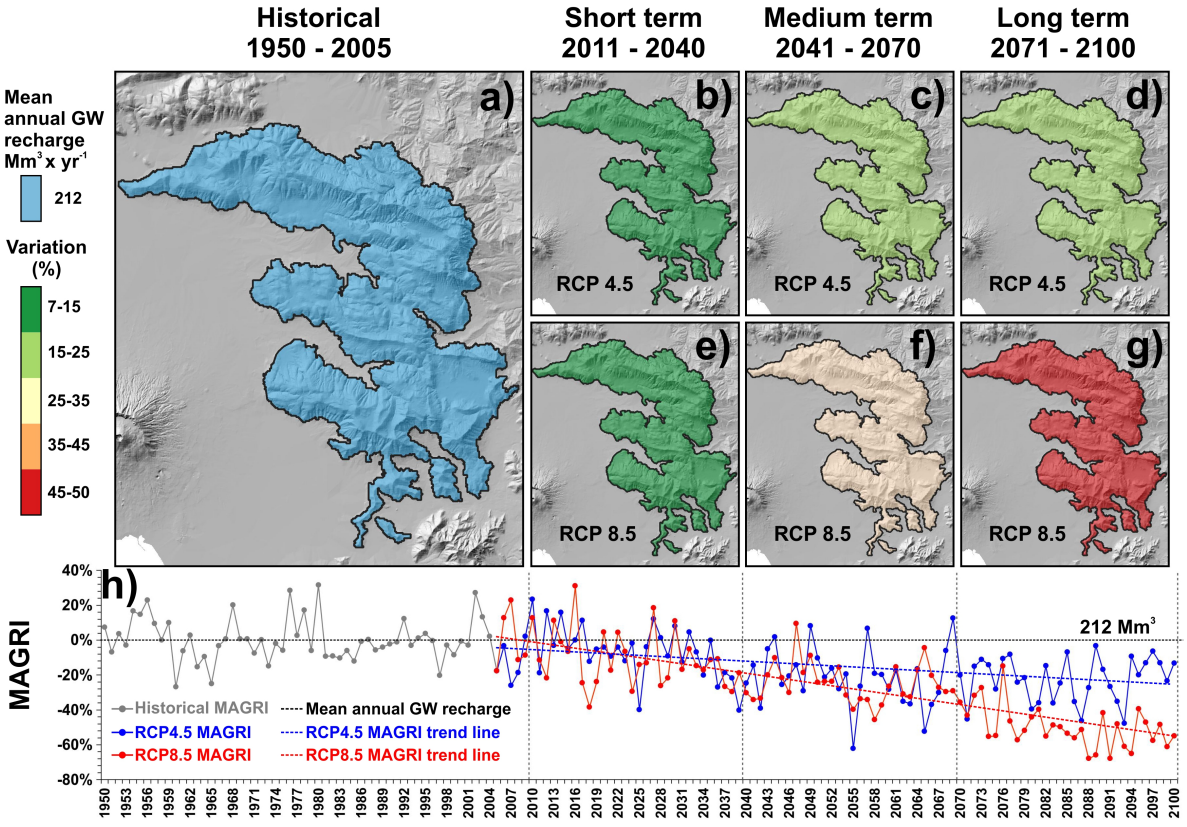


Figure 35 – a) Map of RCM historical mean annual groundwater recharge; maps of RCM recharge variation for the RCP4.5 scenario in the: b) short term, c) medium term; d) long term and for the RCP8.5 scenario in the: e) short term, f) medium term; g) long term; h) MAGRI time series for the historical period (1950-2005) and projected scenarios (2006 to 2100) for both RCP4.5 and RCP8.5 pathways.

Discussion

The recharge RCMs projections show a decreasing trend over time, with more pronounced reductions for the RCP8.5 scenario than for RCP4.5. This behaviour is consistent with the expected effects of increasing air temperatures and decreasing precipitation predicted by the main climate change scenarios. The comparison of recharge values estimated using RCMs projections with those from previous studies aimed to validate the projected future recharge values for various greenhouse gas emission scenarios concerning the Avella karst aquifer. However, RCMs projections are generally underestimated compared to methods based on observed local-scale data (Fig.36). For the period 2000-2019, the recharge estimated using Turc formula (Petrone et al., 2024) is 7.30 m^3/s, which is higher than the RCP4.5 and RCP8.5 projections, equal to 6.26 m^3/s and 6.15 m^3/s, respectively. Similarly, for the period 2010-2021, the SWB method (Soil Water Balance - Petrone et al., 2025) estimated a recharge of 7.75 m^3/s, which exceeds the RCMs values equal to 6.32 m^3/s for RCP4.5 and 5.85 m^3/s for RCP8.5. This small difference can be attributed to the spatial scale between the datasets. The methods based on ground station (Turc and SWB) record local conditions at a higher resolution, capturing the detailed variability essential for complex hydrogeological systems such as karst. In contrast, RCMs operate at larger scales, with a resolution that may not capture the sub-scale recharge variability. An interesting result emerged from the comparison with MODIS data, which estimate a recharge of 6.90 m^3/s (Petrone et al., 2024) for the period 2000-2019, showing a significant correlation with the RCP4.5 and RCP8.5 projections equal to 6.26 m^3/s and 6.15 m^3/s, respectively. This correlation is likely related to the similarity in spatial resolutions of MODIS and RCM, which both operate on regional rather than local scales. The comparison of methods highlights the importance of considering the spatial scale and resolution of data when assessing the accuracy of future projections. This approach helps to validate the models used and improve understanding of the impacts of climate change on groundwater recharge under greenhouse gas emission scenarios, providing useful insights for sustainable water resource management. In addition, a comparison of the recharge estimated by RCMs projections with future water demand would provide a more comprehensive framework for assessing water availability, allowing the identification of potential imbalances between recharge and withdrawal. Such an approach could enhance the development of sustainable water management strategies that address the challenges posed by changes in climate and socio-economic conditions.

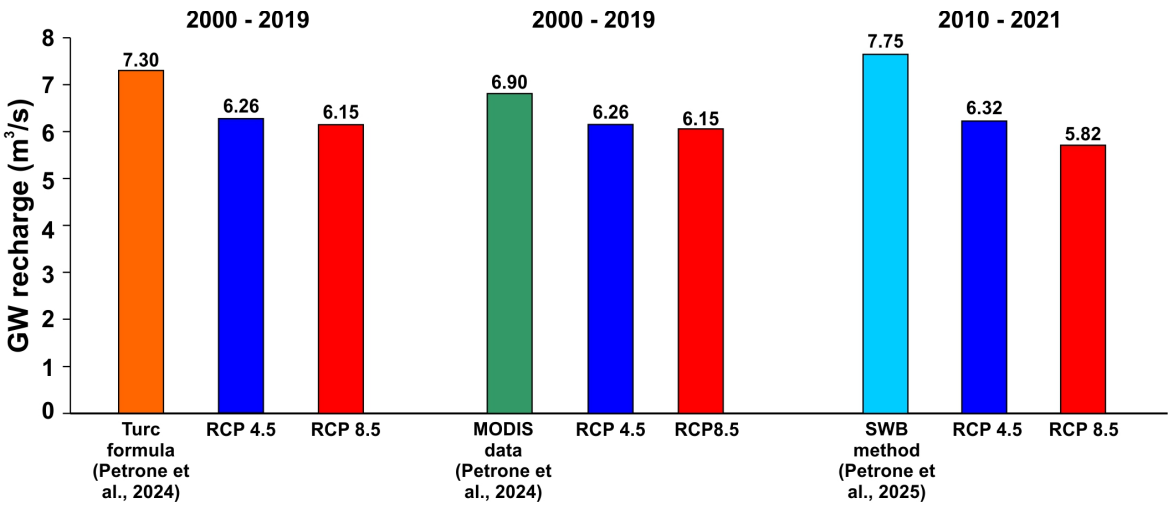


Figure 36 – Comparison of recharge values estimated using Turc formula, MODIS data and SWB methods with those from RCMs under RCP8.5 and RCP4.5 pathways.

Conclusions

The study evaluated the effects of climate change on groundwater recharge in the Avella karst aquifer, employing a methodology that integrates observed climatological data with an ensemble of 15 RCMs from Lepore et al. (2024), with a focus on the RCMs cells within the Avella Mts. domain ($E15_{Avella}$).

The bias correction reduced systematic errors in the RCMs precipitation and air temperature data and improved the accuracy of the $E15_{Avella}$ dataset, aligning it more closely with observed values. After correction, the overestimation of precipitation is negligible (0.001%), while the underestimation of temperature is reduced from 19% to 4%.

Both RCP4.5 and RCP8.5 scenarios project a significant increase in air temperatures and a decrease in precipitation over the 21st century, with considerable interannual variability.

Groundwater recharge is expected to decline significantly under both scenarios, with RCP8.5 showing a more severe reduction compared to RCP4.5. In particular, the RCP8.5 scenario displays a notable decrease (-50%) in the long term projection (2071 – 2100), even if this scenario is the least likely to occur.

When compared to methods based on observed data, such as the Turc formula and SWB, RCMs projections tend to underestimate recharge. This discrepancy can be attributed to the higher resolution of local-scale methods, which capture finer spatial variability. A comparison with MODIS data, instead, showed a significant correlation with the RCMs projections, likely due to the lower spatial resolution of both methods. Furthermore, the

integrated analysis of MAGRI has revealed that the future scenario periods (2006-2100) under both RCP4.5 and RCP8.5 pathways show marked inter-annual fluctuations that coincide with the overall decreasing trends in recharge. The comparison of recharge values obtained from RCMs with those derived from methods based on ground observed data, such Turc formula and SWB method, revealed that the RCMs projections tend to underestimate recharge. This difference is due to the higher resolution of local scale methods, which capture more detailed spatial variability, whereas the RCMs operate at a lower resolution. On the other hand, a comparison with MODIS data showed a significant correlation with the RCMs projections, likely due to the lower spatial resolution of both datasets.

The results highlight the vulnerability of karst aquifers, such as Avella, to climate change, particularly under high greenhouse gas emissions scenarios, and the potential long-term implications for water resource management.

Furthermore, this research demonstrates the potential of using RCMs to define groundwater recharge scenarios under future climate conditions. Although the recharge projections may be subject to a degree of uncertainty, they provide a scientifically based perspective on potential changes.

References

Allocca, V., Celico, F., Celico, P., De Vita, P., Fabbrocino, S., Mattia, C., Monacelli, G., Musilli, I., Piscopo, V., Scalise, A. R., 2007. Carta idrogeologica dell'Italia meridionale. Istituto Poligrafico e Zecca dello Stato.

Allocca, V., Manna, F., De Vita, P., 2014. Estimating annual groundwater recharge coefficient for karst aquifers of the southern Apennines (Italy). Hydrol. Earth Syst. Sci. 18 (2), 803–817.

Celico, P., 1986. Prospezioni idrogeologiche. Vol. I, 1-735. Liguori Editore, Napoli, Italia. ISBN 88-207-1331-4.

D'Oria, M., Tanda, M. G., Todaro, V., 2018. Assessment of local climate change: Historical trends and RCM multi-model projections over the Salento Area Italy. Water Switzerland, 10(8). https://doi.org/10.3390/w10080978.

D'Oria, M., Ferraresi, M., Tanda, M. G., 2019. Quantifying the impacts of climate change on water resources in northern Tuscany, Italy, using high-resolution regional projections. Hydrol. Process. 33, 978–993.

Freeze, R. A., and Cherry, A. (s.d.). JA 1979. Groundwater. Prentice Hall, Inc, Upper Saddle River, NJ, 7458, 213.

Giorgi, F., 2006. Climate change hot-spots. Geophysical Research Letters, 33(8), 2006GL025734. https://doi.org/10.1029/2006GL025734.

Giorgi, F., Jones, C., Asrar, G., 2009). Addressing climate information needs at the regional level: The CORDEX framework. Organization (WMO) Bulletin, 58(July), 175–183.

Hausfather, Z., and Peters, G. P., 2020. Emissions–the 'business as usual'story is misleading. Nature, 577(7792), 618–620.

IPCC. Climate Change, 2014. Synthesis Report. Contribution of Working Groups I, II and III to the Fifth Assessment Report of the Intergovernmental Panel on Climate Change [Core Writing Team, R.K. Pachauri and L.A. Meyer (Eds.)]. IPCC, Geneva, Switzerland,, 151.

Jacob, D. et al., 2014. EURO-CORDEX: New high-resolution climate change projections for European impact research. Reg. Environ. Change 14, 563–578.

Lepore, D., Bucchignani, E., Montesarchio, M., Allocca, V., Coda, S., Cusano, D., De Vita, P., 2024. Impact scenarios on groundwater availability of southern Italy by joint application of regional climate models (RCMs) and meteorological time series.

Scientific Reports, 14:20337. 10.1038/s41598-024-70257-1. https://doi.org/10.1038/s41598-024-70257-1.

Moeck, C., Brunner, P., Hunkeler, D., 2016. The influence of model structure on groundwater recharge rates in climate-change impact studies. Hydrogeology Journal, 24(5), 1171–1184. https://doi.org/10.1007/s10040-016-1367-1.

Nerantzaki, S. D., & Nikolaidis, N. P., 2020). The response of three Mediterranean karst springs to drought and the impact of climate change. Journal of Hydrology, 591(July). https://doi.org/10.1016/j.jhydrol.2020.125296.

Pardo-Igúzquiza, E., Collados-Lara, A. J., Pulido-Velazquez, D., 2019. Potential future impact of climate change on recharge in the Sierra de las Nieves (southern Spain) high-relief karst aquifer using regional climate models and statistical corrections. Environmental Earth Sciences, 78(20), 1–12.

Petrone, P., De Vita, P., Marsiglia, P., Allocca, P., Coda, S., Cusano, D., Lepore, D., Allocca, V., 2024. Hydrogeological conceptual model and groundwater recharge of Avella Mts. karst aquifer (southern Italy): A literature review and update. Journal of Hydrology: Regional Studies, 54, 101871. https://doi.org/10.1016/j.ejrh.2024.101871.

Pulido-Velazquez, D., Collados-Lara, A. J., Alcalá, F. J., 2018. Assessing impacts of future potential climate change scenarios on aquifer recharge in continental Spain. Journal of Hydrology, 567, 803–819.

Ruggieri, G., Allocca, V., Borfecchia, F., Cusano, D., Marsiglia, P., De Vita, P., 2021. Testing Evapotranspiration Estimates Based on MODIS Satellite Data in the Assessment of the Groundwater Recharge of Karst Aquifers in Southern Italy. Water 13 (2), 118, 2021.

Shaw, E., Beven, K. J., Chappell, N. A., Lamb, R., 2010. Hydrology in Practice (CRC Press, 2010).

Sivelle, V., Jourde, H., Bittner, D., Mazzilli, N., Tramblay, Y., 2021. Assessment of the relative impacts of climate changes and anthropogenic forcing on spring discharge of a Mediterranean karst system. J. Hydrol. 598, 126396. https://doi.org/10.1016/j.jhydrol.2021.126396.

Stevanović, Z., 2018. Karst aquifers in the Arid World of Africa and the Middle East: Sustainability or humanity? In Karst Water Environment: Advances in Research, Management and Policy, 1–43.

Stigter, T. Y., Nunes, J. P., Pisani, B., Fakir, Y., Hugman, R., Li, Y., Tomé, S., Ribeiro, L., Samper, J., Oliveira, R., Monteiro, J. P., Silva, A., Tavares, P. C. F., Shapouri, M., Cancela da Fonseca, L., El Himer, H., 2012. Comparative assessment of climate change and its impacts on three coastal aquifers in the Mediterranean. Regional Environmental Change, 14(SUPPL.1), 41–56. https://doi.org/10.1007/s10113-012-0377-3.

Stigter, T. Y., Nunes, J. P., Pisani, B., Fakir, Y., Hugman, R., Li, Y., El Himer, H., 2014. Comparative assessment of climate change and its impacts on three coastal aquifers in the Mediterranean. Regional Environmental Change, 14(1), 41–56.

Teutschbein, C., and Seibert, J., 2012. Bias correction of regional climate model simulations for hydrological climate-change impact studies: Review and evaluation of different methods. Journal of Hydrology, 456–457, 12–29. https://doi.org/10.1016/J.JHYDROL.2012.05.052.

Todaro, V., D'Oria, M., Secci, D., Zanini, A., Tanda, M. G., 2022. Climate change over the Mediterranean region: Local temperature and precipitation variations at five pilot sites. Water, 14(16), 2499. https://doi.org/10.3390/w14162499.

Trzaska, S., and Schnarr, E., 2014. A review of downscaling methods for climate change projections. United States Agency for International Development by Tetra Tech ARD, 1–42.

Turc, L., 1954. Le bilan d'eau des sols: Relations entre les pr´ecipitations, l'´evaporation et l'´eecolument. Ann. Agron. 1954 5, 491–595.

Van Vuuren, D. P., Edmonds, J., Kainuma, M., Riahi, K., Thomson, A., Hibbard, K., et al., 2011. The representative concentration pathways: Anoverview. Climatic Change, 109(1–2), 5–31.

Vitale, S., Ciarcia, S., 2018. Tectono-stratigraphic setting of the Campania region (southern Italy). J. Maps, 2018 14 (2), 9–21.

Voulanas, D., Theodossiou, N., Hatzigiannakis, E., 2021. Assessment of potential hydrological climate change impacts in Kastoria basin (Western Macedonia, Greece)

using EUROCORDEX regional climate models. Global NEST Journal, 23(1), 35–46. https://doi.org/10.30955/gnj.003444.

4.4 Prospective for using of piedmont karst aquifers: the case study of the Baiano District (southern Apennines, Italy)

A. Aquino[1], P. Petrone[2*], M. Ginolfi[3], C. Mazzarotti[4], S. Rosamilia[5], S. Aquino[3], V. Allocca[2*]

[1] MIUR, Ministero dell'Istruzione, dell'Università e della Ricerca
[2] Università degli Studi di Napoli Federico II, Dipartimento di Science della Terra, dell'Ambiente e delle Risorse
[3] Università Telematica Pegaso
[4] Alto Calore Servizi S.p.A.
[5] Provincia di Avellino, Settore Ambiente

[*]Corresponding authors: paola.petrone@unina.it; vincenzo.allocca@unina.it

Riassunto

L'area pedemontana compresa tra i comuni di Avella, Baiano, Mugnano del Cardinale, Quadrelle, Sirignano e Sperone, denominata Mandamento di Baiano (Campania), è di notevole interesse idrogeologico. Questa regione, dal punto di vista idrogeomorfologico, è situata tra la piana di Nola ed il rilievo dei Monti di Avella ed ospita un importante acquifero carsico pedemontano. Sebbene le acque sotterranee siano utilizzate da tempo per l'approvvigionamento idrico delle comunità locali, mancano studi idrogeologici basati sul bilancio e monitoraggio per garantire un uso sostenibile della risorsa.

L'obiettivo di questo lavoro è quello di effettuare una caratterizzazione idrogeologica dell'acquifero carsico pedemontano per valutare: i) la ricarica delle acque sotterranee attraverso il bilancio idrologico; ii) la produttività locale dell'acquifero mediante prove di pompaggio; iii) la qualità idrochimica e microbiologica delle acque.

I risultati evidenziano che l'acquifero carsico pedemontano è caratterizzato da risorse idriche significative (la ricarica annua è mediamente pari a 0,90 m^3/s), di elevata qualità idrochimica e microbiologica e la produttività locale dell'acquifero (la trasmissività è dell'ordine di 10^{-1}-10^{-3} m^2/s) è tra le più alte in Italia.

I risultati aprono nuove prospettive sulla possibilità di utilizzo degli acquiferi carsici pedemontani dell'Appennino meridionale come risorse integrative e/o di riserva per i fabbisogni idrici locali. Tuttavia, nel caso studio del Mandamento di Baiano i prelievi attuali e futuri devono essere autorizzati sulla base di un bilancio idrico aggiornato dei Monti di Avella, dalla scala di bacino a quella locale, ed essere implementati mediante un monitoraggio continuo quali-quantitativo della risorsa, per evitare sovrasfruttamenti ed interferenze con la falda di piana, i centri abitati e le attività antropiche.

Parole chiave: acquifero carsico pedemontano, bilancio idrologico, prove di pompaggio, qualità delle acque, Appennino meridionale

Abstract

The piedmont area situated within the administrative borders of Avella, Baiano, Mugnano del Cardinale, Quadrelle, Sirignano and Sperone municipalities, also called Mandamento of Baiano (Campania region), is of high hydrogeological interest. From a hydrogeomorphological point of view, this region is located between the Nola plain and the Avella Mountains and hosts a strategic piedmont karst aquifer. Although groundwater are used from a long time to supply water to local communities, there aren't water balance-based hydrogeological studies and a groundwater monitoring to ensure sustainable use of the water resource.

The purpose of this paper is to characterize the piedmont karst aquifer to evaluate: i) the groundwater recharge through the hydrological balance; ii) the aquifer productivity by pumping tests; iii) the hydrochemical quality of groundwater.

The results highlight that the piedmont karst aquifer is characterized by significant groundwater resources (annual recharge is about 0,90 m^3/s), with a high groundwater quality and an aquifer productivity (transmissivity is the order of magnitude $10^{-1} \div 10^{-3}$ m^2/s) among the highest in Italy.

The results open new perspectives for using piedmont karst aquifers of southern Apennines as supplementary groundwater resources or reserve for local water needs. However, in the case study of the Baiano District, current and future withdrawals must be authorized on the basis of an updated water balance of the Avella Mountains, from basin to local scale, implementing a continuous monitoring of groundwater, to avoid overexploitation and interference with shallow plain aquifer, urban areas and anthropogenic activities.

Key words: piedmont karst aquifer, hydrological balance, pumping test, groundwater quality, southern Apennines

Introduzione

A scala globale, gli acquiferi carsici ospitano importanti risorse utilizzate per il consumo umano, l'industria e l'agricoltura (Goldscheider, 2012). In molte regioni del mondo svolgono un ruolo vitale per la conservazione degli ecosistemi fluviali e marino-costieri, ospitando patrimoni culturali e ambienti naturali con grande geo e biodiversità (Allocca et al., 2018; 2022; Goldcheider et al., 2020).

In Italia meridionale gli acquiferi carsici da sempre hanno rivestito un'importanza strategica per lo sviluppo socioeconomico ed ambientale (Allocca et al., 2014; 2015). A partire dalla fine '800, le sorgenti carsiche hanno consentito di progettare e realizzare grandi opere idrauliche e infrastrutture acquedottistiche, per alimentare le grandi città, aree metropolitane e rurali (Allocca et al., 2007) costituendo un eccezionale volano di crescita e di miglioramento delle condizioni di vita delle popolazioni.

Sebbene le grandi sorgenti e falde siano, oggi, utilizzate dai grandi sistemi di rete regionali e interregionali, in talune aree carsiche pedemontane possono rinvenirsi volumi idrici che, per posizione altimetrica rispetto alle utenze e qualità delle acque, possono costituire una risorsa integrativa e/o di riserva di interesse locale. Infatti, le zone pedemontane caratterizzate da rocce carbonatiche e ampie fasce detritiche ospitano falde relativamente poco profonde che possono favorire gli interventi di captazione e ridurre i costi di gestione degli impianti. Per queste caratteristiche intrinseche, gli acquiferi carsici pedemontani dell'Appennino meridionale possono costituire una "nuova" risorsa da esplorare in futuro, anche allo scopo di mitigare gli effetti delle variazioni del regime sorgivo sulla disponibilità idrica nei periodi di magra e rendere più resilienti i sistemi di rete agli scenari di crisi connessi con il cambiamento climatico.

Tuttavia, studi idrogeologici basati sul monitoraggio quali-quantitativo per valutare, per esempio, la potenzialità della risorsa, la produttività locale degli acquiferi e la qualità idrochimica delle acque sono necessari, per prevenire fenomeni di sovrasfruttamento e d'inquinamento e garantire una gestione sostenibile della risorsa, a scala locale e di bacino.

L'obiettivo di questo lavoro è quello di caratterizzare l'acquifero carsico pedemontano del cosiddetto Mandamento di Baiano che, per caratteristiche idrogeomorfologiche, rappresenta un caso esemplificativo dell'Appennino meridionale. La caratterizzazione è stata espletata attraverso la valutazione della potenzialità della risorsa, la stima della produttiva locale dell'acquifero e l'analisi della qualità idrochimica e microbiologica delle acque.

La parte restante del lavoro è strutturata come segue. Nel paragrafo 2 sono descritte le caratteristiche dell'area di studio, nel paragrafo 3 sono riportati i dati e metodi utilizzati per la caratterizzazione, nel paragrafo 4 e 5 sono sintetizzati i risultati e le conclusioni.

Descrizione dell'area di studio

L'acquifero carsico pedemontano del Mandamento di Baiano ricade nel settore nord-occidentale del rilievo dei Monti di Avella (Fig. 37a) e comprende i comuni di Avella, Baiano, Mugnano del Cardinale, Quadrelle, Sirignano e Sperone (Fig. 37b).

I Monti di Avella rappresentano un rilievo montuoso tra i più estesi dell'Appenino meridionale, la cui superficie pari a circa 370 km^2 si estende su tutte e cinque le province della Campania. Dal punto di vista geologico il rilievo è costituito da una successione carbonatica di piattaforma di spessore pari a circa 2100 m, formata da calcari e calcari dolomitici cretacico-giurassici e, subordinatamente, da dolomie triassiche, di ambiente di mare basso (Vitale e Ciarcia, 2018).

I versanti carbonatici, con pendenze di 30-35°, sono ricoperti da depositi piroclastici da caduta di origine vesuviana (Fusco et al., 2017) , da depositi detritici ed eluvio-colluviali.

Numerose forme carsiche, sia epigee che ipogee, sono presenti sottoforma di conche endoreiche, grotte, polje e inghiottitoi, in varie zone del rilievo (Allocca et al., 2008; Allocca et al., 2014).

Dal punto di vista idrogeologico, i Monti di Avella rappresentano un acquifero strategico per l'intera regione Campania. Numerosi sono gli Enti pubblici, le società e i soggetti privati che captano, con grandi e piccole opere idrauliche, le acque sotterranee per uso potabile, industriale, irriguo, igienico-sanitario, etc.. A scala di bacino, la falda di base defluisce verso NW, ossia verso l'abitato di Cancello (Civita et al., 1978) dove scaturivano a quota di circa 30 m s.l.m. le sorgenti Calabricito e Mefito (8 e 9 in Fig.1a), e verso SW, ossia verso l'abitato di Sarno (Nicotera e Civita, 1969a, b; Celico, 1983) dove affiorano a quota di 26÷28 m s.l.m. le sorgenti Santa Maria La Foce, Mercato-Palazzo, Cerola, Santa Marina di Lavorate e San Mauro (10, 11, 12, 13 e 14 in Fig.1a). Lauro e Labso (15 e 16 in Fig.1a) che scaturiscono a quota di circa 190÷200 m s.l.m. nella valle del Solofrana sono altre due sorgenti basali, in collegamento con l'inghiottitoio della conca endoreica di Forino (Celico, 1983; Santo et al., 2008).

A partire dalla fine degli anni ’60, le sorgenti di Cancello e Sarno (Fig. 1a) sono state captate mediante gallerie drenanti e campi pozzi in galleria per alimentare importanti sistemi acquedottistici regionali (Acquedotto Campano, GORI SpA, ABC Napoli). Nell’ambito del rilievo numerose sono anche le sorgenti di alta quota (Allocca et al., 2008) alcune delle quali captate mediante bottini di presa per l’alimentazione di acquedotti comunali o provinciali (Fig. 37a).

L’area del Mandamento di Baiano (Fig. 37b), di superficie pari a circa 100 km^2, rappresenta per caratteristiche idrogeomorfologiche un tipico esempio di acquifero carsico pedemontano dell’Appennino meridionale. Essa è, infatti, caratterizzata da versanti calcarei e calcareo-dolomitici, ricoperti da depositi piroclastici ed eluvio-colluviali, con spessori fino a 6-8 metri lungo i versanti (De Vita et al., 2006; Fusco et al., 2017). Alla base dei rilievi, ampie fasce detritiche fanno da raccordo morfologico con i depositi alluvionali di piana. Localmente sono presenti numerose faglie (Fig. 37b) che, con orientazione NE-SW, SW-NE e N-S, dislocano il substrato carbonatico al di sotto dei depositi di piana.

Nella zona pedemontana, dati stratigrafici di pozzi profondi (Fig. 37b e 39) evidenziano una successione di depositi quaternari (prodotti piroclastici, con intercalazioni argillose, Tufo Grigio Campano, depositi detritici e ghiaioso-limosi) di spessore investigato fino a 96 m, poggiante direttamente su un substrato di rocce calcaree fratturate e carsificate (con spessore osservato fino a 350 m circa; pozzo 1 di Fig. 39) passanti verso il basso a dolomie.

L’area pedemontana ospita un importante acquifero carsico, la cui falda di base avente una profondità di qualche centinaio di metri dal p.c. (Fig. 39) è espressione locale della più estesa falda in rete dei Monti di Avella, che alimenta le sorgenti di Sarno. Infatti, sulla base del modello di flusso a scala di bacino (Fig. 37a), le acque sotterranee dirette verso SW in parte travasano verso i depositi di piana (Fig. 37b), in parte defluiscono verso le sorgenti di Sarno (Fig. 37a).

Nel Mandamento di Baiano numerose sono le utenze idriche che per scopo idropotabile (Fig. 37b) (es. Alto Calore Servizi SpA, acquedotti comunali), industriale e, subordinatamente, irriguo, captano le acque della falda di base dei Monti di Avella, mediante pozzi profondi.

Considerata l’importanza della risorsa e la crescita della pressione antropica sull’acquifero dei Monti di Avella negli ultimi decenni, è indispensabile una gestione coordinata che travalichi i confini distrettuali e provinciali, basata sul monitoraggio continuo quali-quantitativo delle acque sotterranee e sul bilancio idrico multi scalare (dalla scala di bacino

a quella locale), che tenga conto di tutte le utenze idriche, per piccole e grandi derivazioni, in atto ed in progetto.

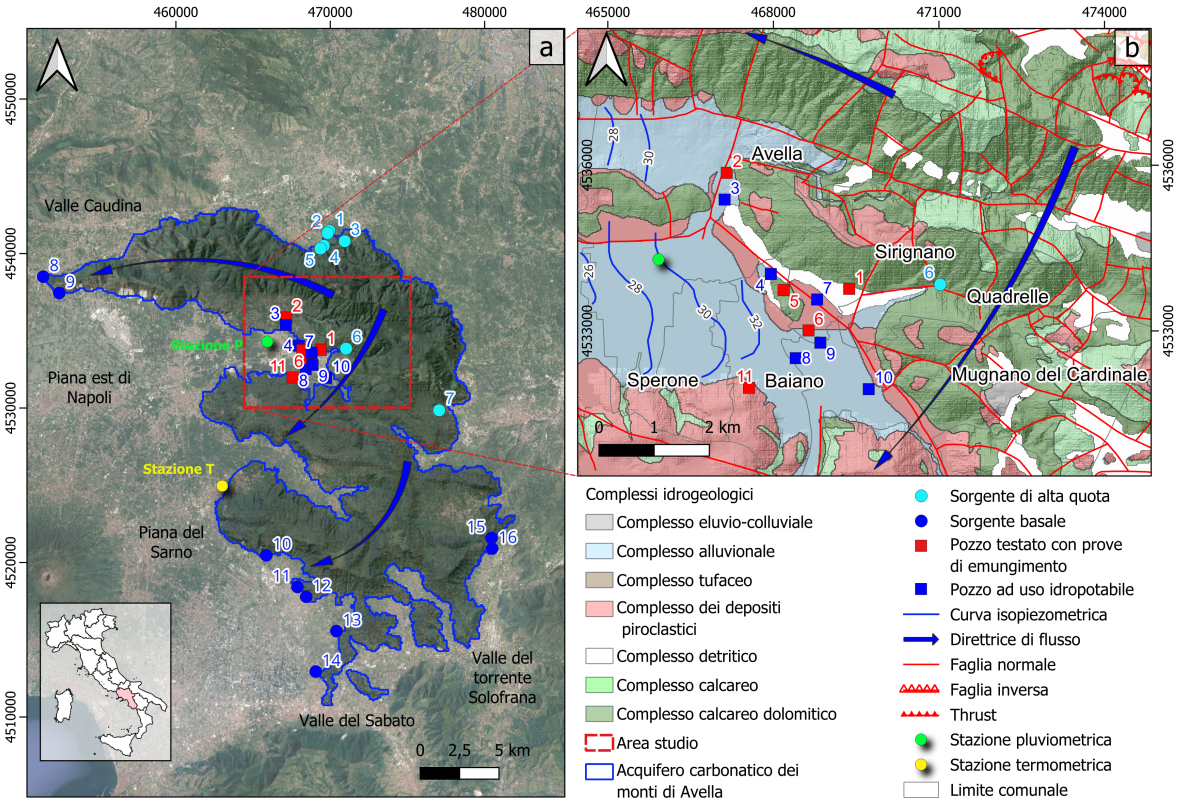


Figura 37 – a) Schema di flusso a scala di bacino dell'acquifero carbonatico dei Monti di Avella, con ubicazione di sorgenti basali e di alta quota, pozzi e stazioni meteoclimatiche (stazione P e T). b) Mappa idrogeologica dell'acquifero carsico pedemontano del Mandamento di Baiano (De Vita et al., 2018 modificato).

Dati e metodi

Bilancio idrologico

Per la stima della ricarica annuale dell'acquifero carsico pedemontano per il periodo 2008÷2022 è stato applicato il codice di calcolo *Soil Water Balance* (SWB, versione 1.2) implementato dall'USGS (*United States Geological Survey*). Il codice SWB è stato implementato mediante la procedura di Figura 38, in un modello discretizzato (di estensione di circa 100 km^2) in celle quadrate (o pixel) con risoluzione 10 m. L'algoritmo si basa sull'approccio modificato del bilancio idrico del suolo di Thornthwaite-Mather (Westenbroek et al., 2010) per calcolare il potenziale di ricarica delle acque sotterranee per ogni singola cella del modello, attraverso la seguente formula (Eq. 12):

$$Recharge = (precipitations + melting\ snow + inflow) - (outflow + ET + interception) - \Delta\ soil\ moisture \quad (12)$$

dove *recharge* (*inches*) è la ricarica annuale; *precipitations* (*inches*) è l'apporto di acqua al suolo sottoforma di pioggia (giornaliera); *melting snow* (*inches*) è la quantità di acqua derivante dalla fusione della neve presente sulla superficie del suolo; *inflow* (*inches*) è l'apporto di acqua superficiale proveniente da aree esterne rispetto alla cella; *outflow* (*inches*) è il deflusso superficiale calcolato con il metodo del Curve Number (USDA, 1972); *ET* (*inches*) è il quantitativo d'acqua di evapotraspirazione reale stimato con il metodo di Thornthwaite e Mather (1955); *interception* (*inches*) è la quantità di pioggia che viene intercettata dalla vegetazione; *Δ soil moisture* (*inches*) è la variazione temporale della quantità di acqua nel suolo. L'applicazione del modello SWB richiede dati di ingresso sia in formato raster (ARC ASCII files) che tabulare (.txt). I dati raster sono stati generati in ambiente GIS e comprendono la mappa della *flow direction*, la mappa del *land use*, la mappa dell'*AWC* (*Available Water Capacity*), la mappa dell'*HSG* (*Hydrological Soil Group*). Inoltre, nel modello sono stati implementati dati tabulari meteoclimatici giornalieri di precipitazione e temperatura dell'aria minima e massima. I dati di pioggia (P) si riferiscono alla stazione di Avella e quelli di temperatura dell'aria (T) alla stazione di Palma Campania, entrambe gestite dal Centro Funzionale Multirischi della Protezione Civile Regione Campania (http://centrofunzionale.regione.campania.it). Infine, il codice utilizza un file di testo (.tvs) per associare ad ogni uso e tipo di suolo i parametri che non vengono specificati nel *grid* e che includono l'intercettazione, la profondità delle radici delle piante e il massimo tasso di ricarica.

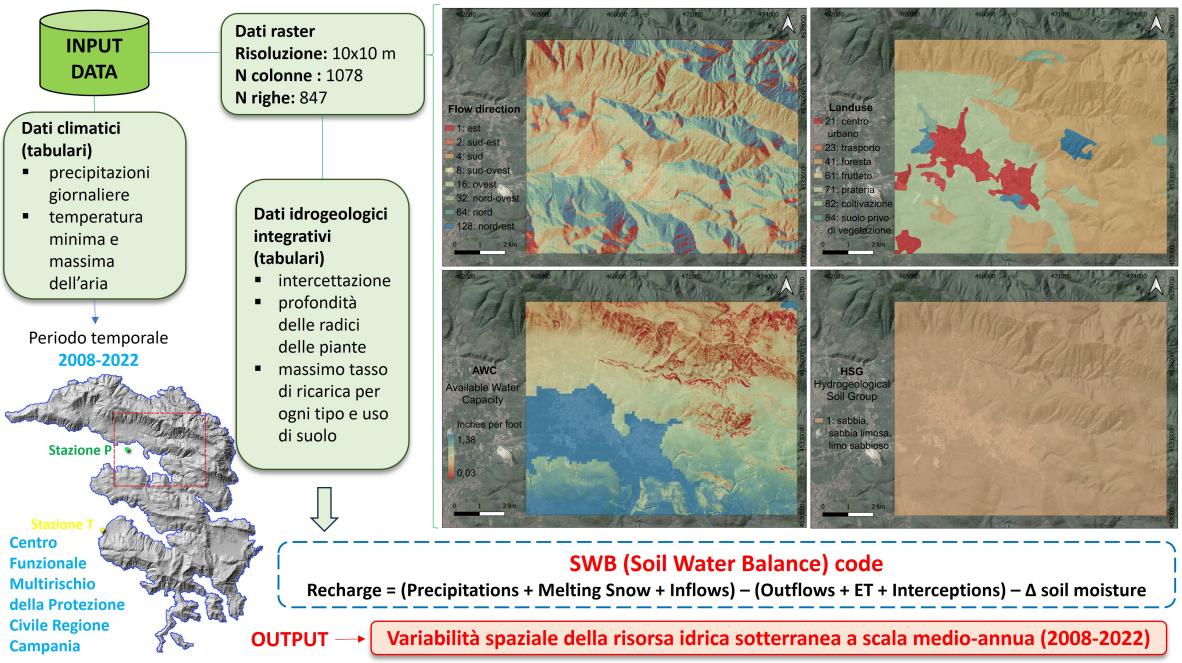


Figura 38 – Flow chart del modello SWB implementato per la stima del bilancio idrologico

Prove di pompaggio

Sono stati analizzati i dati di cinque prove di pompaggio condotte su singoli pozzi attestati nel substrato carbonatico della zona pedemontana ed aventi una profondità fino a 348 metri dal p.c. (Fig. 37b). In Figura 39 sono riportate le stratigrafie dei singoli pozzi testati.

Le prove di pompaggio sono state effettuate in regime di equilibrio, a gradini crescenti di portata, misurando i tempi e le depressioni piezometriche fino alla stabilizzazione. La durata massima delle prove è stata di 70 ore (pozzo 37 in Fig. 39). I dati sono stati utilizzati per costruire la curva caratteristica del pozzo (Fig. 39), stimare la portata critica (Q_c), la portata ottimale del pozzo, la depressione critica (Δh_c) e la portata specifica (Q_s) del pozzo.

Sulla base di equazioni empiriche disponibili in letteratura (e.g. Valigi et al., 2021) è stato, inoltre, possibile ricavare il valore di trasmissività (T) dell'acquifero carsico, mediante l'equazione (Eq. 13):

$$T = \alpha Q s^{\beta} \qquad (13)$$

dove Q_s è la portata specifica (m^2/s), derivata dal rapporto tra Q_c (m^3/s) e Δh_c (m), α e β sono costanti pari a 0.85 e 1.06, rispettivamente, ricavate per gli acquiferi carsici italiani (Valigi et al., 2021).

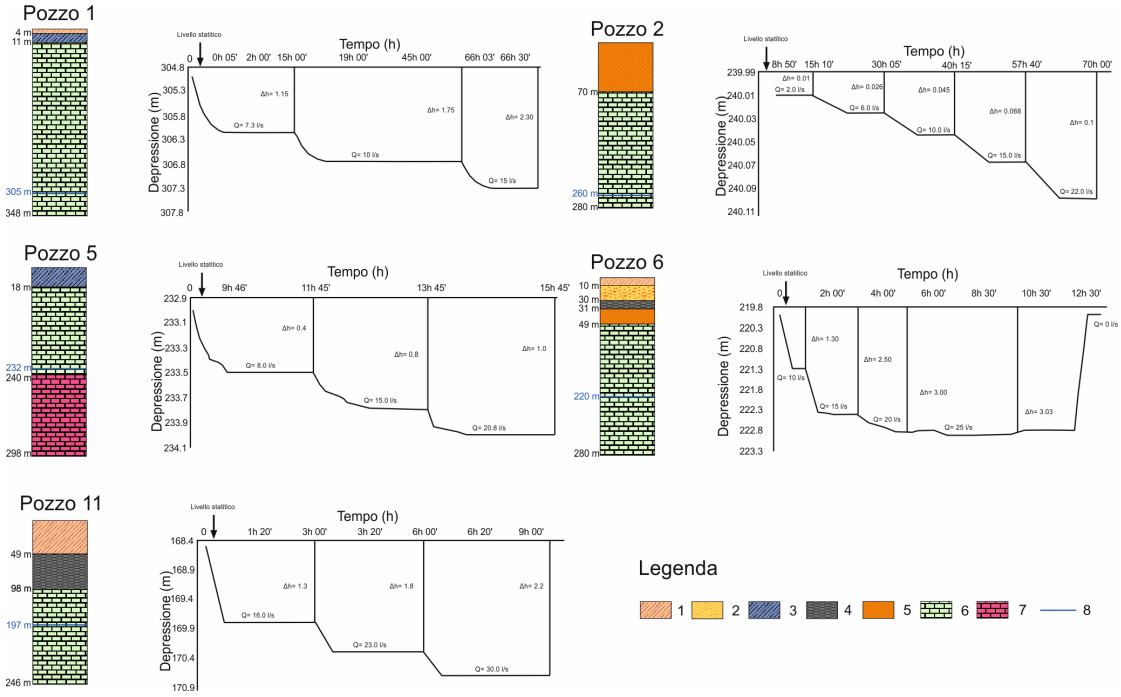


Figura 39 – Stratigrafie dei pozzi e prove di emungimento a gradini di portata crescenti. 1) Depositi piroclastici, 2) Depositi argillosi; 3) Detrito calcareo; 4) Tufo Grigio Campano; 5) Depositi ghiaiosi e limosi; 6) Calcari; 7) Dolomie; 8) Superficie piezometrica (m dal p.c.).

Qualità delle acque

Sono stati analizzati i dati di analisi chimico-fisiche e microbiologiche di 8 punti d'acqua (7 sorgenti di alta quota e 1 pozzo profondo; Figg. 37 e 43) campionati con cadenza quadrimestrale, dal 2018 al 2023.

Al fine di valutare la qualità delle acque ed accertare l'idoneità per il consumo umano (D.L. 31/2001; D.L.vo 152/2006; D.L.vo 18/2023), in Tabella 7 sono riportati i 57 parametri chimico-fisici e microbiologici (33 elementi inorganici, 17 organici e 7 parametri microbiologici) e i relativi valori, minimi e massimi, monitorati negli ultimi 5 anni. Allo scopo di effettuare un confronto con il chimismo delle acque delle sorgenti basali di Cancello e Sarno sono stati utilizzati i dati idrochimici disponibili in letteratura (Celico et al., 1980). Tutti i dati raccolti sono stati elaborati in ambiente Origin 2021 per la realizzazione di diagrammi di classificazione e comparazione di Piper e Schöeller-Berkaloff.

Parametri chimico-fisici e microbiologici	Unità di misura	Vullo	Fontana Stella	Trofa	Ricci	Santo Spirito	Bocca dell'Acqua	Acqua del Pero	Pozzo 1	Calabricito	Mefito	S. Maria la Foce	Mercato Palazzo	Cerola	S. Marina di Lavorate
		2018	2019 - 2020	2018 - 2020	2018 - 2022	2018 - 2022	2018 - 2023	2018 - 2023	2023	Fonte: Celico et al., 1980					
Temperatura	° C	12.70	12.00	11.05	10.90	10.85	10.70	9.80	14.40	13.50	14.00	11.00	12.00	13.80	13.00
Torbidità	NTU	0.76	0.57	0.74	0.88	0.70	1.32	2.75	3.69	n.d.	n.d.	n.d.	n.d.	n.d.	n.d.
pH	unità pH	7.78	8.26	7.97	8.24	7.88	7.98	8.04	7.40	6.80	6.60	7.00	6.80	6.60	6.80
Conducibilità elettrica	µs/cm a 20°C	384.00	437.00	321.50	351.50	364.00	286.50	470.50	473.00	1240.00	847.00	459.00	463.00	1050.00	647.00
Ammonio	mg/l	<0.05	<0.05	<0.05	<0.05	<0.05	<0.05	<0.05	<0.05	n.d.	n.d.	n.d.	n.d.	n.d.	n.d.
Nitrito	mg/l	<0.02	<0.02	<0.02	<0.02	<0.02	<0.02	<0.02	<0.02	n.d.	n.d.	n.d.	n.d.	n.d.	n.d.
Nitrato	mg/l	1.90	3.03	2.45	2.20	2.28	2.97	17.15	13.00	n.d.	n.d.	n.d.	n.d.	n.d.	n.d.
Durezza	°F	17.80	23.15	15.80	17.00	17.35	14.30	19.25	23.50	n.d.	n.d.	n.d.	n.d.	n.d.	n.d.
Calcio	mg/l	60.80	82.40	54.60	61.00	62.20	47.60	66.20	70.00	248.00	193.00	101.00	103.00	248.00	159.00
Magnesio	mg/l	6.20	6.10	5.15	4.30	4.30	5.00	7.20	14.40	59.00	31.00	27.00	26.00	60.00	35.00
Alcalinità	°F	20.50	23.60	18.00	17.40	19.90	13.90	22.40	26.30	n.d.	n.d.	n.d.	n.d.	n.d.	n.d.
Cloruro	mg/l	10.20	16.35	12.75	11.85	14.42	9.90	14.25	28.40	239.00	146.00	60.00	58.00	99.00	53.00
Solfato	mg/l	7.40	5.37	4.40	3.80	5.35	4.30	20.60	5.39	40.00	29.00	38.00	14.00	21.00	16.00
Fluoruro	mg/l	0.61	0.33	0.15	0.28	0.27	0.33	0.52	0.35	n.d.	n.d.	n.d.	n.d.	n.d.	n.d.
Boro	mg/l	n.d.	<0.05	0.34	0.12	0.07	0.06	0.08	<0.05	n.d.	n.d.	n.d.	n.d.	n.d.	n.d.
Cianuro	µg/l	<0.01	<0.01	<0.01	<0.01	<0.01	<0.01	<0.01	<0.01	n.d.	n.d.	n.d.	n.d.	n.d.	n.d.
Ossidabilità -	mg/l O_2	1.04	1.68	0.88	0.84	0.96	1.40	0.76	1.20	n.d.	n.d.	n.d.	n.d.	n.d.	n.d.
Residuo fisso	mg/l	276.00	310.00	231.50	302.50	262.00	212.00	338.50	341.00	n.d.	n.d.	n.d.	n.d.	n.d.	n.d.
Sodio	mg/l	10.20	12.90	9.10	8.37	8.12	7.90	13.97	n.d.	115.00	80.00	33.00	30.00	53.00	26.00
Alluminio	µg/l	<20.00	<20.00	<20.00	<20.00	<20.00	36.00	34.78	<20.00	n.d.	n.d.	n.d.	n.d.	n.d.	n.d.
Potassio	mg/l	5.30	8.50	7.40	6.08	4.62	n.d.	10.14	n.d.	12.00	12.00	10.00	8.00	10.00	11.00
Vanadio	µg/l	<5.00	<5.00	<5.00	<5.00	<5.00	<5.00	5.55	<5.00	n.d.	n.d.	n.d.	n.d.	n.d.	n.d.
Cromo	µg/l	<5.00	<5.00	<5.00	<5.00	<5.00	<5.00	<5.00	<5.00	n.d.	n.d.	n.d.	n.d.	n.d.	n.d.

Manganese	µg/l	<5.00	41.50	<5.00	41.50	<5.00	<5.00	<5.00	<5.00	n.d.	n.d.	n.d.	n.d.	n.d.	n.d.
Ferro	µg/l	<20.00	<20.00	<20.00	<20.00	<20.00	<20.00	<20.00	<20.00	n.d.	n.d.	n.d.	n.d.	n.d.	n.d.
Nichel	µg/l	<2.00	<20.00	<2.00	<2.00	<2.00	<2.00	<2.00	<2.00	n.d.	n.d.	n.d.	n.d.	n.d.	n.d.
Rame	mg/l	<0.01	<0.01	<0.01	<0.01	<0.01	<0.01	<0.01	<0.01	n.d.	n.d.	n.d.	n.d.	n.d.	n.d.
Arsenico	µg/l	1.10	<1.00	<1.00	<1.00	<1.00	<1.00	1.11	<1.00	n.d.	n.d.	n.d.	n.d.	n.d.	n.d.
Selenio	µg/l	<1.00	<1.00	<1.00	<1.00	<1.00	<1.00	<1.00	<1.00	n.d.	n.d.	n.d.	n.d.	n.d.	n.d.
Cadmio	µg/l	<0.50	<0.50	<0.50	<0.50	<0.50	<0.50	<0.50	<0.50	n.d.	n.d.	n.d.	n.d.	n.d.	n.d.
Antimonio	µg/l	<0.50	<0.50	<0.50	<0.50	<0.50	<0.50	<0.50	<0.50	n.d.	n.d.	n.d.	n.d.	n.d.	n.d.
Mercurio	µg/l	n.d.	<0.20	<0.20	<0.20	<0.20	<0.20	<0.20	<0.20	n.d.	n.d.	n.d.	n.d.	n.d.	n.d.
Piombo	µg/l	<1.00	<1.00	<1.00	<1.00	<1.00	<1.00	<1.00	<1.00	n.d.	n.d.	n.d.	n.d.	n.d.	n.d.
Benzo (a) Pirene	µg/l	<0.0025	<0.0025	<0.0025	<0.0025	<0.0025	<0.0025	<0.0025	<0.0025	n.d.	n.d.	n.d.	n.d.	n.d.	n.d.
Benzo (k) Fluorantene	µg/l	<0.01	<0.01	<0.01	<0.01	<0.01	<0.01	<0.01	<0.01	n.d.	n.d.	n.d.	n.d.	n.d.	n.d.
Indeno 1.2.3 (cd) Pirene	µg/l	<0.01	<0.01	<0.01	<0.01	<0.01	<0.01	<0.01	<0.01	n.d.	n.d.	n.d.	n.d.	n.d.	n.d.
Benzo (ghi) Perilene	µg/l	<0.01	<0.01	<0.01	<0.01	<0.01	<0.01	<0.01	<0.01	n.d.	n.d.	n.d.	n.d.	n.d.	n.d.
Benzo (b) Fluorantene	µg/l	<0.01	<0.01	<0.01	<0.01	<0.01	<0.01	<0.01	<0.01	n.d.	n.d.	n.d.	n.d.	n.d.	n.d.
Idrocarburi Policiclici Aromatici	µg/l	<0.025	<0.025	<0.025	<0.025	<0.025	<0.025	<0.025	<0.025	n.d.	n.d.	n.d.	n.d.	n.d.	n.d.
Cloruro di Vinile	µg/l	n.d.	n.d.	n.d.	<0.50	<0.50	<0.50	<0.50	n.d.	n.d.	n.d.	n.d.	n.d.	n.d.	n.d.
Cloroformio	µg/l	n.d.	n.d.	n.d.	<0.25	<0.25	<0.25	<0.25	n.d.	n.d.	n.d.	n.d.	n.d.	n.d.	n.d.
Bromoformio	µg/l	n.d.	n.d.	n.d.	<0.25	<0.25	<0.25	<0.25	n.d.	n.d.	n.d.	n.d.	n.d.	n.d.	n.d.
Dibromoclorometano	µg/l	n.d.	n.d.	n.d.	<0.25	<0.25	<0.25	<0.25	n.d.	n.d.	n.d.	n.d.	n.d.	n.d.	n.d.
Bromodiclorometano	µg/l	n.d.	n.d.	n.d.	<0.25	<0.25	<0.25	<0.25	n.d.	n.d.	n.d.	n.d.	n.d.	n.d.	n.d.

Trialometani totali	µg/l	n.d.	n.d.	n.d.	<0.25	<0.25	<0.25	<0.25	n.d.	n.d.	n.d.	n.d.	n.d.	n.d.	n.d.
Benzene	µg/l	n.d.	n.d.	n.d.	<0.25	<0.25	<0.25	<0.25	n.d.	n.d.	n.d.	n.d.	n.d.	n.d.	n.d.
Tetracloroetilene	µg/l	n.d.	n.d.	n.d.	<0.25	<0.25	<0.25	<0.25	n.d.	n.d.	n.d.	n.d.	n.d.	n.d.	n.d.
Tricloroetilene	µg/l	n.d.	n.d.	n.d.	<0.25	<0.25	<0.25	<0.25	n.d.	n.d.	n.d.	n.d.	n.d.	n.d.	n.d.
Tricloroetilene + Tetracloroetilene	µg/l	n.d.	n.d.	n.d.	<0.25	<0.25	<0.25	<0.25	n.d.	n.d.	n.d.	n.d.	n.d.	n.d.	n.d.
1.2 Dicloroetano	µg/l	n.d.	n.d.	n.d.	<0.25	<0.25	<0.25	<0.25	n.d.	n.d.	n.d.	n.d.	n.d.	n.d.	n.d.
Conteggio colonie 22° C	numero/ml	164.00	21.00	19.00	37.00	32.50	10.00	40.50	247.00	n.d.	n.d.	n.d.	n.d.	n.d.	n.d.
Conteggio colonie 37° C	numero/ml	105.00	6.00	5.00	11.00	13.00	8.00	21.00	91.00	n.d.	n.d.	n.d.	n.d.	n.d.	n.d.
Batteri coliformi 37° C	numero/100ml	3.00	15.00	14.00	15.00	42.00	<1.00	35.00	3.00	n.d.	n.d.	n.d.	n.d.	n.d.	n.d.
Escherichia Coli	numero/100ml	0.00	0.00	1.00	2.00	5.00	<1.00	10.00	0.00	n.d.	n.d.	n.d.	n.d.	n.d.	n.d.
Enterococchi	numero/100ml	0.00	0.00	0.00	<3.00	1.00	<1.00	4.00	0.00	n.d.	n.d.	n.d.	n.d.	n.d.	n.d.
Pseudomonas Aeruginosa	numero/250ml	64.00	0.00	0.00	3.00	15.00	<1.00	50.00	0.00	n.d.	n.d.	n.d.	n.d.	n.d.	n.d.
Clostridium Perfringens	numero/100ml	0.00	0.00	0.00	2.50	<1.00	<1.00	2.00	0.00	n.d.	n.d.	n.d.	n.d.	n.d.	n.d.

Tabella 7 – Parametri (valori medi) chimico-fisici e microbiologici delle acque delle sorgenti di alta quota e del Pozzo 1 (Figg. 37 e 43), per il periodo 2018-2023, e dati idrochimici (Celico et al., 1980) delle sorgenti basali (Calabricito, Mefito, Santa Maria la Foce, Mercato-Palazzo, Cerola, Santa Marina di Lavorate).

Risultati

Valutazione delle risorse idriche sotterranee

L'applicazione del metodo SWB ha fornito un modello spaziale della ricarica medio-annua (Fig. 40a) e la variazione annuale (Fig. 40b e 40c) per il periodo 2008÷2022.

Per l'acquifero carsico pedemontano i valori più elevati di ricarica medio-annua, pari a circa 800 mm, si riscontrano nelle zone altimetricamente più elevate (Fig. 40a). Valori di ricarica medio-annua più bassi, pari a 200 mm si osservano nella zona di piana. La stima del bilancio, inoltre, evidenzia una significativa variabilità inter-annuale della ricarica (Fig. 40b e 40c), strettamente correlata alle variazioni inter-annuali di pioggia e temperatura connesse con le variazioni climatiche in atto. Nel periodo 2008÷2022 si osservano anni di piena, come nel 2010, dove si raggiunge un picco massimo di ricarica pari a 752.2 mm/a, corrispondente a circa 2.17 m^3/s, e anni di magra, come nel 2011, dove si raggiunge un valore minimo di ricarica pari a 245.2 mm/a, equivalente a circa 0.71 m^3/s. Di questa variabilità inter-annuale della risorsa potenzialmente disponibile bisogna tener conto ai fini di una corretta gestione della risorsa, per prevenire crisi idriche e fenomeni di sovrasfruttamento.

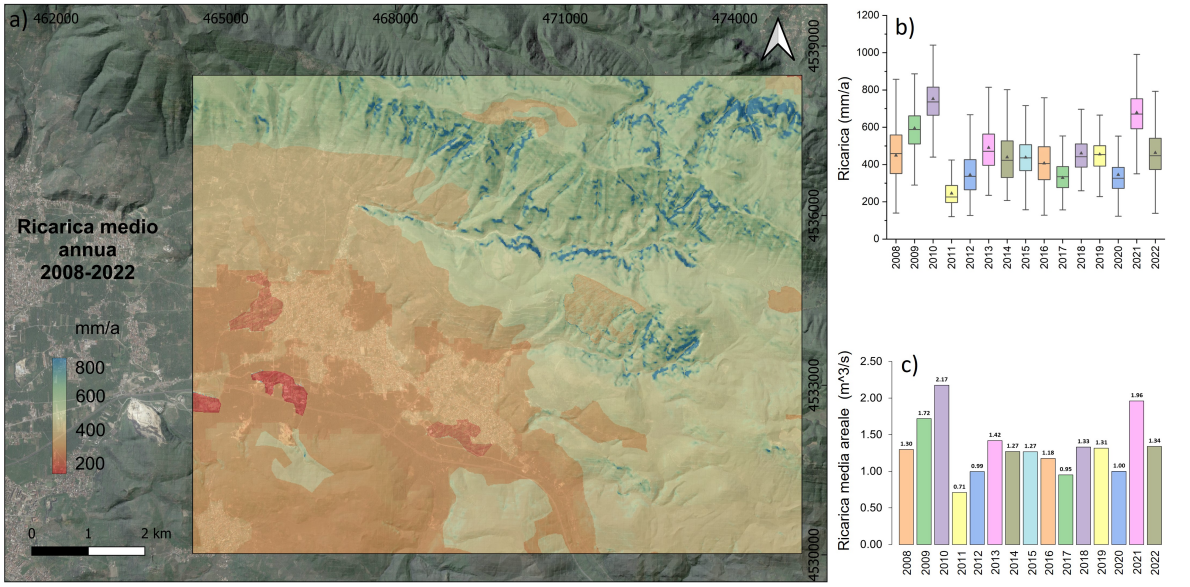


Figura 40 – a) Mappa della ricarica medio-annua (2008÷2022) dell'acquifero carsico pedemontano del Mandamento di Baiano; b) e c) variabilità inter-annuale della ricarica (mm/a e m^3/s).

Prove di pompaggio

In Figura 41 sono riportate le curve caratteristiche dei pozzi (Fig. 37b), mentre in Tabella 8 sono indicati i valori di portata critica, abbassamento critico, portata specifica, trasmissività e portata ottimale di esercizio. Dall'analisi dei dati si evince, complessivamente, un'elevata produttività locale dell'acquifero carsico pedemontano. La portata specifica (Q_s) e la trasmissività (T) variano in un range molto ristretto, dell'ordine di $10^{-1} \div 10^{-3}$ m^2/s. Il valore più alto, dell'ordine di 10^{-1} m^2/s, si osserva per il Pozzo 2 (Fig. 37b), per il quale con una portata ottimale di esercizio di 13,3 l/s si osserva un abbassamento critico è di appena 6,4 cm. Anche per gli altri pozzi evidenziano una buona resa; gli abbassamenti piezometrici critici sono contenuti (fino ad un massimo di 1,8 m), a fronte di portate di esercizio variabili da 5,3 a 11 l/s. Dal confronto con i valori di Q_s e T (Fig. 42) stimati per altri acquiferi carbonatici italiani (Fabbri, 1997; Valigi et al., 2021) si osserva che quelli stimati per l'acquifero carsico pedemontano del Mandamento di Baiano sono tra i più alti riscontrati a livello nazionale (Fig. 41) e coerenti con quelli già stimati in altri acquiferi carsici dell'Appennino meridionale (Celico, 1983; Allocca et al., 2007).

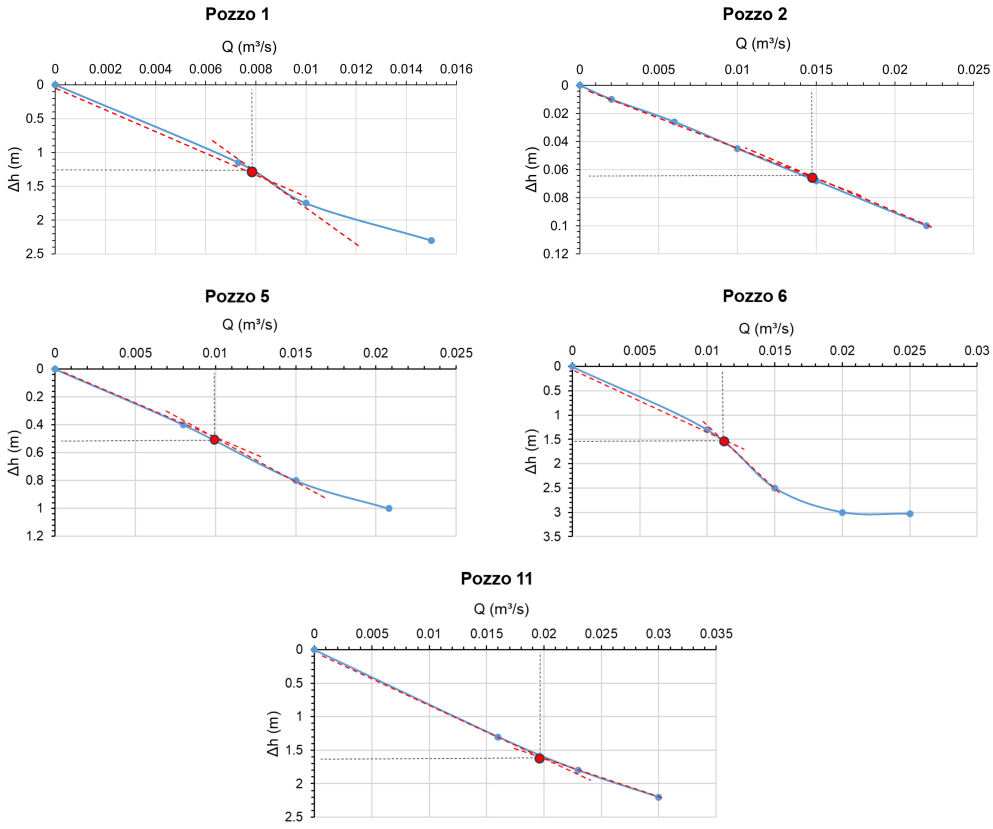


Figura 41 – Curva caratteristica dei pozzi testati con indicazione della portata critica e dell'abbassamento critico (punto rosso).

Pozzo	Portata critica (Q_c)	Abbassamento critico (Δh_c)	Portata specifica del pozzo (Q_s)	Trasmissività dell'acquifero (T)	Portata ottimale di esercizio
	l/s	m	m^2/s	m^2/s	l/s
1	8.5	1.8	4.72E-03	2.91E-03	7.60
2	14.8	0.064	2.31E-01	1.80E-01	13.30
5	5.9	0.48	1.23E-02	8.01E-03	5.30
6	11.0	1.5	7.33E-03	4.64E-03	9.90
11	19.5	1.6	1.22E-02	7.95E-03	11.00

Tabella 8 – Parametri idraulici del sistema acquifero-pozzo stimati attraverso le prove di pompaggio

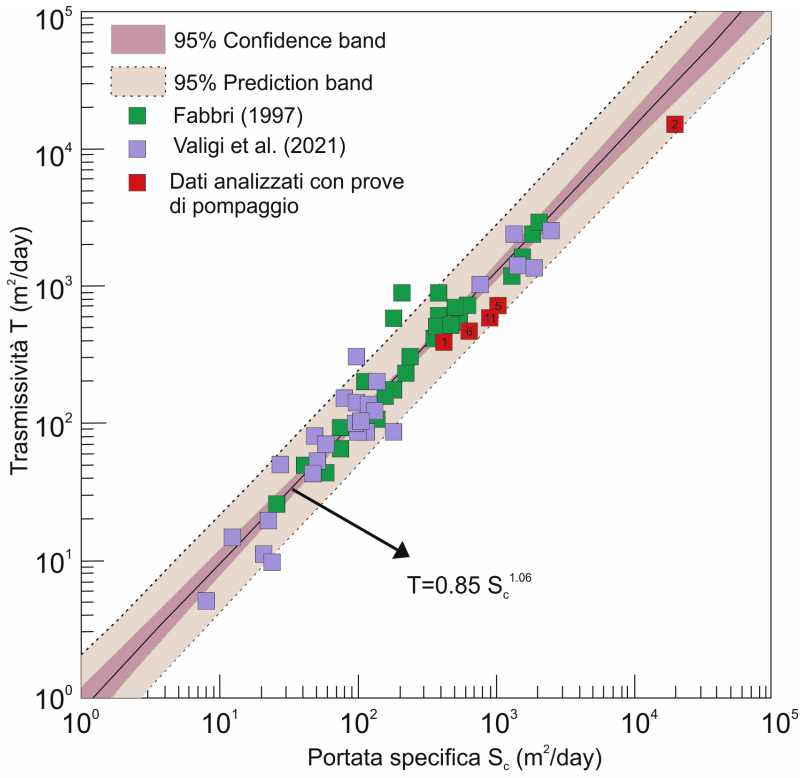


Figura 42 - Confronto tra i valori Q_s-T di prove di pompaggio eseguite in acquiferi carbonatici italiani (Fabbri, 1997; Valigi et al., 2021) e nei pozzi dell'area di studio

Qualità delle acque

Il diagramma di Piper (Fig. 43a) mostra che le acque sotterranee di tutti i campioni analizzati (sorgenti di alta quota, sorgenti basali e Pozzo 1) hanno una facies bicarbonato-alcalino-terrosa, a conferma della stessa natura e litologia della roccia-serbatoio. Il range ristretto di

valori minimi e massimi mostrati in Tabella 7 per il periodo di monitoraggio 2018-2023 testimonia una discreta stabilità idrochimica (inter-annuale e stagionale). Il diagramma di Shöeller-Berkaloff (Figg. 43b e 43c) evidenzia che tra i vari elementi maggiori prevalgono (meq/l), per i cationi, il calcio, magnesio e il sodio, mentre per gli anioni, il bicarbonato di calcio, i solfati e cloruri.

Dai dati di temperatura e conducibilità elettrica (Tab. 7) e dai profili idrochimici (Fig. 43b e 43c) si osserva che le acque delle sorgenti basali sono relativamente più calde e mineralizzate, rispetto alle acque delle sorgenti di alta quota, in linea con i tempi più lunghi di residenza delle acque all'interno dell'acquifero. Infine, dall'analisi di tutti i parametri inorganici, organici e microbiologici (Tab. 7) è possibile constatare un'elevata qualità idrochimica e microbiologica di tutte le acque analizzate e l'idoneità delle stesse al consumo umano, tenuto conto che gli stessi valori misurati (minimi e massimi) per l'intero periodo di monitoraggio rientrano nei limiti imposti dalla normativa italiana (D.L.vo 31/2001; D.L.vo 152/2006; D.L.vo 18/2023).

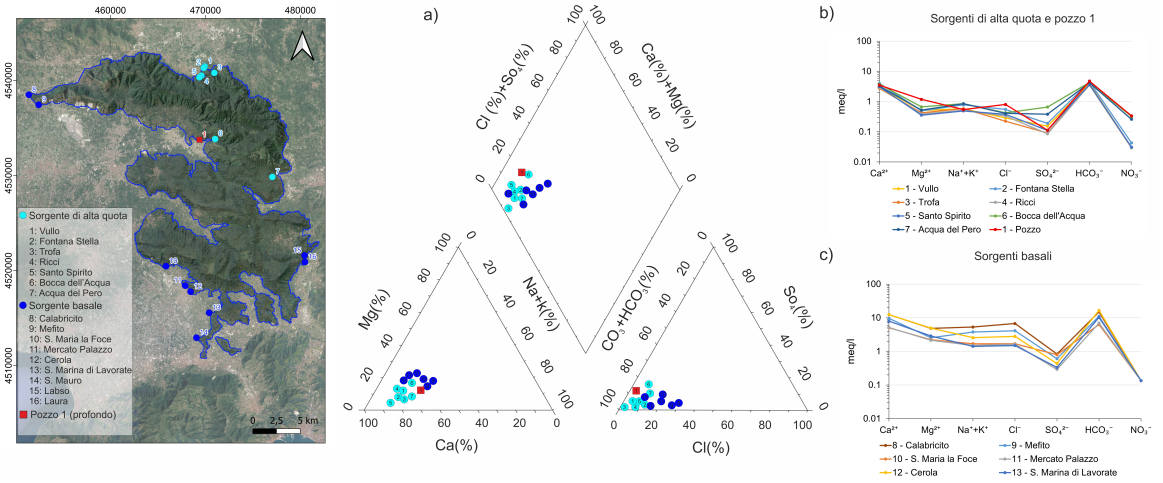


Figura 43 – a) Diagramma di Piper dei campioni analizzati; b) Diagramma di Shöeller-Berkaloff dei campioni di acqua analizzati delle sorgenti di alta quota e del Pozzo 1; c) Diagramma di Shöeller-Berkaloff dei campioni di acqua analizzati delle sorgenti basali (Celico et al., 1980).

Conclusioni

La caratterizzazione dell'acquifero carsico pedemontano del Mandamento di Baiano ha fornito interessanti risultati riguardanti le caratteristiche idrogeologiche e qualitative delle acque sotterranee.

A scala locale, il *Soil Water Balance* ha evidenziato un'infiltrazione medio-annua pari a 2.86×10^7 m^3/a, equivalente a circa 0,90 m^3/s. Per il periodo 2008÷2022 è stata osservata una significativa variabilità inter-annuale (valori minimi di ricarica fino a 0,71 m^3/s), legata alle variazioni climatiche inter-annuali, di cui bisogna tener conto per evitare crisi idriche e sovrasfruttamenti della risorsa.

Il modello di flusso a scala di bacino evidenzia che le acque sotterranee del Mandamento di Baiano in parte travasano verso i depositi di piana, in parte defluiscono verso le sorgenti di Sarno.

Le prove di pompaggio, condotte su cinque pozzi profondi attestati nel substrato carbonatico pedemontano, hanno evidenziato un'elevata produttività locale dell'acquifero. I valori di portata specifica e trasmissività, dell'ordine di $10^{-1}\div10^{-3}$ m^2/s, sono tra i più alti in Italia e in Appenino meridionale.

Le analisi chimico-fisiche e microbiologiche, effettuate dal 2018 al 2023, su 7 sorgenti di alta quota e un pozzo profondo hanno evidenziato la presenza di acque di ottima qualità, aventi un chimismo bicarbonato-calcico tipico degli acquiferi carbonatici dell'Appennino meridionale. I valori minimi e massimi dei parametri inorganici, organici e microbiologici monitorati rientrano nei limiti della normativa italiana per le acque da destinare al consumo umano.

I risultati aprono nuove prospettive sulla possibilità di utilizzo degli acquiferi carsici pedemontani dell'Appennino meridionale come risorse integrative e/o di riserva per i fabbisogni idrici locali, mitigare gli effetti delle variazioni del regime sorgivo sulla disponibilità idrica nei periodi di magra e rendere più resilienti i sistemi di rete agli scenari di crisi connessi con il cambiamento climatico. Nel caso studio del Mandamento di Baiano, tuttavia, i prelievi in atto e futuri dovranno tener conto del bilancio idrico dell'acquifero dei Monti di Avella, dalla scala di bacino a quella locale, e devono essere implementati attraverso un continuo monitoraggio quali-quantitativo della risorsa, per prevenire fenomeni di sovrasfruttamento ed interferenze con le acque di piana, i centri abitati e le attività antropiche.

Ringraziamenti

Gli Autori ringraziano l'Alto Calore Servizi SpA e i Comuni del Mandamento di Baiano per aver la disponibilità e condivisione di dati delle analisi chimico-fisiche e microbiologiche e delle prove di pompaggio.

Bibliografia

Allocca V., Celico F., Celico P., De Vita P., Fabbrocino S., Mattia C., Monacelli G., Musilli I., Piscopo V., Scalise A. R., Summa G., Tranfaglia G., 2007. Note illustrative della Carta Idrogeologica dell'Italia Meridionale. Mem. Ist. Pol. Zecca Stato, 1-211 (2007), ISBN 88-448-0215-5.

Allocca V., Aquino S., Esposito L., Celico P., 2008. Le acque sotterranee dell'Irpinia (Italia meridionale): stato delle conoscenze e prospettive future. L'ACQUA, 6 (2008), 39-66.

Allocca V., Manna F., De Vita P., 2014. Estimating annual groundwater recharge coefficient for karst aquifers of the southern Apennines (Italy). Hydrology and Earth System Sciences 18(2), 803–817.

Allocca V., De Vita P., Manna F., Nimmo J.R., 2015. Groundwater recharge assessment at local and episodic scale in a soil mantled perched karst aquifer in southern Italy. Journal of Hydrology, 529(2015), 843-853.

Allocca V., Marzano E., Tramontano M., Celico F., 2018. Environmental impact of cattle grazing on a karst aquifer in the southern Apennines (Italy): quantification through the grey water footprint. Ecological Indicators, 93, 830-837.

Allocca V., Marzano E., Tramontano M., Celico F., 2022. The Impact of Cattle Grazing on Recreational Ecosystem Services in a Park Area: a Gray Water Footprint Assessment. Journal of Environmental Accounting and Management 10(3) (2022) 269-278.

Celico P., de Riso R. 1978. Il ruolo della Valle Caudina nella idrogeologia del Casertano e del Sarnese (Campania). Mem. e Note Ist. Geol. Appl., 14, 1–25, Napoli.

Celico P., De Gennaro M., Ferreri M., Ghiara M., Russo D., Stanzione D., Zenone F., 1980. Il margine orientale della Piana Campana: indagini idrogeologiche e geochimiche. Period. Miner. 49, 241–270.

Celico P., 1983. Idrogeologia dei massicci carbonatici, delle piane quaternarie e delle aree vulcaniche dell'Italia centromeridionale (Marche e Lazio meridionale, Abruzzo, Molise e Campania). Quaderni della Cassa per il Mezzogiorno, 4/2, 1–203, Roma.

Civita M., de Riso R., Nicotera P., 1970. Sulla struttura idrogeologica alimentante le sorgenti del Fiume Sarno e le falde pedemontane profonde della parte sud-orientale della Conca Campana. Atti I Conv. Intern. Acque Sott., IAH, 1-24, Palermo.

Fabbri P., 1997. Transmissivity in the geothermal Euganean Basin; a geostatistical analysis. Ground Water (1997), 35, 881–887.

De Vita P., Agrello D., Ambrosino F., 2006. Landslide susceptibility assessment in ash-fall pyroclastic deposits surrounding Mount Somma-Vesuvius: Application of geophysical surveys for soil thickness mapping. Journal of Applied Geophysics 59(2), 126– 139.

De Vita P., Allocca V., Celico F., Fabbrocino S., Mattia C., Monacelli G., Musilli I., Piscopo V., Scalise A.R., Summa G., Tranfaglia G., Celico P. 2018. Hydrogeology of continental southern Italy. Journal of Maps, 14:2, 230-241.

Fusco F., Allocca V., De Vita P., 2017. Hydro-geomorphological modelling of ash-fall pyroclastic soils for debris flow initiation and groundwater recharge in Campania (southern Italy). Catena 158 (2017) 235–249.

Goldscheider N., 2012. A holistic approach to groundwater protection and ecosystem services in karst terrains. Aquat. Mundi Am., 2012, 06046, 117–124.

Goldscheider N., Chen Z., Auler A.S., Bakalowicz M., Broda S., Drew D., Hartmann H., Jiang G., Moosdorf N., Stevanovic Z., Veni G., 2020. Global distribution of carbonate rocks and karst water resources. Hydrogeology Journal (2020) 28:1661–1677.

Nicotera P., Civita M. 1969a. Ricerche idrogeologiche per la realizzazione delle opere di presa delle sorgenti Mercato e Palazzo in Sarno (Campania). Mem. e Note Ist. Geol. Appl. (1969), Vol. 11, 1-59, Napoli.

Nicotera P., Civita M. 1969b. Indagini idrogeologiche per la captazione delle sorgenti S. Marina di Lavorate (Sarno). Mem. e Note Ist. Geol. Appl. (1969), Vol. 11, 1-50, Napoli.

Santo A., Prete, S., Giulivo I., 2008. Nuove ipotesi sulla formazione dei piping sinkhole in aree alluvionali: il caso della piana di Forino (Avellino, Campania). Alpine and Mediterranean Quaternary 21.2: 395-408.

Thornthwaite C.W., Mather, J.R.,1955. The Water Balance. Publ. Climatol. Drexel Institute of Climatology, Centerton, New Jersey, 8.1: 1-104.

USDA, 1972. Soil Conservation Service, National Engineering Handbook. Hydrology Section 4 Chapters 4-10, Washington, D.C: USDA.

Valigi, D., Cambi, C., Checcucci, R., Di Matteo, L. 2021. Transmissivity Estimates by Specific Capacity Data of Some Fractured Italian Carbonate Aquifers. Water, 13(10), 1374.

Vitale S., Ciarcia S., 2018. Tectono-stratigraphic setting of the Campania region (southern Italy). Journal of Maps, 14.2: 9-21.

Westenbroek S.M., Kelson V.A., Dripps W.R., Hunt R.J., Bradbury K.R. 2010. SWB - A modified Thornthwaite-Mather Soil-Water-Balance code for estimating groundwater recharge. U.S. Geological Survey Techniques and Methods, Book 6-A31, 60 p.

4.5 Groundwater recharge estimation using HYDRUS-1D model in Foce hydrogeological karst observatory

Keywords: Groundwater Recharge, HYDRUS-1D, Numerical Modelling, Unsaturated Zone

Abstract

The estimation of groundwater recharge is a critical aspect of efficient and sustainable aquifer management. In the carbonate mountain ranges surrounding volcanic centres in the Campania region (southern Italy), ash-fall pyroclastic deposits play a significant role in modulating recharge processes to underlying karst aquifers. These deposits affect infiltration dynamics in the unsaturated zone due to their variable thickness, stratigraphy and hydraulic properties. In this study, a one-dimensional numerical model was developed using HYDRUS-1D to simulate water infiltration within the unsaturated pyroclastic soil mantle of the Foce hydrogeological karst basin (0.90 km²), hydraulically connected to the Avella karst aquifer. A hydrogeological observatory was installed in the basin to provide real-time and continuous monitoring of the main hydrological variables. Data from this monitoring, combined with detailed stratigraphic characterization and hydraulic parameters determination, were implemented in HYDRUS-1D for a 3-year simulation period (2021-2024). Model calibration was performed using inverse modelling techniques and multi-level soil moisture data, resulting in a good agreement between observed and simulated values (R^2 = 0.72883, mass balance error = 0.033%). The simulations showed differences in infiltration rates between the upper and lower soil layers, highlighting the influence of soil matrix structure and hydraulic properties on water infiltration. Seasonal dynamics were evident, with higher infiltration rates during wet and cold months and increased evapotranspiration during dry and warm periods. The results also emphasized the role of canopy interception in modifying effective precipitation and its contribution to the hydrological balance.

While the model performed well, limitations related to the short observation period and the spatial resolution of some input parameters were challenging for validation.

Introduction

Karst aquifers are globally recognised as vital groundwater reservoirs and environmental assets, supporting ecosystems with wide geo- and biodiversity (Goldscheider, 2012). In southern Italy, these aquifers are mainly exploited for drinking water, providing an estimated

annual yield of $4{,}100\times10^6$ m³, with outflows from huge springs and/or through other adjacent aquifers (Celico, 1983; Allocca et al., 2007). However, in the Campania region, karst aquifers are covered by ash-fall pyroclastic deposits erupted mainly by the Somma-Vesuvius and, subordinately, the Phlegrean Fields volcanic centres during the last 39 ka. These deposits act as a regulatory layer exerting relevant hydrological control on groundwater recharge processes (Fusco et al., 2017; Cusano et al., 2024) due to their variable thickness and hydraulic features. The pyroclastic origin of the soil cover imparts high water retention capacity (De Vita et al., 2013; Fusco et al., 2017), which, when coupled with the dense vegetation, contributes to water uptake by plant roots and high evapotranspiration rates.

The complex interaction between soil properties, vegetation and climatic conditions emphasises the need for advanced methodologies to accurately estimate recharge in these contexts. Unsaturated zone modelling provides a reliable approach to estimating recharge by simulating drainage below the root zone. It assumes that water percolates vertically to reach the aquifer (Scanlon et al., 2002). Traditional approaches to recharge estimation include Boussinesq equation (Su, 1994), the water table fluctuation method (Healy, 2010; Healy and Cook, 2002) and chemical and isotopic techniques (Allison et al., 1994; Nogueira et al., 2015). With advances in computational capabilities, numerical models have become an important tool for integrating complex data sets and simulating hydrological processes. One-dimensional models, such as HYDRUS-1D, are particularly applied to estimate groundwater recharge in vadose zones (Šimůnek et al., 2008; Adomako et al., 2010; Assefa et al., 2013; Awan et al., 2013; Dickinson et al., 2013; Ficklin et al., 2010; Gates et al., 2011; Huo et al., 2014; Ibrahim et al., 2014; Jimenez-Martinez et al., 2009; Kurtzman et al., 2011; Le Coz et al., 2013; Leterme et al., 2012; Lu et al., 2011; Mastrocicco et al., 2010; Scott et al., 2000; Turkeltaub et al., 2014; Wang et al., 2009). These models simulate main hydrological processes, such as infiltration, root water uptake and evapotranspiration, considering the dynamic interactions between soil properties, vegetation and climatic conditions (Sprenger et al., 2016; dos Santos et al., 2021). Furthermore, numerical approaches provide a flexible alternative to field techniques, enabling recharge assessments under varying scenarios and future projections (Brandenburg, 2020; Neto et al., 2015).

In this study, HYDRUS-1D (Šimůnek et al., 1998, 2008) was applied to model water balance dynamics in the vadose zone of the Avella karst aquifer, focusing on the site-specific scale of the Foce hydrogeological basin. A soil profile of 1.75 m was implemented using

stratigraphic data and hydraulic parameters based on the van Genuchten equations (van Genuchten et al., 1980), derived from detailed field and laboratory tests. Calibration was performed using inverse modelling techniques, integrating multi-depth water content measurements to refine model performance.

The Foce basin was selected as a typical example of a karst aquifer in the Campania region, characterised by a discontinuous pyroclastic cover with a complex hydrogeological dynamic. A significant innovation of this study is the experimental hydrogeological observatory established within the basin, which provides continuous, real-time monitoring of key water balance parameters which are essential for the implementation and calibration of the HYDRUS-1D model. Given the representativeness of the study site, the results and the investigative approach used in this study have significant potential for application to the other karst aquifers in the Campania region, providing a transferable model for the assessment and management of recharge processes in similar contexts.

Foce hydrogeological karst observatory

The Foce hydrogeological karst observatory is located in the southern sector of the Avella Mts., specifically on the southern slope of Torre Savaio (847 m a.s.l.), part of the Sarno Mts. (Fig. 44a). It extends approximately 0.90 km² and is composed of a carbonate bedrock of Mesozoic limestone (Fig. 44b). The bedrock, extensively fractured and karstified due to tectonic activity during the Miocene and Pliocene-Pleistocene periods, hosts a local karst aquifer hydraulically connected to the Avella aquifer system. This aquifer feeds the basal spring of S. Maria La Foce (32 m a.s.l.), which has been used for drinking water since 1962 when a drainage tunnel was built.

Overlying the carbonate bedrock, discontinuous ash-fall pyroclastic deposits, with a maximum thickness of 8 m (Fig. 44c), were deposited which derived from the Phlegraean Fields and Somma-Vesuvius volcanic systems (Di Crescenzo and Santo, 2005). These deposits include the Ancient Pyroclastic Complex (APC), predominantly represented by Ignimbrite Campana flow deposits (dated to ~39 k-years), and the Recent Pyroclastic Complex (RPC), formed by more recent Somma-Vesuvius eruptions (Rolandi et al., 1998, 2000).

The volcanoclastic sequence is not uniformly complete within the basin, due to denudation processes controlled by erosive and gravitational phenomena, which are influenced by the

morphology of the slopes. These are characterised by straight profiles with an inclination of about 35° (Brancaccio et al., 2000). In morphologically conservative areas, where slopes have an inclination of less than 28°, a detailed stratigraphic and pedological characterisation of the pyroclastic deposits was carried out (De Vita et al., 2006b).

The pyroclastic cover, from top to bottom, consists of several distinct horizons. The uppermost A horizon, classified as highly organic soil (Pt), is rich in organic material with sparse pumice clasts. Below this, the B horizon consists of pumice clasts ranging from coarse to fine fractions, classified as sand with silt (SM). The C horizon is composed of pumice clasts in a matrix of poorly to well-graded sand and gravel (GW and GP). The basal layers, including the Bb and Cb horizons, comprise residual pyroclastic deposits with advanced pedogenetic features. At the lowest layer, a highly developed basal paleosol (Bb_{basal} horizon), classified as sand with silt (SM), is observed. This horizon covers the carbonate bedrock and fills the open discontinuities in the rock mass.

The hydrogeological regime of the pyroclastic soil mantle plays a significant role in regulating the groundwater recharge of the underlying karst aquifer (Fusco et al., 2017). This influence is mainly attributed to the high water retention capacity of the soils, which allows significant storage of water in the soil (Napolitano et al., 2016; De Vita et al., 2013) and consequently, its loss to the atmosphere through evapotranspiration processes.

The pyroclastic deposits support dense vegetation that varies along the altitudinal gradient (Fig. 44d). The upstream areas are mainly covered by deciduous woods, with chestnut (Castanea sativa) as the dominant species, and transitional woodland-shrub zones. In contrast, downstream areas have a more heterogeneous land use, including oak woodlands interspersed with natural grasslands and agricultural zones.

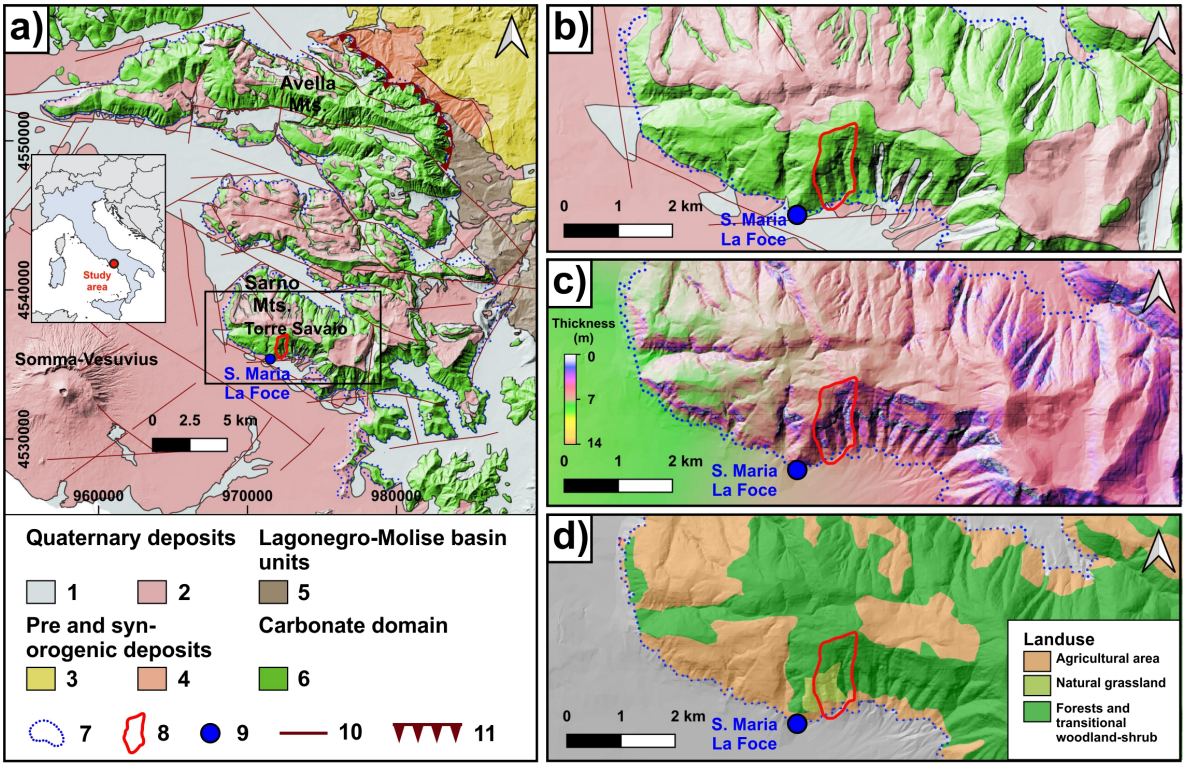


Figure 44 – a) Hydrogeological map of Avella Mts. (Petrone et al., 2024, modified); b) Excerpt from the hydrogeological map; c) Excerpt from the map of the pyroclastic deposits thickness (De Vita and Nappi, 2013, modified); d) Excerpt from land use map (Corine Land Cover, 2018, simplified).

Data and methods

Characterization of the experimental site

Laboratory and field tests were conducted to assess the stratigraphic, hydraulic, physical and index properties of the pyroclastic soil cover at the downstream site of the Foce experimental basin. A trench measuring 1.75 m deep and 2.00 m wide was excavated to enable a detailed stratigraphic analysis of the soil layers. Three reworked samples at depths of 0.30 m (Foce B_{30}), 0.80 m (Foce C_{80}), and 1.20 m (Foce C_{120}), were collected for standard laboratory tests: bulck density, grain size analysis using sieving methods, Atterberg limits (w_L and w_P) and Plasticity Index ($PI = w_L - w_P$). Porosity (n) and void ratio (e) were also estimated. Hydraulic properties were determined in the laboratory using the multistep outflow experiments performed on the four undisturbed soil samples, collected two each at 0.30 m (Foce $B_{30\text{-}1}$ and $B_{30\text{-}2}$) and 0.80 m (Foce $C_{80\text{-}1}$ and $C_{80\text{-}2}$) in depth. Fully saturated soil samples were placed in the Tempe cells (2 replicates for each soil) and were slowly drained using increasing pressure

head steps (0.1-1,000 cm H_2O). Therefore, the SWRCs were reconstructed by means of the van Genuchten model (van Genuchten et al., 1980) (Eq. 14):

$$\theta(h) = \theta_r + \frac{\theta_s + \theta_r}{[1 + |\alpha/|h||^n]^m} \quad (14)$$

where θ_s ($m^3 \cdot m^{-3}$) is the saturated volumetric water content, θ_r ($m^3 \cdot m^{-3}$) is the residual volumetric water content, h (m) is the soil matric pressure head, α (m^{-1}) is the inverse of the air entry head, n (dimensionless) is the pore size distribution parameter, and m= 1-1/n.

An optimization procedure was used to fit the experimental data by means of RETC software (van Genuchten et al., 1991).

The laboratory characterisation of SWRCs allowed the estimation of the Available Water Capacity (AWC), determined as the difference between the water content corresponding to the Field Capacity (θ_{FC}) and Permanent Wilting Point (θ_{PWP}).

In situ, infiltrometer experiments were carried out at 0.10 m, 0.40 m and 0.90 m depths to determine the saturated hydraulic conductivity (K_{sat}) of the soil.

Field monitoring

A continuous and remote hydrological monitoring system was designed and implemented in the experimental karst basin for real-time collection of all water balance parameters.

Hydrologic monitoring started in 2000 and is ongoing both upstream and downstream. Over the years, the monitoring network has been progressively expanded with additional instruments. Currently, the Foce hydrogeological observatory includes a wide array of monitoring systems designed to characterise the complex hydrodynamic processes that govern the hydrological balance of the whole basin (Fig. 45a).

Weather stations monitor (Fig. 45b) a wide range of atmospheric parameters, including air temperature, precipitation, humidity, wind speed, solar radiation, and conductivity. Two of these stations are located outside the forest, one operating since January 2000 and the other since April 2024. Additionally, a third station, operational since July 2023 and strategically placed inside the forest, focuses exclusively on precipitation measurements to estimate leaf interception.

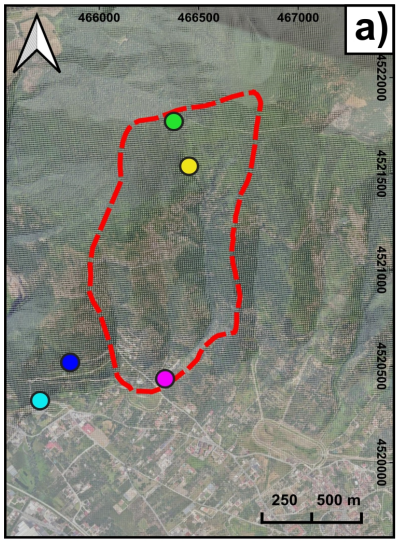
A continuous monitoring system was implemented to analyse the hydrological regime of the pyroclastic cover. Two multilevel probes were installed in June 2022 at upstream and downstream sites to monitor soil water content and temperature up to a depth of 1.20 m at

0.10 m intervals (Fig. 45c). In April 2024, the system was expanded at the upstream site with two additional multilevel probes and six water potential sensors, further improving the spatial and temporal resolution of soil water content and matric potential measurements.

The basal spring of S. Maria La Foce has been continuously monitored since February 2021 by the Sarno aqueduct (GORI SpA). This monitoring system, installed within the drainage tunnel of the spring, includes level (Fig. 45d) and flow velocity sensors to measure groundwater levels and spring discharge. The collected data are essential for understanding the dynamics of the aquifer, particularly its response to rainfall and seasonal variations, to provide effective management of the drinking water resource.

A multi-level lysimeter station was specifically designed and constructed in the field (Fig. 45e) in July 2023 to measure water infiltration in the pyroclastic cover, allowing a detailed analysis of vertical water movement through the soil and its potential contribution to the recharge of the karst aquifer. The station was installed in a trench specifically excavated for stratigraphic observations of the study area. Four horizontal boreholes were drilled at depths of 40 cm, 80 cm, 120 cm and 160 cm. Funnels were inserted into each borehole and connected by tubes to rain gauges placed in a protective box. This simple yet innovative configuration allows easy and efficient monitoring of water infiltration at different depths in the pyroclastic cover.

To complement these systems, a monitoring station for surface runoff was installed in March 2024 in a detention tank at the base of the experimental basin (Fig. 45f). This station, powered by a solar panel, verifies the activation of surface water outflows and measures continuously and remotely the flow rates. It is equipped with a stainless-steel Venturi channel coupled with a radar sensor for water level monitoring and a surveillance camera with remote access linked to the operational centre of GORI SpA, ensuring comprehensive real-time control. In addition, a 30 cm concrete weir was built to channel the surface runoff into the Venturi channel.



Ubication	Instrument	Monitored parameter	Date
●	1 multilevel probe	soil water content, water temperature	June 2022
●	1 weather station, 2 multilevel probes, 6 water potential sensors	precipitation, air temperature and humidity, wind speed, solar radiation, soil water content, water temperature, conductivity, matric potential	April 2024
●	1 weather station (inside forest), 1 multilevel probe, 1 natural multilevel lysimeter, 2 levels and velocity sensors	soil water content, water temperature,	June 2022
		precipitation, interception, soil water content, water temperature, water percolation and actual evapotranspiration,	July 2023
		piezometric levels and spring discharges	2020
●	Venturi flume channel and radar sensor	surface runoff	March 2024
●	1 weather station (outside forest)	precipitation	2000









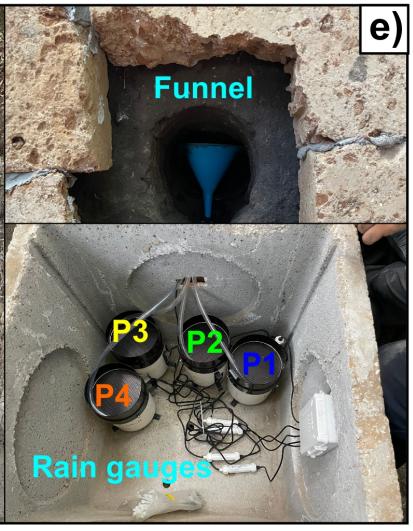




Figure 45 – Foce hydrogeological observatory: a) ubication of monitoring stations; b) weather station; c) multilevel probes for the soil water content measurements; d) groundwater level sensor; e) multi-level lysimeter station; f) Venturi channel.

HYDRUS-1D model, calibration and validation

To simulate the infiltration rate in the vadose zone profiles the HYDRUS-1D model (Šimůnek et al., 2016) was used. HYDRUS-1D is a finite element model, which is a numerical solution of the one-dimensional Richards equation (Richard, 1931) (Eq. 15):

$$\frac{\delta\theta}{\delta t} = \frac{\delta}{\delta z}\left[k\,(h)\left(\frac{\delta h}{\delta z} + 1\right)\right] - S(h) \tag{15}$$

where θ ($L^3\ L^{-3}$) is the volumetric water content, t (T) is the time variable, z (L) is a vertical coordinate, K (h) ($L\ T^{-1}$) is the unsaturated hydraulic conductivity function, h (L) is the pressure head and S (T^{-1}) is a sink term accounting for water uptake by plant roots.

In this study, the HYDRUS-1D simulation only used data from the downstream monitoring network. The simulation focused on a period of approximately 3 years, from 1 January 2021 to 27 March 2024. The model was set up with a total depth of 1.75 m and was divided into three layers. For each layer, specific hydraulic parameters derived from experimental data were defined, such as k_{sat}, θ_r, θ_s, α and n. In the numerical model, the soil hydraulic properties and the unsaturated hydraulic conductivity are described by the unimodal van Genuchten-Mualem (VGM) model (van Genuchten et al., 1980).

The HYDRUS-1D simulation includes boundary conditions for precipitation and evapotranspiration. For precipitation, a correction was needed due to the limited availability of precipitation data inside the forest, as direct measurements of precipitation below the canopy were only available from July 2023. To ensure consistency with the simulation period starting in January 2021, precipitation data recorded outside the forest from 2021 to 2024 were used and corrected for interception by the forest canopy.

The correction was implemented by estimating the reduction in rainfall due to interception using the following equation (Eq. 16):

$$\Delta P\ (\%) = \frac{(P_{out} - P_{in})}{P_{out}} \tag{16}$$

where ΔP (%) is the reduction of the precipitation due to interception, P_{out} (cm) is the precipitation measured outside the forest and P_{in} (cm) is the precipitation measured under the forest canopy. This reduction was calculated monthly to account for seasonal variability

in interception, which is influenced by both the phenological stage of the forest (e.g. leaf growth) and rainfall intensity.

The corrected precipitation outside the forest ($P_{out\text{-}corrected}$) was then calculated using the formula (Eq. 17):

$$P_{out-corrected} = P_{out} \times (100/(100 + \Delta P)) \quad (17)$$

The potential evapotranspiration (Ep_i) for month i (cm) was estimated using the Thornthwaite-Mather (1957) formula, which is expressed as (Eq. 18):

$$Ep_i = k \times \left[1.6 \times \left(10 \times \frac{T_i}{I}\right)^{\alpha}\right] \quad (18)$$

where k is a correction coefficient that depends on the mean monthly daylight hours and is a function of latitude and month, T_i is the mean monthly temperature (°C), I is the annual heat index and α is an empirical exponent.

A free drainage boundary condition was applied at the bottom of the model, neglecting the presence of a phreatic surface within the domain. This condition permits unrestricted water flow at the lower boundary.

The Feddes Root Water Uptake Model (Feddes et al., 1978) was used to simulate the movement of water removed due to vegetation in the area.

The model calibration was conducted using observed soil moisture data collected from 2022 to 2024. The calibration process involved the optimization of soil hydraulic parameters through inverse modelling using Marquardt-Levenberg Optimization Algorithm (Marquardt, 1963; Šimůnek et al., 2018) algorithm integrated within HYDRUS-1D. A total of 12 observation points, corresponding to the depths of sensor installation (every 10 cm up to 120 cm), were used to compare measured and simulated water content. Hydraulic parameters (k_s, θ_r, θ_s, α and n) were iteratively adjusted to minimize the difference between simulated and observed soil moisture.

Results

Physical and hydraulic properties of the site

At the downstream site of the Foce basin, the soil cover reaches a maximum thickness of 2 m underlain by the karst bedrock, with the water table located at 29 m a.s.l. Three different soil horizons were identified in the exploratory trench: the A horizon (0.09 m thick), the B horizon (0.44 m thick) and the C horizon (1.22 m thick) (Fig. 46a). Laboratory tests provided detailed physical and index properties for each soil horizon, summarized in Table 9. These analyses determined, water content (w), bulk unit weights (γ_{nat}, γ_{dry}, γ_{sat}, γ_s), porosity (n), void index (e), Relative Density (Dr), Atterberg limit (w_L, w_P, w_S, PI, SI, LI, CI) and organic matter content (OMC). Based on granulometric analysis and stratigraphic observations, A horizon was identified as humus, B horizon as very loose gravelly sand, and C horizon as very loose sand, consistent with AGI classification (1977).

The SWRCs show slight differences in water retention capacity, with the B horizon (θs = 0.397, θr = 0.075) retaining more water than the C horizon (θs = 0.367, θr = 0.024) (Fig. 46b). These differences correspond to the measured porosity values of 47.52% for the B horizon and 53.88% for the C horizon. The results obtained are consistent with the field capacity and permanent wilting point values calculated using the van Genuchten equation, which provided an AWC of 0.56 for the B horizon (θ_{FC} = 8.2%, θ_{PWP} = 2.6%) and 0.4 for the C horizon (θ_{FC} = 2.6%, θ_{PWP} = 2.2%) (Tab. 10).

K_{sat} values of 692 cm/day for the B horizon and 2,643 cm/day for the C horizon are consistent with this characterisation. Although laboratory tests were only carried out on samples from the B and C horizons, field measurements provided a K_{sat} for the A horizon of 3,119 cm/day. This high value indicates that the A horizon facilitates rapid water movement due to its organic-rich composition.

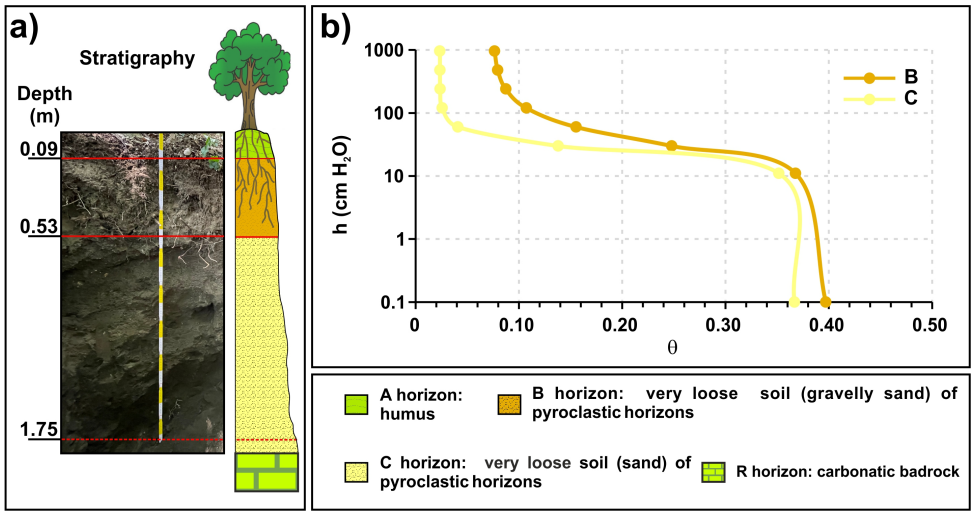


Figure 46 – a) 1D Geological model of the monitoring station site; b) SWRCs for B and C horizon

Physical-volumetric and index parameters		**Foce B_{30}**	**Foce C_{80}**	**Foce C_{120}**
Water content	θ (%)	3.87	6.60	7.82
Natural unit weight	Υ_{nat} (gr/cm^3)	1.341	1.339	1.325
Dry unit weight	Υ_{dry} (gr/cm^3)	1.287	1.230	1.199
Saturated unit weight	Υ_{sat} (gr/cm^3)	1.762	1.744	1.762
Specific gravity	Υ_s (gr/cm^3)	2.45	2.53	2.75
Void index	e	0.91	1.06	1.29
Porosity	n (%)	47.52	51.40	56.36
Relative density	Dr (%)	88.70	78.62	77.62
Liquid limit	w_L(%)	38.41	40.45	42.03
Plastic limit	w_P (%)	30.41	32.39	36.18
Shrinkage limit	w_S (%)	16.77	16.77	16.77
Plasticity Index	PI (%)	7.99	8.06	5.85
Shrinkage Index	SI (%)	13.64	15.61	19.41
Liquid Index	LI	-3.32	-3.20	-4.85
Consistency Index	CI	4.32	4.20	5.85
Organic Matter Content	OMC (%)	3.34	2.74	2.44
AGI classification		Gravelly sand	Slightly gravelly sand	Sand

Table 9 - Physical-volumetric and index parameters and AGI classification of soil samples from laboratory tests.

Horizon	Ksat (cm/day)	θ_s (-)	θ_r (-)	α (m^{-1})	n (-)	θ_{FC} (%)	θ_{PWP} (%)
A	3,119	-	-	-	-	-	-
B	692	0.397	0.075	4.397	2.37	8.2	2.6
C	2,643	0.367	0.024	4.511	3.98	2.6	2.2

Table 10 - Parameters of hydraulic characterization.

Hydrological monitoring and model calibration

For the HYDRUS-1D simulations, the results of the stratigraphic and hydraulic characterisation of the pyroclastic soil cover were integrated with the hydrogeological monitoring data collected at the downstream site of the Foce basin. Same of this data were used both for the HYDRUS-1D model implementation and calibration.

A comparative analysis was carried out between rainfall measured outside and inside the forest canopy over the period 2021-2024 (Fig. 47a) to assess leaf interception. Precipitation in the forest is consistently lower than in open areas. On average, the presence of the forest canopy reduced precipitation reaching the ground by 48% compared to outside measurements. The precipitation affected by interception was implemented as a climatic parameter in the HYDRUS-1D model simulation, allowing a more realistic representation of the water balance within the study area.

The spring hydrogram (Fig. 47b) provides indications of the temporal variations in the S. Maria La Foce spring discharge, both captured by the drainage tunnel and by the wells field, managed by GORI for drinking use. The sum of the captured discharge represents the natural spring discharge whose trend is a useful tool for analysing the dynamics of the karstic aquifer in response to precipitation. The average discharge is 1.70 m^3/s, with a minimum typically below 1 m^3/s observed during the spring depletion period between April and May, corresponding to the gradual reduction of groundwater reserves accumulated during the wet winter season. In contrast, the maximum discharge exceeds 3 m^3/s during the recharge phase, which begins in November and December and is closely linked to the increased autumn and winter precipitation that replenishes the aquifer.

The results of the lysimetric observations (Fig. 47c), show the infiltration trends from July 2023 to March 2024 at different depths. The lysimetric station recorded episodes of effective infiltration, with a maximum value of 0.40 mm, only at a depth of 0.80 m (rain gauge P2).

These events correspond to rainfall observed at the end of September 2023, between October and November 2023 and March 2024.

Surface runoff was related to precipitation events for the period from 1 March 2024 to 3 October 2024, as shown in Figure 47d. Runoff peaks (maximum of 0.06 l/s) were recorded immediately after significant rainfall events, such as those in June, September and October 2024.

The calibration process was performed in HYDRUS-1D using an inverse modelling approach based on observed soil water content data from multi-level probe with sensors installed at 12 different depths in the soil profile, every 10 cm, up to 120 cm. Figure 47e shows the temporal variation of soil water content at different depths, correlated with precipitation events. The graph shows that the soil at 15 cm below the surface exhibits the highest sensitivity to climatic variations, as evidenced by pronounced peaks in response to precipitation and evapotranspiration dynamics. In contrast, at greater depths, the water content curves show a more moderated response, reflecting reduced influence from short-term climatic fluctuations. The data also highlight seasonal trends, with soil water content increasing during cooler and wetter periods and decreasing during warmer and drier conditions.

Figure 47f shows the average monthly water content for 2022, 2023 and 2024, as well as stratigraphic details, θ_{FC} and θ_{PWP} limits (Tab. 10) derived from SWRCs. Water content generally increases during wetter months and decreases during drier periods. The data indicate that the C horizon has a higher water content than the other horizons, while the B horizon consistently has the lowest water content. Values above θ_{FC} during the wettest periods occur in the C horizon and indicate water infiltration in the soil.

The hydraulic parameters (K_{sat}, θr, θs, α, and n) were iteratively adjusted to minimize the difference between the simulated and observed soil water content at each observation point. The calibration results indicate a good agreement between observed and simulated data, with R^2 of 0.72883, a minimal mass balance error of 0.0330%, and a final objective function value of 0.3640.

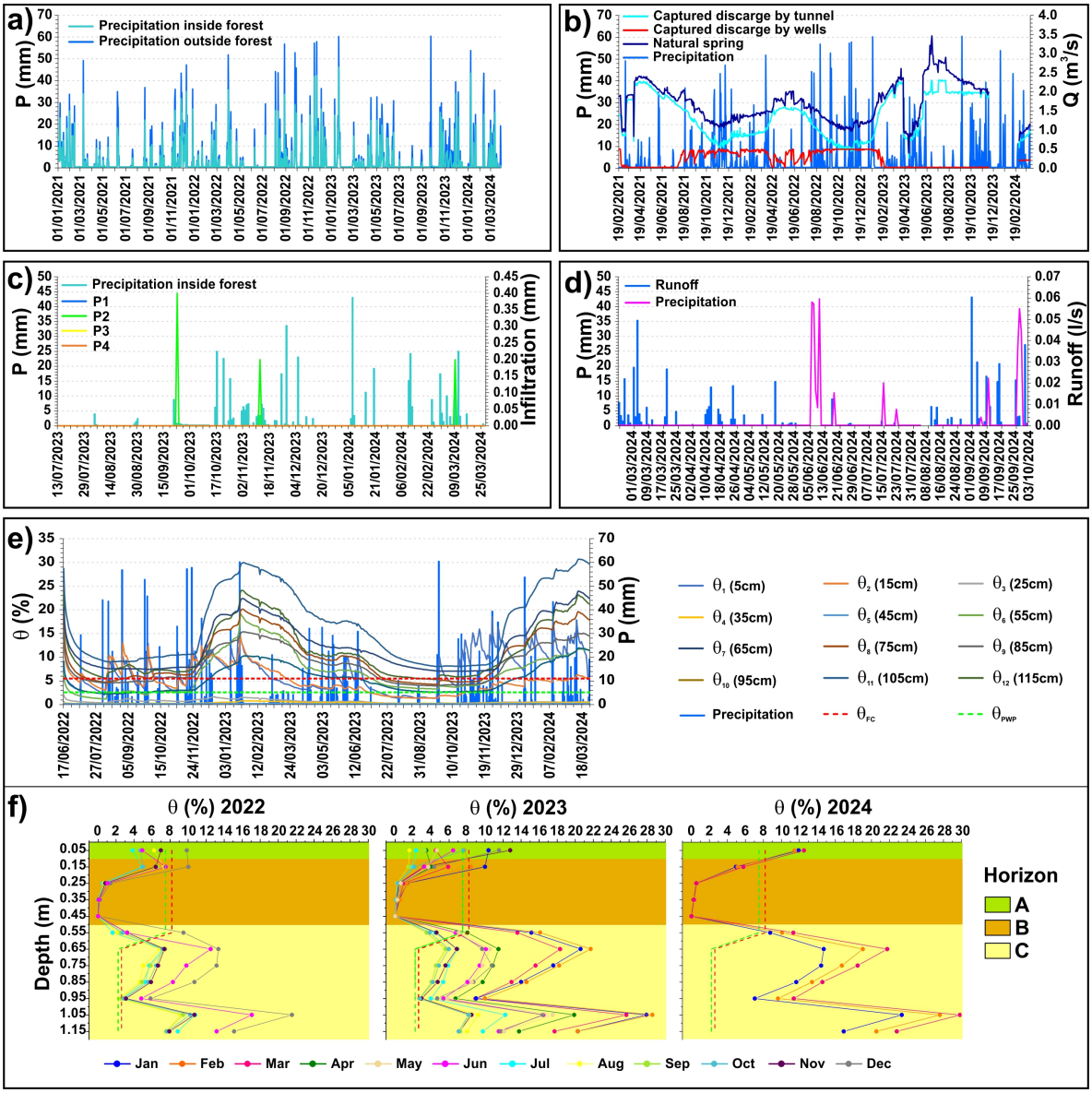


Figure 47 – Results of hydrogeological monitoringa) Comparison between precipitation measured inside and outside the forest; b) spring hydrogram of S. Maria La Foce spring; c) infiltration measured by multilevel lysimeter; d) superficial runoff; e) soil water content at different depths; 7) average monthly water content for 2022, 2023 and 2024.

Groundwater recharge simulation

The simulation performed using HYDRUS-1D shows the trend of selected water balance components over a period of about three years, from January 2021 to April 2024 (Fig. 48a). The variables analysed include the actual infiltration occurring at the top and bottom of the HYDRUS-1D model (Fig. 48d) and the actual evapotranspiration, related to the rainfall

measured inside the forest, where interception processes play a significant role. The results show a consistently higher infiltration rate at the top of the HYDRUS-1D model than observed at the bottom, mainly due to the higher permeability of the upper soil layers, which facilitates water percolation. In addition, the temporal variability of climatic conditions has a more pronounced effect on the upper soil layer, where infiltration shows sharp peaks in response to precipitation events. In contrast, infiltration in the lower layer shows a more regular and moderate pattern over time. This difference can be attributed to the buffering effect of the soil profile: as water percolates through the subsurface, the redistribution and retention processes dampen the intensity of the temporal fluctuations, resulting in a less variable infiltration rate at deeper levels.

The results further highlight a strong seasonal variability of the hydrogeological variables over the simulation period: during wet and cold months, higher infiltration rates are observed at both the top (maximum value of 45.7 mm/day in January 2023) and bottom (maximum value of 0.003 mm/day in January 2021) layers, associated with reduced evapotranspiration rates (minimum value of 0.3 mm/day in January 2024) (Fig. 48b). Conversely, during dry and warm months, evapotranspiration increases (maximum value of 4.1 mm/day in August 2022), while infiltration decreases at both the top (minimum value of 0.003 mm/day in September 2023) and bottom (minimum value of 0.003 mm/day in September 2021) (Fig.48c).

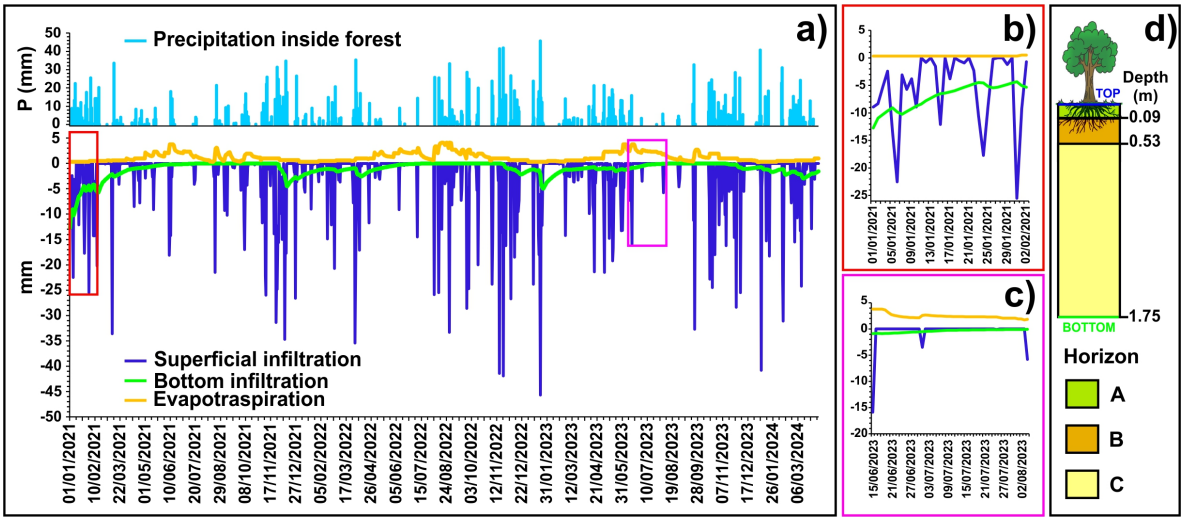


Figure 48– a) The hydrogeological variables simulated by HYDRUS-1D; b) simulation during wet and cold months c) simulation during dry and warm months; d) 1D geological model implemented in HYDRUS-1D.

Discussion

The results of the HYDRUS-1D simulation provide significant insights concerning the temporal dynamics of the water balance components in the pyroclastic soil cover of the Foce hydrogeological observatory. The higher infiltration rates observed at the top of the soil profile compared to the bottom highlight the influence of stratigraphic heterogeneity of the soil matrix and the greater permeability of the upper soil layer. The seasonal variability highlighted in the simulation, characterised by increased infiltration during wet and cold months and increased evapotranspiration during dry and warm months, is consistent with expected hydrological behaviour under Mediterranean climatic conditions. These results are also consistent with previous studies (Calder, 1996), which emphasise the role of interception processes in reducing effective precipitation under forest canopies. The observed divergence in infiltration trends between the top and bottom layers, with the latter showing a more moderated temporal pattern, reflects the damping effect of soil processes on climatic fluctuations as water percolates through the profile. This highlights the importance of soil matrix structure and hydraulic properties in controlling the downward movement of the water and, hence, recharge potential in the underlying karst aquifer.

The calibration process of the HYDRUS-1D model was essential to achieve a good representation of the observed soil water dynamics. Using inverse modelling techniques, hydraulic parameters such as saturated hydraulic conductivity, residual and saturated water content and pore size distribution were iteratively adjusted to minimise discrepancies between observed and simulated data. The calibration results showed good agreement, demonstrating the capability of the model to reproduce the general trends in soil moisture variation observed in the field.

While the calibration process provided good results, the validation of the HYDRUS-1D model at the site-specific scale of the Foce experimental basin remains challenging due to limitations in the available observed data set. Although the monitoring network provides a wide range of data on the hydrogeological variables of the water balance (soil water content, precipitation in and out of the forest, infiltration and runoff), the relatively short time frame of data collection, particularly for infiltration and runoff, limits the robustness of model validation.

Conclusions

Based on detailed field data collected from the downstream monitoring network and hydraulic properties determined from laboratory and field experiments, this study applied the HYDRUS-1D model to simulate the infiltration process within the pyroclastic soil cover of the Foce experimental karst basin. The main results of this research can be summarised as follows:

- Calibration of the HYDRUS-1D model using inverse modelling techniques and observed soil moisture data from multi-level probes provided a good agreement between simulated and measured data ($R^2 = 0.72883$, mass balance error = 0.033%).
- The model showed a significant difference in infiltration rates between the top and bottom soil layers.
- The simulation highlighted strong seasonal variability in water balance components, with higher infiltration rates during wet and cold months and increased evapotranspiration during dry and warm months.
- The divergence in infiltration trends between the top and bottom layers further demonstrated the role of the soil matrix structure and hydraulic properties in controlling water percolation and potential recharge. The response of the top to rainfall was more variable, reflecting short-term climatic fluctuations, while the bottom layer exhibited more moderated behaviour, highlighting the buffering effects of deeper soil profiles.
- The comparative analysis of precipitation measured inside and outside the forest confirmed the influence of interception processes on effective precipitation, with a significant impact on the water balance of forest areas.

The results highlight the complexity of the infiltration process at the site-specific scale, influenced by the spatial heterogeneity of the pyroclastic soil matrix and the presence of preferential pathways. Even though the HYDRUS-1D model was able to capture the temporal dynamics of the water balance components with good calibration criteria, limitations of the dataset, including the short monitoring period and the limited spatial resolution, restricted the model validation. To overcome these limitations, it would be useful to extend the monitoring period and increase the spatial resolution of some of the monitored parameters (e.g. lysimeter infiltration and runoff). These future developments would improve the reliability of the model, reduce uncertainties and deepen the understanding of

hydrological processes in the pyroclastic soil systems of karst aquifers, thus enabling wider applications of the HYDRUS-1D model.

References

Adomako, D., P. Maloszewski, C. Stumpp, S. Osae, T. T. Akiti. 2010. Estimating groundwater recharge from water isotope (δ2H, δ18O) depth profiles in the Densu River basin, Ghana. - Hydrological Sciences Journal, 55, 8, 1405- 1416.

Allison, G.B., Gee, G.W., Tyler, S.W., 1994. Vadose-Zone Techniques for Estimating Groundwater Recharge in Arid and Semiarid Regions. Soil Sci. Soc. Am. J. 58, 6-14. https://doi.orq/10.2136/sssai1994.03615995005800010002x.

Allocca, V., Celico, F., Celico, P., De Vita, P., Fabbrocino, S., Mattia, S., Monacelli, G., Musilli, I., Piscopo, V., Scalise, A.R., Summa, G., and Tranfaglia, G., 2007. Illustrative Notes of the Hydrogeological Map of Southern Italy. Istituto Poligrafico e Zecca dello Stato, Rome, 1–211, ISBN 88-448-0223-6.

Assefa, K.A., Woodbury, A. D., 2013. Transient, spatially varied groundwater recharge modeling. - Water Resources Research, 49, 4593–4606. https://doi.org/10.1002/wrcr.20332.

Associazione Geotecnica Italiana (A.G.I.), 1977. Raccomandazioni sulla programmazione ed esecuzione delle indagini geotecniche.

Awan, U. K., Tischbein B., Martius C., 2013. Combining hydrological modeling and GIS approaches to determine the spatial distribution of groundwater recharge in an arid irrigation scheme. - Irrig. Sci., 31, 793–806. https://doi.org/10.1007/s00271-012-0362-0.

Brancaccio, L., Cinque, A., Russo, F., Sgambati, D., 2000. Le frane del 5-6 maggio 1998 sul gruppo montuoso Pizzo d'Alvano (Campania): osservazioni geomorfologiche sulla loro distribuzione e sulla dinamica delle connesse colate. Quaderni di Geologia Applicata, 7, 1.

Brandenburg, J. P., 2020. Geologic frameworks for groundwater flow models. 25 Disponivel em: www.gw-proiect.org.

Calder, I. R., 1996. Dependence of rainfall interception on drop size: 1. Development of the two-layer stochastic model. Journal of hydrology, 185(1-4), 363-378.

Celico, P., 1983. Idrogeologia dei massicci carbonatici, delle piane quaternarie e delle aree vulcaniche dell'Italia centro-meridionale: Marche e Lazio meridionali, Abruzzo, Molise e Campania. Cassa per il Mezzogiorno.

Corine Land Cover. 2018. https://land.copernicus.eu/pan-european/corine-land-cover.

Cusano, D., Lepore, D., Allocca, V., De Vita, P., 2024. Control of soil mantle thickness and land cover types on groundwater recharge of karst aquifers in Mediterranean areas. Journal of Hydrology. 630, 130770. https://doi.org/10.1016/j.jhydrol.2024.130770.

De Vita, P., Agrello, D., Ambrosino, F., 2006b. Landslide susceptibility assessment in ash-fall pyroclastic deposits surrounding Mount Somma-Vesuvius: Application of geophysical surveys for soil thickness mapping. Journal of Applied Geophysics, 59(2), 126-139.

De Vita, P., and Nappi, M., 2013. Regional Distribution of Ash-Fall Pyroclastic Soils for Landslide Susceptibility Assessment. In Landslide Science and Practice pp. 103–109. Springer Berlin Heidelberg.

De Vita, P., Napolitano, E., Godt, J.W., Baum, R.L., 2013. Deterministic estimation of hydrological thresholds for shallow landslide initiation and slope stability models: case study from the Somma-Vesuvius area of southern Italy. Landslides 10, 713–728. https://doi.org/10.1007/s10346-012-0348-2.

Di Crescenzo, G., and Santo, A., 2005. Nuovo contributo sul ruolo svolto dai livelli pomicei nelle aree di distacco delle frane di colata rapida dei massicci carbonatici campani. Convegno Nazionale La mitigazione del rischio da colate di fango a Sarno e negli altri Comuni colpiti dagli eventi del maggio 1998. Napoli, 2 e 3 maggio 2005 - Sarno 4 e 5 maggio 2005.

Dickinson, J. E., Ferré, T. P. A., Bakker M., Crompton B., 2014. A screening tool for delineating subregions of steady recharge within groundwater models, Vadose Zone Journal 13, 6, 15. https://doi.org/10.2136/vzj2013.10.0184.

Dos Santos, R. M., Koide, S., Tåvora, B. E., De Araujo, D. L., 2021. Groundwater recharge in the cerrado biome, Brazil—a multi-method study at experimental watershed scale. Water (Switzerland), 13, 1, 1—28. https://doi.orq/10.3390/w13010020.

Feddes, R. A., Kowalik, P. J., Zaradny, H., Taylor, S. A., Ashcroft, G. L., Vrugt, J. A., Diks, C. G., Gupta, H. V., Bouten, W., and Verstraten, J. M., 1978. Physical edaphology. The physics of irrigated and nonirrigated soils, Monogr. PUDOC,Wageningen, 41, 1–17, https://doi.org/10.1029/2004WR003059.

Ficklin, D. L., Luedeling, E., Zhang, M., 2010. Sensitivity of groundwater recharge under irrigated agriculture to changes in climate, CO 2 concentrations and canopy structure. - Agricultural Water Management, 97, 7, 1039-1050.

Fusco, F., Allocca, V., De Vita, P., 2017. Hydro-geomorphological modelling of ash-fall pyroclastic soils for debris flow initiation and groundwater recharge in Campania (southern Italy). Catena 158, 235–249. https://doi.org/10.1016/j.catena.2017.07.010.

Gates, J. B., Scanlon, B. R., Mu, X., Zhang, L., 2011. Impacts of soil conservation on groundwater recharge in the semi-arid Loess Plateau, China. – Hydrogeology Journal, 19, 865–875.

Goldscheider, N., 2012. A holistic approach to groundwater protection and ecosystem services in karst terrains. Aqua Mundi – Am, 06046, 117–124.

Healy, R. W. and Cook, P. G., 2022. Using groundwater levels to estimate recharge, Hydrogeol. J., 10, 109. https://doi.org/10.1007/s10040-001-0178-0.

Healy, R.W. 2010. Estimating groundwater recharge. Cambridge University Press. https://doi.orq/10.1017/CB0978051 1780745.

Huo, S., Menggui J., Liang, X., Lin, D., 2014. Changes of vertical groundwater recharge with increase in thickness of vadose zone simulated by one-dimensional variably saturated flow model, Journal of Earth Science, 25, 6, 1043-1050.

Ibrahim, M., Favreau, G., Scanlon, B. R., Seidel, J. L., Le Coz, M., Demarty, J., Cappelaere B., 2014. Long-term increase in diffuse groundwater recharge following expansion of rainfed cultivation in the Sahel, West Africa. - Hydrogeology Journal, 22, 6, 1293-1305.

Jimenez-Martinez, J., Skaggs, T. H., van Genuchten, M. Th., Candela, L., 2009. A root zone modelling approach to estimating groundwater recharge from irrigated areas. - J. Hydrol., 367, 1-2, 138-149.

Kurtzman, D., Scanlon, B. R., 2011. Groundwater recharge through Vertisols: Irrigated cropland vs. natural land, Israel. - Vadose Zone Journal, 10, 2, 662-674.

Le Coz, M., Favreau, G., Ousmane, S. D., 2013. Modeling increased groundwater recharge due to change from rainfed to irrigated cropping in a semiarid region. Vadose Zone Journal, 12, 2, 12. https://doi.org/10.2136/vzj2012.0148.

Leterme, B., Mallants, D., Jacques, D., 2012. Sensitivity of groundwater recharge using climatic analogues and HYDRU S-1D. - Hydrol. Earth Syst. Sci., 16, 2485–2497, doi:10.5194/hess-16-2485-2012. https://doi.org/10.5194/hess-16-2485-2012.

Lu, X., Jin, M., van Genuchten, M. Th., Wang, B., 2011. Groundwater recharge at five representative sites in the Hebei Plain of China: Case study. - Ground Water, 49, 2, 286-294.

Marquardt, D. W., 1963. An Algorithm for Least Squares Estimation of Nonlinear Parameters, J. Soc. Ind. Appl. Math. 11, 431-441.

Mastrocicco, M., Colombani, N., Salemi E., Castaldelli G., 2010. Numerical assessment of effective evapotranspiration from maize plots to estimate groundwater recharge in lowlands. - Agricultural Water Management, 97, 9, 1389-1398.

Napolitano, E., Fusco, F., Baum. R. L., Godt, J. W., De Vita, P., 2016. Effect of antecedent hydrological conditions on rainfall triggering of debris flows in ash-fall pyroclastic mantled slopes of Campania (southern Italy). Landslides, 13(5), 967-983.

Neto, D. C., Chang, H. K., van Genuchten, M. Th., 2015. A Mathematical View of Water Table Fluctuations in a Shallow Aquifer in Brazil. Groundwater.

Nogueira, G.E.H., Kiang, C.H., 2015. Simulaqäo numérica de fluxo de åguas subterräneas do aquifero rio Claro, porqäo nordeste do municipio de Rio Claro, SP. Åguas Subterråneas, 29, 175. https://doi.orq/10.14295/ras.v29i2.28304.

Petrone, P., De Vita, P., Marsiglia, P., Allocca, P., Coda, S., Cusano, D., Lepore, D., Allocca, V., 2024. Hydrogeological conceptual model and groundwater recharge of Avella Mts. karst aquifer (southern Italy): A literature review and update. Journal of Hydrology: Regional Studies, 54, 101871. https://doi.org/10.1016/j.ejrh.2024.101871.

Richards, L. A., 1931. Capillary conduction of liquids through porous mediums. Physics, 1(5), 318–333.

Rolandi, G., Petrosino, P., Mc Geehin, J., 1998. The interplinian activity at Somma–Vesuvius in the last 3500 years. Journal of Volcanology and Geothermal Research, 82(1-4), 19-52.

Rolandi, G., Bertollini, F., Cozzolino, G., Esposito, N., Sannino, D., 2000. Sull' origine delle coltri piroclastiche presenti sul versante occidentale del Pizzo d'Alvano (Sarno-Campania). Quaderni di Geologia Applicata, 7(1), 37-48.

Scanlon, B. R., Healy, R.W., and Cook, P. G., 2002. Choosing appropriate techniques for quantifying groundwater recharge, Hydrogeol. J., 10, 18–39. https://doi.org/10.1007/s10040-001-0176-2.

Scott, R. L., Shuttleworth, W. J., Keefer, T. O., Warrick, A. W., 2000. Modeling multiyear observations of soil moisture recharge in the semiarid American Southwest. -Water Resour. Rer., 36, 8, 2233-2247.

Šimůnek, J., Huang, K., van Genuchten, M. Th., 1998. The HYDRUS code for simulating the one-dimensional movement of water, heat, and multiple solutes in variably saturated media. Version 6.0, Research Report No. 144, U.S. Salinity Laboratory, USDA, ARS, Riverside, California, 164.

Šimůnek, J., Köhne, J. M., Kodešová, R., & Šejna, M., 2008. Simulating non equilibrium movement of water, solutes, and particles using HYDRUS: a review of recent applications. Soil and Water Research, 3(Special Issue 1), S42–S51.

Šimůnek, J., van Genuchten, M. Th., Šejna, M., 2016. Recent Developments and Applications of the HYDRUS Computer Software Packages, Vadose Zone J., 15, vzj2016.04.0033, https://doi.org/10.2136/vzj2016.04.0033.

Šimůnek, J., Šejna, M., van Genuchten, M. Th., 2018. New features of version 3 of the HYDRUS (2D/3D) computer software package. Journal of Hydrology and Hydromechanics, 66(2), 133-142.

Sprenger, M., Seeger, S., Blume, T.; Weiler, M., 2016. Travel times in the vadose zone: Variability in space and time. Water Resources Research, v. 52, n. 8, p. 5727—5754. https://doi.orq/10.1002/2015WR018077.

Su, N. 1994. A formula for computation of time-varying recharge of groundwater. Journal of Hydrology, 160, 123-135. https://doi.orq/10.1016/0022-1694(94)90037-X.

Thornthwaite, C.W., Mather, J.R., 1957. Instructions and tables for computing potential evapotranspiration and the water balance. Centerton, New Jersey, Laboratory of Climatology, Publications in Climatology 10 (3): 185–311.

Turkeltaub, T., Dahan, O., Kurtzman, D., 2014. Investigation of groundwater recharge under agricultural fields using transient deep vadose zone data. - Vadose Zone Journal, 13, 4, 13, https://doi.org/10.2136/vzj2013.10.0176.

van Genuchten, M. Th., 1980. A closed-form equation for predicting the hydraulic conductivity of unsaturated soils 1. Soil Science Society of America Journal, 44(5), 892–898.

van Genuchten, M. Th., Leij, F.J., Jates, S.R., 1991. The Retc code for quantifying the hydraulic functions of unsaturated soils. U.S. Department of Agriculture, Agricultural Research Service, Report IAG-DW12933934, Riverside, CA.

Wang, T., Zlotnik, V. A., Šimůnek, J., Schaap, M. G., 2009. Using pedotransfer functions in vadose zone models for estimating groundwater recharge in semiarid regions. Water Resour. Res., 45, 12. https://doi.org/10.1029/2008WR006903.

5. Conclusions

The research results highlight how an integrated multi-method approach represents a valuable tool for the multi-temporal estimation and modelling, of groundwater recharge processes at different scales of analysis in the study area.

By integrating remote sensing data (e.g. MODIS real evapotranspiration) with ground-based hydrological observations, the study provided more accurate recharge estimates, particularly in high-altitude areas where systematic data collection is limited.

The SWB code is a highly versatile method, which was applied at different temporal (annual, monthly and daily) and spatial (aquifer and basin) scales, allowing the model to be adapted to local hydrogeological and climatic characteristics. Furthermore, the results of the SWB applied at the sectoral scale, combined with pumping tests and the hydrogeochemical quality data, highlighted the high potential and good quality of the groundwater resources in the piedmont karst aquifer sector, which can serve as a complementary water resource during dry periods.

The integration of the RCMs data allowed the simulation of different climate change scenarios, assessing the impact of future changes in temperature and precipitation on groundwater resources, particularly on the recharge dynamics.

At the site-specific scale a karst basin was equipped as a natural hydrogeological observatory for continuous and multiparametric field measurements in space and time of all hydrological variables of the water balance. The data collected from this monitoring system were used for the implementation and calibration of a numerical model in HYDRUS-1D, which allowed accurate simulation of key hydrological balance processes (e.g. evapotranspiration and infiltration) within the unsaturated zone of the ash-fall pyroclastic soil cover.

An important achievement of this research is the potential to export the proposed integrated approach to similar hydrogeological contexts, providing a basis for future analyses, both in terms of academic research and practical applications. The integrated methods represent a significant contribution to the understanding of the role of climatic, hydrogeological and geological variables in recharge processes, providing the basis for the development of strategies for more sustainable management of groundwater resources in karst aquifers.

Acknowledgments

I would like to express my deepest gratitude to my supervisor, Prof. Vincenzo Allocca, for his constant guidance, support and valuable advice that accompanied every step of my Ph.D. His experience and dedication were important to my professional and personal growth.

I thank my co-supervisor, Prof. Pantaleone De Vita, for his support and availability.

Special thanks are due to the guys of DiSTAR hydrogeology group for their scientific and human support, which was never lacking, and for creating a stimulating and collaborative environment that enriched this experience.

I am grateful to Dr. Enrico Di Clemente for guiding me through the laboratory experience.

I would like to thank GORI SpA for making this research possible and for the results obtained.

Finally, I would like to thank Prof. Radká Kodešová for welcoming me during my Ph.D.visit to the University of Life Sciences in Prague. The experience at her institution was an extraordinary opportunity for my growth, both professionally and personally.

I thank the referees for referencing the thesis.

References

Allocca, V., Celico, F., Celico, P., De Vita, P., Fabbrocino, S., Mattia, S., Monacelli, G., Musilli, I., Piscopo, V., Scalise, A. R., Summa, G., Tranfaglia, G., 2007. Illustrative Notes of the Hydrogeological Map of Southern Italy. Istituto Poligrafico e Zecca dello Stato, Rome, 1–211, ISBN 88-448-0223-6.

Allocca V., Aquino S., Esposito L., Celico P., 2008. Le acque sotterranee dell'Irpinia (Italia meridionale): stato delle conoscenze e prospettive future. L'ACQUA, 6 (2008), 39-66.

Allocca, V., Manna, F., De Vita, P., 2014. Estimating annual groundwater recharge coefficient for karst aquifers of the southern Apennines (Italy). Hydrology and Earth System Sciences, 18(2), 803–817.

Allocca, V., De Vita, P., Manna, F., Nimmo, J. R., 2015. Groundwater recharge assessment at local and episodic scale in a soil mantled perched karst aquifer in southern Italy. Journal of Hydrology, 529, 843–853.

Beck, H. E., Zimmermann, N. E., McVicar, T. R., Vergopolan, N., Berg, A., Wood, E. F., 2018. Present and future Köppen-Geiger climate classification maps at 1-km resolution. Scientific Data, 5, Article 180214. https://doi.org/10.1038/sdata.2018.214.

Bonardi, G., D'Argenio, B., Perrone, V., 1988. Carta geologica dell'Appennino meridionale alla scala 1: 250.000. Memorie della Società Geologica Italiana, 41.

Brancaccio, L., Cinque, A., & Sgrosso, I., 1978. L'analisi morfologica dei versanti come strumento per la ricostruzione degli eventi neotettonici.

Brancaccio, L., Cinque, A., Russo, F., Sgambati, D., 2000. Le frane del 5-6 maggio 1998 sul gruppo montuoso Pizzo d'Alvano (Campania): osservazioni geomorfologiche sulla loro distribuzione e sulla dinamica delle connesse colate. Quaderni di Geologia Applicata, 7, 1.

Bull, W. B., 2007. Tectonic geomorphology of mountains, a new approach to paleoseismology, Blackwell Publishing, Malden, USA, 316.

Celico, P., 1978. Schema idrogeologico dell'Appennino carbonatico centromeridionale. Memorie e Note Istituto di Geologia Applicata, Napoli 14, 1–97.

Celico P., de Riso R. 1978. Il ruolo della Valle Caudina nella idrogeologia del Casertano e del Sarnese (Campania). Mem. e Note Ist. Geol. Appl., 14, 1–25, Napoli.

Celico P., De Gennaro M., Ferreri M., Ghiara M., Russo D., Stanzione D., Zenone F., 1980. Il margine orientale della Piana Campana: indagini idrogeologiche e geochimiche. Period. Miner. 49, 241–270.

Celico, P., 1983. Idrogeologia dei massicci carbonatici, delle piane quaternarie e delle aree vulcaniche dell'Italia centromeridionale (Marche e Lazio meridionale, Abruzzo, Molise e Campania). Quaderni della Cassa per il Mezzogiorno 4 (2), 1–203, Roma.

Celico, F., Musilli, I., Naclerio, G., 2004. The impacts of pasture- and manure-spreading on microbial groundwater quality in carbonate aquifers. Environmental Geology 46(2).

Celico, F., Petrella, P., Celico, P., 2006. Hydrogeological behaviour of some fault zones in a carbonate aquifer of Southern Italy: an experimentally based model, Terra Nova, 18, 308–313.

Celico F., Naclerio G., Bucci A., Nerone V., Capuano P., Carcione M., Allocca V., Celico P., 2010. Influence of pyroclastic soil on epikarst formation: a test study in southern Italy. Terra Nova, 22, 110-115.

Civita M., de Riso R., Nicotera P., 1970. Sulla struttura idrogeologica alimentante le sorgenti del Fiume Sarno e le falde pedemontane profonde della parte sud-orientale della Conca Campana. Atti I Conv. Intern. Acque Sott., IAH, 1-24, Palermo.

Compagnucci, R. et al. Nigel Arnell (UK) and Chunzhen Liu (China). 2001. Climate Change 2001: Impacts, Adaptation, and Vulnerability: Contribution of Working Group II to the Third Assessment Report of the Intergovernmental Panel on Climate Change 2, 191.

Corine Land Cover. 2018. https://land.copernicus.eu/pan-european/corine-land-cover.

Cusano, D., Allocca, V., Fusco, F., Tufano, R., De Vita, P., 2019. Multi-scale assessment of groundwater vulnerability to pollution: study cases from Campania region (southern Italy). Italian Journal of Engineering Geology and Enviroment (Special Issue).

Cusano, D., Coda, S., De Vita, P., Fabbrocino, S., Fusco, F., Lepore D., Nicodemo, F., Pizzolante, A., Tufano, R., Allocca V., 2023. Comparison of methods for assessing groundwater vulnerability in karst aquifers: the case study of Terminio Mt. aquifer (Southern Italy). Sustainable Environment Research (2023) 33:42. https://doi.org/10.1186/s42834-023-00204-8.

Cusano, D., Allocca, V., Coda, S., Di Clemente, E., Fabbrocino, S., Lepore, D., Panza, R., Petrone, P., De Vita P., 2024a. Effects of ash-fall pyroclastic soil mantle on groundwater recharge of Terminio Mt. peri-volcanic karst aquifer. Journal of Hydrology: Regional Studies. 53 (2024) 101844. https://doi.org/10.1016/j.ejrh.2024.101844

Cusano, D., Lepore, D., Allocca, V., De Vita, P., 2024b. Control of soil mantle thickness and land cover types on groundwater recharge of karst aquifers in Mediterranean areas. Journal of Hydrology 630, 130770. https://doi.org/10.1016/j.jhydrol.2024.130770.

D'Argenio, B., Pescatore, T., & Scandone, P., 1973. Schema geologico dell'Appennino meriodionale (Campania e Lucania). Verlag nicht ermittelbar.

De Vita, P., Agrello, D., Ambrosino, F., 2006a. Landslide susceptibility assessment in ash-fall pyroclastic deposits surrounding Mount Somma-Vesuvius: Application of geophysical surveys for soil thickness mapping. J. Appl. Geophys. 2, 126-139. https://doi.org/10.1016/j.jappgeo.2005.09.001.

De Vita P., Agrello D., Ambrosino F., 2006b. Landslide susceptibility assessment in ash-fall pyroclastic deposits surrounding Mount Somma-Vesuvius: Application of geophysical surveys for soil thickness mapping. Journal of Applied Geophysics, 59(2), 126-139.

De Vita, P., Allocca, V., Manna, F., Fabbrocino, S., 2012. Coupled decadal variability of the North Atlantic Oscillation, regional rainfall and karst spring discharges in the Campania region (southern Italy). Hydrology and Earth System Sciences, 16(5), 1389–1399.

De Vita, P., Nappi, M., 2013. Regional distribution of ash-fall pyroclastic deposits in Campania (southern Italy) for landslide susceptibility assessment. In: Landslide Science and Practice (Margottini C., Canuti P, Sassa K. eds.), 3, Spatial Analysis and Modelling, Springer-Verlang, 103-110. https://doi:10.1007/978-3-642-31310-3_15.

De Vita, P., Allocca, V., Celico, F., Fabbrocino, S., Mattia, C., Monacelli, G., Musilli, I., Piscopo, V., Scalise, A.R., Summa, G., Tranfaglia G., Celico, P., 2018. Hydrogeology of continental southern Italy. Journal of Maps, 14:2, 230–241.

De Vivo B., Rolandi G., Gans P., Calvert A., Bohrson W., Spera F., Belkin H., 2001. New constraints on the pyroclastic eruptive history of the Campanian volcanic Plain (Italy). Mineralogy and Petrology, v. 73, no. 1, p. 47-65.

Deino, A. L., Orsi, G., de Vita, S., Piochi, M., 2004. The age of the Neapolitan Yellow Tuff caldera-forming eruption (Campi Flegrei caldera–Italy) assessed by 40Ar/39Ar dating method. Journal of Volcanology and Geothermal Research, 133(1-4), 157-170.

Del Prete, M., Del Prete, R., Guadagno, F. M., Revellino, P., 2005. Observations on 1998 Campanian debris avalanches and debris flows. Giornale di Geologia Applicata, 1, 63-72.

Di Crescenzo, G., and Santo, A., 2005. Nuovo contributo sul ruolo svolto dai livelli pomicei nelle aree di distacco delle frane di colata rapida dei massicci carbonatici campani. Convegno Nazionale La mitigazione del rischio da colate di fango a Sarno e negli altri Comuni colpiti dagli eventi del maggio 1998. Napoli, 2 e 3 maggio 2005 - Sarno 4 e 5 maggio 2005.

Di Vito M., Sulpizio R., Zanchetta G., 1997. Relazioni tra depositi vulcanici e sedimentari nella Piana Campana negli ultimi 37 ka. GNV, 1996 Annual Meeting Abstract Volume, 31-32.

Di Vito, M.A., Sulpizio, R., Zanchetta, G., 1998. I depositi ghiaiosi della valle dei torrenti Clanio e Acqualonga (Campania centro-orientale): significato stratigrafico e ricostruzione paleoambientale. Il Quaternario, 11 (2), 273–286.

Fiorillo, F., 2009. Spring hydrographs as indicators of droughts in a karst environment. Journal of Hydrology 373(3–4), 290–301.

Fiorillo, F. and Guadagno, F.M. 2012., Long karst spring discharge time series and droughts occurrence in Southern Italy. Environmental Earth Sciences 65(8), 2273–2283.

Fiorillo, F. 2013., Spring hydrographs recession and analysis of the Caposele Spring (Southern Italy) during dry periods. Italian Journal of Engineering Geology and Environment 2013, 51–64.

Ford, D., and Williams, P., 2007. Karst hydrogeology and geomorphology. Wiley J. & Sons, Ltd, 1-576, ISBN 978-0-470-84996-5.

Fusco, F., Allocca, V., De Vita, P., 2017. Hydro-geomorphological modelling of ash-fall pyroclastic soils for debris flow initiation and groundwater recharge in Campania (southern Italy). Catena 2017, 158, 235–249.

Fusco, F., Bordoni, M., Tufano, R., Vivaldi, V., Meisina, C., Valentino, R., Bittelli M., De Vita, P. 2022. Hydrological regimes in different slope environments and implications on rainfall thresholds triggering shallow landslides. Natural Hazards, 114(1), 907-939.

Geiger, R., 1954. Klassifikation der Klimate nach W. Köppen. Landolt-Börnstein: Zahlenwerte und Funktionen aus Physik, Chemie, Astronomie, Geophysik und Technik, Alte Serie, Vol. 3. Springer 603, 607.

Giorgi, F., 2006. Climate change hot-spots. Geophysical Research Letters, 33(8), 2006GL025734. https://doi.org/10.1029/2006GL025734.

Goldscheider N., 2012. A holistic approach to groundwater protection and ecosystem services in karst terrains. Aquat. Mundi Am., 2012, 06046, 117–124.

IPCC. Climate Change, 2014. Synthesis Report. Contribution of Working Groups I, II and III to the Fifth Assessment Report of the Intergovernmental Panel on Climate Change [Core Writing Team, R.K. Pachauri and L.A. Meyer (Eds.)]. IPCC, Geneva, Switzerland,, 151.

ISPRA, 2017. Geological maps of Italy, scale 1:50,000. Sheets 431, 432, 448, 449, 466, 467, 485. ISPRA – Istituto Superiore per la Protezione e la Ricerca Ambientale, Servizio Geologico d'Italia. Retrieved from http://www.isprambiente.gov.it/Media/carg/campania.html.

Köppen, W., 1936. Das geographische system der klimat. Handbuch der klimatologie, 46.

Kresic, N. and Stevanović, Z., 2010. Groundwater hydrology of springs: engineering, theory, management, and sustainability. Butterworth-Heinemann, Oxford.

Lepore, D., Bucchignani, E., Montesarchio, M., Allocca, V., Coda, S., Cusano, D., De Vita, P., 2024. Impact scenarios on groundwater availability of southern Italy by joint application of regional climate models (RCMs) and meteorological time series. Scientific Reports, 14:20337. 10.1038/s41598-024-70257-1. https://doi.org/10.1038/s41598-024-70257-1.

Manna, F., Allocca, V., Fusco, F., Napolitano, E., De Vita, P., 2013a. Effect of the North Atlantic Oscillation on groundwater recharge in karst aquifers of the Cilento Geopark (Italy). Rendiconti Online Società Geologica Italiana 28, 106–109.

Manna, F., Allocca, V., De Vita, P., Fusco, F., Napolitano, E. 2013b. Groundwater recharge assessment in karst aquifers of southern Apennines (Italy). Rendiconti Online Società Geologica Italiana 24, 202–204.

Mirus, B.B., Nimmo, J.R., 2013. Balancing practicality and hydrologic realism: a parsimonious approach for simulating rapid groundwater recharge via unsaturated-zone preferential flow. Water Resour. Res. 49, 1458–1465.

Mostardini, F., and Merlini, S., 1989. Appennino centro-meridionale, sezioni geologiche e proposta di modello strutturale, Mem. Soc. Geol. Ital., 35,177-20.

Naclerio, G., Petrella, E., Nerone, V., Allocca, V., De Vita, P., Celico, F., 2008. Influence of topsoil of pyroclastic origin on microbial contamination of groundwater in fractured carbonate aquifers. Hydrogeology Journal 16(6), 1057–1064.

Napolitano, E., Fusco, F., Baum. R. L., Godt, J. W., De Vita, P., 2016. Effect of antecedent hydrological conditions on rainfall triggering of debris flows in ash-fall pyroclastic mantled slopes of Campania (southern Italy). Landslides, 13(5), 967-983.

Nicotera, P., Civita, M., 1969a. Ricerche idrogeologiche per la realizzazione delle opere di presa delle sorgenti Mercato e Palazzo in Sarno (Campania). Mem. e Note Ist. Geol. Appl. (1969), Vol. 11, 1-59, Napoli.

Nicotera, P., Civita, M., 1969b. Indagini idrogeologiche per la captazione delle sorgenti S. Marina di Lavorate (Sarno). Mem. e Note Ist. Geol. Appl. (1969), Vol. 11, 1-50, Napoli.

Patacca, E., and Scandone, P., 2007. Geology of the southern Apennines. Bollettino della Società Geologica Italiana, 7, 75-119.

Pescatore, T., and Ortolani, F., 1973. Schema tettonico dell'Appennino campano-lucano.

Pescatore, T., and Sgrosso, I., 1973. I rapporti tra la piattaforma campano-lucana e la piattaforma abruzzese-campana nel casertano.

Petrella, E., Capuano, P., Celico, F., 2007. Unusual behaviour of epikarst in the Acqua dei Faggi carbonate aquifer (Southern Italy). Terra Nova 19(1), 82–88.

Petrella, E., Falasca, A., Celico, F., 2008. Natural-gradient tracer experiments in epikarst: a test study in the Acqua dei Faggi experimental site, southern Italy. Geofluids 8(3), 159–166.

Petrone, P., Allocca, V., Fusco, F., Incontri, P., De Vita, P., 2023. Engineering geological 3D modeling and geotechnical characterization in the framework of technical rules

for geotechnical design: the case study of the Nola's logistic plant (southern Italy). Bulletin of Engineering Geology and the Environment, 82(1), 12.

Putignano, M. L., Ruberti, D., Tescione, M., Vigliotti, M., 2007. Evoluzione tardo quaternaria del margine casertano della Piana Campana (Italia meridionale). Bollettino della Società geologica italiana, 126, 11-24.

Rolandi G., Maraffi S., Petrosino P., Lirer L., 1993a. The Ottaviano eruption of Somma-Vesuvio (8000 y BP): a magmatic alternating fall and flow-forming eruption. Journal of Volcanology and Geothermal Research, 58(1-4), 43-65.

Rolandi G., Mastrolorenzo G., Barrella A. M., Borrelli A., 1993b. The Avellino plinian eruption of Somma-Vesuvius (3760 yBP): the progressive evolution from magmatic to hydromagmatic style. Journal of Volcanology and Geothermal Research, 58(1-4), 67-88.

Rolandi G., Petrosino P., Mc Geehin J., 1998. The interplinian activity at Somma–Vesuvius in the last 3500 years. Journal of Volcanology and Geothermal Research, 82(1-4), 19-52.

Rolandi G., Bertollini F., Cozzolino G., Esposito N., Sannino D., 2000, Sull'origine delle coltri piroclastiche presenti sul versante occidentale del Pizzo d'Alvano (Sarno-Campania). Quaderni di Geologia Applicata, 7(1), 37-48.

Rolandi G., Munno R., Postiglione A., 2004. The 472 AD eruption of Somma volcano. Journal of Volcanology and Geothermal Research, v. 129, p. 289-318.

Rolandi G., Paone A., Di Lascio M., Stefani G., 2007. The 79 AD eruption of Somma: The relationship between the date of the eruption and the southeast tephra dispersion. Journal of Volcanology and Geothermal Research 169, 87–98.

Rosi M., Principe C., Vecci R., 1993. The 1631 Vesuvius eruption. A reconstruction based on historical and stratigraphical data. Journal of Volcanology and Geothermal Research, 58(1-4), 151-182.

Ruggieri, G., Allocca, V., Borfecchia, F., Cusano, D., Marsiglia, P., De Vita, P., 2021. Testing Evapotranspiration Estimates Based on MODIS Satellite Data in the Assessment of the Groundwater Recharge of Karst Aquifers in Southern Italy. Water 13 (2), 118, 2021.

Santangelo, N., Ciampo, G., Di Donato, V., Esposito, P., Petrosino, P., Romano, P., Russo Ermolli, E., santo, A., Toscano, F., Villa, I., 2010. Late Quaternary buried lagoons in the northern Campania plain (southern Italy): evolution of a coastal system under the influence of volcano-tectonics and eustatism. Ital. J. Geosci. 129 (1), 156e175.

Santo, A., Liguori, M., Aquino, S., Galasso, M., 1998. Problemi di geologia ambientale nei polje appenninici: l'esempio della Piana di Forino (Campania). Il Quaternario 11(2), 233–245.

Santo, A., Prete, S., Giulivo, I., 2008. Nuove ipotesi sulla formazione dei piping sinkhole in aree alluvionali: il caso della piana di Forino (Avellino, Campania). 21, 395–408.

Santo, A., Santangelo, N., De Falco, M., Forte, G., Valente, E., 2019. Cover collapse sinkhole over a deep buried carbonate bedrock: The case study of Fossa San Vito (Sarno-Southern Italy). Geomorphology 345, 106838. https://doi.org/10.1016/j.geomorph.2019.106838.

Terribile F., Basile A., De Mascellis R., Di Gennaro A., Vingiani S., 2000. I suoli delle aree di crisi di Quindici e Sarno: proprietà e comportamenti in relazione ai fenomeni franosi del 1998. Quaderni di Geologia Applicata 7 (1), pp. 60-79.

Tufano, R., Allocca, V., Coda, S., Cusano, D., Fusco, F., Nicodemo, F., Pizzolante, A., De Vita, P., 2020. Groundwater vulnerability of principal aquifers of the Campania region (southern Italy). Journal of Maps, 2020, 16:2, 565-576.

USDA, 2014. Keys to soil taxonomy. United States Department of Agriculture Natural Resources Conservation Service 12th edition, pp. 372.

Valente, E., Allocca, V., Riccardi, U., Camanni, G., Di Martire, D., 2021. Studying a Subsiding Urbanized Area from a Multidisciplinary Perspective: The Inner Sector of

the Sarno Plain (Southern Apennines, Italy). Remote Sens. 2021, 13, 3323. https://doi.org/10.3390/rs13163323.

Vicente-Serrano, S.M., López-Moreno, J.I., Beguería, S., Lorenzo-Lacruz, J., Sanchez-Lorenzo, A., García-Ruiz, J.M., Azorin-Molina, C., Morán-Tejeda, E., Revuelto, J., Trigo, R., Coelho, F., and Espejo, F., 2014. Evidence of increasing drought severity caused by temperature rise in southern Europe. Environ. Res. Lett. 9 (4). https://doi.org/10.1088/1748-9326/9/4/044001.

Vitale, S., Ciarcia, S., 2018. Tectono-stratigraphic setting of the Campania region (southern Italy). Journal of Maps, 2018, 14(2), 9-21.